

Geochemical Perspectives



VOLUME 12, NUMBER 2 | OCTOBER 2023

ERIC H. OELKERS
SIGURDUR R. GISLASON

Carbon Capture and Storage: From Global Cycles to Global Solutions





Each issue of **Geochemical Perspectives** presents a single article with an in-depth view on the past, present and future of a field of geochemistry, seen through the eyes of highly respected members of our community. The articles combine research and history of the field's development and the scientist's opinions about future directions. We welcome personal glimpses into the author's scientific life, how ideas were generated and pitfalls along the way. *Perspectives* articles are intended to appeal to the entire geochemical community, not only to experts. They are not reviews or monographs; they go beyond the current state of the art, providing opinions about future directions and impact in the field.

This article is distributed under Creative Commons Attribution Non-Commercial No-Derivatives 4.0 License (CC BY-NC-ND 4.0), anyone is free to share (copy and redistribute) the material in any medium or format under the condition that:

- appropriate credit is given to the original author and publication
- a mention is included if changes were made to the original material
- a link to the license is provided



However, the material cannot be adapted (remixed, transformed, built upon) or used for commercial purposes without prior permission from the author.

For information on *Geochemical Perspectives*, visit: www.geochemicalperspectives.org.

The publisher assumes no responsibility for any statement of fact or opinion expressed in the published material.

ISSN 2223-7755 (print)

ISSN 2224-2759 (online)

DOI 10.7185/geochempersp.12.2

Principal Editor for this issue

Mihály Pósfai, University of Pannonia, Hungary

Reviewers

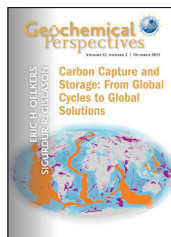
Jérôme Gaillardet, IPGP Université de Paris Cité, France

Stuart Haszeldine, University of Edinburgh, UK

Cover Layout Pouliot Guay Graphistes

Typesetter Info 1000 Mots

Printer Deschamps impression



About the cover

Locations of feasible geological formations for *in situ* mineral carbonation. Map showing the potential onshore and offshore targets for *in situ* mineral storage of CO₂. Oceanic ridges younger than 30 Ma are shown in orange, and oceanic igneous plateaus and continental flood basalts are shown in purple (FROM SNAEJORNSDOTTIR ET AL., 2020, INCLUDING AUTHOR CORRECTION).

EDITORIAL BOARD



JANNE BLICHERT-TOFT
ENS Lyon, France



DON CANFIELD
University of Southern Denmark,
Denmark



SARAH GLEESON
GFZ Potsdam, Germany



KLAUS MEZGER
University of Bern, Switzerland



RICHARD PANCOST
University of Bristol, UK



MIHÁLY PÓSFAI
University of Pannonia,
Hungary



Editorial Manager
MARIE-AUDE HULSHOFF
European Association of Geochemistry



Graphical Advisor
ROBERT DENNEN
Geoscience Editing

CONTENTS

Abstract	179
1. Introduction	181
1.1 How Did We Become Geochemists?	181
Text Box 1.1 – Eric: Beginnings of <i>Geochemical Perspectives</i>	185
1.2 A Brief History of the Link between CO ₂ and Global Warming	187
2. The Global Carbon Cycle and Climate	192
2.1 The Basics	192
2.2 Demonstration of the Feedback between Increasing Global Temperature, Continental Weathering and the Drawdown of CO ₂ from the Atmosphere	198
2.2.1 Quantifying Riverine Chemical Concentrations and Fluxes in 8 NE Iceland Rivers	198
2.2.2 Quantifying the Effect of Increasing Temperature on Weathering Rates	205
2.2.3 The Strength of the Weathering Feedback on Distinct Elements	209
Text Box 2.1 – Summary: Major Observations on the Weathering-Climate Feedback from Long Term Weathering Studies	211



2.2.4	The Increase in Elemental Weathering Rates from 1960 to 2005.	211
2.2.5	The Carbon Drawdown Rates of Icelandic Rivers.	213
2.2.6	Assessing the Potential for Increased Natural Weathering to Address Global Warming	214
	Text Box 2.2 – The Carbon Dioxide Weathering Feedback and the Proof of Divine Intervention	215
2.3	Other Factors Influencing Weathering Rates	216
2.3.1	Rock Age.	216
2.3.2	River Damming.	218
2.3.3	Glacial Cover	220
	Text Box 2.3 – Summary: Factors Affecting Weathering Rates.	222
2.4	The Significance of Suspended Material Transport to the Oceans on the Global Cycles of the Elements.	222
2.5	Deglaciations, Particulate Material, and the Oxygenation of the Earth’s Atmosphere	228
3.	Anthropogenic Influences.	233
3.1	Human Intervention in the Global Carbon Cycle.	233
3.2	The Fate of Anthropogenic Carbon Emissions	235
3.3	Atmospheric CO ₂ Concentrations and Human Health	238
4.	Carbon Capture and Storage (CCS).	240
4.1	History of Conventional Carbon Capture and Storage (CCS)	240
4.1.1	Conventional Carbon Capture and Storage: Practicalities	242
4.2	Is Enhanced Oil Recovery (EOR) Carbon Storage?	243
4.3	Carbon Capture and Storage via Mineral Carbonation at the Earth’s Surface	245
4.4	The Beginning of CarbFix	250
4.4.1	Pre-Injection Field Observations	255
4.4.2	Pre-Injection Experimental Studies	257
4.4.3	Characterising Subsurface Flow Paths	261
4.4.4	Pre-Injection Reactive Transport Modelling of the CarbFix1 Injection	263
4.5	CarbFix1	266
4.5.1	The CarbFix1 Injection Well	266
4.5.2	The Chemistry of the Monitoring Well Fluids.	271
4.5.3	The Saturation State of the Monitoring Well Fluids	273
4.5.4	Quantifying the Mass of CO ₂ Fixed in Minerals.	275
4.5.5	Development of Novel Isotopic Tracers to Quantify the Fate of CO ₂ Injected into the Subsurface	278
4.5.6	Toxic and Trace Element Mobility in Response to the CarbFix1 Injections	282



4.5.7	The Co-Injection of CO ₂ + H ₂ S and End of the CarbFix1 Injections	283
4.5.8	CarbFix1 Epilogue.....	283
4.6	CarbFix2	284
4.7	Money Changes Everything	294
4.8	Water Demand and the Use of Seawater.....	297
4.9	Coupling Subsurface Mineralisation with Direct Air Capture (DAC).....	299
4.10	Carbon Storage Alternatives	301
4.10.1	Carbon Storage in Clathrates or Hydrates	301
4.10.2	Combining CO ₂ Hydrate Storage with CH ₄ Recovery	304
4.10.3	Deep Ocean Storage of Liquid CO ₂	305
4.10.4	Carbon Storage through Forestry.....	305
4.11	How Much Carbon Capture and Storage: Incentives and Costs?.....	307
5.	The Future	311
5.1	Will Carbon Capture and Storage Ever Be Large Enough to Help Limit Global Warming?.....	313
5.2	Will Mineral Carbon Storage Move Forward?.....	314
5.2.1	<i>Ex situ</i> Mineralisation.....	315
5.2.2	<i>In situ</i> Mineralisation	315
5.3	Future Carbfix Projects.....	316
5.4	Other Future Subsurface Mineral Storage Projects.....	318
5.4.1	Subsurface Basalt-Hosted Carbon Mineralisation in Other Parts of the World.....	318
5.4.2	Subsurface Mineralisation in Ultramafic Rocks	318
5.5	Future Research Directions.....	319
5.6	Over and Out.....	321
	References	323
	Index	347



CARBON CAPTURE AND STORAGE: FROM GLOBAL CYCLES TO GLOBAL SOLUTIONS

ABSTRACT

Anthropogenic carbon emissions have overwhelmed the natural carbon cycle, leading to a dramatic increase in atmospheric CO₂ concentration. The rate of this increase may be unprecedented in Earth's history and is leading to a substantial increase in global temperatures, ocean acidification, sea level rise and potentially human health challenges. In this *Geochemical Perspectives* we review the natural carbon cycle and its link to global climate. Notably, as directly observed by field observations summarised in this volume, there is a natural negative feedback loop between increasing global temperature, continental weathering rates, and CO₂ that has tended to limit Earth climate changes over geological time scales.

Due to the rapid increase in atmospheric carbon concentrations, global average temperatures have increased by more than 1.2 °C since the start of the industrial revolution. One way to slow or even arrest this increasing global average temperature is through Carbon Capture and Storage (CCS). Carbon dioxide can be captured either from large industrial point sources or directly from the atmosphere. Taking account of the natural carbon cycle, the most secure



approach to storing captured CO₂ is by reacting it with mafic or ultramafic rocks to form stable carbonate minerals, a process referred to as “mineral carbonation”. Although mineral carbonation can occur and be accelerated at the Earth’s surface, due to the required scale and required time frames it is most effective in the subsurface. This subsurface mineralisation approach was developed into an industrial scale process through an academic-industrial collaboration called CarbFix. The history of CarbFix, from its beginnings as a concept through its installation as an industrial process is presented in detail.

This *Geochemical Perspectives* concludes with an assessment of the future of subsurface mineralisation as a means to help address the global warming challenge, as well as a detailed list of potential research directions that need to be addressed to further upscale and optimise this carbon storage approach.

Note to readers:

Throughout this issue, the spelling of places mentioned in figures as well as names of authors in the reference list follows that of the original sources. In all other cases, the spelling of Icelandic personal names is without the Icelandic characters.

For clarity, Siggi is a nickname for the Icelandic name Sigurður.



1.1 How Did We Become Geochemists?

We have in the past thought that our writing should always focus on our science. In part because we always have so much science to share and because this is what we have in common with our readers – the desire to solve some of the great questions and challenges of our world. Our opinions began to change somewhat at the 2013 Goldschmidt meeting in Florence. At a bar across from the Medici Chapel, over far too many beers, we were surrounded by a suite of students and postdocs, not asking details of our science, but trying to find out how we got to where we were, what motivated us, and how we got our ideas. This has been repeated again and again at subsequent conferences. Though we cannot, we suspect, really determine where our ideas come from, perhaps a bit of our background can provide some insight.

Quite curiously our backgrounds are very different, though in some ways this has always been our strength. Siggí grew up in Reykjavík and in rural Iceland, raising animals and shooting game. Eric grew up in New York City where the only farm animals were found in the refrigerator section of the local grocery store, and the only game animals in the local zoo. As a geochemist, Siggí's background was largely field based and Eric's largely computational and experimental based. The combination of our backgrounds, however, made it possible for us to go far beyond what either of us could do on our own.

Siggí: I was born and raised in Iceland. As a young boy, I spent summers at my grandfather's farm in southeast Iceland, downstream from the glacier-covered Katla volcano. In the evenings, I would listen to stories of eruptions, ash falls and my grandfather galloping on his horse in front of the glacier's outburst flood associated with the 1918 eruption of the Katla volcano. At the peak of the flood, it was the largest river on Earth. My interest in volcanoes and geology was kindled.

My high school teacher further inspired me to study geology at the University of Iceland. There I learned from Stefan Arnorsson and Sigurdur Steinthorsson about the power of thermodynamics, and how it helps to interpret water-rock interactions. After graduation in the spring of 1980, I took my first job as a geologist at the Nordic Volcanological Institute in Iceland, before heading to Johns Hopkins University for graduate school that fall. We got two eruptions that summer, and I was paid to study them. I spent my last week in Iceland on the slopes of the erupting Hekla volcano before my departure for the US in late August 1980. I took one day to pack and received a culture shock when I arrived for the first time in New York and then onwards to Baltimore. There I was to study gas buffers in basaltic geothermal systems with Hans Eugster at



Johns Hopkins University. Hans was a great mentor, scientist, and artist. We had Friday seminars at his and Elaine's farm in Western Maryland, surrounded by his paintings. Elaine, Hans' wife, was a professor of mathematics at Goucher College in Baltimore. For my PhD thesis, I did field and laboratory studies of meteoric water-basalt interactions with Hans (Gislason and Eugster, 1987a,b; Fig. 1.1).

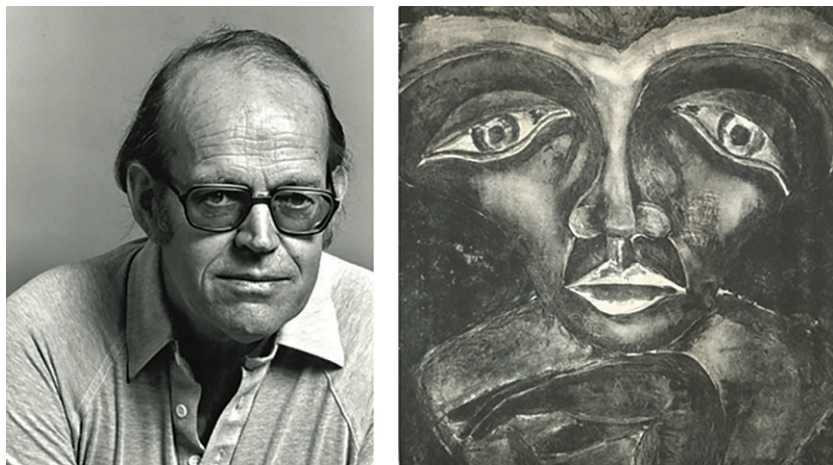


Figure 1.1 Photo of Hans P. Eugster taken few years before he died in 1987 and his Self Portrait 1962, Lithograph. From Spencer and Chou (1990) with permission from the Geochemical Society.

I had a few postdoc options in USA and Canada in 1985, but my wife Malla, an architect and urban planner, received an excellent offer from an Icelandic architectural firm, so I followed her back to Iceland and started working on a soft money post at the University of Iceland. I went back to Hopkins for few months during 1987, working with Dave Veblen on a TEM study of alteration products created during my low temperature PhD experiments. At the end of our stay at Hopkins in early autumn, we drove to Martha's Vineyard where Hans and Elaine were building a summerhouse. When we left on the ferry, Hans waved for a long time, which was unusual for him. This was the last time I saw him, he died two months later from an infection, at the age of 62, virtually with his boots on.

Just before Christmas in 1987, the same day that Hans died, I got a permanent position at University of Iceland. Few years later in 1994, I went on a sabbatical to Toulouse, France, to work with Jacques Schott on dissolution rate experiments on moganite (a novel silica polymorph) and quartz. Peter Heaney, a Hopkins friend, had then recently shown that chalcedony and chert specimens from around the world contained a mixture of very small crystals of quartz and moganite. Chalcedony generally contains between 5 and 15 wt. % moganite, whereas chert from evaporitic environments may include more than 50 wt. %



moganite. The aim was to define moganite's dissolution rates and its thermodynamic properties (Gislason *et al.*, 1997). On my first visit to the lab in Toulouse I ran into Eric Oelkers. Eric was and is direct, brilliant, honest, trustworthy and a lot of fun. We have been the very best of friends and collaborators from that day. My family and I were frequent visitors to Toulouse over the next 15 years and enjoyed the hospitality of Eric, Stacey, and Jacques. With PhD students and postdocs, we quantified the dissolution rates of volcanic glasses, climate control of weathering of basaltic rocks, the role of river suspended material in the carbon cycle and the effect of crystallinity on dissolution rates and CO₂ consumption capacity of silicates, as discussed in Section 2 of this volume.

The tide changed in 2007 with the beginning of the CarbFix project in Iceland. In February 2005 the Kyoto protocol entered into full force, committing countries to limit CO₂ emission. To address this challenge, the Icelandic President approached Eric and I, along with Einar Gunnlaugsson at Reykjavík Energy, Iceland, Wally Broecker at Columbia University, USA, to design a project, later referred to as CarbFix, to aid in limiting greenhouse gas emissions in Iceland. After nearly a decade of experiments, obtaining permissions and the preliminary injections, Reykjavík Energy and other members of CarbFix laid the foundation of industrial scale gas capture from concentrated gas streams and directly from the atmosphere, followed by injection and mineralisation at the Hellisheiði site in Southwest Iceland as described in Section 4.

Eric: I am proud to have been born and raised in the Bronx and to have grown up in New York City. Much of the surface of New York is covered in asphalt or large buildings, so this is hardly a hotbed of geology. In fact, it's likely as far as one can get from the natural environment and still be on the surface of our planet. After graduating from schools with such catchy names as P.S. 203, I.S. 74, and Cardozo High School, I left home to study Chemistry at the Massachusetts Institute of Technology.

The defining moment convincing me to try geology occurred the summer of my first year at university. I had an internship at Southwest Specialty Chemicals in Deer Park, Texas. A memorable feature of Deer Park was that the colour of the sky was always a different shade of purplish grey each day. My job was to collect samples from trucks arriving with solvents, such as acetone and ammonia, and measure their purity. Apparently, a common practice at the time was to add water to these solvents diluting these down to the minimum spec. limit to maximise profits. If below the purchased quality I was to send the truck away.

This was boring work. So boring, I began to calculate the number of minutes left in my work day, every five minutes. Within weeks I was convinced that I could not be a career chemist. Upon returning to MIT, I took my first geology class, Introduction to geology taught by John Southard. This was fun. Visiting outcrops, hammering on rocks, and perhaps most important I was able to see scientific principles right in front of me in the field.

Not wanting to start work after graduation, I applied to a large number of graduate programmes, and despite having only average grades got into all of



these. I decided to go to Berkeley, California. I recall my largest motivation was all of the California beach and surfing movies I watched as an adolescent, but for some reason Harold Helgeson seemed to think I moved to California to study geochemistry, so he offered me a research assistantship as part of his research group “Prediction Central” (see Fig. 1.2).



Figure 1.2

Prediction Central 1983. From left to right: Mike Salais, Barbara Ransom, Eric Oelkers, Joan Bossart, Harold Helgeson, Everett Shock, Cathy Wilson, John Tanger, Peter Lichtner, William Murphy, and Jay Ague.

I regret that many of you reading this volume never had the chance to meet Helgeson. He was a classic “work hard, play harder” professor. Perhaps the closest person in personality to the character Morris Zapp in the book *Changing Places* by David Lodge. He was a generous and very loyal advisor, and he changed geochemistry by creating the mineral-fluid-gas thermodynamic database (Johnson *et al.*, 1992). While there, Helgeson drove into our heads the minute details of thermodynamics and kinetics. Peter Lichtner, there at the time, introduced me to geochemical reactive transport modelling.



Geology, being cyclical, was out of favour when I graduated and jobs in the United States were scarce. My best opportunity was to move to France to work with Jacques Schott, an experimental geochemist working largely on mineral-fluid reaction rates. Jacques was far different in personality than Helgeson. Jacques is highly cultured, always curious, loves hiking, and always has time to discuss any scientific detail one has in mind. After two years I was recruited at the CNRS and I continue to work with Jacques to this day.

Funding experimental research, however, proved challenging, but the European Commission had the answer in the form of Research and Training Networks. All one needed to do was to organise a set of like-minded scientists located in different European countries and agree on a collaborative research and training programme. This turned out to be the path to great friends, great collaborators, and great science. Siggí and I gathered a close group of very motivated and talented geoscientists including Manolo Prieto (Spain), Vala Ragnarsdóttir (UK and Iceland), Andrew and Christine Putnis (Germany), Susan Stipp (Denmark), Björn Jamtveit (Norway), Per Aagaard (Norway), Jordi Bruno (Spain), and Liane Benning (UK and Germany) who ran research and training networks together with more than 100 PhD students and postdocs since 1999. The keys to success of these networks were mutual respect and complete trust among us so we could share all of our ideas. Science can be a rough career. As is the case for all scientists, our work is commonly criticised, many of our grant proposals and papers are rejected, and most of our publications barely read. It is this group of friends and our students and postdocs that have kept us moving and motivated. It is only their encouragement and support that made it possible to continue pursuing scientific research over our careers.

Text Box 1.1 – Eric: Beginnings of Geochemical Perspectives

Although I always wanted this journal *Geochemical Perspectives* to be forward looking, I feel compelled to take advantage of this opportunity to look back, to provide some of the history of the origins of this journal. The idea for *Geochemical Perspectives* was hatched in 2009 at the Goldschmidt conference during a lunch discussion with Elsevier. At that time, during my tenure as EAG president, we were in negotiations with Elsevier in an attempt to acquire funds to support student attendance at conferences. The connection between the EAG and Elsevier went back to the late 1980's when the EAG made *Chemical Geology* the official journal of the society. When asked for funds for student support, we were told that there was no reason for Elsevier to provide funds to the EAG, as the society provided little for them. I pointed out to them that in addition to providing most of their published papers, our community provided hundreds of reviews of manuscripts free of charge for *Chemical Geology*, as well as their other journals. The response was that the reviewers were happy to provide these for free, so why did they owe anything. They, however, proposed that they might be able to provide from \$10,000 to perhaps as much as \$30,000 if we allowed them to run the Goldschmidt meeting. I left my meeting angry. The income of the Goldschmidt meeting, run by EAG every two years, is far in excess of that amount even without a for-profit company attempting to maximise their profit from it.



I also noted that only a few years before, the combined geochemical and mineralogical community joined together and launched the journal *Elements*. *Elements* was produced and mailed to members of our community anywhere in the world at a cost of less than \$2.00 *per issue*. In contrast, the cost of many of Elsevier's journals exceeded \$100 per issue. So why could the EAG not start a community owned and operated journal at a far less cost than the major profit making publishing company?

We at the EAG then approached the Geochemical Society with the idea of joining forces to launch one or more journals. The Geochemical Society declined as they were involved in separate negotiations with Elsevier themselves at the time. Still at the 2009 Davos Goldschmidt meeting, the EAG treasurer, Christa Göpel, pointed out that the costs of launching the journal would not be excessive, and could be taken on by the EAG alone.

Tim Elliott, Susan Stipp, and Liane Benning agreed to join with me to generate a scientific and business plan. We wanted to start with a new concept and something that was high profile and, at least from the start, easy to manage. We noted that many of our senior colleagues had many ideas that were lost upon their retirement. At times these ideas were controversial and perhaps lacked sufficient evidence making them difficult to publish. Many of these ideas could be testable hypotheses for the future, particularly as new information and tools became available to our community. Many were critical open questions that could/should be further explored. Others were consequences of their past work that could not be added to the discussion parts of shorter scientific communications.

From these beginnings *Geochemical Perspectives* was born. Our goal was to motivate senior scientists to open up after long careers to write monographs revealing their ideas in a loose format, giving each the leeway to speculate if they cared to, to suggest new research directions, and to provide new ideas for the future generation of Earth Scientists. I hope that *Geochemical Perspectives* has been able to do so.

I personally have been inspired by a number of our past issues. Two in particular stand out in my head. The first is that of Wally Broecker's second monograph *CO₂ the Earth Climate Driver* (Broecker, 2018), which clearly laid out the evidence connecting the atmospheric CO₂ concentrations and global climate, by focusing on what we know about 6 episodes of Earth history. In many cases he pointed out what we have, and have not observed, and proposed new directions that would further enlighten our understanding of the current climate CO₂ feedback. The second issue that particularly inspired me was *Natural Resources in a Planetary Perspective* (Sverdrup and Ragnarsdottir, 2014). In this issue, Harald and Vala make their best estimates of when the global supplies of various essential elements will run out and speculate on the consequences. This issue was particularly controversial and motivated a second *Geochemical Perspectives* issue in response (Arndt *et al.*, 2017), which presented the counter argument that there are many more economic resources available, so long as we find them. In either case, the message is clear. Our community needs to continue to find new resources and to develop effective methods of recycling to ensure the future of society. What stands out to me from each of these issues is that our geochemical community holds the key knowledge and perhaps the responsibility to help manage our Earth for the benefit of all.



PREQUEL

When starting to develop this *Geochemical Perspectives*, we decided to focus on the global carbon cycle and how our understanding of the natural Earth surface might be used to limit future carbon emissions to the atmosphere. We chose to limit our attention to the natural and anthropogenically influenced carbon cycle, both because we have worked extensively in this area over the past two decades and to focus attention on the critical societal need to limit global warming in the coming decades. We hope that by creating this perspective we can inspire members of our community to help develop effective and large scale solutions to attenuate carbon dioxide emissions to our atmosphere, building on our knowledge of natural processes.

1.2 A Brief History of the Link between CO₂ and Global Warming

Interest in the connection between the CO₂ content of the atmosphere and global temperature goes back for over a century. Perhaps the first scientific report linking increasing CO₂ content to global climate was the study of Arrhenius (1896). Using model calculations, he concluded that the halving of the atmosphere's CO₂ content could lead to an ice age, but doubling this content could increase global temperature by 5 to 6 °C.

Scientific efforts connecting atmospheric CO₂ content with global temperature accelerated beginning in the 1960's. This acceleration was due to two major scientific efforts. First, beginning in 1957, Charles Keeling began measuring the CO₂ content of the atmosphere on Mauna Loa, Hawaii, and in Antarctica. By 1965, a clear temporal increase in atmospheric CO₂ concentrations was evident (Brown and Keeling, 1965; Pales and Keeling, 1965). At approximately this time, the first comprehensive compilations of the temporal evolution of global temperature were published by Mitchell (1963, 1972). Mitchell's 1963 global temperature curve is shown together with several others in Figure 1.3. These studies showed that global temperature increased steadily from the 1880's until approximately 1940, after which it decreased into the 1970's. This apparent discrepancy was attributed primarily to the increase in aerosols in the atmosphere. Broecker (1975), in the first scientific study to use the expression "global warming", concluded that the global cooling trend from 1940 to 1975 would soon come to an end. He concluded that the exponential increase in atmospheric carbon dioxide content would drive global temperatures beyond the limits experienced during the previous 1,000 years.

Scientific research over the following decade generated a unified view of the factors influencing global climate, including the role of greenhouse gases, aerosols, orbital forcing and solar radiation (Manabe and Stouffer, 1980; Hansen *et al.*, 1981). The message was clear. Anthropogenic increases in atmospheric CO₂ concentrations could lead to a dramatic and rapid increase in global



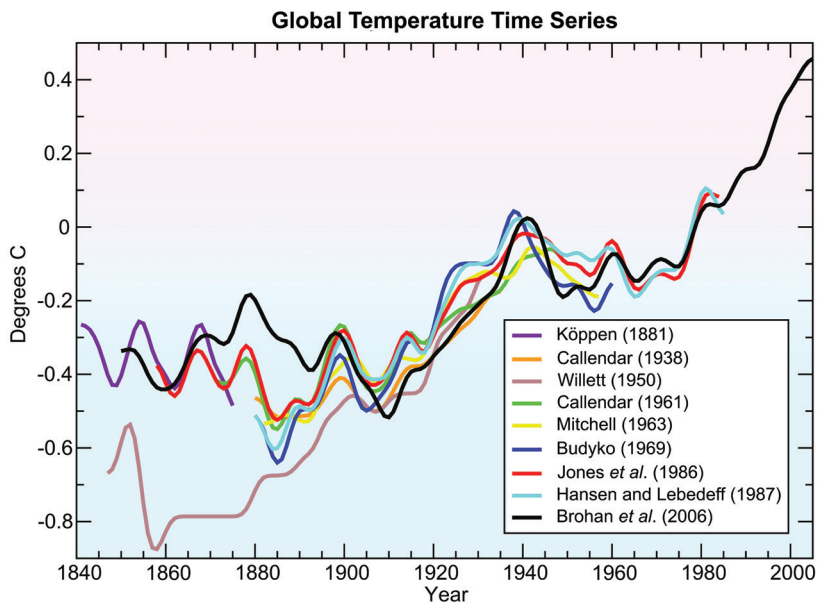


Figure 1.3 Comparison of various published historical global temperature records through 2007. These records include: Köppen (1881), based on land air temperature. Callendar (1938) and Willett (1950) estimated global average temperature using land station measurements; Callendar (1961) estimated average temperature from 60°N to 60°S using land station measurements; Mitchell (1963) estimated global average using land station measurements; Budyko (1969) estimated Northern Hemisphere temperatures using land station measurements and ship reports; Jones et al. (1986a,b) estimated global average using land station measurements; Hansen and Lebedeff (1987) estimated global average using land station measurements; Brohan et al. (2006) estimated global average temperature using land air temperature and sea surface temperature data. All time series were smoothed using a 13 point filter. To make the curves comparable, all time series were adjusted to have the mean of their last 30 years identical to that of Brohan et al. (2006). From Le Treut et al. (2007).

temperatures. This wake-up call motivated the United Nations to organise the first Intergovernmental Panel on Climate Change (IPCC) in 1988. Since that time the IPCC has delivered five assessment reports (<https://www.ipcc.ch/reports/>). In 1990, the First IPCC Assessment Report summarised climate change research and its global consequences. The Second Assessment Report in 1995 provided material leading to the adoption of the Kyoto Protocol in 1997. The Third Assessment Report, in 2001, outlined the likely impacts of climate change. The Fourth Assessment Report, delivered in 2007, laid the groundwork for a post-Kyoto agreement, focusing on limiting global warming to 2 °C. The Fifth



Assessment Report was delivered in 2014 and provided the scientific input for the Paris Agreement. The Sixth Assessment Report is expected to be finalised during 2023. Each report is an extensive and informative review of the science of climate change and public policy.

The international impact of the IPCC has been great. This impact was further enhanced by a number of highly visible supporters, including Al Gore, the United States Vice President at that time (1993 to 2001), who gave a large number of presentations and created a popular film publicising the evidence for and the consequences of global warming. For their efforts the IPCC and Al Gore shared the 2007 Nobel Peace Prize. At the invitation of the President of Iceland, Siggí met Al Gore for a working dinner at President Grimsson's residency in April 2008, and later in the year he met Rajendra Kumar Pachauri, the chairman of the IPCC in Iceland for an afternoon tea to discuss carbon capture and storage *via* the CarbFix method described in Sections 4.4–4.6.

One of the major ways to address the challenge of global warming is carbon capture and storage (CCS). Although the impact of the IPCC reports and international interest in arresting global warming was great, the number of operating, in construction and planned CCS facilities, as shown in Figure 1.4, peaked in 2011 and declined in terms of total CCS capacity by more than 50 % from 2011 through 2017. This decline was largely due to stopping projects that were in construction or planned. There are several reasons for this large drop in interest in CCS over these years, much of it due to a public misinformation campaign in part supported by the energy and electrical utility industry. This campaign was aimed at making the public suspicious of global warming and of the scientific community in general (Brulle, 2019; Franta, 2021). Some of this misinformation stems from the complexity of the controls on global climate. Notably, the link between CO₂ and global temperature has been controversial over the past several decades, as this link has not been direct over geologic time (Broecker, 2018). Moreover, the interpretation of various evidence has changed over time. For example, one of the figures shown by Al Gore in his film *An Inconvenient Truth* is reproduced in Figure 1.5. This figure shows what appears to be a strong correlation between an increase in global temperature and atmospheric CO₂ content. A subsequent and more detailed study of these ice core records shows that, in fact, the change in CO₂ concentrations lagged the change in temperature by approximately 800 years (*e.g.*, Caillon *et al.*, 2003). The simple explanation for this lag is the retrograde solubility of CO₂ in seawater. When global temperature is driven by orbital planetary cycles, an increase in ocean temperature decreases the solubility of CO₂ in seawater. This decrease in solubility leads to the exsolution of CO₂ from the oceans into the atmosphere and the CO₂ content of the atmosphere increases. The 800 year lag is approximately twice the residence time of dissolved CO₂ in the oceans, and close to the mixing time of the marine system.





Figure 1.4 Estimated global CCS capacity from 2010 to 2020 including facilities in operation, in development and in construction. From the Global CCS Institute 2022 annual report (https://status22.globalccsinstitute.com/wp-content/uploads/2023/03/GCCSI_Global-Report-2022_PDF_FINAL-01-03-23.pdf).

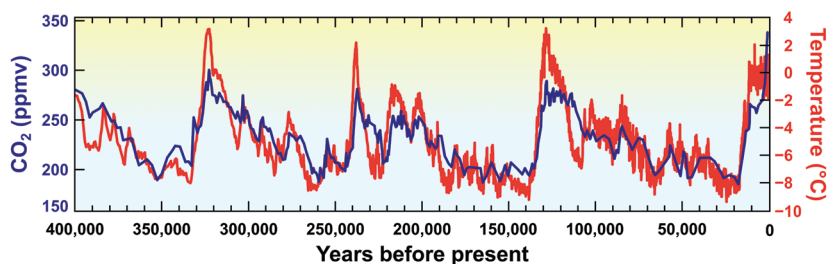


Figure 1.5 Variation of atmospheric CO₂ concentrations (blue) and estimated global temperature (red) estimated from Vostok ice core data over time. Data from Petit *et al.* (1999), figure reproduced from Oelkers and Cole (2008), with permission from the Mineralogical Society of America.

Nevertheless, doubt originating from this lag between increasing CO₂ concentrations and global temperature rise and a global financial downturn, helped slow considerably the pace of CCS activities by the end of the decade. This slowdown was further reinforced by an incident referred to by the popular press at that time as “Climategate”. In November 2009, more than 1,000 emails among the scientists at the Climate Research Department of the University of East Anglia were stolen and made public (Leiserowitz *et al.*, 2012). These emails



included some that discussed how to best describe and present sensitive climate data to illustrate the extent of global warming. The publication of these emails was used to discredit the scientists as well as the whole scientific field of climate research. Others claimed that the emails invalidated the conclusions of the 2007 IPCC report confirming the Earth was warming due to anthropogenic activities. Although 1) nothing in the leaked emails contravened the evidence for global warming, and 2) to date the people responsible for leaking these emails have not been revealed, these emails were seized upon as evidence that scientists cannot be trusted, and that the whole of global warming was a hoax created by scientists to obtain attention and grant funding.

It is only over the past few years that the evidence for global warming has become so overwhelming that the mountain of misinformation has been overcome. As we are writing this section, during the summer of 2022, Europe is experiencing the hottest summer on record and experiencing an historic drought (Rousi *et al.*, 2022). The effects of global warming are leading to extreme and destructive weather events worldwide (Thompson *et al.*, 2022). The seven warmest years directly measured in history have occurred since 2015 (World Meteorological Organization, 2022). These events have altered dramatically public opinion in favour of addressing the challenges of CO₂ reduction and global warming. The change in public opinion helped motivate the development of financial incentives, including tax breaks for CCS and emission trading schemes. Together these more recent developments have motivated a resurgence in CCS research and industrial scale projects shown in Figure 1.4.



2.1 The Basics

The transfer of carbon among the various reservoirs of the Earth both influences the global climate and makes possible life itself. The relative size of the major carbon reservoirs is shown in Figure 2.1. The atmosphere is a relatively small carbon reservoir. In pre-industrial times it contained roughly 600 gigatons of carbon, C. This has increased to approximately 900 gigatons of carbon since that time. These masses of carbon are equivalent to 2,200 and 3,300 gigatons of carbon dioxide, CO₂, respectively. Note that some literature sources, including this one, refer at times to masses of C and at times to masses of CO₂, potentially leading to confusion. The terrestrial biosphere contains approximately 2,000 gigatons of carbon. This carbon is mostly stored in organic material including live or decaying plants and microbes. The oceans contain roughly 38,000 gigatons of carbon, equal to about 40 times that of the atmosphere. The relatively large mass of carbon in the ocean compared to the atmosphere implies that a relatively small release or take up of carbon by the oceans can change substantially the CO₂ content of the atmosphere. Far larger than these reservoirs is the lithosphere, which is estimated to contain 3×10^8 gigatons of carbon. Most of the carbon in the lithosphere is present within carbonate minerals. It is estimated that approximately 25 % of the carbon in the lithosphere is in the form of kerogen, resulting from the transformation of organic material (Falkowski *et al.*, 2000). The mass of fossil fuels, including coal, oil and natural gas is only ~10,000 gigatons of carbon, yet the burning of even this relatively small carbon reservoir has notably increased the CO₂ content of the atmosphere. The mantle is estimated to be a larger carbon reservoir than the lithosphere at 1.5×10^9 gigatons of carbon (Lee *et al.*, 2019).

The processes and rates at which carbon moves among these reservoirs differ dramatically, as shown in Figure 2.2. The transfer of carbon among the atmosphere, the oceans and the terrestrial biosphere is relatively fast. This transfer is often referred to as the short term carbon cycle. More than 20 % of the carbon in the atmosphere is cycled into and out of the oceans and the terrestrial biosphere annually. This carbon is largely:

- 1) Dissolved into and exsolved out of the oceans. This reaction is sufficiently fast that the CO₂ concentration of surface ocean water is usually close to equilibrium with respect to CO₂ in the atmosphere. Thus, an increase in the CO₂ concentration of the atmosphere will increase the CO₂ concentration of the oceans. This process leads to ocean acidification (Mackenzie and Anderson, 2013).



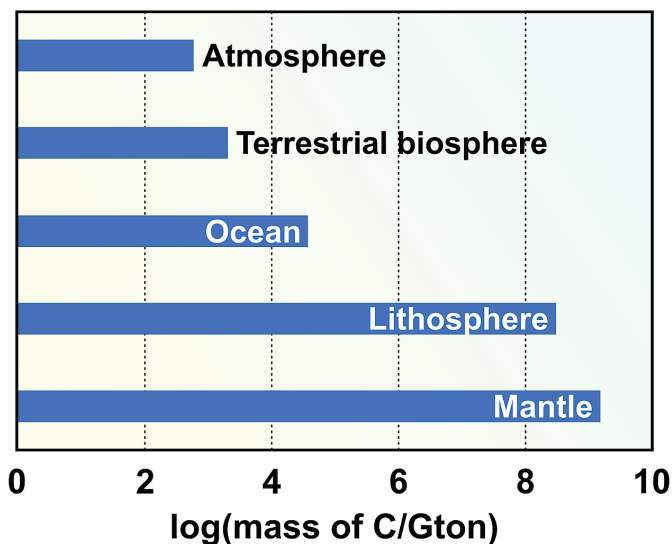


Figure 2.1 Masses of carbon in major terrestrial reservoirs in pre-industrial times. Data summarised by Lee *et al.* (2019). Note the logarithmic scale of the horizontal axis.

- 2) Transferred into and out of the terrestrial biosphere *via* photosynthesis and decay. These are two sides of the same reaction, which can be summarised as



The forward reaction is photosynthesis and draws CO_2 out of the atmosphere forming organic molecules, represented here by CH_2O . The reverse reaction is organic decay and returns the CO_2 back to the atmosphere. These reactions are fast and lead to measurable annual oscillations in the CO_2 concentration of the atmosphere. The reverse of Equation 2.1 is an oxidation reaction that provides energy for animal life including our own, and a similar oxidation reaction of hydrocarbons runs most of our automobiles.

Far slower is the transfer of material into and out the crust and mantle. The mass of carbon going into and out of the crust is estimated to be on the order of 0.2 gigatons *per* year, and within the crust it consists of both buried carbonate minerals and organic material. This mass is small compared to the 3×10^8 gigatons of carbon contained in the crust, such that the average residence time of carbon in the crust is in excess of a hundred million years.



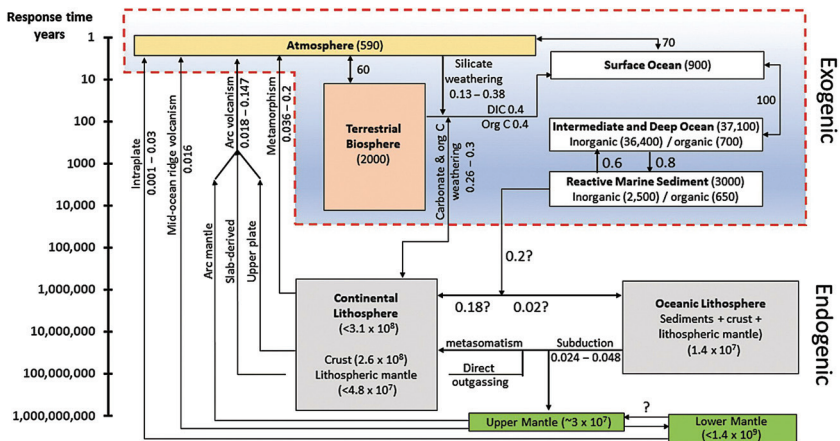


Figure 2.2

The pre-industrial carbon cycle, after Lee *et al.* (2019). The numbers in the boxes indicate the mass of carbon in each reservoir in units of gigatons carbon (Gt C). The numbers on the arrows connecting the reservoirs correspond to the estimated annual mass flux of carbon transferred between these reservoirs annually in gigatons carbon (Gt C yr⁻¹). The vertical scale on the left side of the figure indicates the average residence time, which approximates the average residence time of carbon in each of the reservoirs. Note that one gigaton of carbon is equivalent to 3.67 gigatons of CO₂. Plots of the carbon cycle such as shown in this figure have been made and updated since Goldschmidt published an early figure of the quantified global carbon cycle in 1934 (Goldschmidt, 1934).

The cycling of carbon into and out of the crust and mantle is commonly referred to as the long term carbon cycle and is summarised in Figure 2.3. Carbon dioxide and methane are released from the crust to the atmosphere through volcanic activity, metamorphism, sedimentary organic carbon weathering and diagenesis. Methane added to the modern atmosphere oxidises to CO₂ within decades. This CO₂ is returned to the crust either by:

- 1) the formation of carbonate minerals by the dissolution of the gaseous CO₂ into rainwater, where dissolved CO₂ can react with silicate minerals to form carbonate minerals, or by
- 2) the formation of organic material by photosynthesis followed by the burial of these carbon-bearing products.

Perhaps the most amazing feature of the global carbon cycle and terrestrial processes in general is the feedback between global temperature, the chemical weathering of the planet and atmospheric CO₂ content. The feedback between continental weathering and the atmospheric CO₂ content was first proposed by



Ebelmen (1845). He observed that the chemical weathering of silicate minerals consumes CO_2 making carbonate minerals, and that volcanic activity adds CO_2 to the atmosphere. This work was mostly forgotten for more than 100 years when the independent deduction of the major CO_2 and O_2 -controlling processes was reported by Urey (1952) and others (Berner, 2012). As mentioned in Section 1, evidence starting with Arrhenius (1896) linked increasing atmospheric CO_2 content to increased global temperatures through the greenhouse effect. Taken together, these processes provide a mechanism that has largely regulated global temperature over much of geologic time.

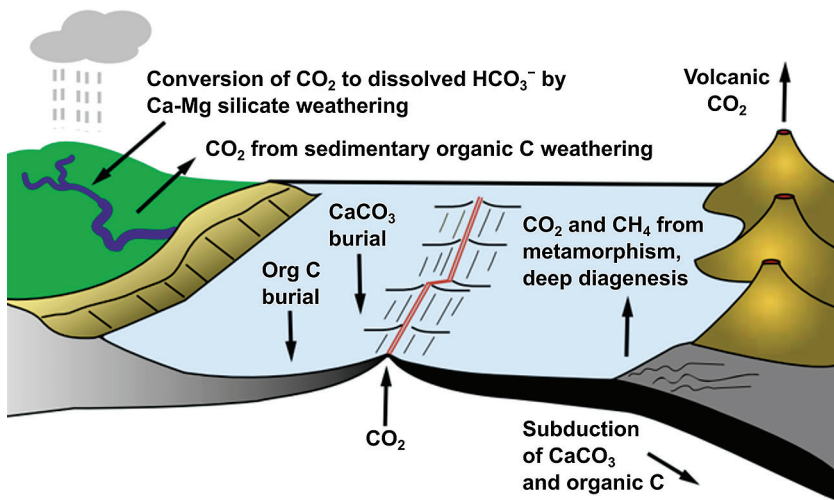


Figure 2.3 Summary of the long term carbon cycle providing the major processes transferring carbon into and out of the Earth's crust. Modified from Berner (2004).

The feedback between global temperature, continental weathering and atmospheric CO_2 is summarised in Figure 2.4. Global warming could be increased due to external forcing such as by increased solar radiation levels or by planetary orbital variations. The resulting warmer temperature then accelerates global silicate weathering rates and the drawdown of CO_2 . In contrast, colder climates slow weathering, permitting buildup of CO_2 and warming (Walker *et al.*, 1981; Berner *et al.*, 1983). This process is thought to be responsible for the continuous habitability of Earth over the past 4 billion years (Kasting, 2019) and for the re-establishment of climate and carbon cycle equilibrium following perturbations (Penman *et al.*, 2020).

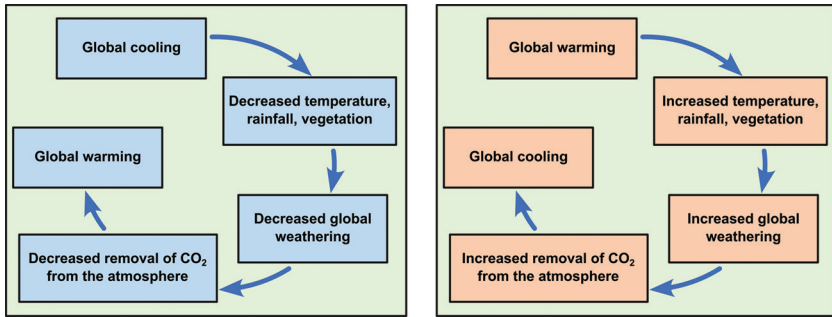


Figure 2.4 Schematic illustration of the feedback between increased global temperature, continental weathering and atmospheric CO₂ content.

A simple set of chemical reactions can summarise this process. The dissolution of CO₂ into rainwater produces carbonic acid:



which can dissociate into bicarbonate and carbonate decreasing the fluid pH and promoting silicate mineral dissolution in accord with:



and



Due to the rapid dissolution of CO₂ and its subsequent dissociation, the current average pH of rainwater is approximately 5.7. The interaction of acidic, CO₂-charged rainwater with silicate rocks consumes the CO₂ through the formation of carbonate minerals *via* a multi-step process. For example, the dissolution of anorthite, the Ca-bearing plagioclase end member dissolving incongruently on the continents, forming the clay mineral kaolinite could occur by:



The dissolved calcium and bicarbonate ions are transported to the sea where they can combine and precipitate as calcite or aragonite:

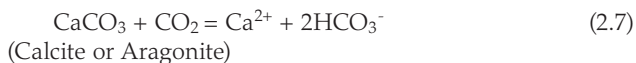


This latter reaction can occur inorganically due to the higher pH of the oceans, though in modern times this is almost completely driven by biotic processes, for example shell growth. Note that although the dissolution of anorthite consumed two CO₂ molecules, these remain in the fluid phase until CaCO₃ precipitated. The precipitation of CaCO₃ returned one of these CO₂ molecules back to the



atmosphere. An example of marine precipitated CaCO_3 is shown in Figure 2.5. The dissolution of silicates on the continent by, for example reaction 2.5 can also be promoted by sulfuric and/or nitric acids (*e.g.*, Galy and France-Lanord, 1999).

Note that the weathering of carbonate minerals on the continental surface can have a short term effect on atmospheric CO_2 content and global temperature. Increased atmospheric CO_2 concentrations can promote the dissolution of calcite on the continents by the reverse of Equation 2.6:



Although the CO_2 consumed by Equation 2.7 is returned to the atmosphere by Equation 2.6 in the oceans, CO_2 is removed from the atmosphere over the short term, for the time from the dissolution of the calcite on the continents until its subsequent precipitation in the oceans. Furthermore, an increase in atmospheric CO_2 will also drive Equation 2.7 to the right in the oceans, dissolving some calcite and potentially increasing dissolved carbon stored in the oceans. Not all carbonate weathering on the continents, however, removes CO_2 from the atmosphere. The oxidation of pyrite coupled to carbonate weathering can act as a source of CO_2 to the atmosphere (Li *et al.*, 2008; Burke *et al.*, 2018).



Figure 2.5 Photograph of Mons Klint, a 6 km long limestone and flint cliff located on the east coast of Mon Island in the Baltic Sea. Limestones such as these contain up to 1.19 tons of CO_2 per m^3 of rock. Photo credit: Joseph Greaves.



2.2 Demonstration of the Feedback between Increasing Global Temperature, Continental Weathering and the Drawdown of CO₂ from the Atmosphere

The feedback between global temperature, atmospheric CO₂ content, and silicate weathering had been extensively verified through theory and modelling, but was not demonstrated in the field before the 1990's. Field verification is extremely challenging because it requires studying pristine regions of the continents over sufficient time frames to determine unambiguous changes in weathering rates and associated CO₂ consumption in response to climate change. In 1998, however, the opportunity to perform such a large scale, long term study came to us through a national effort to exploit the hydropower resources in Northeast Iceland. This opportunity arose due to the OSPAR¹ commission (<https://www.ospar.org/about>) to protect the marine environment of the North East Atlantic, and the Arctic Monitoring and Assessment Programme (<https://www.amap.no/>), which came into effect during 1998. These international agreements required the detailed quantification of the environmental consequences of human activities on the chemical transport by rivers to the oceans and thus required the regular monitoring of the mass transport of elements of rivers located in North-east Iceland destined to be dammed during the early 2000's. Eydis Eiriksdottrir (Fig. 2.6) was hired at University of Iceland to run the project from 1998 to 2013, in collaboration with scientists and engineers at the Hydrological Survey of the National Energy Authority, Iceland, which later became the Hydrological Survey of the Icelandic Meteorological Office.

2.2.1 Quantifying Riverine Chemical Concentrations and Fluxes in 8 NE Iceland Rivers

Our monitoring efforts focused on defining the chemical transport to the oceans due to weathering in eight rivers located in NE Iceland; the location of these rivers and the sampling sites are presented in Figure 2.7. River studies provide average weathering rates of the rocks in the river catchments (Viers *et al.*, 2014). Water discharge and suspended and dissolved element fluxes of the eight basaltic river catchments in NE Iceland were measured directly for five years, from 1998 to 2003, before two of the rivers, the Jökulsá á Dal and Jökulsá í Fljótssdal, were dammed. These rivers are relatively unique in the world in that they drain nearly uninhabited catchments with little to no agriculture, and prior to most of our work were undammed. These conditions provided us the opportunity to quantify river processes in the absence of nearly all anthropogenic influences. Samples were collected 44 times from each sampling site, except from the Fjarðará, which

1. OSPAR refers to the original Oslo and Paris Conventions. OSPAR is the mechanism by which 15 Governments and the EU cooperate to protect the marine environment of the North-East Atlantic.





Figure 2.6 Eydis Salome Eiríksdóttir sampling from the Háslón reservoir north of the Vatnajökull glacier in Iceland during 2010. This reservoir was formed after damming of the Jökulsá á Dal river in 2004. Photo credit: Egill Axelsson.

was sampled 20 times and Jökulsá á Brú, which was sampled 24 times. Five years after the completion of the dams, some of the rivers were sampled again during 2008–2013, to assess the impact of river damming (Eiríksdóttir *et al.*, 2017). Over 30 dissolved element concentrations were measured as were several isotopic pairs. The suspended inorganic matter (SIM) mass concentration, its grain size distribution, its chemical composition, and its BET specific surface area were measured, as well as the suspended particle organic carbon and phosphorus concentrations (POC and POP), and the dissolved organic carbon concentrations (DOC) in the river waters. Throughout this period there was continuous monitoring of river discharge and climate within these catchments. The net and gross primary production of vegetation in the river catchments for the years 2000–2006 were also monitored in collaboration with NASA (Kardjilov, 2008).

The rocks in the studied catchments are predominantly basaltic lavas and hyaloclastite (glassy basalt), with some acidic intrusions associated with extinct central volcanoes (Eiríksdóttir *et al.*, 2008). The ages of these basalts generally increase from east to west, the youngest basalts are found in the Jökulsá á Fjöllum river catchment and are on average 0.3 million years old. The oldest

basalts are found in the Fjarðará river catchment and are on average 11 million years old (Moorbath *et al.*, 1968; Johannesson and Saemundsson, 1998). Five of the eight river catchments are partially glaciated. As the catchment rocks contain nearly identical lithologies, the comparison of the behaviours of these essentially monolithologic catchments provides insight into the role of rock age and the presence of glacial cover on continental weathering rates.

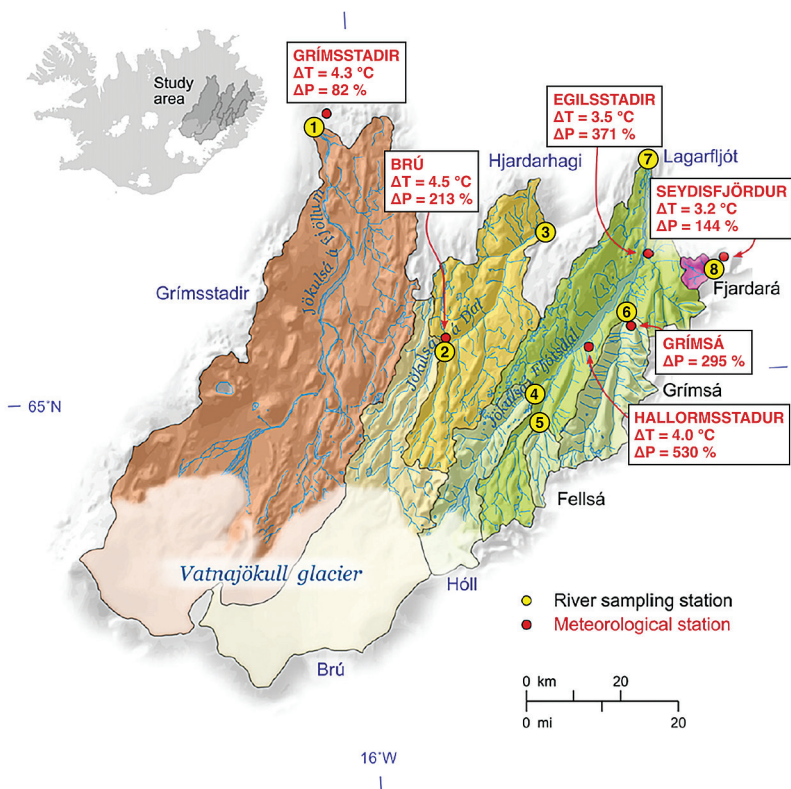


Figure 2.7

Map showing the locations of the catchments investigated in NE Iceland, the sampling stations, the meteorological stations, and the variation in mean annual temperature, ΔT and percent variation in annual rainfall, ΔP from 1961–2005. The studied rivers from west to east are 1) Jökulsá á Fjöllum at Grímsstaðir, 2) Jökulsá á Dal at Brú, 3) Jökulsá á Dal at Hjarðarhagi, 4) Jökulsá í Fljótsdal at Hóll, 5) Fellsá, 6) Grímsá, 7) Lagarfljót and 8) Fjarðará. The word Jökulsá in Icelandic means a glacier-fed river. The names of glacier-fed rivers and catchments are shown in blue letters. The Fellsá, Grímsá, and Fjarðará are direct runoff rivers, the Jökulsá á Dal, Jökulsá í Fljótsdal, and Lagarfljót are a mixture of glacier and direct runoff, and the Jökulsá á Fjöllum is a mixture of spring, glacier and direct runoff waters. Water flow of the Lagarfljót and Grímsá rivers is now influenced by dams. The catchments of these 8 rivers cover a total of 11,350 km². From Gislason *et al.* (2009) with permission from Elsevier.



The suspended material in all of the studied rivers is basaltic; it is composed of 51–53 wt. % SiO₂ and 7–11 wt. % CaO (Gislason *et al.*, 2006). The suspended material in the easternmost and oldest glaciated catchment, that of the Jökulsá í Fljótssdal, has the highest SiO₂ and lowest CaO content. The composition of the suspended material of each catchment is relatively constant; the standard deviation of SiO₂ and CaO concentrations in the suspended material from the glacier-fed river catchments is less than 4 % and 8 % of the absolute concentration, respectively, and there is no compositional correlation with discharge (Gislason *et al.*, 2006).

The Hydrological Service of the National Energy Authority had continuously monitored the discharge of these rivers and the suspended load of the glacial rivers over the three to four decades prior to 1998 (Tomasson, 1990; Pálsson and Vigfusson, 1996; Tomasson *et al.*, 1996; Adalsteinsson, 2000; Gislason *et al.*, 2006, 2009; Johannesson *et al.*, 2007; Eiríksdóttir *et al.*, 2008, 2013, 2015, 2017). These data were used together with those collected in 1998–2002, to build rating curves for the dissolved and suspended chemical fluxes in each river.

Many authors (*e.g.*, Walling and Webb, 1986; Gislason *et al.*, 2006, 2009; Tipper *et al.*, 2006; Calmels *et al.*, 2011; Eiríksdóttir *et al.*, 2013, 2015) showed that the variation of the concentrations of elements in river water with water discharge can be described by the power law:

$$C = aQ^b \quad (2.8)$$

where C represents concentration, a refers to a constant, Q denotes river discharge, and b stands for a constant describing the power dependence of river concentration with discharge. If b is equal to zero, the concentration of the element is independent of discharge. If b is equal to -1 , the river water concentration of the element may be controlled by its dilution by pure water. Previous studies (*e.g.*, Walling and Webb, 1986; Gislason *et al.*, 2006) showed that b is greater than zero for river suspended inorganic matter, meaning its concentration increases with increasing discharge. In contrast, b is between 0 and -1 for soluble dissolved constituents, with the majority of rivers falling in the range of 0 to -0.4 , with an overall mean of -0.17 (Walling and Webb, 1986; Eiríksdóttir *et al.*, 2015). This suggests that dissolved element concentrations decrease with increasing discharge, but less than if they were diluted with pure water.

Representative examples of the application of Equation 2.8 to describe measured element concentrations are shown in Figure 2.8a and b. This figure illustrates the measured suspended and dissolved Ca concentrations as a function of discharge in the river Jökulsá á Dal, at Brú. The power b is equal to 1.16 for the suspended Ca concentration and -0.356 for the dissolved concentration. Concentration of suspended Ca increases with discharge but dissolved Ca decreases with discharge, but less than if it were diluted by pure water. The suspended Ca concentrations were determined by multiplying the suspended inorganic matter (SIM) by the Ca concentration fraction in this suspended material.



The instantaneous flux of dissolved and suspended constituents can be calculated by multiplying the river water concentrations by discharge at the time of sampling (Gislason *et al.*, 2006, 2009; Eiríksdóttir *et al.*, 2015), increasing the power in Equation 2.8 by 1;

$$F = C Q = a Q^{b+1} \quad (2.9)$$

where F designates the river flux. Examples of this are provided in Figure 2.8c and d. These results confirm that with increasing runoff the suspended Ca flux to the oceans is enhanced far faster than the dissolved Ca flux.

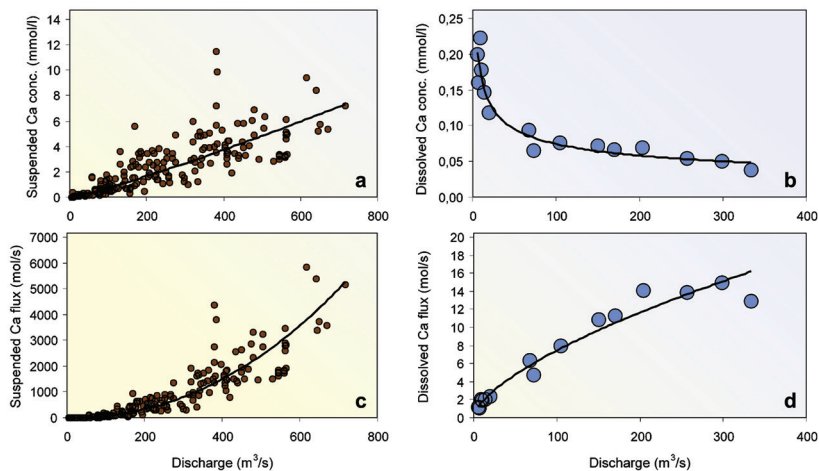


Figure 2.8 Suspended material and dissolved Ca concentrations and fluxes in the Jökulsá á Dal river at Brú. (a) Suspended material Ca concentration vs. discharge. (b) Dissolved Ca concentration vs. discharge. (c) Suspended material Ca flux vs. discharge. (d) Dissolved Ca flux vs. discharge. Note that for this catchment, discharge of 100 m³/s is equivalent to a runoff of 600 mm/yr. Modified from Gislason *et al.* (2006).

We extended the application of Equations 2.8 and 2.9 to quantify the riverine fluxes of numerous elements, suspended inorganic matter, and particle organic carbon (Eiríksdóttir *et al.*, 2015). Some examples of this effort are shown in Figure 2.9 that show the discharge dependence of the concentration of suspended inorganic particulate matter (SIM) and dissolved Na and Fe in the representative glacial Jökulsá á Dal river at Hjarðarhagi (for location see Fig. 2.7). Na and Fe concentrations were chosen for this figure as they are representative of the behaviour of soluble and insoluble major elements in basalt, respectively. The suspended inorganic matter concentration increases in response to increasing discharge, whereas the dissolved concentration of the soluble element Na decreases with increasing discharge, consistent with fluid dilution. A similar



relationship holds for dissolved Ca concentrations for the Jökulsá á Dal at Brú (Fig. 2.8). In contrast, the dissolved concentration of the insoluble Fe is nearly independent of discharge and exhibits significant scatter. The effect of dilution on the concentration of insoluble elements such as Fe is low because its concentration in the river waters is likely controlled by the low solubility of fine grained secondary minerals, such as ferrihydrite (Eiriksdottir *et al.*, 2015).

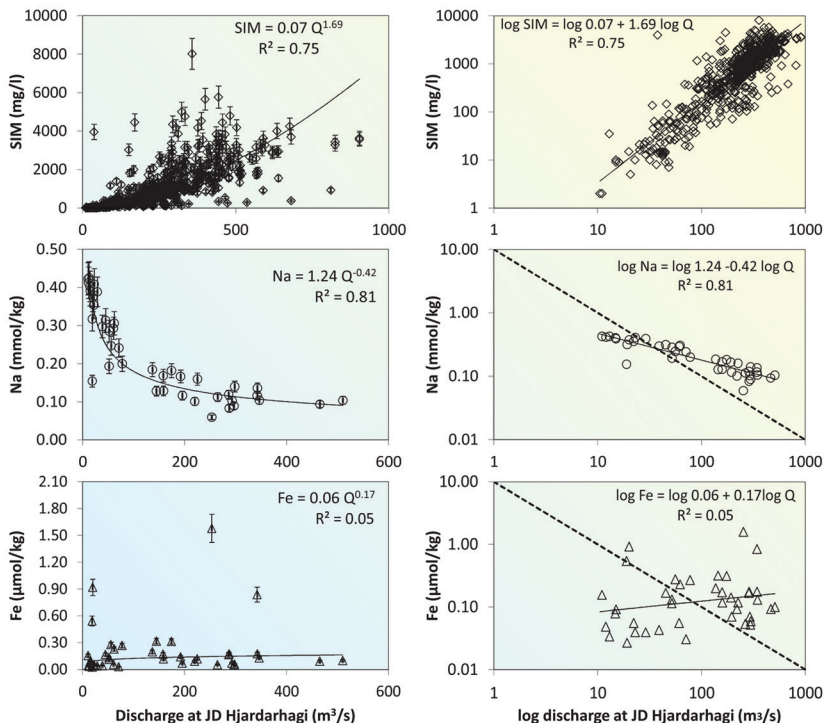


Figure 2.9

The discharge dependence of the concentration of suspended inorganic material (SIM), and concentrations of dissolved Na and Fe on linear-linear and log-log scales in the Jökulsá á Dal at Hjarðarhagi. Note the data for the dissolved samples were collected over the years 1998–2003, whereas data for SIM were collected over the years 1961–2003. The dashed lines are the conservative mixing lines and show how concentrations would evolve if they were controlled solely by the dilution of the catchment waters. The solid lines and curves correspond to least squares fits of the data, consistent with the equations given in each plot, where Q stands for the discharge in m³/s. A 10 % uncertainty is estimated for the measured concentrations. From Eiriksdottir *et al.* (2015) with permission from Elsevier.



Once the concentrations of the elements and particulate material have been defined as a function of river discharge, the instantaneous flux of all dissolved and suspended constituents can be calculated by multiplying the river water concentrations by the river discharge at the time of sampling. To enable this calculation for each day over a 40 year time frame we used correlations for fluid elemental concentrations *versus* discharge, such as shown in Figures 2.8 and 2.9 together with the average daily discharge of each river as reported by the Hydrological Service over the time span of 1962–2003 (Johannesson *et al.*, 2007). The effect of the dam construction on the riverine fluxes, described by Eiriksdottir *et al.* (2017) and discussed in more detail in Section 2.3.2, showed

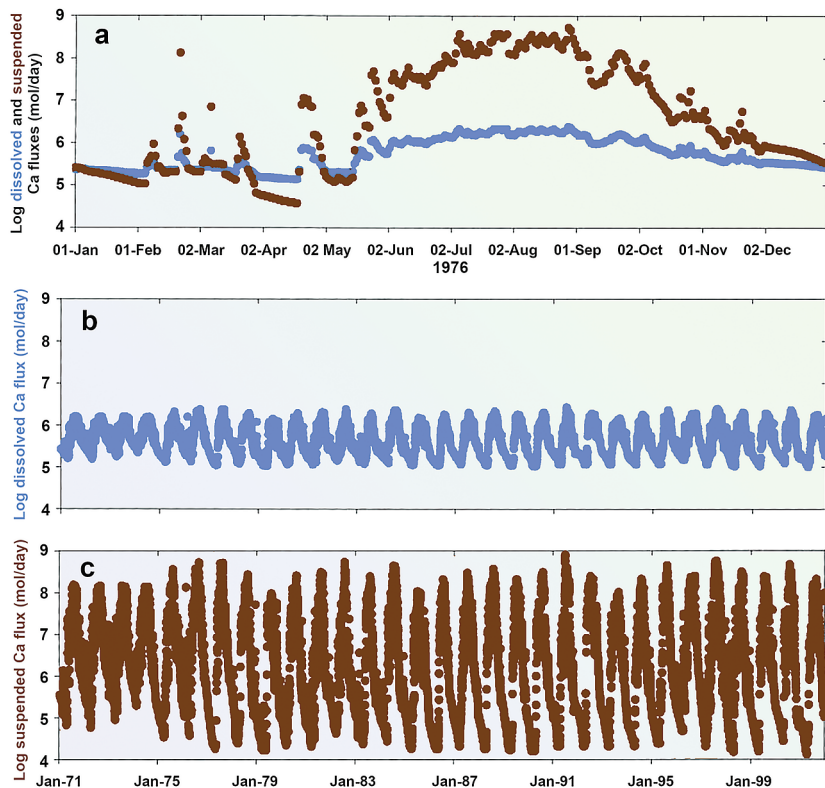


Figure 2.10

Logarithm of daily average suspended and dissolved Ca fluxes of river Jökulsá á Dal at Brú, Northeastern Iceland: (a) for year 1976, (b) dissolved and (c) suspended Ca fluxes from the year 1971 to 2003. Modified from Gíslason *et al.* (2006).



that although the damming of the glacial rivers changed discharge dramatically, the concentration-discharge correlation of dissolved major elements and most trace elements has not changed significantly. This observation provides evidence that the dissolved element concentration-discharge correlations are stable over long time periods and can be used to calculate the dissolved fluxes back in time. An example of the calculated daily average suspended and dissolved Ca fluxes for the river Jökulsá á Dal at Brú is shown in Figure 2.10a, for the year 1976 and in Figures 2.10b and c over the years 1971–2003. The scales of Figures 2.10b and 2.10c are identical, facilitating the comparison of these fluxes.

It is evident in Figure 2.10 that both the suspended and dissolved Ca fluxes exhibit seasonal variations, with a summer maximum and a winter minimum. The suspended material Ca flux, however, depends far more on seasonal variations than dissolved Ca flux. The average difference between the annual maximum and minimum daily suspended Ca flux is four orders of magnitude, whereas this difference for dissolved Ca flux is only approximately one order of magnitude. As a consequence, during the summer, discharge is high and suspended Ca flux is much greater than the dissolved Ca flux. In the winter, discharge is low, and the suspended Ca flux is less than the dissolved flux.

2.2.2 Quantifying the Effect of Increasing Temperature on Weathering Rates

The long term and regular sampling of the rivers enabled us to quantify the weathering processes in the catchments. For example, we observed a strong correlation between alkalinity and dissolved silica concentrations as shown in Figure 2.11. This correlation indicates that the contribution of carbonate mineral dissolution to the dissolved load of these rivers is negligible compared to silicate dissolution and that the river water chemistry reflects the weathering of silicate rather than carbonate rocks. These observations directly contravene the argument of Jacobson *et al.* (2015) who attempted to determine the origin of alkalinity in Icelandic rivers indirectly through the measurement of the Ca isotopic composition of these waters. The observation that silicate weathering dominates the alkalinity generation in these rivers is particularly significant as it means that this alkalinity generated in these catchments leads to long term carbon storage (*e.g.*, from Equations 2.5 and 2.6) rather than a short term drawdown (*e.g.*, from the combination of Equations 2.6 and 2.7). This differs from many catchments, whose chemistry is largely influenced by the dissolution of carbonate minerals, even if the relative proportion of carbonate minerals is small, as carbonate minerals dissolve orders of magnitude faster than silicate minerals (*e.g.*, Blum *et al.*, 1998; Quade *et al.*, 2003).



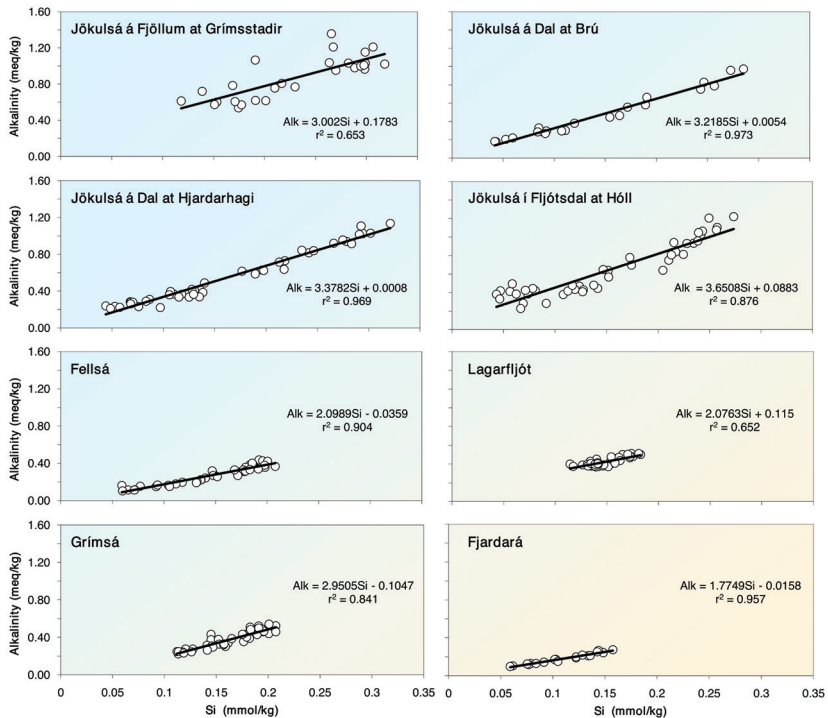


Figure 2.11

Measured alkalinity *versus* dissolved silicon concentration for 8 Icelandic rivers. All plots have the same scale. Data from rivers draining the youngest catchment rocks are on the top and those from rivers draining the oldest rocks are shown near the bottom. All the data were linearly regressed. The equation and coefficient of determination (r^2) of the linear regressions are provided in each plot. From Gislason *et al.* (2009) with permission from Elsevier.

What makes the rivers of the NE Iceland river catchments distinct is that the rocks in these catchments are dominated by relatively young volcanic rocks. Alkalinity is relatively higher in the rivers draining young rocks. The relationship between Si and alkalinity in Jökulsá á Fjöllum at Grímsstaðir is less clear than other young glacial-fed rivers because a considerable fraction of its discharge comes from groundwaters and there is some geothermal component in the river waters (Eiriksdóttir *et al.*, 2008). The range in alkalinity and dissolved silicon concentration is diminished since the damming of the Lagarfljót and Grímsá rivers.



The ability to estimate the dissolved and suspended chemical fluxes of the pristine rivers of Northeast Iceland provided the opportunity to quantify directly the changes in weathering rates due to climate change in each catchment and the consequences of river damming in some of these (Gislason *et al.*, 2006, 2009; Kardjilov, 2008; Eiriksdottir *et al.*, 2013, 2015, 2017). By working on individual catchments, we limited potential ambiguities associated with topographic relief, rock type, vegetation, and glacier cover, which could mask the effects of temperature and precipitation/runoff on weathering (*e.g.*, Edmond *et al.*, 1995) and lead to considerable data scatter (*e.g.*, Li *et al.*, 2016).

As the alkalinity flux of the rivers of Northeast Iceland is dominated by the weathering of silicate minerals, these alkalinity fluxes are directly related to the long term drawdown of CO₂ from the atmosphere. As discussed in Section 2.1, the atmospheric CO₂ content is linked to climate through the greenhouse effect. Increased CO₂ leads to warmer temperatures and an overall increase in runoff, which leads to increased weathering rates and increased CO₂ drawdown from the atmosphere, which cools the climate (Walker *et al.*, 1981). Consequently, the drawdown of CO₂ from the weathering of silicate rocks, as shown for the catchments of Northeast Iceland, is a major process limiting global warming over geologic time scales.

Due to variations in annual temperature in Northeast Iceland and the general global increase in temperatures, our long term studies of the weathering rates of Northeast Iceland allowed us to measure directly the effect of temperature on natural weathering rates. Towards this goal we first calculated the annual fluxes of each dissolved element and of suspended material by summing up the average daily fluxes from each river, for example as shown in Figure 2.10 for each year from 1962 to 2003. The summing of the daily rates over each year was essential to overcome the strong seasonal variation of these fluxes. The resulting annual fluxes are plotted as a function of the average annual temperature for the case of the Jökulsá í Fljótssdal catchment at Holl in Figure 2.12. The slope of the regression lines in Figure 2.12 indicates a 16 % increase in runoff, a 21 % increase in SIM flux, and a 14 % increase in Ca²⁺ and total dissolved inorganic carbon (DIC) chemical weathering fluxes, for each degree increase in annual air temperature. The DIC is shown in this figure as bicarbonate (HCO₃⁻) as it is the dominating carbonate species. Carbonic acid (H₂CO₃) and dissolved CO₂ amounts to less than 10 % of the total.

We were extremely excited by this result. For decades the geochemical community proposed that an increase in air temperature leads to increased CO₂ drawdown due to silicate weathering, providing a feedback mechanism limiting global temperature variations. However, only this 40 year time series on nearly pristine rivers provided direct evidence for this process proposed long ago.



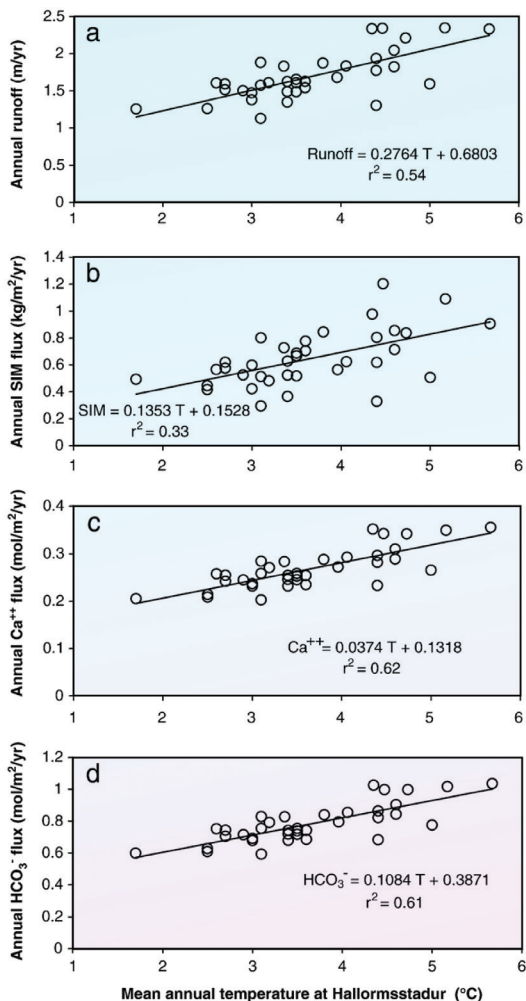


Figure 2.12 Annual river fluxes in the Jökulsá í Fljótssdal river at Hóll as a function of the annual mean air temperature at the Hallormsstadur station (Fig. 2.7). **(a)** Annual runoff, **(b)** annual suspended inorganic material (SIM) flux, **(c)** annual dissolved Ca²⁺ flux, and **(d)** annual total dissolved inorganic carbon (DIC) depicted as bicarbonate (HCO₃⁻), as it is the dominating (>90 %) carbon species flux. The symbols correspond to measured fluxes but the line represents a least squares fit of each data set. The equation and coefficient of determination (r^2) of the fit are provided in each plot. From Gíslason *et al.* (2009) with permission from Elsevier.



2.2.3 The Strength of the Weathering Feedback on Distinct Elements

Calculations such as shown in Figure 2.12 were used to determine the strength of the climate-weathering feedback for individual dissolved elements and suspended particulate material, depicted as a response to one percent rise in river runoff in Figure 2.13, and as a response to one degree °C rise in temperature in Figure 2.14. The weathering rates are found to increase by an average 5 to 15 % percent for each degree of temperature increase for the soluble elements including Ca and Mg. This result has since been validated by comparing the weathering rates of basaltic terrains worldwide by Li *et al.* (2016). It can also be seen that the non-soluble elements are more affected by climate change (*e.g.*, temperature and runoff) than soluble elements. Where this becomes significant is that most limiting nutrients in the ocean, including iron and phosphorus are highly insoluble, suggesting a closer link between climate, silicate weathering and the primary productivity of the oceans.

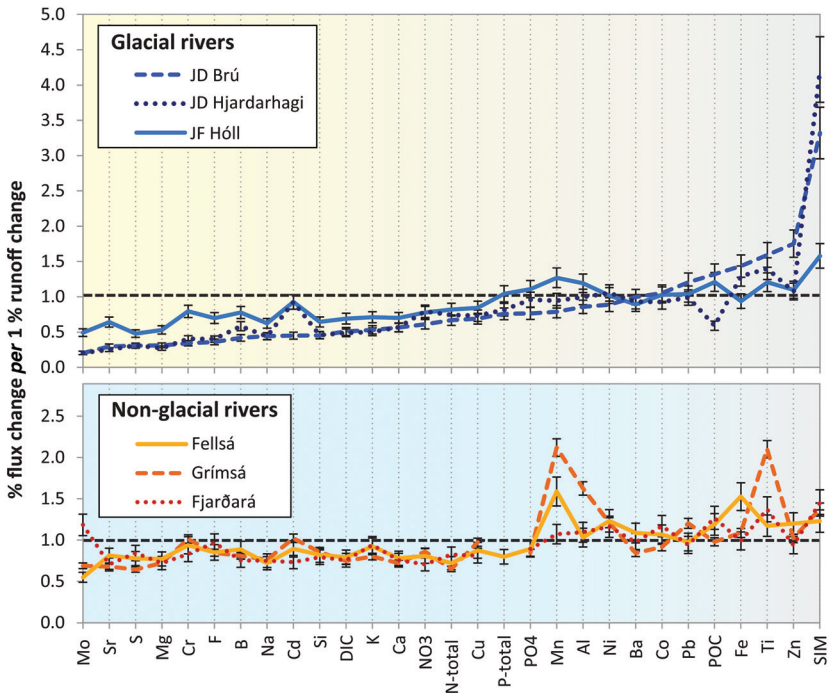


Figure 2.13 Percent change in the annual average flux of the indicated dissolved elements, suspended inorganic material (SIM) and particulate organic carbon (POC), per 1 % increase in river runoff. The error bars show the propagation of variance of the fluxes, which is 11 % . The order of elements in this figure was set by



the increasing values of these fluxes in the Jökulsá á Dal river at Brú, to best show this variation among the elements. The dashed horizontal line corresponds to a 1 % flux increase for a 1 % increase in runoff; a situation when element concentrations are runoff invariant. From Eiriksdottir *et al.* (2015) with permission from Elsevier.

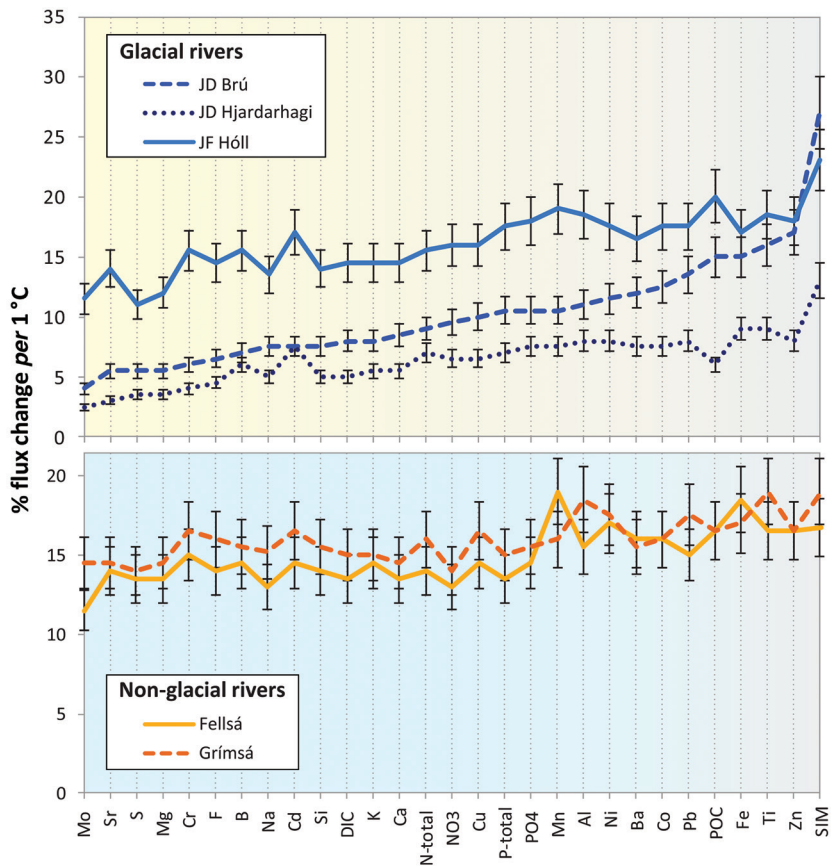


Figure 2.14 Percent change in the annual average flux of the indicated dissolved elements, suspended inorganic material (SIM), and particulate organic material (POC), per 1 °C temperature change. The order of elements is the same as in Figure 2.13, fixed by the increasing values of this flux dependence for the river Jökulsá á Dal river at Brú, to best show this variation among the elements. From Eiriksdottir *et al.* (2015) with permission from Elsevier.



The variation of weathering rates with temperature and runoff among the elements tends to be more pronounced for the glacial compared to the non-glacial rivers. The dilution of the soluble elements by increasing discharge in the glacial rivers is enhanced by a relatively low amount of water-rock interaction; increased runoff due to glacial melting tends to be collected rapidly into river channels, limiting water-rock interaction.

The climate (temperature and runoff) effect on suspended inorganic matter transport (SIM) from the glacial rivers is far higher than for any of the dissolved elemental fluxes. This observation, together with the finding that the flux to the oceans of bio-limiting elements such as P and Fe is dominated by particulates (Fig. 2.23), suggest that particulate transport by melting glaciers has a relatively strong effect on the feedback between continental weathering, atmospheric chemistry, and climate regulation over geologic time.

Text Box 2.1 – Summary: Major Observations on the Weathering-Climate Feedback from Long Term Weathering Studies

The weathering fluxes of the elements controlling the long term inorganic carbon cycle, such as Ca and DIC, increase by 5–15 % per 1 °C increase in average annual air temperature.

The weathering fluxes of the elements controlling the long term organic carbon cycle, including Fe, P, Si, POC, and SIM, increase by 9–19 %, 7–18 %, 5–15 %, 6–20 %, and 13–27 %, respectively, per 1 °C rise in temperature.

Particle transport from the glacial rivers is far higher than all other measured fluxes. This observation, together with the finding that the flux to the oceans of bio-limiting elements such as P and Fe is dominated by particulates, suggest that particulate transport by melting glaciers has a particularly strong effect on the feedback between continental weathering, atmospheric chemistry, and climate regulation over geologic time through the organic carbon cycle.

2.2.4 The Increase in Elemental Weathering Rates from 1960 to 2005

Global warming has led to increased temperatures worldwide. The average annual temperature of the studied Icelandic catchments increased on average from 1.5 to 4 °C from 1960 to 2005; some individual years experienced more dramatic temperature extremes. The average annual temperatures of two of our studied river catchments over this time period are shown in Figure 2.15. The annual average rainfall and glacial melting in the region also increased over time in response to rise in temperature. An increase of rainfall with rise in temperature is observed worldwide (Adler *et al.*, 2008), leading to a corresponding increase in river runoff (Labat *et al.*, 2004). Overall, for the studied NE Iceland rivers, the annual rainfall over our 26–42 year study period increased by 0.2 to 2.0 cm/yr.



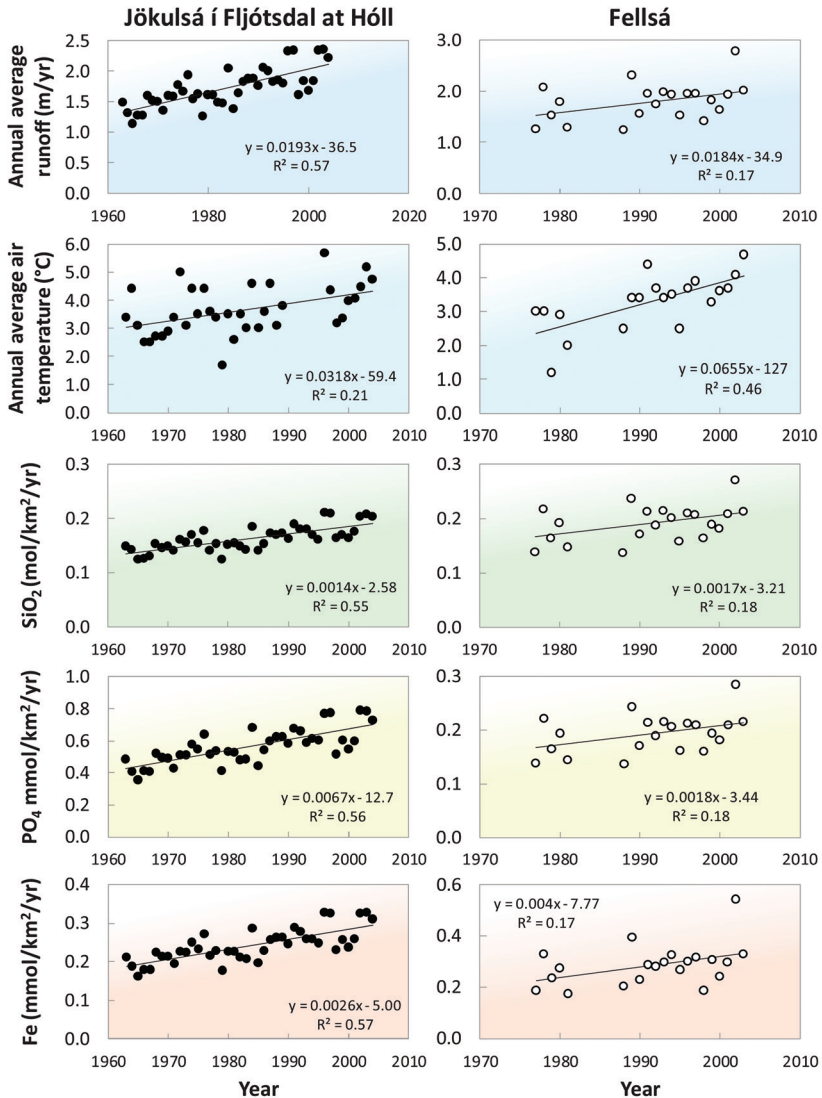


Figure 2.15 Temporal variations in runoff, annual average air temperature, and absolute fluxes of dissolved SiO₂, PO₄ and Fe for the catchments of Fellsá and Jökulsá í Fljótssdal at Hóll, exhibiting the largest temporal flux increases for this period. All the parameters increase demonstrating the link between climate change and elemental fluxes to the oceans. From Eiríksdóttir *et al.* (2015) with permission from Elsevier.



Due to this additional rainfall and the presence of glaciers, the runoff of the rivers in Northeast Iceland increases by 8–17 % for each degree °C increase in local average air temperature (Eiríksdóttir *et al.*, 2013). This increase far exceeds the global average. The combination of increased temperature and increased rainfall over time has led to a substantial increase in weathering rates in Northeast Iceland from 1960 to 2005 (Eiríksdóttir *et al.*, 2013). An example of the largest temporal increases for this period, which were found for the direct river catchment of Fellsá and the glacier-fed river catchment of Jökulsá í Fljótssdal at Hóll, is shown in Figure 2.15. Overall, the studied rivers experienced approximately a 30–75 % rise in annual dissolved Si, PO₄, and Fe bio-limiting fluxes over the 26 to 42 year study period. The rise is larger for Fe and PO₄ than Si, consistent with the stronger climate dependence of these fluxes as shown in Figures 2.13 and 2.14.

2.2.5 The Carbon Drawdown Rates of Icelandic Rivers

Silicate weathering captures CO₂ from the atmosphere, adding it to rivers as dissolved inorganic carbon. This dissolved carbon is mostly in the form of bicarbonate (HCO₃⁻); less than 10 % is undissociated carbonic acid (H₂CO₃) when the pH of the river water is about 7.5, as it is in NE Icelandic rivers. The temporal evolution of the annual area-normalised DIC flux of the glacier-fed Jökulsá í Fljótssdal at Hóll is shown in Figure 2.16a. This river catchment has the largest climate response of the rivers in NE Iceland. For each degree rise in annual temperature the annual fluxes of Ca and DIC towards the oceans increase by about 14 %, and the other two main contributors to alkalinity (bicarbonate) production, Mg and Na increase by 12 and 14 %, respectively (Fig. 2.14). Taking account of the rate of alkalinity production, the calculated total mass flux of CO₂ captured by silicate weathering within the 560 km² Jökulsá í Fljótssdal catchment is shown in Figure 2.16b. During the initial years of our study starting in 1963, the weathering within this catchment captured about 16,000 tons of CO₂ from the atmosphere annually. This amount increased to about 22,000 tons/yr in 2003, translating into 29–39 t CO₂ km⁻² yr⁻¹ or 8–11 g C m⁻² yr⁻¹ when averaged over the whole catchment. The weathering of silicates in all of Iceland that has an area of 103,000 km² was estimated to capture 3.1 Mt CO₂ per year (Gislason, 2008), based on chemical denudation-runoff correlations from 30 river catchments of variable rock age and runoff in different parts of Iceland (Gislason *et al.*, 1996; Louvat *et al.*, 2008) and the total runoff for Iceland as reported by Rist (1956). This translates to an average of 30 t CO₂ km⁻² yr⁻¹ or 8 g C/m²yr. This value can be compared to the average global rate of CO₂ drawdown by silicate weathering on the continents, estimated to be 0.5 Gt CO₂ yr⁻¹ (Gaillardet *et al.*, 1999a; Hartmann *et al.*, 2009), equal to approximately 4 t CO₂ km⁻² yr⁻¹. The land area normalised CO₂ capture rate of Icelandic silicates is thus about 7–8 times greater than that of the global average.



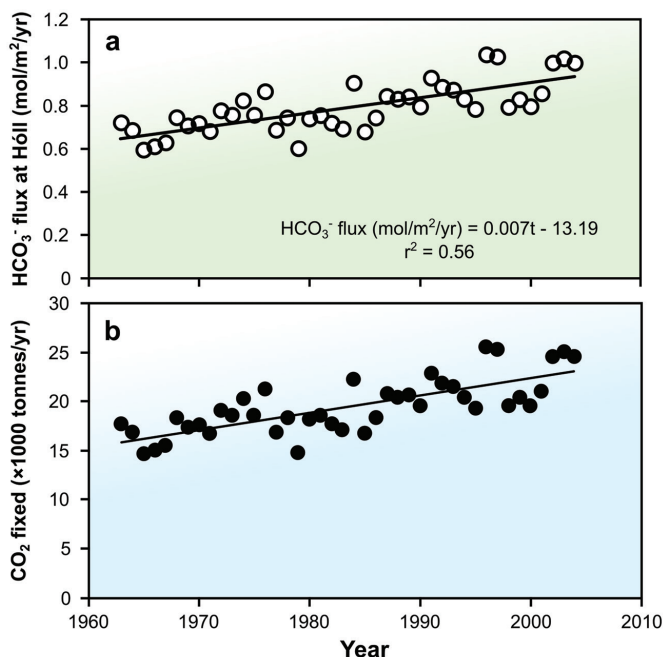


Figure 2.16

Annual CO₂ captured as dissolved inorganic carbon (mostly bicarbonate) provoked by chemical weathering and denudation within the Jökulsá í Fljótsdal river catchment at the Hóll sampling station during 1963–2003. **(a)** Annual average area-normalised DIC flux (mol/m²/yr). **(b)** Total dissolved inorganic carbon captured within the 560 km² catchment annually. Modified from Gislason (2008) and Gislason *et al.* (2009).

2.2.6 Assessing the Potential for Increased Natural Weathering to Address Global Warming

It is enlightening to compare the natural CO₂ drawdown due to weathering to that of engineered Carbon Capture and Storage (CCS) operations. The Carbfix company is currently capturing about 12,000 tons of CO₂ per year from the Hellisheiði geothermal power plant in SW Iceland as described in Section 4.6. Plans call for upscaling this CCS effort by 2025 to capture about 95 % of the CO₂ from the powerplant for a total of about 35,000 tons of CO₂ per year. This future CO₂ mass, to be captured from the Hellisheiði power plant, is comparable to the CO₂ mass that natural silicate weathering captures from the weathering of roughly one thousand square km of Iceland each year, or about 1 % of Iceland. This



comparison illustrates how relatively effective natural weathering processes are in drawing CO₂ out of the atmosphere and the large effort that must be made to engineer substantial carbon removal.

Although the climate-weathering feedback evidenced in the Icelandic catchments demonstrates that there is an increase in carbon drawdown due to increasing terrestrial air temperature, this increase is far too low to effectively address the rate of anthropogenic carbon emissions as temperature warms. The Greenhouse Effect is estimated to result in about 3 degrees rise in global temperature if we double the 280 ppm pre-industrial CO₂ concentration in the atmosphere to 560 ppm (IPCC, 2014). The strength of the weathering climate feedback for the CO₂ drawdown and major cations, Ca²⁺, Mg²⁺ and Na⁺ released during weathering of the basaltic catchments in Northeastern Iceland is only 5–15 % *per* degree °C. The strength of the alkalinity weathering feedback, which is mostly bicarbonate alkalinity (HCO₃⁻), *per* one °C in temperature is also 5–15 %, as this alkalinity is the direct result of the dissolution of the silicates, releasing these cations to water as depicted for Ca²⁺ in Equation 2.5. Silicate weathering alkalinity fluxes from the terrestrial environment of the Earth are estimated to capture 0.5 Gt CO₂ yr⁻¹ (Gaillardet *et al.*, 1999a; Hartmann *et al.*, 2009). An increase in silicate weathering rates due to a 3 °C rise in temperature will result in maximum 45 % (= 3 × 15 %) increase in the silica weathering rate, leading to a global maximum of 0.8 Gt CO₂/yr drawdown from the atmosphere. This rate of carbon drawdown is negligible compared to the current ~40 Gt CO₂/yr anthropogenic CO₂ emissions.

Text Box 2.2 – The Carbon Dioxide Weathering Feedback and the Proof of Divine Intervention

As Eric tells the story, he was surfing the internet in February 2006 – shortly after we published our paper in *Geology* on the role of river suspended material on the global carbon cycle (Gislason *et al.*, 2006) – and he found out that we had just provided new scientific evidence for the existence of God.

This incredible interpretation of our work appeared in the newsletter of *Reasons to Believe*, an organisation that “uses scientific advances to answer questions and identify evidence of God’s existence, his or her character, and the Bible’s reliability”. A direct quote concerning our research in this newsletter states: “Research into material transport *via* rivers provides further evidence that a supernatural designer has fashioned Earth to support life. One reason the planet does not undergo runaway heating is that calcium helps remove carbon dioxide (CO₂) from the atmosphere, thereby reducing the greenhouse effect. A team of European scientists has shown that the amount of suspended calcium is similar to dissolved calcium in rivers as they discharge into the ocean. However, the suspended calcium varies much more widely than dissolved calcium due to annual fluctuations in water levels. This means that there is both a baseline amount of calcium (dissolved) to assist in CO₂ removal and a much more variable amount of calcium (suspended) to provide a stronger negative feedback to stabilise Earth’s temperature against greenhouse heating. Complex controls in the global carbon cycle would be expected in a biblical creation model positing that a supernatural Creator designed this life-support planet” (Ross, 2006).



We found this amusing, so Siggi added the following link to his website with the heading: “You never know where and how your papers are cited”. According to the website of *Reasons to Believe* (<https://reasons.org/explore/publications/articles/more-knobs-to-control-global-environment>) we have “provided powerful new reasons from science to believe in God”.

We got no comments or response to this link until 11 years later. Siggi was going to give a plenary talk on the CarbFix project and its future in October 2017 at the annual meeting of the German Development Bank (KfW) that has over 7,300 employees. Although the bank was just going to cover the cost of Siggi’s transportation to Frankfurt and hotel, still, he had to sign a very formal 3 page contract for his contribution. At the final page of the contract there was a long paragraph on Other Provisions: “The Contractor is aware that KfW rejects the goals of the Scientology sect and its techniques [...] and does not accept the application of these in training. The Contractor provides assurance that he is not a member of the Official Church of Scientology.”

The German Bankers did not get the joke, or perhaps they wanted to be on the safe side. After Siggi’s talk, he removed the *Reasons to Believe* link from his website – to be on the safe side.

2.3 Other Factors Influencing Weathering Rates

2.3.1 Rock Age

The effects of numerous factors on the chemical weathering rate in catchments can be quantified using the Total Chemical Denudation Rate (TCDR). The TCDR is defined as the sum of the major rock derived, river dissolved fluxes, excluding carbon. The TCDR is calculated by summing mass fluxes of the soluble elements Si, Na, Ca, Mg, S and K (e.g., Gislason *et al.*, 1996; Gislason, 2005; Vigier *et al.*, 2006; Louvat *et al.*, 2008). The annual TCDR of 32 Icelandic river catchments are shown as a function of river runoff and of rock age in Figure 2.17. The runoff from these catchments ranges from 914 mm yr⁻¹ to 6,000 mm yr⁻¹, and the catchment rocks are predominantly glassy and crystalline basalts. The average ages of the rocks in these catchments range from 0.2 to 8 Ma. The filled circles represent average annual TCDR rates for each catchment, based on 17–23 monthly samples taken over two years from 1972 to 1974 in south and west Iceland (Gislason *et al.*, 1996). The 15 open circles depict rates based on single grab samples from individual catchments sampled around Iceland, within a week in late May 1996 (Louvat, 1997). There is a strong linear correlation between total chemical denudation rate and runoff as shown in Figure 2.17a. The largest outlier is the Ytri-Rangá catchment in South Iceland. This spring-fed river received magmatic gases from the Hekla volcano at the time of sampling (Flaathen *et al.*, 2009a). The magmatic derived SO₄²⁻ and F⁻ originating from the volcanic gases increase the dissolution rate of glassy rocks and feldspars at the early stage of weathering (Wolff-Boenisch *et al.*, 2004a; Flaathen *et al.*, 2009b).



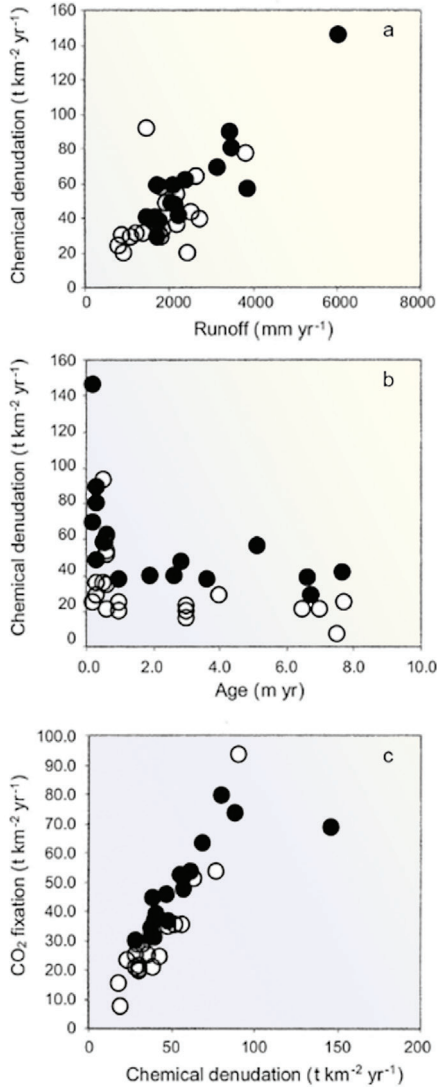


Figure 2.17

(a) The total chemical denudation rate (TCDR) of 32 Icelandic rivers versus runoff. (b) The TCDR versus rock age. (c) Uptake of CO₂ versus TCDR for the Icelandic catchments. The filled circles represent average rates for each catchment, based on 17–23 continuous monthly samples taken from 1972 to 1975 (Gislason *et al.*, 1996). The open circles depict rates based on a single sample from individual catchments (Louvat, 1997).



The total chemical denudation rate decreases with increasing rock age (Fig. 2.17b, Gislason *et al.*, 1996; Louvat *et al.*, 2008; Vigier, 2006). The early sharp decrease in denudation rates with age stems from the presence of glass and olivine in the rocks younger than 3 Ma (Gislason and Eugster, 1987b; Gudbrandsson *et al.*, 2011). These solids rapidly dissolve once the basalt is exposed to weathering. Other factors influencing this trend include the higher permeability of the younger rocks (Sigurdsson and Ingimarsson, 1990), which results in higher reactive surface areas for the water-rock interaction, and that the young rocks receive a larger volcanic dust flux (Arnalds *et al.*, 2014). Younger rocks also tend to have higher runoff as they are commonly present at higher elevations and in catchments of greater relief. Despite the large influence of runoff, Stefansson and Gislason (2001) showed that the total TCDR normalised to runoff increased with the abundance of glassy rocks in the catchment areas. Fresh glass and some highly reactive minerals such as olivine tend to be rapidly dissolved from basalts, leaving behind less reactive minerals over time. This process leads to decreasing chemical weathering rates as rocks age. This observation has been confirmed by the measurements of the rates of altered basalts reported by Delerce *et al.* (2023a,b), as well as by numerous field studies (Bluth and Kump, 1994; Hartmann, 2009; Li *et al.*, 2016).

The relatively rapid chemical weathering rate of fresh rocks leads to a rapid drawdown of CO₂ from the atmosphere following large scale volcanic events, mitigating the effect of volcanic CO₂ emissions to the atmosphere over geologic time scales. Evidence for enhanced chemical weathering following major volcanic events have been reported in a number of past studies (*e.g.*, Pogge von Strandmann *et al.*, 2013; Sun *et al.*, 2018).

2.3.2 River Damming

Water management has altered extensively the world's river systems to meet societies' need for water, energy, and transportation. One of the goals of our river weathering studies was to assess the impact of the installation of the Kárahnjúkar Dam in Eastern Iceland on the transport of riverine dissolved and particulate material to the ocean by the Jökulsá á Dal and the Lagarfljót rivers (Eiríksdóttir *et al.*, 2017). This dam (Fig. 2.18), completed in 2007, collects water into the 2.2 km³ Háslón reservoir and diverts water from the Jökulsá á Dal river into the Lagarfljót lagoon *via* a headrace tunnel. These river catchments are partially glaciated, with glaciers covering 43 % of the Jökulsá á Dal catchment and 6 % of the Lagarfljót catchment. After the Háslón reservoir is filled in late summer each year, it overflows into the Jökulsá á Dal river channel and changes dramatically the river discharge and the concentration of suspended and dissolved material of this river downstream to the Hjarðarhagi monitoring station. The impact of the damming was evaluated by sampling water from both the Jökulsá á Dal and the Lagarfljót rivers, first from 1998–2003 and then from 2008–2013.



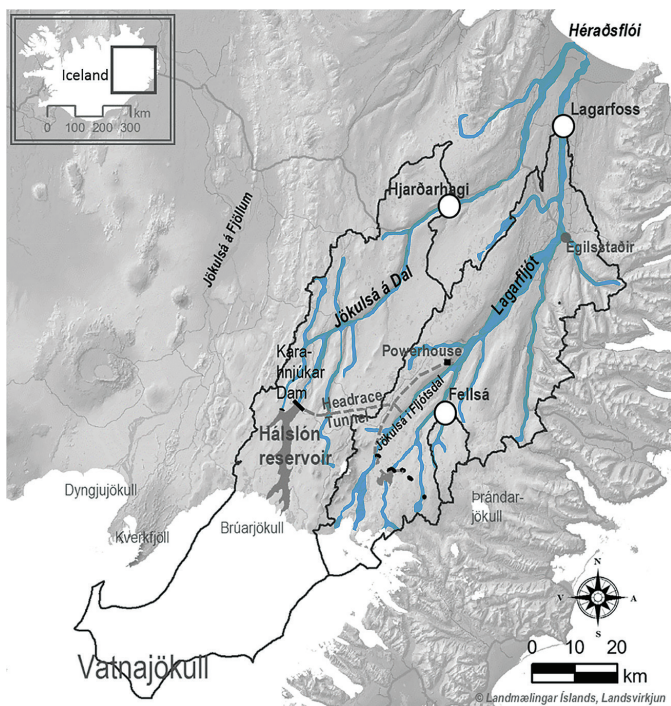


Figure 2.18

Map showing the location of the two river catchments affected by the damming of the Jökulsá á Dal glacial river in Eastern Iceland, the location of the sampling sites (white circles), the Háslón reservoir (dark grey area) created by the dam (black thick line), the headrace tunnels (grey hatched curves) and the power plant (black square). The Vatnajökull glacier is shown in white in the lower left corner. From Eiríksdóttir *et al.* (2017) with permission from Elsevier; map from the National Land Survey of Iceland and Landsvirkjun; National Power Company of Iceland.

The net effect of damming on the combined annual fluxes of dissolved and suspended material of the Jökulsá á Dal and the Lagarfljót rivers is shown in Figure 2.19. The combined runoff of the rivers increased by 11 % from 1998–2003 to 2008–2013 due to increased glacial melting and rainfall in the catchments. This is indicated by the broken line in Figure 2.19. The combined suspended inorganic matter (SIM) flux in these rivers to the oceans decreased by approximately 85 %, as most of the original riverine transported mass of particulate material was trapped by the dam. The SIM flux, however, of the Lagarfljót river itself increased as the diverted water from the dammed glacial Jökulsá á Dal river had much higher SIM load, even though most of the larger grained SIM was retained by the dam. The particulate material that exits the reservoir tends to be

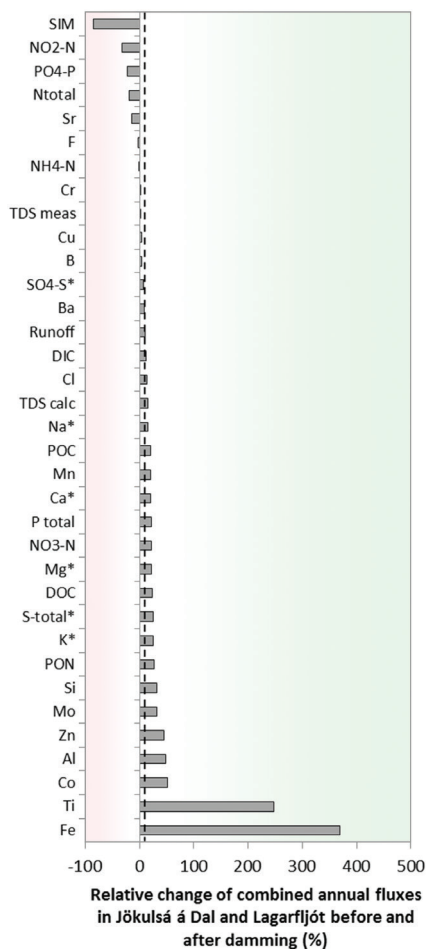


Figure 2.19 Relative changes in the combined elemental fluxes of the Jökulsá á Dal river at Hjarðarhagi and the Lagarfljót river at Lagarfoss. Negative numbers refer to decreased fluxes and positive numbers refer to increased fluxes due to the damming. Runoff in these combined rivers increased by 11 % from 1998–2003 to 2008–2013, as indicated by the broken line. Elements labelled with * have been corrected for atmospheric input. From Eiriksdóttir *et al.* (2017) with permission from Elsevier.

relatively fine grained, increasing the average specific surface area of the particulate matter that continues to flow towards the ocean.

In contrast, the combined annual flux of most dissolved elements running through the Hjarðarhagi and Lagarfoss monitoring stations increased due to the damming, although much of this increase is similar to the increase in combined runoff in these rivers. For example, the DIC flux grew by 13 %. This is similar to the combined increase in the runoff of the combined rivers over this period. The fluxes of dissolved Zn, Al, Co, Ti and Fe, however, increased most by damming. The distinct effect of damming on these element fluxes can be attributed to changed saturation states of common secondary minerals in the Jökulsá á Dal due to reduced discharge, increased residence time, and dissolution of suspended material, and, to a lesser degree, reduced photosynthesis due to less transparency in the Lagarfljót lagoon.

2.3.3 Glacial Cover

The major effect of glacial cover on weathering rates stems from the grinding of rocks at the base of the glaciers. This leads to a huge increase in rates, as can be seen in Figure 2.20. The mechanical denudation rates of much of non-glaciated Iceland is less than 50 ton km⁻¹ yr⁻¹. In contrast, the same rates of the glaciated parts of Iceland tend to exceed 3,000 ton



$\text{km}^{-1} \text{yr}^{-1}$, leading to a large increase in SIM fluxes observed in the rivers draining glaciated catchments compared to non-glaciated river catchments (Eiriksdottir *et al.*, 2015) (Fig. 2.21). Whereas the catchment area-normalised dissolved Si flux to the oceans in the glacial Jökulsá í Fljótssdal is similar to that of the non-glacial Fellsá river, the corresponding suspended Si flux is approximately 2 orders of magnitude greater in the glacial river. This difference has major consequences for the effect of melting glaciers on trace elements and limiting nutrient delivery to the oceans, as the arrival of these elements to the oceans is dominated by particulate transport (see Section 2.4). In contrast to the large effect of glacial cover on mechanical denudation, there is no general relationship between the total chemical denudation rate (*e.g.* transport of dissolved material to the oceans) and glacial cover in Iceland (Gislason *et al.*, 1996; Louvat, 1997).

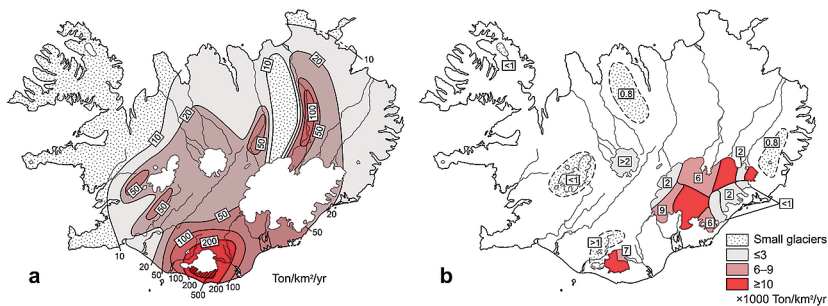


Figure 2.20 The spatial variation of the mechanical denudation rates for Iceland in (a) glacier-free areas, (b) glaciated regions. Note the scale in (b) is 1,000 times greater than that of map (a). After Tomasson (1990).

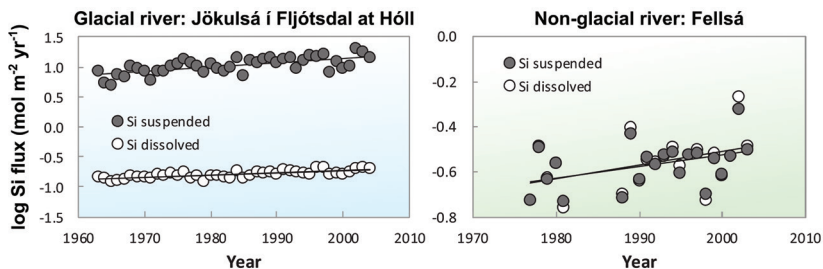


Figure 2.21 The logarithm of annual total Si transported towards the oceans as suspended particles and in dissolved form in the glacial Jökulsá í Fljótssdal river at Hóll and the non-glacial Fellsá river. The Jökulsá í Fljótssdal river catchment is 27 percent covered by the Vatnajökull glacier, whereas there is no glacial cover in the Fellsá catchments. After Eiriksdottir *et al.* (2015).



Text Box 2.3 – Summary: Factors Affecting Weathering Rates

Rock age: Fresher rocks have faster chemical weathering rates largely due to the presence of rapidly dissolving minerals that are replaced over time by more stable, less reactive minerals.

Damming: Dams tend to trap larger particulate material, lowering SIM transport to the oceans but have only a minor effect on most major dissolved element fluxes.

Glaciers: The presence of glaciers increases greatly particulate fluxes towards the oceans, whereas they have little effect on dissolved element fluxes.

2.4 The Significance of Suspended Material Transport to the Oceans on the Global Cycles of the Elements

A major observation of our river studies is the that flux of suspended material to the oceans is more dependent on temperature and rainfall changes than the corresponding dissolved fluxes. This observation led us to propose that the suspended material flux to the oceans dominates the feedback between temperature and weathering (Gislason *et al.*, 2006).

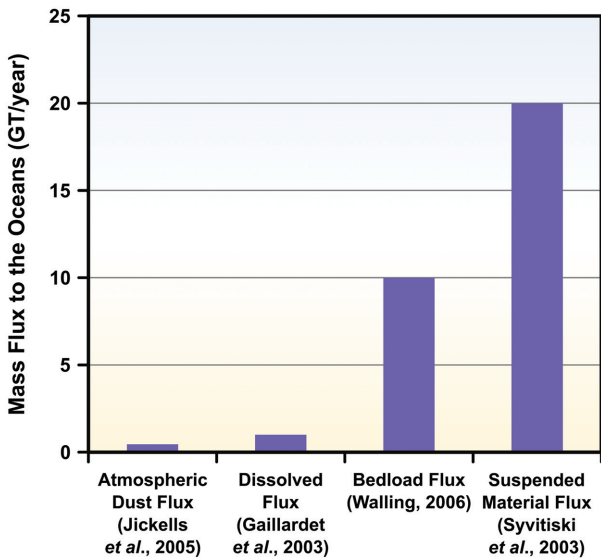


Figure 2.22 Estimated total mass of material transported from the continents to the oceans by selected processes. After Oelkers *et al.* (2012).



The potential influence of suspended material flux on the global cycles of the elements and ocean chemistry is evidenced by the total mass of suspended material arriving to the oceans, as illustrated in Figure 2.22. Riverine transported suspended material is the largest source of continental material to the oceans. Its annual flux is estimated to be $\sim 20 \text{ Gt yr}^{-1}$. This amount compares to only 10 Gt yr^{-1} of bedload mass, 1 Gt yr^{-1} of dissolved riverine transported mass, and 0.45 Gt yr^{-1} of windblown dust (see Fig. 2.22). The relative importance of suspended particulate material depends greatly on the identity of the element. The relative flux of each element transported to the oceans by suspended particulate transport in global rivers is compared to the corresponding dissolved flux, such as shown in Figure 2.23. The riverine fluxes of all elements other than Na

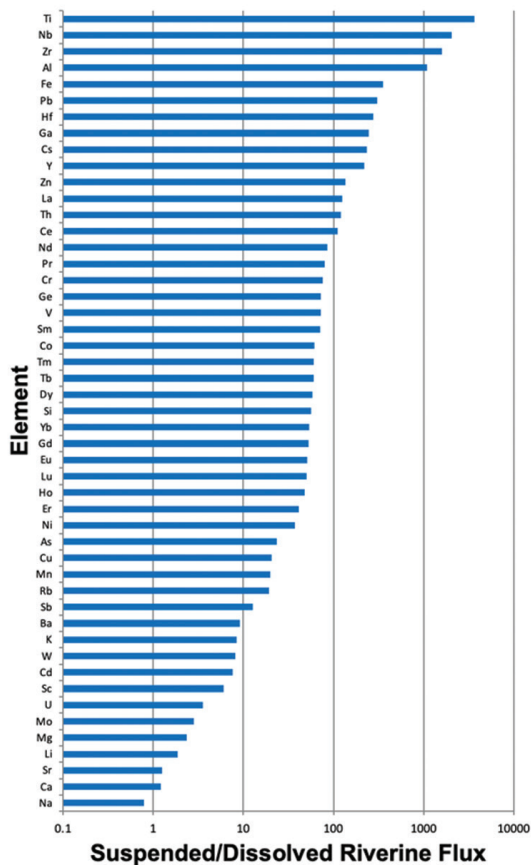


Figure 2.23

The ratio of riverine suspended particulate fluxes of the elements to the corresponding dissolved fluxes. Data from Viers *et al.* (2009) and Gaillardet *et al.* (1999b, 2003). After Oelkers *et al.* (2011).



are dominated by suspended particulate transport to the oceans. Suspended particulate material transport is most important for the least soluble elements, including Fe, which is a common limiting element for primary productivity. Of the least soluble elements, more than 100 times the amount arrives to the oceans within suspended particles than in dissolved form. It should be noted that the comparison of fluxes shown in Figure 2.24 does not include the transport of riverine bedload material, which is estimated to contain about 50 % as much mass as the suspended particles, see Figure 2.22.

Riverine transported particulates can influence seawater chemistry if they dissolve once they arrive to the ocean. We tested this potential by running laboratory batch experiments (Jones *et al.*, 2012a); some representative results are shown in Figure 2.24. Several observations are apparent. Nearly all elements were rapidly added to seawater. The rates that elements are released to seawater increases measurably with increasing temperature. Apparently, with time the concentrations of many elements added to seawater maximise, then decrease. This behaviour is likely due to the precipitation of secondary minerals; many minerals that are saturated or supersaturated in seawater and will begin to precipitate as fluid concentrations increase. This is part of the early diagenesis process, where less stable minerals are replaced by more stable minerals through seawater-particulate interaction. This process makes it challenging to define the total amount of elements released from the particulate material during its interaction with seawater, and therefore may be available to marine biota.

The compositional variation of the seawater during its interaction with natural particulate material suggests that the precipitation of secondary phases masks the overall extent of particulate dissolution. To overcome this challenge we used stable isotope techniques to distinguish the dissolution of the particulates from the precipitation of secondary minerals. This was done by assuming the conservative release of, for example Sr isotopes, from the particles during dissolution and the conservative uptake of Sr isotopes by secondary phases. Mass balance calculations were then used to estimate the mass of Sr originally released from the particulates (Jones *et al.*, 2012b). An example of the results of this approach is shown in Figure 2.25. Such results confirmed the combined dissolution-reprecipitation process, and that the addition of elements to the oceans from dissolving particulate material is far greater than what might be deduced from the concentrations of elements in seawater. The rapid dissolution of particulates in the oceans are promoted by the high surface areas of the particulate material that is commonly in excess of $10 \text{ m}^2/\text{g}$ (Jones *et al.*, 2012a,b; Eiriksdottir *et al.*, 2017).



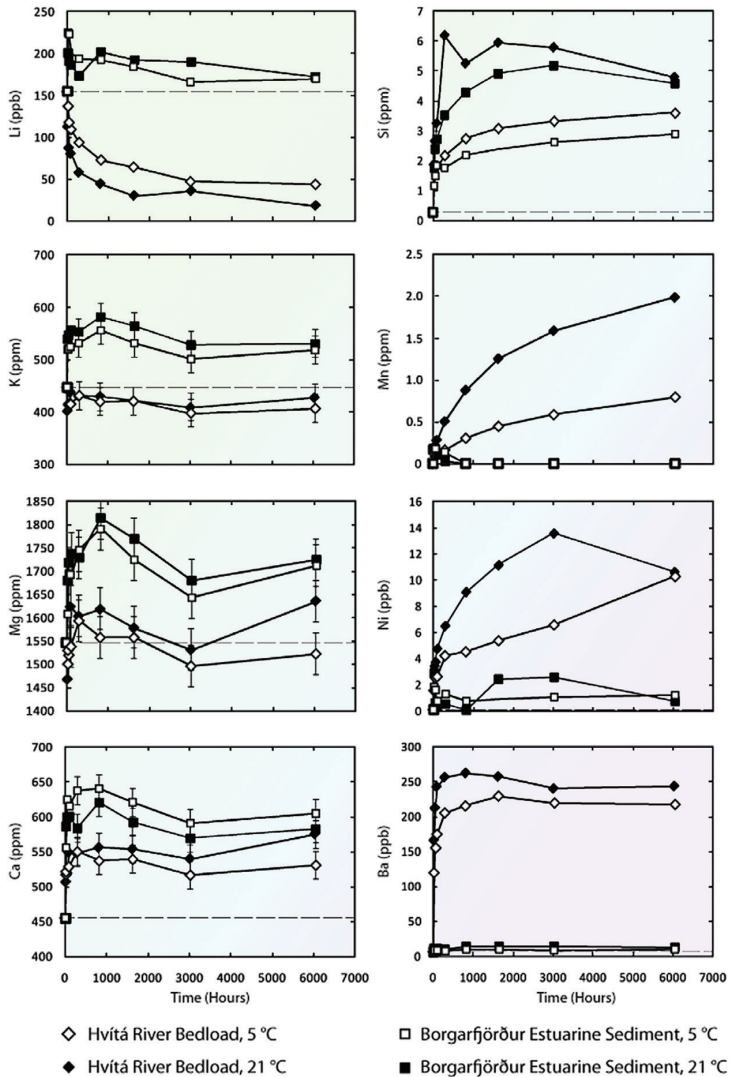


Figure 2.24 The concentrations of selected elements in seawater when reacted in batch reactors with Hvitá river bedload material and Borgarfjörður estuarine sediment at 5 °C and 21 °C. After Jones *et al.* (2012a).



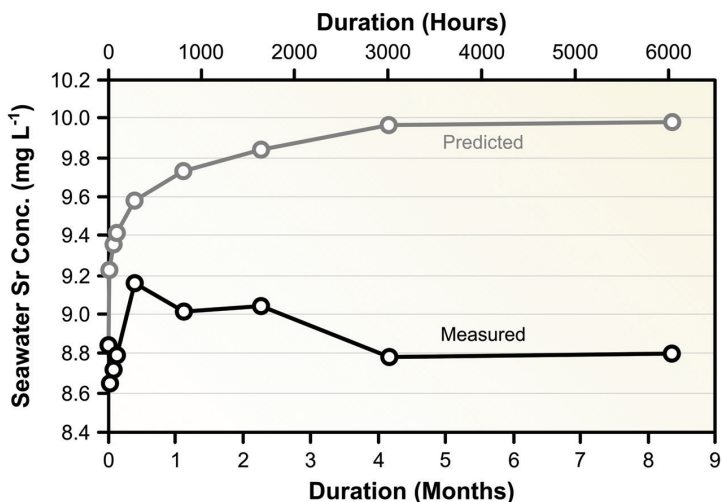


Figure 2.25

Comparison of the measured Sr concentrations in seawater during interaction of seawater with Hvítá bedload material in a batch reactor at 5 °C, with the corresponding calculated Sr concentrations determined from the measured change of the $^{87}\text{Sr}/^{86}\text{Sr}$ ratio of the fluid phase. The predicted curve was calculated assuming that no Sr was incorporated into secondary phases during the experiment. The difference in the curves can be attributed to the uptake of Sr by secondary phases. After Jones *et al.* (2012b).

To assess if this same process occurs in natural systems, and to demonstrate the reactivity of particulate material as it arrives in the oceans, we performed a number of studies in the Borgarfjörður Estuary (Pearce *et al.*, 2013; Jones *et al.*, 2014). This estuary is located ~100 km north of Reykjavík (see Fig. 2.26). We sampled the water and coexisting suspended particulate material and bedload. The measured Sr isotopic ratios of these samples are plotted as a function of the chlorine content of the estuary water samples in Figure 2.27. Both the suspended particulate and the bedload Sr isotope compositions approach that of seawater as they move through the estuary towards the ocean. The Sr isotope composition of the suspended particulates, however, plots well above the pure mechanical mixing curve. Similarly, the Sr isotope composition of the water samples plots below the corresponding pure mechanical mixing curve. These observations indicate the dissolution of the particulate material and bedload into the aqueous phase in the estuaries as they move towards the ocean. Mass balance calculations reported by Jones *et al.* (2014) indicate that greater than 90 % of the dissolved Sr in the estuary waters in the middle of the mixing zone originated from the particulate material.



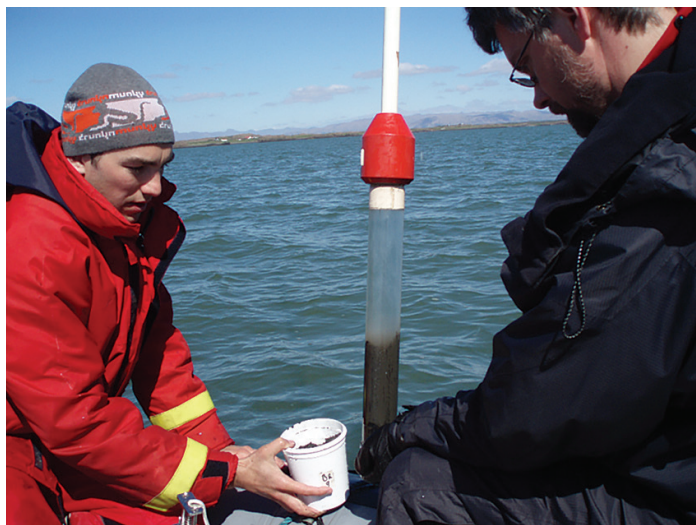


Figure 2.26 Chris Pearce sampling particulate and bedload material from the Borgarfjörður estuary together with Haraldur R. Ingvason from Natural History Museum of Kópavogur Iceland, in 2009.

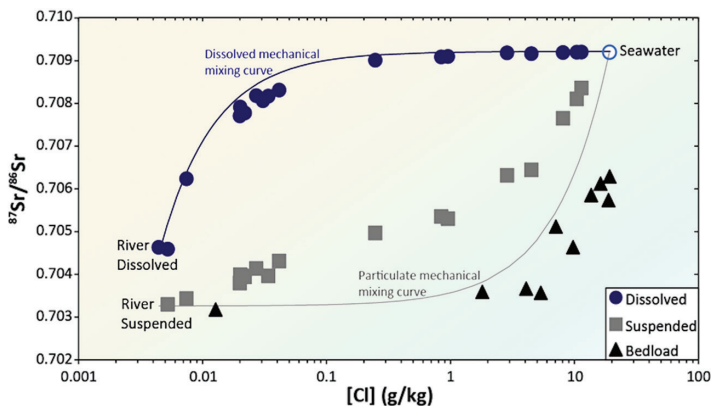


Figure 2.27 The measured $^{87}\text{Sr}/^{86}\text{Sr}$ ratios from dissolved (dark blue circles), suspended (grey squares), and bedload (black triangles) Borgarfjörður Estuary samples as a function of the corresponding dissolved chloride concentrations in estuarine water. The Cl concentration increases as the water enters the ocean. The solid curves represent the predicted $^{87}\text{Sr}/^{86}\text{Sr}$ ratios from a mechanical, non-reactive two component mixing model of the riverine and seawater end members. Errors for individual points are within the size of the symbols. After Jones *et al.* (2014).

The arrival of particulate material to the oceans lead to the release of elements to seawater, coupled to the consumption of much of these released elements by secondary phase precipitation. The major consequences of a coupled process in the oceans include:

- 1) The isotopic compositions of elements dissolved in seawater are significantly affected by particulate-seawater interaction. This effect stems from the difference in isotopic compositions of elements in the dissolving particulate material and in the precipitating secondary phases. Such effects have been widely observed in natural systems. Notably, Jeandel and co-workers reported that particulate-seawater interaction influences greatly the Nd isotopic composition of the oceans, a process they call boundary exchange (Arsouze *et al.*, 2007; Jeandel and Oelkers, 2015; Ayache *et al.*, 2016; Jeandel, 2016). Little *et al.* (2016, 2018) reported that particulate-seawater interactions affect significantly the availability and isotopic compositions of Cu and Zn. Jones *et al.* (2014) noted that particulate-seawater interactions greatly affect the marine compositions of Sr. This process is also likely to affect the availability and isotopic compositions of numerous other elements in the ocean (Jeandel, 2016).
- 2) Particulate material can provide the nutrients for primary productivity, notably by acting as a slowly dissolving source for limiting nutrients. This process is particularly significant as limiting nutrients are primarily transported to the oceans by riverine particulates. The close link between particulate material mass and primary productivity has been evidenced by experimental results reported by Grimm *et al.* (2019).

The degree to which particulates influence marine processes will depend greatly on the element and the identity of the particulate material (*e.g.*, Jones *et al.*, 2012b, 2014). To date the global significance for each element has yet to be quantified, *yet all* evidence suggests this influence will be large on a global scale and helps to balance the global elemental cycles of many elements.

2.5 Deglaciations, Particulate Material, and the Oxygenation of the Earth's Atmosphere

One of the most debated topics in the Earth Sciences is what caused the oxidation of Earth's atmosphere. There was negligible oxygen in the atmosphere for the first 2 billion years of Earth history (Holland, 1962; Canfield, 2005). The oxygenation of our atmosphere was dominated by two subsequent events, the Great Oxygenation Event (GOE) and the Neoproterozoic Oxygenation Event (NOE). Each of these events is temporally linked to the end of snowball Earth events (Luo *et al.*, 2016; Gumsley *et al.*, 2017).



Numerous processes have been proposed to explain these oxygenation events. Some have advocated that the oxygenation of our planet's atmosphere is due to changes in the mass and/or composition of volcanic gases emitted to the atmosphere (Holland, 2009; Gaillard *et al.*, 2011). A decrease in the serpentinisation rates of ultramafic rocks over time has been proposed as a contributing factor (Leong *et al.*, 2021). Others have proposed that the oxygenation of the atmosphere was provoked by the formation of supercontinents leading to extensive mountain building, increased weathering, increased nutrient transport to the oceans, and an explosion of algal and bacterial growth (Campbell and Allen, 2008). Indeed, the first of the global oxygenation events, the GOE, occurred ~2.45 billion years ago and coincided with the establishment of large, thick continental land masses, with relatively high mafic composition compared to the present (Kump, 2008; Smit and Mezger, 2017). Increased weathering of the continents as a process to increase the atmospheric oxygen content during the Proterozoic has also been advocated (Mills *et al.*, 2014). Few of these suggested processes, however, link directly the oxygenation of the planet to the global glacial events that preceded the major atmospheric oxygenation events.

The oxygenation of Earth's atmosphere could have been provoked by the organic carbon cycle, through the combination of photosynthesis and the burial of produced organic material. Photosynthesis creates oxygen *via*



where the product CH_2O signifies the produced organic carbon. Organic decay will reverse this reaction, so the net addition of oxygen to the Earth's surface requires organic carbon burial as well as photosynthesis. Although it might be attractive to attribute the oxidation of our atmosphere to the rise of photosynthesis itself, significant evidence indicates that photosynthesising microorganisms were active on the Earth's surface a half billion years before the GOE (Buick, 2008; Lyons *et al.*, 2014; Planavsky *et al.*, 2014). The long delay between the appearance of oxygenic photosynthesis and the GOE, however, suggests that although biotic productivity and organic carbon burial could lead to the oxygenation of the planet, a process other than the appearance of photosynthesis likely triggered this event (*e.g.*, Catling and Claire, 2005).

The observations reviewed in Sections 2.2 to 2.4 suggest a different possible process, linking the snowball Earth and the oxygenation of our planet's atmosphere, notably, enhanced organic productivity and burial triggered by glacial melting. The melting of glaciers greatly increases the transport of particulate material to the oceans. This particulate material (1) dominates the transport of limiting elements to the oceans (Oelkers *et al.*, 2011, 2012), and (2) releases a substantial percentage of their elements upon their arrival to the oceans (Jones *et al.*, 2011, 2014; Pearce *et al.*, 2013). Although global glaciation would have dramatically slowed biotic primary production, the large addition of limiting nutrients to the oceans at the end of large scale glacial events would



have induced cyanobacterial blooms (Kirschvink *et al.*, 2000). The large addition of particulate material will enhance the burial of the organic carbon formed by these bacterial blooms (Müller and Suess, 1979; Henrichs and Reeburgh, 1987; Ingall and Van Capellen, 1990). There are numerous observations suggesting organic material burial was significantly increased at the end of snowball Earth events. Notably, although carbon isotope values of carbonate minerals suggest that the organic fraction of the overall global carbon burial is close to constant at between 10 to 20 % over most of geologic time, there were several dramatic transient increases in this organic burial fraction: notably during the Lomagundi-Jatuli event, close to the time of the initial GOE, and again near the end of the Neoproterozoic snowball Earth, concurrent with the NOE (Kasting, 2013). Other studies have suggested that the oxygenation of our planet's atmosphere has been influenced strongly by changes in the burial rate of organic carbon in sedimentary rocks (Kipp *et al.*, 2021; Krissansen-Totton *et al.*, 2021) or in subduction zones (Duncan and Dasgupta, 2017). The overall modelling of the role of enhanced organic burial on Earth's atmospheric composition is, however, complicated by the burial of other redox sensitive elements, notably iron and sulfur. The burial of these elements can also contribute to the global oxygen cycle (Catling and Claire, 2005).

Direct evidence linking increasing particulate material concentrations to increasing biotic productivity was presented by Grimm *et al.* (2019) who grew *Synechococcus sp.*, a common photosynthesising bacterium, in the absence and presence of both basaltic Icelandic suspended riverine particles and continental Mississippi river bedload material. After an initial exponent growth stage, due the consumption of initially available aqueous nutrients, bacterial growth continued in the presence of particulate material but net bacterial death was observed in the absence of particulate material (Fig. 2.28). Grimm *et al.* (2019, 2023) also reported a direct correlation between the mass of particulate material and the post-exponential stage growth rate of these bacteria. Such results confirm the aforementioned field and experimental observations, suggesting a major role of the arrival of riverine particulate material in providing nutrients and promoting bacterial growth. The acquisition of these nutrients by the biota may be indirect due to the dissolution of the particulate material followed by the acquisition of the nutrients from the aqueous solution or from the direct contact of the bacteria to the particulates. The direct colonisation of nutrient-bearing particulates has been observed both in laboratory experiments and in the field (see Fig. 2.29). For example, the ability of microbes to acquire limiting nutrients directly from the mineral phase has been shown by numerous studies, including those by Bailey *et al.* (2009), Rogers and Bennett (2004), Bonneville *et al.* (2011), Smits *et al.* (2012) and Sudek *et al.* (2017).

It is possible there will never be a consensus in our community on the exact process that led to the Great Oxygenation Event and the Neoproterozoic Oxygenation Event. Direct evidence of the trigger for such processes may be



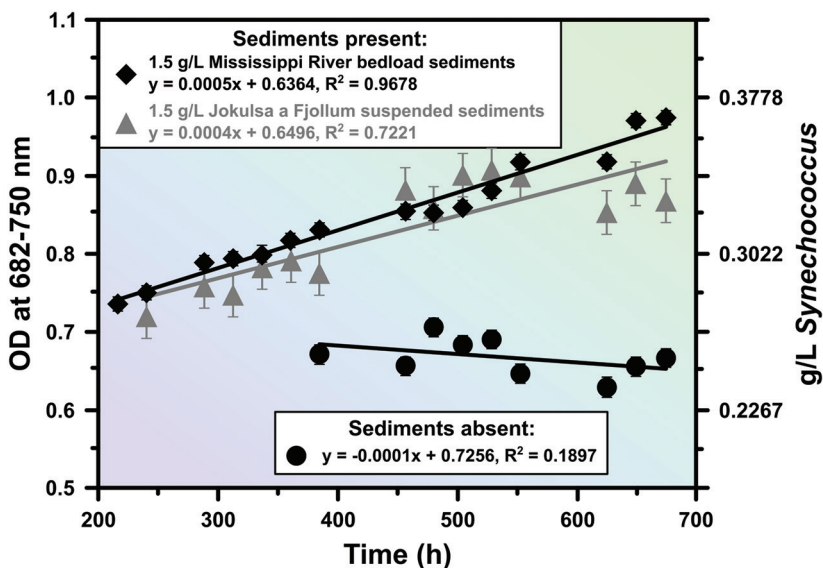


Figure 2.28 Temporal evolution of optical density (OD) and corresponding concentration of *Synechococcus* in g/l, dry weight during cyanobacterial growth experiments in the presence and absence of riverine particulate material. The filled diamonds, triangles and circles correspond to measured bacterial concentrations in the presence of 1.5 g/l of Mississippi River bedload sediments, 1.5 g/l of Jökulsá á Fjöllum suspended sediments, and in the absence of sediments, in the reactor. Results shown were obtained after the completion of the exponential growth phase of the experiments (see Grimm *et al.*, 2019).

difficult to ever identify unambiguously as these events occurred hundreds of millions and billions of years ago. Nevertheless, the observations reviewed above suggest that the enhanced delivery of particulate material due to melting glaciers provides a possible trigger for the oxygenation of our planet as it simultaneously would enhance primary productivity and organic carbon burial. This mechanism provides a close link between the GOE and NOE with the end of snowball Earth epochs. It is also certainly possible, however, that other proposed factors also play a role. Active mountain building, potentially related to volcanic activity, would lead to increased particulate transport to the oceans when coupled to glacial melting. Mountain building and the melting glaciers would have delivered huge quantities of particulate material to the global oceans. The combined ability of these particulates to provide the nutrients for biotic growth, and the ability of these particulates to promote enhanced organic burial supports greatly the possibility that this process was the trigger for the GOE and NOE.

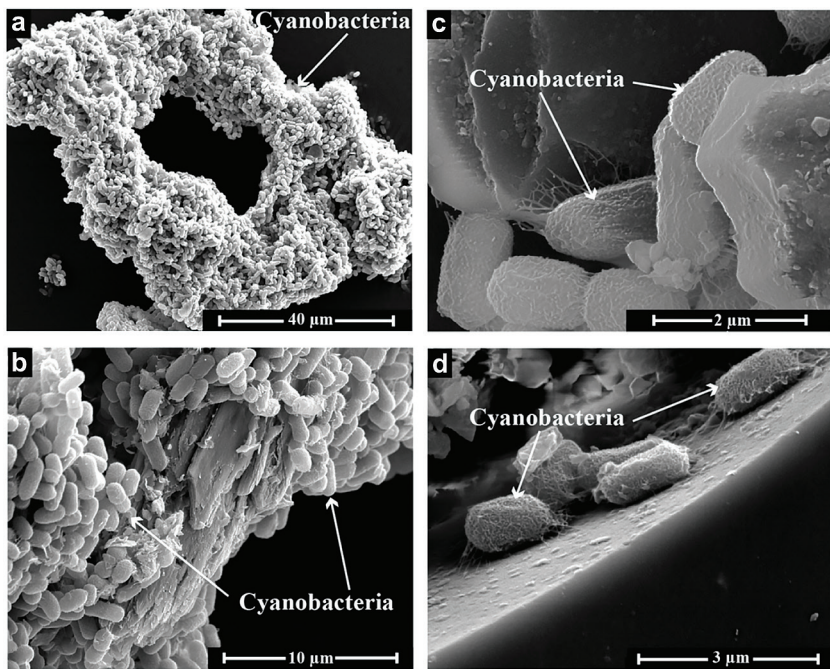


Figure 2.29 SEM microphotographs of Mississippi (a-b) and Iceland (c-d) riverine particulate material sampled during the exponential growth phase collected during the experiments presented in Figure 2.28. Modified from Grimm *et al.* (2019).



3.1 Human Intervention in the Global Carbon Cycle

The natural carbon cycle described in the last section has been greatly influenced by human activity. Human intervention in the global carbon cycle is so large that it is often referred to as a new geologic epoch, “The Anthropocene” (Kolbert, 2011; Crutzen 2002). This epoch, however, has not yet been officially approved as a subdivision of geologic time.

The beginning of Anthropocene is debated widely by the scientific community (Waters and Turner, 2022). Its start could be as early as 8,000 years ago when, as suggested by Ruddiman (2003), human activities saved us from a new ice age by the burning of forests and the cultivating of land. Such processes are now referred to as “land use change”. More often, the beginning of the Anthropocene is placed in the mid-18th century when the initial impact of the Industrial Revolution became evident. Notably, at this time, CO₂ emissions increased due to coal burning and the CO₂ concentration in air bubbles in ice from the South Pole began to increase from about 280 ppm (Etheridge *et al.*, 1996; Petit *et al.*, 1999; MacFarling Meure *et al.*, 2006). The Intergovernmental Panel on Climate Change defines the pre-industrial era as prior to the year 1750. It uses this year as the baseline to define anthropogenic changes in atmospheric greenhouse gases and climate. Others suggest that the beginning of the Anthropocene was the mid-20th century, marked by the rapid rise in CO₂ emission due to the addition of the widespread use of oil and gas. This rapid, more recent rise in CO₂ emission coincides with the peak in radionuclides fallout from atomic bomb testing during the 1950s, the first atomic bomb in 1945, and the Partial Nuclear Test Ban Treaty in 1963.

The total annual human induced CO₂ emission to the atmosphere from various sources is shown in Figure 3.1, spanning the years from 1850 to 2020. Land use change was the dominant source of human induced CO₂ emission from 1850 up to about 1950. After this time, fossil fuel emission dominates. With the exception of a few years, the rise in CO₂ emissions after 1950 continuously increases up to 2019, whereafter the 2020 emission dropped from the previous year by 5.4 % (1.9 Gt CO₂ yr⁻¹). This is the impact of Covid-19 on the global economy and is the largest annual emission decline since 1950. Emissions rebounded towards their pre-COVID-19 levels in 2021 (Friedlingstein *et al.*, 2022).

The mass of CO₂ released to the atmosphere by human activity was about 40 Gt CO₂/yr in 2019. Compared to the natural sources and sink fluxes in the long term global carbon cycle this anthropogenic emission is large. The combined CO₂ emission from the Earth’s mantle *via* the mid-ocean ridges, oceanic islands, arcs, and continental rifts amounts between 0.31 and 1.1 Gt CO₂/yr with an



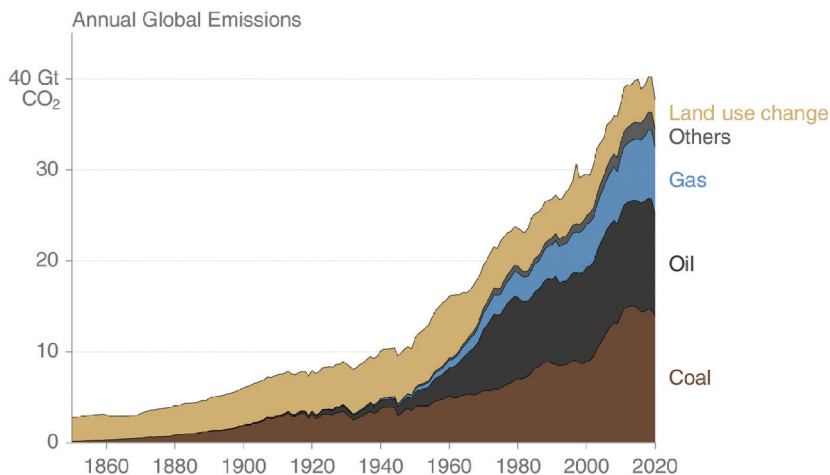


Figure 3.1 Total annual human induced global CO₂ emission by source from the year 1850 to 2020. “Others” represent emissions from gas flaring and carbonate decomposition. Modified from Friedlingstein *et al.* (2022) and The Global Carbon Project (2021) <https://www.globalcarbonproject.org/>.

average estimate of 0.705 Gt CO₂/yr (Marty and Tolstikhin, 1998; Dasgupta and Hirschmann, 2010; Burton *et al.*, 2013; Lee *et al.*, 2016; Tucker *et al.*, 2018; Suarez *et al.*, 2019). The anthropogenic CO₂ emissions during 2019 are 83 times larger than the average rate of mantle degassing to the atmosphere. It took humans only one week in 2019 to emit more CO₂ to the atmosphere than all the volcanoes on the Earth emit on average in a year.

It is somewhat difficult to imagine the scale of human CO₂ emissions. A gigaton is equal to 1 billion tons or 10¹² kg. To put this into perspective one can consider the volume occupied by a gigaton of CO₂. At ambient temperature and pressure, one gigaton of CO₂ occupies approximately 550 km³. The density of supercritical CO₂ at 50 °C and 150 bars of pressure is 0.70 g/cm³ (Duan *et al.*, 1992), such that a gigaton of CO₂ at these conditions has a volume of 1.4 km³. Similarly, as the density of calcite is 2.71 g/cm³ (DeFoe and Compton, 1925) and contains 44 % CO₂ by weight, the volume required to store a gigaton of CO₂ as pure calcite is 0.84 km³ (Oelkers *et al.*, 2022). Another way of looking at this mass is the *per capita* emissions of CO₂ globally. Considering the current global population of 8 billion, the 40 Gt CO₂/yr emission in 2019 equals 5 tons of CO₂ *per person* annually. For many of us this number is difficult to imagine, as we do not see CO₂ being emitted to the atmosphere as it is colourless and odorless. Yet, carbon emissions from each of us are substantial. For example, many car drivers fill their gas tank twice a month. Each fill-up uses at least 50 litres of gasoline, equal to approximately 36.7 kg of gasoline. The burning of each kg of



gasoline produces ~3.1 kg CO₂ such that each 50 litre tank of gasoline produces about 113 kg of CO₂ (Oelkers and Cole, 2008). Thus, 24 annual fill-ups translate roughly into 2.7 tons of CO₂/year.

3.2 The Fate of Anthropogenic Carbon Emissions

Due to the fast exchange among the Earth surface carbon reservoirs involved in the short term carbon cycle shown in Figure 2.2 in Section 2.1, human-induced CO₂ emissions are rapidly partitioned between the atmosphere, terrestrial biosphere, and the ocean. Carbon has relatively short residence time in each of these reservoirs, ranging from one to several hundreds of years. The residence time is defined as the average amount of time each carbon atom persists in the reservoir. This is calculated by dividing the mass of carbon in the reservoir by the annual flux of carbon out of this reservoir. The residence time of carbon in the crust, however, is much longer, counted in millions of years as described in Section 2.1. (e.g., Berner, 2004; Lee *et al.*, 2019). The size and carbon transfer rate among these reservoirs is shown in Figure 3.2. Atmospheric carbon has the shortest residence time, less than 5 years, as CO₂ in the atmosphere is readily dissolved into seawater and incorporated into the biota. The residence time of carbon in the terrestrial biosphere is 33 years, in the surface ocean 13 years, in the intermediate and deep ocean 370 years, and in reactive marine sediments about 5,000 years (Lee *et al.*, 2019). As anthropogenic emissions to the atmosphere continue, the carbon content of each of these reservoirs continues to grow, since the fluxes into the long term carbon cycle are too slow to keep up with the man-made emissions.

Close to 700 Gt of anthropogenic CO₂ have been added to the atmosphere since 1850. Human-induced CO₂ emissions have increased steadily over the past 150 years or more, and this emission rate has been accelerating over time, as shown in Figure 3.3. The high growth in 1987, 1998, and during 2015–16 is thought to reflect a strong El Niño effect that weakens the terrestrial biosphere sink (NOAA, 2022; Friedlingstein *et al.*, 2022). Roughly 45 % of all anthropogenic emissions have remained in the atmosphere, despite the near continuous growth in CO₂ emissions (NOAA, 2022; Friedlingstein *et al.*, 2022). The distribution of total global emissions and total global sinks is depicted over time in Figure 3.3.

The sources and sinks of CO₂ to the atmosphere vary over the globe. Fossil CO₂ emissions dominate in the Northern Hemisphere, while land use change emissions are relatively more important in the tropics. Tropical, temperate, and boreal forests are the major terrestrial carbon sinks (Friedlingstein *et al.*, 2022). The North Atlantic and Southern Ocean are net carbon sinks, while the tropical ocean tends to be a net source of CO₂ (Takahashi *et al.*, 2009; Canadell *et al.*, 2021). This is due to the retrograde solubility of CO₂ in water. As the temperature of seawater goes up, the solubility CO₂ in this water decreases and the gas tends to exsolve into the atmosphere. Nevertheless, there has been a net increase in the mass of CO₂ in the oceans; roughly 45 % of anthropogenic CO₂ emissions



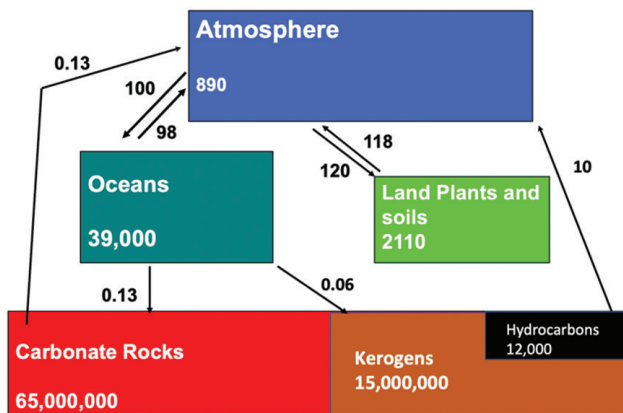


Figure 3.2 Schematic illustration of major terrestrial carbon reservoirs and the annual transfer of carbon among these reservoirs in 2022. The numbers in the boxes representing the reservoirs correspond to the mass of carbon in Gt and the numbers next to the arrows provide the estimated annual fluxes in carbon in Gt carbon/year. Note that these masses and fluxes are provided in terms of carbon rather than CO₂, as CO₂ is converted to organic carbon by some of the processes depicted in this illustration (1 Gt carbon = 3.67 Gt CO₂).

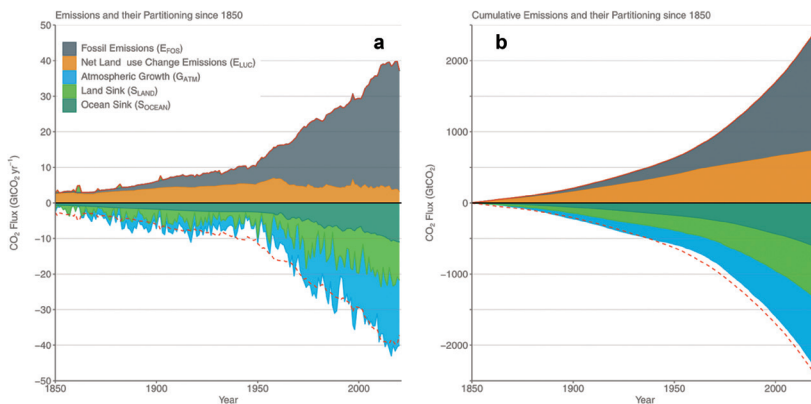


Figure 3.3 The partitioning of anthropogenic carbon emission among the atmosphere and carbon sinks on land and in the ocean over the years 1850 to 2020. **(a)** Annual anthropogenic CO₂ emissions and their partitioning into the short term carbon reservoirs since 1850. **(b)** Cumulative anthropogenic CO₂ emissions and their partitioning into the short term carbon reservoirs since 1850. The difference between the red dashed curves in each plot and the blue to green shaded areas represents an “imbalance” between total emissions and total sinks, likely due to uncertainties in the various measurements. From Friedlingstein *et al.* (2022) and The Global Carbon Project (2021) <https://www.globalcarbonproject.org/>.



are stored in the oceans. This CO₂ influx has resulted in ocean acidification (e.g., MacKenzie and Andersson, 2013). For example, the pH of North Atlantic surface waters north of Iceland has dropped continuously from 8.14 in 1984 to 8.08 in 2009 (Olafsson *et al.*, 2009); the average annual pH of the global oceans has decreased from 8.11 to 8.05 from 1985 to 2020 (Canadell *et al.*, 2021).

Anthropogenic activities, and in particular the burning of fossil fuels, are adding carbon dioxide to the atmosphere and oceans from the crust at a rate that is approximately 700 times faster than natural processes. This is far faster than the rate of natural processes that return this CO₂ back into the crust. As a result, the concentration of CO₂ in the atmosphere has been increasing at a rate unprecedented over the past million years (Fig. 3.4). The increase in global temperature during the past century correlates closely with the corresponding increase in the atmospheric CO₂ concentration over this time, as shown in Figure 3.5. The forcing of global temperature due to increasing atmospheric CO₂ concentration is closely consistent with the role of greenhouse gases influencing global temperatures, as summarised in Section 1.3.

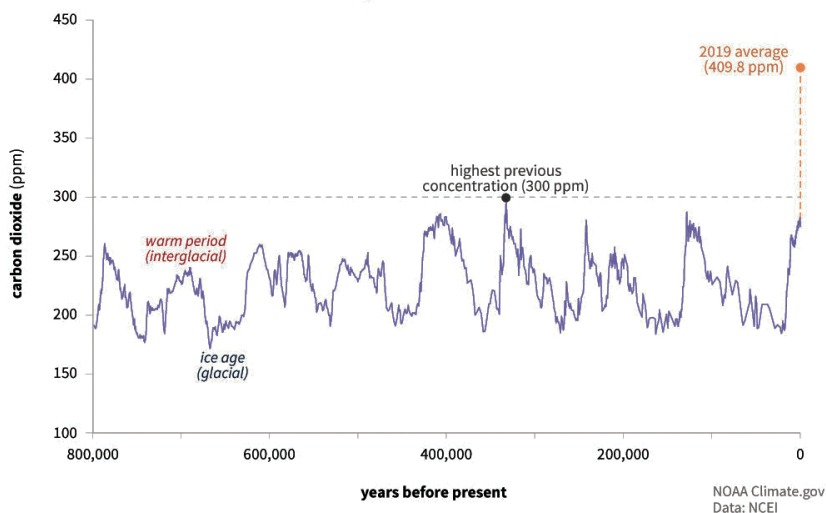


Figure 3.4

Atmospheric CO₂ content over the past 800,000 years. The blue curve shows concentrations based on ice core measurements, whereas the dashed orange curve is based on direct measurement. From NOAA Climate.gov <https://www.climate.gov/media/13685>.



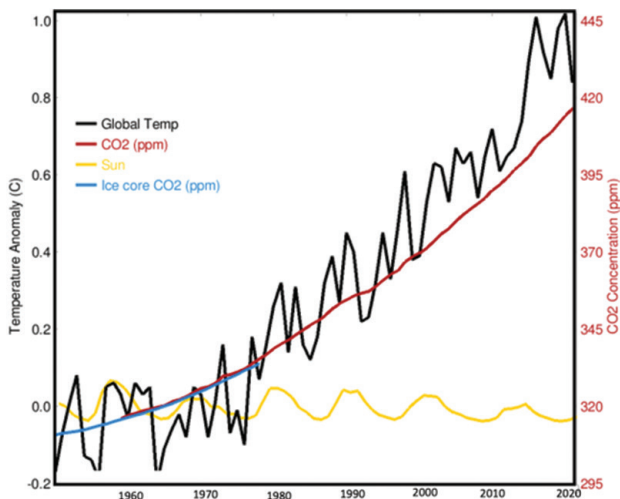


Figure 3.5 Evolution of global average temperature (black), atmospheric CO₂ concentration (red), CO₂ concentration in air trapped in Antarctic ice cores (blue) and solar activity (yellow) 1950 to 2020. Temperature and CO₂ are scaled relative to each other. The solar activity curve shows the average number of sun spots *per year*; its amplitude is scaled from the observed correlation of solar and temperature data. Data taken from the website RealClimate: Climate Science From Climate Scientists (<http://www.realclimate.org/>). This graphic was produced using the climate widget available at <http://herdsoft.com/climate/widget/>.

3.3 Atmospheric CO₂ Concentrations and Human Health

Compared to the threat of increased global warming, the threats to human health due to increasing atmospheric CO₂ contents have been relatively ignored (Jacobson *et al.*, 2019; Karnauskas *et al.*, 2020). It is well established that elevated CO₂ contents have grave consequences on human health. Exposure to >15 % concentrations of CO₂ for over several minutes leads to unconsciousness convulsions, coma and death (OSHA, 1989). Headaches, dizziness, and dyspnea are evident when exposed to CO₂ concentrations in excess of 2 % (OSHA, 1989). Yet there is evidence of less drastic, but substantial health risks at far lower CO₂ concentrations that may be attained by anthropogenic activities.

Atmospheric CO₂ concentrations were stable at ~280 ppm throughout human evolution, and humans may therefore not be adapted to chronic or intermittent exposures to elevated CO₂ (Jacobson *et al.*, 2019; Duarte *et al.*, 2020). Robertson (2001) estimated that lifetime exposure to as little as 426 ppm CO₂



would have detrimental effects on human health. Even at this relatively low CO₂ concentration, which was attained during several days in April-June this year (2023) at the Mauna Loa monitoring station (NOAA, 2023), the average pH of human blood will measurably decrease (Duarte *et al.*, 2020). Reduced pH can lead to an increased incidence of acidosis, leading to poorer lung function and depressed breathing. A decrease in blood pH from 0.1 to 0.4 units, reached after the long term exposure to ~500 to 800 ppm CO₂ can provoke proteome malfunction, leading to such problems as obesity, cancer and neurological disorders. Numerous studies have noted that in poorly ventilated rooms, where the indoor atmosphere CO₂ concentrations exceed 600 ppm, some of the occupants display one or more of the classic symptoms of carbon dioxide poisoning including difficult breathing, headache, and fatigue (Robertson, 2006).

Equally notable is that measurable cognitive and neurological effects have been observed at relatively dilute atmospheric CO₂ concentrations (Azuma *et al.*, 2018; Lowe *et al.*, 2018; Karneckas *et al.*, 2020). Satish *et al.* (2012) reported that the performance on seven of nine decision-making activities decreased by 11 to 23 % after subjects were exposed to 1,000 ppm CO₂ for 2.5 hours, compared to the performance attained after a 2.5 hour exposure to 600 ppm. After an exposure to 2,500 ppm CO₂ for 2.5 hours, the performance results were 44–94 % lower. Allen *et al.* (2016) found that cognitive function scores were 15 % lower at 950 ppm and 50 % lower at 1,400 ppm compared to a baseline of 480 to 600 ppm. In a further study Allen *et al.* (2018) found negative impacts on air pilot performances when increasing the atmospheric CO₂ concentration from 700 to 1500 ppm.

Anthropogenically provoked CO₂ increases can also affect the nutritional content of food. Smith and Myers (2020) reported that numerous food crops grown under a 550 ppm CO₂ atmosphere have 3 to 17 % less protein, iron, and zinc than those grown under current atmospheric conditions. They estimate that this would lead to 175 million people to be zinc deficient, and 122 million people becoming protein deficient worldwide.

Evidence for the potential for the potential effects of anthropogenic CO₂ emissions on human health and cognitive abilities are both limited and scattered at present. Nevertheless, such potential effects are concerning and likely deserve more research effort considering the possible global consequences.



Over time it has become apparent that the increase in the CO₂ concentration of the atmosphere, induced by anthropogenic activities, was and is continuing to provoke global warming, sea-level rise, ocean acidification and potentially global health issues (see Section 3). Concerns over these and other consequences of anthropogenic carbon emissions have led many to call for a global effort to attenuate or even reverse the trend of concentration change of CO₂ in our atmosphere. Decreasing the rate of increase of atmospheric CO₂ concentration can be attained either by 1) replacing carbon-emitting processes such as fossil fuel burning, or 2) carbon capture and storage, or a combination thereof.

The global effort to address Carbon Capture and Storage (CCS) has been initiated by the Intergovernmental Panel on Climate Change (IPCC). Their Special Report on Carbon Dioxide Capture and Storage was approved in September 2005 and represented a formally agreed statement summarising the understanding of CO₂ capture and storage at that time (IPCC, 2005). It was a landmark report and stimulated scientists, funding agencies and politicians to tackle this challenge. The definition of CCS in 2005 was “Carbon dioxide (CO₂) capture and storage (CCS) is a process consisting of the separation of CO₂ from industrial and energy-related sources, transport to a storage location and long term isolation from the atmosphere”. Carbon dioxide capture can be applied to large point sources. The CO₂ would then be compressed and transported for storage in geological formations, in the ocean, in carbonate minerals, or for use in industrial processes. At this time about 60 % of CO₂ emission to the atmosphere came from point sources (Benson and Cole, 2008). The report further stated that “Storage of CO₂ as mineral carbonates does not cover deep geological carbonation or ocean storage with enhanced carbonate neutralisation”. In other words, subsurface mineral carbonation in reactive rocks was not considered in the 2005 IPCC report. However, the 2005 IPCC report indicated that no single technology option would provide all the emission reductions needed to achieve stabilisation; instead, a portfolio of mitigation measures would be needed.

4.1 History of Conventional Carbon Capture and Storage (CCS)

In 1996 the Norwegian state company Statoil, which has since changed its name to the more environmentally benign name Equinor, began to inject a little less than million tons *per* year of carbon dioxide into the Utsira formation 800–1,000 metres beneath the bottom of the North Sea (Torp and Gale, 2003; Fig. 4.1). The formation is a saline aquifer consisting mostly of porous quartz sandstone. The CO₂ was separated from the natural gas produced from a different rock formation located beneath the Utsira formation, to meet the requirements for the sale of this



gas in Europe. Statoil could have emitted the CO₂ to the atmosphere and paid a 50 USD *per* ton of CO₂ Norwegian tax, but they decided instead to inject it into a sub-seabed aquifer, thus beginning this new approach for limiting CO₂ emissions to the atmosphere: carbon dioxide capture and sequestration (CCS). Since then, several large scale CCS projects have started, and in 2021 about 40 million tons (Mt) of CO₂ were captured and injected into the subsurface annually worldwide, and other projects are in development (Global CCS Institute, 2021). Most of the projects in operation today are enhanced oil recovery (EOR) projects, which lead to a net increase rather than a decrease in carbon emissions (see Section 4.2). Subtracting the EOR projects from the current global effort, the annual conventional CCS storage shrinks down to about 4 Mt CO₂/yr. This is only about 0.01 % of the annual 40 Gt CO₂ anthropogenic CO₂ emission in 2021.

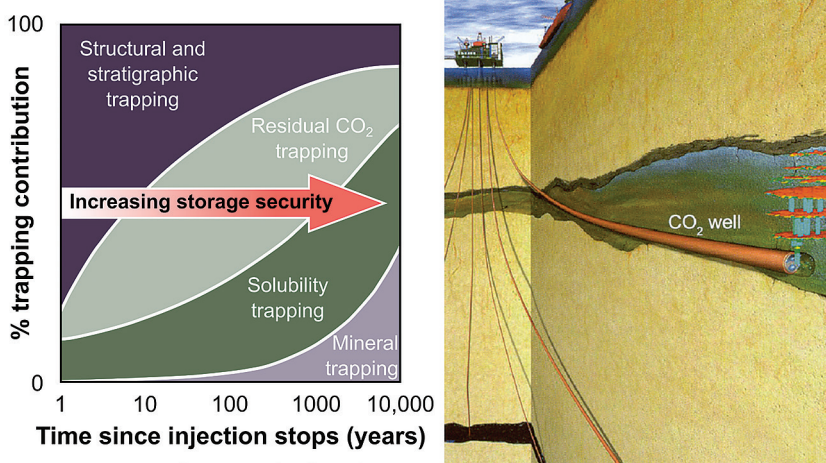


Figure 4.1

Left: Schematic illustration of the expected trapping mechanisms following the injection of CO₂ into a subsurface sedimentary basin storage site. **Right:** Schematic illustration of carbon storage in sedimentary basins, such as the Utsira formation located 800 metres beneath the bottom of the North Sea. Storage in sedimentary basins proceeds *via* the injection of pure liquid CO₂ into porous sedimentary rocks. Ideally this CO₂ is trapped below an impermeable cap rock *via* structural and stratigraphic trapping. Eventually some of this CO₂ becomes stuck in small pores, limiting its mobility *via* residual trapping. Over time, some of the CO₂ dissolves in the formation water leading to its solubility trapping. Some of this dissolved CO₂ may react to form stable carbonate minerals leading to its mineral trapping. As one progresses from structural to mineral trapping, the CO₂ becomes less mobile and its storage more secure, though this process can take thousands of years or more (Gunter *et al.*, 1997; IPCC, 2005a; Gilfillan *et al.*, 2009). Modified from Benson *et al.* (2005) and Torp and Gale (2003). Note the x axis, on the often reproduced left plot provides a quantitative time scale, yet this scale is largely illustrative. In storage reservoirs where no divalent metal-bearing silicate minerals are present, such as a pure quartz sandstone, mineral trapping may never occur, but within sedimentary rocks containing abundant mafic or ultramafic fragments mineral trapping can be significant within several years (see Sections 4.3 to 4.6).



4.1.1 Conventional Carbon Capture and Storage: Practicalities

As defined in the 2005 IPCC special report, conventional CCS consists of CO₂ capture from large point sources, compression of this gas to liquid state, transportation of the liquid to an injection site, and the injection of this liquid into a subsurface storage formation. This injection could lead to a supercritical CO₂ fluid at depth, depending on the geothermal gradient and injection depth. If injected into saline sedimentary aquifers (Fig. 4.1), the supercritical CO₂ is buoyant and tends to rise toward the surface of the Earth. An impermeable cap rock above the injection formation is necessary to prevent the buoyant CO₂ to rise to the Earth's surface. This leads to the physical trapping of the CO₂. Some of this rising CO₂ becomes trapped in small pores on its way towards the surface, limiting its mobility. This process is commonly referred to as residual or capillary trapping. Over time the supercritical CO₂ dissolves into the saline water, making the CO₂-charged saline water denser than the formation water. Once dissolved, CO₂-charged saline water sinks down in the rock formation, increasing storage security. This process is commonly referred to as solubility storage. Finally, some fraction may be converted to stable carbonate minerals, the most permanent form of geological storage (Gunter *et al.*, 1997) through a process called mineral trapping. This series of sequential steps is illustrated in Figure 4.1. Mineral trapping is believed to be comparatively slow, potentially taking a thousand years or longer in sedimentary rocks, which contain relatively little divalent metal cations in silicate rocks. Although some Mg-bearing silicate clay such as smectite may be abundant, these minerals are relatively slow to dissolve and liberate their Mg for mineralisation reactions. Nevertheless, the permanence of mineral storage, combined with the potentially large storage capacity present in some geological settings, makes mineral trapping desirable.

Insight into the fate of CO₂ stored *via* conventional CCS in sedimentary rocks can be attained through observations obtained during the enhanced oil recovery efforts at the Weyburn oil fields. Although the net carbon storage in this system may be negative, as much of the injected CO₂ was mined from the subsurface and the injection of CO₂ was used to produce additional petroleum from this field, it provides a well studied example of the fate of CO₂ injected into sedimentary rocks.

The Weyburn oil fields are located southeast of Regina in southern Saskatchewan, Canada. The oil field consists of two main producing layers: the upper Midale Marly and the lower Midale Vuggy. These reservoirs are dominated by carbonate minerals (Hutcheon *et al.*, 2016). The Marly is a low permeability dolostone with an average porosity of 26 %. The Vuggy is a heterogeneous limestone with an average porosity of 15 %, and an average permeability of 20 mD. The reservoir caprock seal consists of low permeability evaporites (Wilson *et al.*, 2004).

A detailed study of the chemical evolution of the Weyburn system by Shevalier *et al.* (2013) presented the results of the pre-injection baseline characterisation of the reservoir geochemistry (*e.g.*, prior to CO₂ injection in August



2000), and 16 monitoring campaigns performed over a 10 year period following the start of CO₂ injection. The CO₂ concentration measured in the gases collected from the wells increased progressively as the injected CO₂ plume spread in the subsurface system and reached the production wells. The median concentration of CO₂ in these gases was 4.1 mol. % prior to injection, but close to 64 mol. % CO₂ by 2010, 10 years after the start of the injection.

The CO₂ injected into the Weyburn subsurface was found to be contained in four forms: 1) free phase supercritical CO₂, 2) CO₂ dissolved in oil, 3) CO₂ dissolved in brine, and 4) CO₂ precipitated as calcite. Hutcheon *et al.* (2016) estimated how the injected CO₂ was distributed among these sinks through detailed modelling. This model took account of the mineralogical data produced from 100 cores collected from different layers of the Weyburn reservoir, and the reservoir fluid chemistry obtained *via* the baseline monitoring to define the initial conditions for the model. At the end of the 50 year modelled period, more than 50 % of the subsurface CO₂ was dissolved in the oil remaining in the reservoir. A further 38 % of the CO₂ was stored *via* stratigraphic trapping, locking some of the injected CO₂ as a free phase bounded by the evaporite caprock. Solubility and mineral trapping were predicted to account for no more than 9 % and 2 % of the CO₂ stored, respectively. In a separate study based on isotopic signature of the injected CO₂, Raistrick *et al.* (2006) found that nearly 20 % of the dissolved inorganic carbon present in the subsurface water at Weyburn originated from the dissolution of calcite originally present in the rock and approximately 80 % from the direct dissolution of injected CO₂ into these brines. Taken together this case study confirms the overall pathway of trapping mechanisms illustrated schematically in Figure 4.1.

4.2 Is Enhanced Oil Recovery (EOR) Carbon Storage?

As of 2020, only 26 Carbon Capture and Storage (CCS) facilities were operating globally and these facilities had a combined CO₂ capacity of approximately 40 Mt CO₂/year (Global CCS Institute, 2020). Of these, most operations at present are dedicated to enhanced oil recovery (EOR); EOR projects may account for as much as 90 % of the current ongoing subsurface carbon injections (Global CCS Institute, 2020). EOR is widely promoted as carbon storage (*e.g.*, Tanzer and Ramirez, 2019), but does it really lead to a net reduction of CO₂ in the atmosphere?

EOR is a method to obtain additional petroleum from the subsurface by the injection of CO₂ into oil field reservoirs (Mungan, 1981, 1992; Stewart *et al.*, 2018). The injection of CO₂ into petroleum reservoirs enhances recovery in a number of ways, notably much of the injected CO₂ dissolves into the petroleum reducing the viscosity of the crude oil. This allows for petroleum to more readily migrate towards the production wells pushed by the increased pressure of the injected CO₂. The CO₂ dissolved in the oil returns to the surface with the recovered petroleum where it is either released to the atmosphere, captured, or a combination thereof (*e.g.*, Nunez-Lopez and Moskal, 2019).



A surprisingly limited number of studies have been published attempting to inventory the net CO₂ storage gained from the current EOR projects. These are difficult to compare to one another as the studies do not tend to include all of the same factors in their inventories, and differing EOR projects have different degrees of success in carbon storage and petroleum recovery.

Nevertheless, a very simple inventory of EOR carbon storage can be made. Traditional onshore EOR projects have reported to permanently store 200–300 kg of CO₂ *per* additional barrel of oil produced (Stewart and Haszeldine, 2014). In contrast, the average estimated CO₂ emissions from burning a barrel of oil for energy is 500 kg of CO₂ *per* barrel (Oil-Climate Index, 2015). So, using just a very crude calculation, considering the difference between the amount of carbon stored *versus* that added to the atmosphere from the burning of the additional petroleum obtained from EOR activities, this process basically adds two tons of CO₂ into the atmosphere for each ton of CO₂ injected into a subsurface oil field as part of EOR efforts.

The overall net addition of CO₂ emissions to the atmosphere due to EOR may be far worse than the above suggests. Enhanced oil recovery at the present time uses a combination of CO₂ captured from industrial sources and mined CO₂. Traditionally, more than 85 % of the CO₂ used for EOR is mined rather than captured (Nichols *et al.*, 2012). Note that CO₂ that is obtained directly from the subsurface would not otherwise be in the atmosphere. Consequently, of the 200 to 300 kg of CO₂ retained in the subsurface due to current EOR activities, on average 85 % was already stored in the subsurface to begin with. So, we are left wondering if it is best to refer to oil generated by EOR as CO₂-enhanced oil recovery rather than a CO₂ storage approach.

The crude estimate of net carbon emissions made here likely underestimates greatly the current net carbon emissions of EOR operations, as it only takes into account the net difference between the CO₂ stored in the subsurface and that added by burning an average barrel of oil. It does not take into account the carbon emissions originating from the acquisition, transport and injection of the CO₂ itself, among other sources (Stewart and Haszeldine, 2014; Cooney *et al.*, 2015). The additional effect of such sources to the net CO₂ emissions to the atmosphere can be considerable. For example, in a study of 5 EOR systems in North America, Jaramillo *et al.* (2009) taking account of carbon emissions originating from the acquisition, transport and its injection determined that between 3.7 and 4.7 tons of CO₂ were emitted to the atmosphere for each ton of CO₂ injected into the subsurface.

This is not to say, however, that EOR could not eventually be fine tuned to provide net carbon storage. The primary goal of CO₂-EOR at present, however, is to produce more oil with less purchased CO₂. If an incentive to store CO₂ was put into place, through a tax credit or a carbon market, CO₂-EOR could be optimised to store CO₂ more efficiently (*e.g.*, Stewart and Haszeldine, 2015; Nunez-Lopez and Moskal, 2019; Nunez-Lopez *et al.*, 2019). This could largely be accomplished by increasing substantially the CO₂ storage *per* barrel of oil produced



at a temperature of 25 °C and atmospheric CO₂ pressure of 400 ppm has a Gibbs free energy of reaction of -43.3 kJ/mol. So, in each case, these reactions are thermodynamically favourable and chemically spontaneous.

Using reactions such as (4.1) and (4.2) to capture and store CO₂ at the Earth's surface, however, is hindered by several challenges. First, the rates of these reactions are generally slow on a human time scale at Earth surface conditions. If these rates were far faster, these reactions would lead to low atmospheric CO₂ concentrations, global cooling and a dramatic decrease in photosynthesis on our planet. A second challenge is that there are many other mineral reactions, such as the formation of some clay minerals, that compete with carbonate minerals for the divalent metal cations liberated by silicate dissolution reactions.

The number of processes that can accelerate the dissolution of divalent metal-bearing silicate minerals is limited. In some cases, such reaction rates can be accelerated by low fluid pH (*e.g.*, Schott *et al.*, 2009). Low pH conditions, however, are unfavourable for the precipitation of carbonate minerals. The addition of organic ligands can accelerate the dissolution rates of divalent metal silicates at some conditions (Oelkers and Schott, 1998), yet the widespread addition of organic ligands to the Earth's surface to promote mineral carbonation seems impractical. The most practical way to accelerate the rates of reactions such as (4.1) and (4.2) appears to be the extensive grinding of divalent metal-bearing silicate minerals. Grinding makes the particles smaller and increases their surface area. Silicate mineral dissolution rates are widely considered to be proportional to the mineral-water interfacial surface area (*e.g.*, Brantley, 2008). Consequently, the finer the minerals are ground, the faster mineral carbonation reactions likely proceed.

Such observations have motivated a large number of studies investigating the carbonation of mafic and ultramafic mine tailings piles (Oskierski *et al.*, 2013; Wilson *et al.*, 2014). These piles have the advantage that the tailings have been finely ground during mining operations, leading to small rock grain sizes and high grain surface areas. A number of these studies observed substantial mineral carbonation of ultramafic mine tailings, although most carbonation stems from the dissolution of brucite (Mg(OH)₂) and the precipitation of hydrous Mg-carbonate minerals (Assima *et al.*, 2013; Harrison *et al.*, 2013; Boschi *et al.*, 2017; Zarandi *et al.*, 2017). Brucite is characterised by far faster dissolution rates than the silicate minerals at the near neutral pH of most Earth surface waters (Fig. 4.2; Pokrovsky and Schott, 2004; Schott *et al.*, 2009). The brucite in ultramafic mine waste generally formed together with serpentine from the high temperature aqueous alteration of olivine-rich rock (*e.g.*, Hostetler *et al.*, 1966). The rapid dissolution of brucite leads to a strong increase both in fluid pH and dissolved Mg concentration in the aqueous fluid. These strong increases are necessary to promote the carbonation of the dissolving brucite, as the most stable Mg carbonate mineral, magnesite, is extremely sluggish to precipitate or does not precipitate at all at ambient temperatures (Saldi *et al.*, 2009, 2012). Consequently, at ambient temperature, aqueous fluids need be sufficiently concentrated and of sufficiently high pH to precipitate the less stable hydrous magnesium carbonate



minerals, nesquehonite, dypingite and/or hydromagnesite. In contrast to the behaviour of brucite, serpentine and other Mg-bearing silicates in the ultramafic mine waste appear to be relatively inert, consistent with their far slower dissolution rates, particularly at the high pH of fluids resulting from brucite-water interaction. Nevertheless, some have argued that from 190 to 320 million tons of CO₂ could be captured from the air and stored annually by the carbonation of silicate mineral mine waste globally (Renforth *et al.*, 2011). Such huge estimates, which are approximately equal to the half of the total current natural carbonation of the whole of the Earth surface, may be overly optimistic. This scale of carbon capture and storage would require the efficient carbonation of both the silicate and hydroxide minerals in the mine waste piles, and the bulk of these minerals have extremely sluggish reaction rates (Fig. 4.2). It seems likely that the practical global total may be much lower. Nevertheless, in certain instances the carbonation of mafic and ultramafic mine waste can offset a significant percentage of the carbon emissions created by the mining industry.

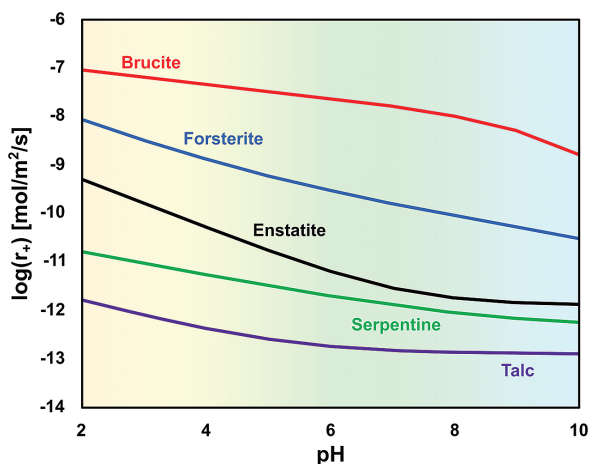


Figure 4.2 Logarithm of the 25 °C far from equilibrium BET² surface area-normalised dissolution rates (r_a) brucite, forsterite, enstatite, serpentine, and talc as a function of pH. Rates were calculated using equations and parameters reported by Pokrovsky and Schott (2004) and Hermanska *et al.* (2022, 2023).

The carbonation of olivine and numerous other Mg silicate minerals is challenging on the Earth's surface due to their slow reaction rates (*e.g.*, Fig 4.2; Brantley, 2008; Oelkers *et al.*, 2018). Due to its slower dissolution rates and to the lack of low temperature magnesite precipitation, olivine carbonation occurs

2. BET surface area measurements are determined from the adsorption of an inert gas on the surfaces of minerals (Brunauer *et al.*, 1938).

in only a few limited environments on the Earth surface. One example is alkaline lakes (Shirokova *et al.*, 2013; Power *et al.*, 2019), where the lack of lake drainage and high evaporation rates serves to concentrate the dissolved Mg. In such systems the carbonation of the dissolved Mg is also promoted by the presence of cyanobacteria that increase fluid pH during photosynthesis (*e.g.*, Power *et al.*, 2007; Mavromatis *et al.*, 2012). A second process that may successfully carbonate olivine is through its interaction directly with seawater (Montserrat *et al.*, 2017). Seawater is mildly supersaturated with respect to calcite. The dissolution of olivine or other minerals in mafic rocks can increase locally the pH and alkalinity of the seawater, provoking the precipitation of calcite or aragonite. Essential to the success of such an approach is that the Si liberated to the seawater is eventually precipitated within a solid that does not consume divalent metal cations. The formation of Mg clays, for example sepiolite, would tend to liberate protons back the seawater, potentially dissolving the calcite originally precipitated by the initial dissolution of the olivine or lowering the alkalinity of seawater (Rigopoulos *et al.*, 2018). The precipitation of Mg clays in the oceans might be avoided through the activity of diatoms that scavenge dissolved Si to form their amorphous SiO₂ frustules (*e.g.*, Thamatrakoln and Hildebrand, 2008). The quantification of the overall mass of carbon drawdown by the addition of olivine to the oceans, however, will be challenging, and perhaps impossible, as the dissolution products will be rapidly dispersed in the global oceans. A potential approach to quantify carbon drawdown through olivine-seawater interaction might be through the use of closed system basins or pools, where a detailed inventory of inputs and outputs from the fluid phase can be determined directly.

A potential process for promoting Mg silicate carbonation at the near-Earth surface that has received some recent attention is the addition of finely ground mafic materials, notably olivine or basalt, to agricultural soils (Moosdorf *et al.*, 2014; Kantola *et al.*, 2017; Beerling *et al.*, 2018, 2020; Andrews and Taylor, 2019). It has been proposed that such additions to soils would have two benefits. First, the dissolution of these materials could enhance agricultural yields by increasing the pH of soil waters and adding essential nutrients such as phosphorus and iron to soils. Second, the carbonation of these materials could be enhanced by their relatively rapid dissolution rates in the acidic soil waters, characterised by a relatively high organic ligand concentration and a higher CO₂ content than in Earth surface waters. The potential of this approach to drawdown large quantities of CO₂ from the atmosphere has proved difficult to quantify due to the large number of processes that occur in soils, and to the relatively slow rates of the process. A recent study of Linke *et al.* (2023), however, successfully quantified this process, but concluded that it might be too slow to make a global impact. Linke *et al.* (2023) concluded that drawing down a gigaton of CO₂ through alkalinity production would require adding basaltic dust to a land area approximately equal that of the whole of the United States.

Despite these challenges, the carbonation of mafic or ultramafic rocks at or near the Earth's surface deserves consideration, as it may provide a low cost alternative to relatively expensive and energy intensive direct-from-the-air carbon



capture technologies. Of note in this regard is the use of mineral reactions at the Earth surface for direct air capture through the process called mineral cycling (Keith *et al.*, 2018; Kelemen *et al.*, 2020; McQueen *et al.*, 2020). Mineral cycling for air capture consists of sequentially combining the decarbonation and carbonation of minerals such as calcite and lime. Specifically, calcite can be decarbonated through heat in a kiln, similar to the production of cement, in accord with



This reaction releases a pure CO_2 gas stream that can be captured and stored. The produced lime can be added into water and exposed to the atmosphere, leading to the reactions:



and

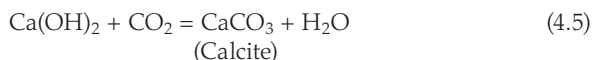


Figure 4.3 Tom Sawyer “Whitewashing the Fence”, 1936. Illustration for *The Adventures of Tom Sawyer*. Norman Rockwell Museum Digital Collections. Whitewashing consists of painting a Ca(OH)_2 bearing aqueous solution onto a wall. Carbon dioxide dissolves directly into the solution and reacts with the dissolved Ca to make a thin white layer of calcite on the wall. Eric used this technique to paint ceilings at his country house and discovered that one needs to protect oneself from direct contact with the Ca(OH)_2 aqueous solution as its high pH leads to nasty chemical burns on the skin.



These later reactions are spontaneous and rapid in the atmosphere. The calcite produced by Equations 4.4 and 4.5 can be returned to the kiln completing the cycle. This process is neither new nor novel, they form the basis for limewashing or whitewashing, which is a method of painting and preserving buildings, a technique going back to at least ancient Egypt. Many of us may have learned about this first through the reading of *Tom Sawyer* by Mark Twain, where Tom was obliged to whitewash a fence (although he got his friends to do it for him; Fig. 4.3). Despite its simplicity, this long known mineral cycling process may prove to be the most economic approach for the direct capture of CO₂ from our atmosphere. This possible is beginning to be explored by the scientific community (e.g., Fasihi *et al.*, 2019; Kelemen *et al.*, 2020; McQueen *et al.*, 2020; Gadikota, 2021).

4.4 The Beginning of CarbFix

During the first commitment period of the Kyoto protocol, 37 industrialised nations and the European Union committed to reduce greenhouse gas emissions to an average of five percent below their levels in 1990. To explore this challenge the President of Iceland, Olafur Ragnar Grimsson, along with Siggí and Wally Broecker, organised a “closed roundtable” meeting January 2006 in Iceland. Representatives from University of Iceland, Columbia University, CNRS in Toulouse, the Icelandic power companies, Reykjavík Energy, Landsvirkjun Power and HS-Orka, and other Icelandic stakeholders were in attendance. After two days of discussion, a working group was formed, chaired by Siggí, with representatives from the Icelandic power companies, the Icelandic Geosurvey and the President’s Office to select the best possible site for a pilot study. After a few meetings over the following weeks, Reykjavík Energy offered the Hellisheiði site for the pilot, and everyone agreed that it would be ideal. The Icelandic President then approached us, representing University of Iceland and CNRS in Toulouse France, together with Einar Gunnlaugsson at Reykjavík Energy Iceland, and Wally Broecker at Columbia University, New York USA, to design a project to curb the greenhouse gas emissions in Iceland (Fig. 4.4). Preparations for a pilot project started in full force in February 2006, while President Grimsson of Iceland prepared the Global Roundtable on Climate Change meeting to be held in May 2006, where the CarbFix project would be introduced (Global Roundtable on Climate Change, 2022). President Grimsson hosted the “Roundtable”, which was chaired by Jeffrey Sachs, Director of Earth Institute, Columbia University. At this meeting, Kristin Ingólfssdóttir, the Rector of the University of Iceland and Jeffrey Sachs signed a memorandum of understanding (MOU) by the two Universities to collaborate on a carbon capture and storage project. The discussion of subsurface carbon storage in Iceland was not limited to scientists and politicians. This subject was also extensively debated at that time in the popular press (see Fig 4.5).





Figure 4.4 Original members of the CarbFix scientific steering committee together with the former President of Iceland at Hellisheiði Geothermal Power Plant in September 2009. From left to right: Einar Gunnlaugsson, Sigurdur Gislason, former President of Iceland Olafur Ragnar Grimsson, Wally Broecker and Eric Oelkers. Photo credit: Sigfus Mar Petursson.

The efforts of the CarbFix “Scientific Steering Committee” and of the managers and lawyers of the partners culminated with the signing of a legal document between the four founding partners in October 2007. By that time seven PhD students, a project manager, Holmfridur Sigurdardottir, and a CarbFix project manager for University of Iceland, Domenic Wolff-Boenish, had been hired. The main scientific and decision-making group during the first few years were 1) from Columbia University Wally Broecker, Juerg Matter, Martin Stute, and at the first stage Klaus Lackner, 2) from University of Iceland; Sigurdur (Siggí) Gislason, Domenic Wolff-Boenisch and at the beginning Andri Stefansson, 3) from Reykjavík Energy, Einar Gunnlaugsson, Holmfridur Sigurdardottir, Bergur Sigfusson, Ingvi Gunnarsson and at the first stage, Grimur Bjornsson and Thorleifur Finnsson and, 4) from CNRS in Toulouse France, Eric Oelkers. Additionally, from the Icelandic Geosurvey, which were subcontractors of Reykjavík Energy came Gudni Axelsson and Thrainn Fridriksson. Representatives from Lawrence Berkeley National Laboratory USA, a subcontractor of Reykjavík Energy, included Eric Sonnenthal, who helped with the development and application of the reactive transport code *ToughReact*. From Mannvit Engineering in Reykjavík, a subcontractor of Reykjavík Energy, came the engineers Teitur Gunnarsson and Magnus Arnarsson.



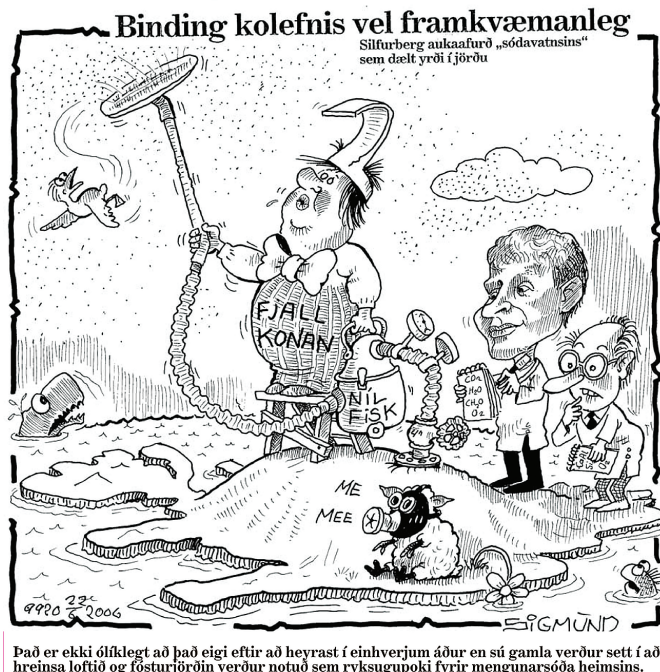


Figure 4.5

Cartoon appearing in the Morgunblaðið newspaper 22 June 2006 following Siggí's national television interview on the possibility of direct air capture of CO₂ and its mineralisation in the subsurface. Icelandic text on top of the panel: "Carbon capture and mineralisation is doable". Small font: "Calcite (Iceland Spar), product of the injection of soda water". Icelandic text at bottom of the panel: "The Icelanders will have doubts about using Iceland as a dustbag for the global polluters of the atmosphere". "Fjall-Konan" is a metaphor for the mother of Iceland.

Carbon storage in Iceland poses a challenge due to the country's geology. Iceland is the largest part of the Mid-Atlantic Ridge that rises above sea level. It is tectonically active with fractures and faults, and the island consists mostly of basaltic rocks. It lacks the stable sedimentary basins that are commonly thought of as favourable geologic storage hosts of single phase buoyant supercritical CO₂, as shown in Figure 4.1. Basalts, however, contain about 20–30 % by weight of calcium, magnesium, and iron oxides (e.g., Oelkers and Gislason, 2001; Schaefer *et al.*, 2010; Alfredsson *et al.*, 2013). Basaltic rocks are also far more reactive in water than sedimentary silicate rocks, and the divalent metals contained in basalts are potentially available to combine with injected CO₂ to form stable carbonate minerals (Oelkers and Gislason, 2001; Wolff-Boenisch *et al.*, 2004b, 2006; Gudbrandsson *et al.*, 2011). Hence, we were optimistic in 2007 that basalt



could provide an opportunity to mineralise CO₂ injected into the subsurface. The evolution of CarbFix took longer than we would have expected at that time; a brief timeline of the CarbFix project is shown in Figure 4.6.

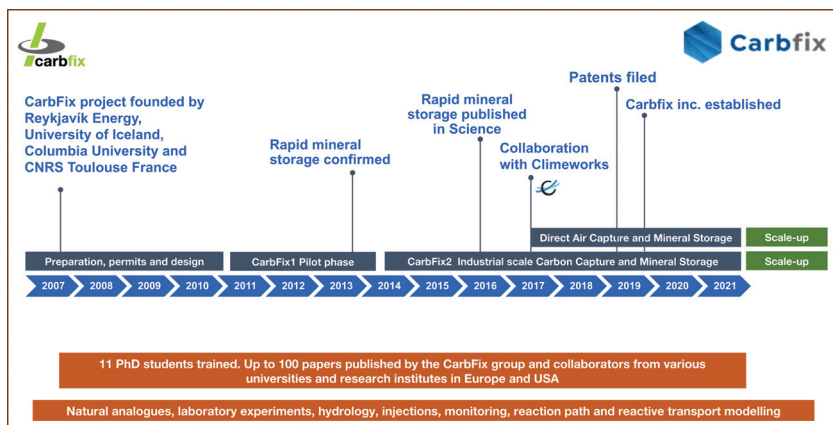


Figure 4.6 The CarbFix project timeline. During the CarbFix1 pilot, pure CO₂ and a CO₂-H₂S-H₂ gas mixture were injected at 350 m depth and 20–50 °C in 2012. In 2014, a water dissolved CO₂ + H₂S gas mixture was continuously injected at a depth below 700 m into a hotter part of the geothermal system (>250 °C). This is referred to as the CarbFix2 injection. The annual capacity of this upscaled injection was ca. 15,000 tons of CO₂-H₂S gas mixture in 2017. Direct Air Capture (DAC) started in 2017.

In the wake of the publication of the IPCC special report on carbon capture and storage in 2005 (IPCC, 2005a,b) and the implementation of the Kyoto protocol the same year, other carbon mineralisation projects were brewing. Pete McGrail and co-workers defined the potential for carbon dioxide mineralisation in some of the major terrestrial flood basalts (McGrail *et al.*, 2006), and two years later, Dave Goldberg and co-workers at Columbia University estimated the storage capacity of carbon dioxide in deep sea basalts (Goldberg *et al.*, 2008). Peter Kelemen and Juerg Matter at Columbia University were keen on trying mineralisation in ultramafic rocks (Kelemen and Matter, 2008). Parallel with CarbFix, the Wallula project led by Pete McGrail at the Pacific Northwest National Laboratory USA injected 1,000 tons of pure liquid CO₂ into the Columbia River flood basalts near Wallula, Washington, USA (McGrail *et al.*, 2014, 2017). The CarbFix1³ injection

3. Throughout this text, CarbFix refers to the overall project, CarbFix1 to the first demonstration injection at a depth of 350 m run during 2012, CarbFix2 refers to the second and ongoing injection at depth of 700 m. The company that was formed late December 2019 is referred to as Carbfix.

occurred in the beginning of year 2012 (Fig. 4.6; Gislason and Oelkers, 2014; Sigfusson *et al.*, 2015; Matter *et al.*, 2016), whereas the Wallula injection occurred during 2013 (McGrail *et al.*, 2017).

Before and during CarbFix we needed to raise funds and we had to “sell” the project. Eric co-edited an issue of the journal *Elements* on Carbon Capture and Storage, published in 2008 (Cole and Oelkers, 2008), with introduction from both President Grimsson of Iceland and Wally Broecker, and a paper by us and Juerg Matter on carbon mineralisation (Oelkers *et al.*, 2008).

Wally Broecker was very much focused on CO₂ and climate solutions (Fig. 4.7). He wrote an inspiring book with Robert Kunzig, who later became the environmental editor of National Geographic, on *Fixing Climate* (Broecker and Kunzig, 2008). Wally later published two issues of *Geochemical Perspectives* where he discussed the geochemistry of past and present climate on Earth (Broecker, 2012, 2018). The second of these, *CO₂: Earth’s Climate Driver*, came out a few weeks before he died. Siggı got an autographed issue in the mail from him signed: “To Siggı, The CO₂ Undertaker!” – he knew what was coming.



Figure 4.7 Wally Broecker discussing carbon storage in Iceland in January 2006. From left to right Siggı Gislason, Eric Oelkers (partially obscured), Wally Broecker, Jon Olafsson, Klaus Lackner, and Juerg Matter.



Perhaps the most challenging issues of starting a subsurface carbon storage project are the legal details. Regulations pertinent to CarbFix at its beginning were 1) The Planning Act, 2) The Environmental Impact Assessment Act (EIA), 3) Regulations concerning prevention of groundwater contamination, 4) Health and safety regulations, 5) Law on nature conservation, 6) Radiation safety regulations, and from 2009, 7) Regulation of certain substances that increase greenhouse effects, and 8) Directive 2009/31/EC on the geological storage of carbon dioxide. At least ten permits were needed prior to CarbFix1 CO₂ injection. Some of these permits needed to be renewed every year. No doubt the challenge of obtaining all the permissions required for any subsurface carbon storage is a major hurdle for the worldwide implementation of subsurface carbon storage.

After several meetings led by Siggí in early 2006 with Icelandic power companies and the Icelandic Geosurvey, Reykjavík Energy identified the injection and monitoring wells locations near their Hellisheiði Geothermal power plant, which was inaugurated in September 2006 and located 40 km east of Reykjavík.

4.4.1 Pre-Injection Field Observations

While applying for permits, we studied the chemistry of the groundwater system into which we planned to inject the CO₂, quantified the rock composition and mineralogy, assessed the saturation state of the primary and secondary minerals and glasses, and predicted the saturation state of these minerals as CO₂-charged water entered the basaltic rocks, and finally, we measured the CO₂ “soil” fluxes from surface lava flows (Gislason *et al.*, 2010; Alfredsson *et al.*, 2013). The state of the bacteria in the well fluids before the gas injection was also defined (Trias *et al.*, 2017).

A study of the rocks at the CarbFix1 injection site was performed prior to CO₂ injection. The first appearance of aragonite (CaCO₃) in drill chips sampled from the injection (HN-02) and monitoring (HN-04) wells was observed at below 150 m to 200 m depth, and calcite (CaCO₃) first appeared below 250 to 300 m depth (Fig. 4.8). The presence of these carbonate minerals served as a proof of concept, as these minerals resulted from the interaction of naturally CO₂-charged water with the primary volcanic rocks in the subsurface. Deeper in the subsurface, Ca-rich zeolites and some Na zeolites are common secondary phases. These observations motivated us to target the original CarbFix1 injection to enter the subsurface basalts at ~500 m depth. The major alteration phases at this depth, according to XRD measurements, are pore-filling Mg-Fe-Ca smectite, Ca-rich zeolites (mesolite and chabazite) and calcite (Alfredsson *et al.*, 2013; Fig. 4.8). Formation temperatures, estimated from the sequence of the alteration minerals, ranged from 25 °C at a depth of 500 m to 180 °C at a depth of 1500 m. The well fluids below 400 m depth were at calcite and aragonite saturation before the CO₂ injection (Alfredsson *et al.*, 2013). All major host rock primary and secondary minerals and glasses were estimated to be strongly undersaturated



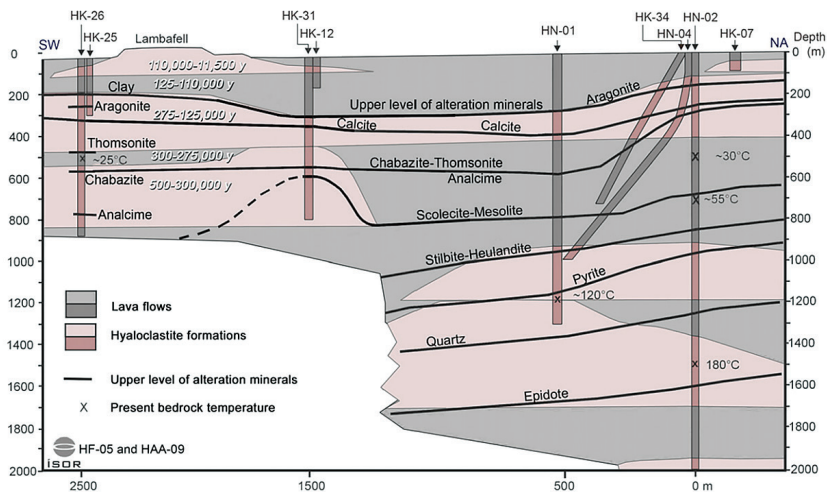


Figure 4.8 Geologic cross section, SW-NE showing the stratigraphy of the Hellisheiði, SW Iceland CarbFix1 injection site. The locations of the CarbFix1 wells are shown in the figure; HN-2 is the injection well, HN-1 is the water source well (1 km toward west) and HN-4, HK-34, HK-31, HK-25, HK-7b, HK-12 and HK-25 are monitoring wells. The major stratigraphy consists of glassy hyaloclastite basalt formations (pink) and more crystalline basalt lava formations (grey). The first appearances of secondary minerals with depth, before the CO₂ injection, are shown as black lines. The estimated rock ages are shown in the upper left part of the figure. From Alfredsson *et al.* (2013) with permission from Elsevier.

with respect to the proposed gas-charged injection waters (Alfredsson *et al.*, 2013). Thus, CO₂-charged water injections were expected to create porosity in the near vicinity of the injection well by dissolving primary and secondary minerals.

As the CarbFix1 injection was being developed and approved, we embarked on a number of field analogue studies to gain insight into the fate and consequences of injecting CO₂ into basalt rocks. Among the most notable of these was work performed by Wiese *et al.* (2008). In a study of the CO₂ mineralisation in three active Icelandic high-temperature geothermal systems, Wiese *et al.* (2008) found that up to 150 kg of CO₂ per m³ of basalt precipitated into calcite in the up-flow zones of these systems. This result provided us with a way to estimate subsurface storage capacity of basalts, and suggested that a maximum CO₂ storage by the CarbFix approach would be approximately 5 wt. % of the target reservoir rock volume.

We performed another field study with Teresa Flaathen to assess the risk of toxic metal mobility induced by the injection of CO₂ into basalts. These efforts focussed on the groundwater system draining the Hekla volcano in South Iceland. This volcano erupted in 1947, 1970, 1980, 1991 and 2000. Flaathen *et al.* (2009a)



demonstrated that heavy metals released at the early stage of CO₂-charged water and basalt interaction are incorporated into secondary minerals such as carbonates and ferrihydrite. Similarly, our work with Jonas Olsson (Olsson *et al.*, 2014a,b) indicated that toxic metals, including As, Ba, Cd, Sr and Pb were likely scavenged by carbonate mineral precipitation. These observations demonstrated the likelihood that the toxic metals released by basaltic and ultramafic rocks in an engineered CO₂ injection project would be taken up by mineralised carbon, minimising risk to water quality.

4.4.2 Pre-Injection Experimental Studies

Concurrently, with some of these field analogue studies, and prior to the initial CarbFix1 injection, many of us focused on characterising the reactivity of basaltic rocks through laboratory experiments (Oelkers and Gislason, 2001; Gislason and Oelkers, 2003; Wolff-Boenisch *et al.*, 2004a,b, 2006, 2011; Gudbrandsson *et al.*, 2011, 2014; Gysi and Stefansson, 2011, 2012a,b; Stockmann *et al.*, 2011, 2012, 2013, 2014; Galeczka *et al.*, 2013, 2014). The motivation for this work was to enable accurate temporal and spatial modelling of CO₂ injection into basalt. The CO₂-charged water injected into the subsurface is acidic, which is neutralised due to its interaction with basalt, provoking the precipitation of carbonate minerals. Hence, an accurate reactive transport modelling of the CO₂ mineralising process in basalts requires reliable rates as a function of temperature and pH. Examples of the results of some of our experiments are shown in Figures 4.9 and 4.10.

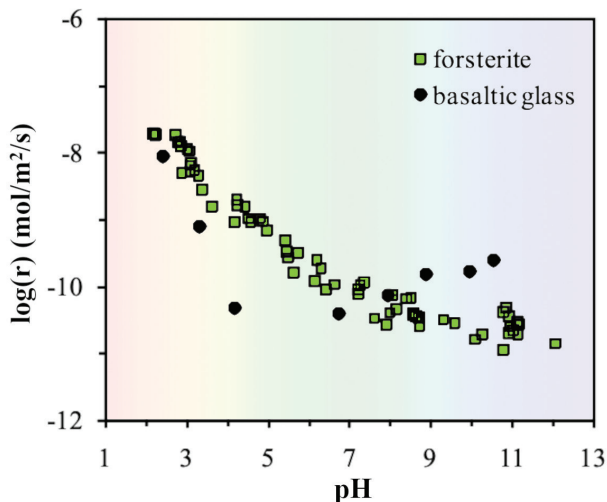


Figure 4.9 Far from equilibrium surface area-normalised dissolution rates of forsterite based on Si release at high undersaturation at 25 °C (Pokrovsky and Schott, 2000), and corresponding rates of the Stapafell basaltic glass from SW Iceland, the composition of which is close to the Mid-Ocean Ridge Basalt (MORB) composition, at 30 °C. Modified from Gislason and Oelkers (2003).



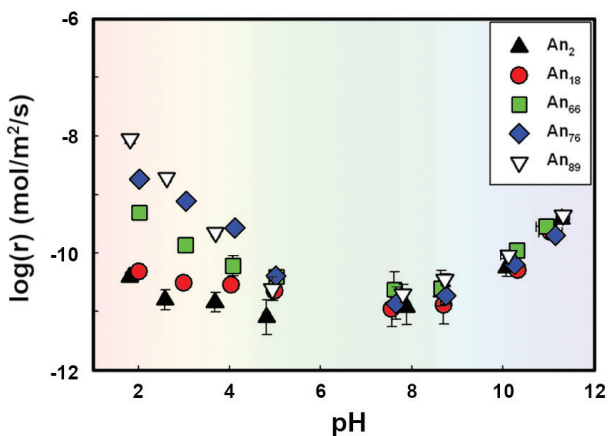


Figure 4.10 Far from equilibrium plagioclase dissolution rates at 25 °C based on Si release rate. Modified from Gudbrandsson *et al.* (2014).

The dissolution rate of forsterite is the fastest of the major primary silicate minerals of ultramafic and basaltic rocks at acidic conditions, but its rate declines continuously with pH (Fig. 4.9). A similar behaviour is observed for other Mg silicate minerals including enstatite, diopside and talc (Oelkers and Schott, 2001; Saldi *et al.*, 2007). Note that the dissolution rates of basaltic glass and most plagioclases decline and minimise at a pH of 6 to 7 at 25 °C, then increase at higher pH (Figs. 4.9 and 4.10). At pH greater than 9, the dissolution rates of basaltic glass and Ca-rich plagioclase are larger than that of forsterite. This has consequences for the stoichiometry of Ca, Mg and Fe release from crystalline basalt at far from equilibrium conditions, and likely for the identity of the carbonate minerals formed in response to the injection of CO₂ into basalts. Carbon dioxide-rich waters injected into subsurface basalts have an acidic pH of 3.5–4.5. At these acidic conditions basalts will preferentially release Mg and Fe (see Fig. 4.11), such that Mg and Fe-bearing carbonates might be the first carbonate minerals to form. As the pH of these fluids increased due to further basalt dissolution, Ca release from basalt begins to dominate and calcite may dominate carbonate precipitation. Natural basaltic groundwater systems have a pH of 9 to 10 (*e.g.*, Alfredsson *et al.*, 2013); at these pH values carbonation is likely dominated by Ca carbonate precipitation.

The effects of the presence of calcite or bacteria coatings on silicate mineral dissolution rates were investigated in collaboration with Gabriella Stockmann (Stockmann *et al.*, 2011, 2012, 2013, 2014). The concern was that carbonate or bacterial coatings on glass, olivine, pyroxene or plagioclase would slow or even stop the dissolution of the primary phases of basalt, arresting mineral precipitation in the subsurface. In all cases, the biotic or abiotic surface coatings had



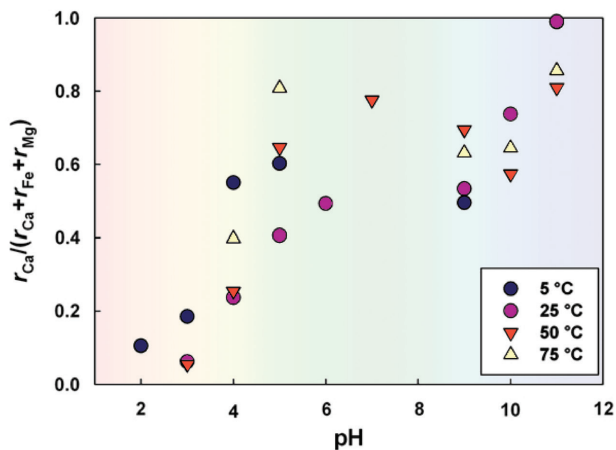


Figure 4.11 The release rate of Ca from crystalline basalt, divided by the sum of the corresponding release rates of the divalent cations as a function of pH at the indicated temperatures. Modified from Gudbrandsson *et al.* (2011).

negligible effect on the dissolution rate of the underlying primary mineral. These experiments also provided insight into the nucleation preference of calcite. Calcite precipitated relatively rapidly on labradorite, olivine, and enstatite surfaces, but more slowly on augite and basaltic glass. Calcite precipitation rates, however, became independent of substrate identity and mass over time during 70 day long experiments. In all cases, these experiments suggested that the precipitation of carbonate minerals will have no detrimental effects on the rates of mineral carbonation.

The overall reaction path between injected CO₂-charged water and a host basalt was investigated through a series of experiments performed by Alex Gysi. In these batch experiments basaltic glass was reacted at 40 °C with CO₂-charged water having initial CO₂ partial pressures of 10 and 30 bar for up to 260 days (Gysi and Stefansson, 2012a). These were the conditions expected to be present in the subsurface during the CarbFix1 injections. In the experiments, the measured divalent metal cation concentrations in the fluid phase were observed to decrease continuously with time, and this decrease was most efficient at higher initial fluid *p*CO₂. The major minerals precipitated in the experiments were a smectite clay and a mixed Mg, Fe, Ca carbonate. The formation of these clays may enhance carbonate mineral precipitation (Molnar *et al.*, 2021, 2023). The eventual formation of zeolite minerals was also suggested by the reactive fluid compositions during the experiments. The modelling of these experimental results indicated the rapid transformation of the original basaltic glass and illuminated the efficiency of the mineral carbonation process (Gysi and Stefansson, 2011, 2012b). Some of the results of this modelling are shown in Figure 4.12. Several

insightful observations are apparent. First, mineralisation occurs more rapidly at high $p\text{CO}_2$ than low $p\text{CO}_2$. Second, abundant non-carbonate secondary minerals form, notably amorphous SiO_2 , Al silicate clay minerals, smectite and zeolites. These results match well both the experimental observations made by Gysi and Stefansson (2011) and also the observed mineral assemblages in the CarbFix1 injection site and other hydrothermally altered basaltic systems (Neuhoff *et al.*, 1999; Alfredsson *et al.*, 2013).

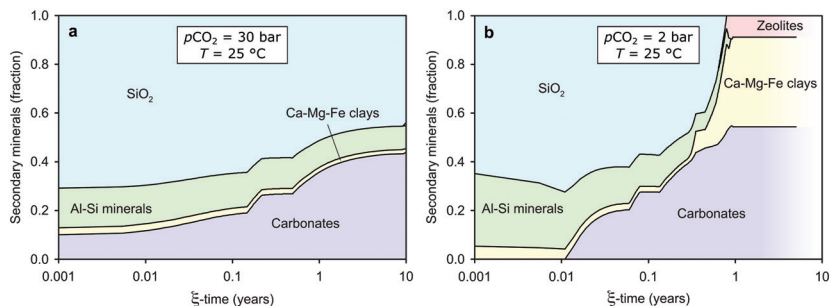


Figure 4.12 Mole fraction of secondary minerals formed as a function of reaction progress at 25 °C in accord with the modelling results of Gysi and Stefansson (2012b). The calculations are based on the reaction of basaltic glass with Icelandic natural spring water initially saturated with (a) 30 bar and (b) 2 bar CO_2 . Modified from Gysi and Stefansson (2012b).

In an attempt to recreate a natural flow system in experiments, we first considered building and running a 50 m long flow reactor. By creating such a reactor, we could “build a bridge” between the bench scale experiments and the subsurface system. Reykjavík Energy gave us preliminary permission to construct this long flow reactor within the Hellisheiði power plant. After making a preliminary design we decided that this was impractical, largely because of the huge quantity of basalt that would be needed to fill, and be analysed after, each experiment. Instead, we settled on building a 2.5 m long, high pressure reaction column made of titanium (Galeczka *et al.*, 2013, 2014; Clark *et al.*, 2019). Experiments were performed by the injection of pure water and CO_2 -charged water into the column filled with basaltic glass at 22 °C and 50 °C, and at $10^{-5.7}$ to 22 bar initial partial pressure of CO_2 . These temperature and CO_2 pressure conditions span those at the CarbFix1 injection site before and after the injection (Alfredsson *et al.*, 2013). Geochemical modelling matched well the observations in these plug flow experiments, validating the use of modelling codes and the application of thermodynamic and kinetic parameters measured from our laboratory bench scale experiments. The column length and thus the residence time of the fluid in the reactor of less than 8 hours were too short to provoke the precipitation of carbonate minerals. Once this fluid exited the reactor, however, carbonate minerals precipitated as the fluid degassed.



4.4.3 Characterising Subsurface Flow Paths

Inert tracer tests were performed prior to CO₂ injection at the Hellisheiði CarbFix1 injection site during 2008 to 2011 to define the subsystem hydrology and to develop pre-injection reactive transport models (Khalilabad, 2008; Khalilabad *et al.*, 2008; Aradottir *et al.*, 2012a,b, 2015). A schematic illustration of the CarbFix1 injection site is provided in Figure 4.13. This site consists of a series of lava flows and glassy hyaloclastite formations. It is equipped with several wells for the injection of CO₂-charged water and the sampling of this water after its interaction with the subsurface basalts. The chosen injection well was HN-02, and the closest potential monitoring well was HN-04, situated towards the west (Fig. 4.13). The distance between the two wells is ~60 m at 400 m depth, 150 m at 650 m depth and 360 m at 800 m depth. Tracer tests were conducted both under natural and forced flow conditions to define the fluid flow paths between these wells.

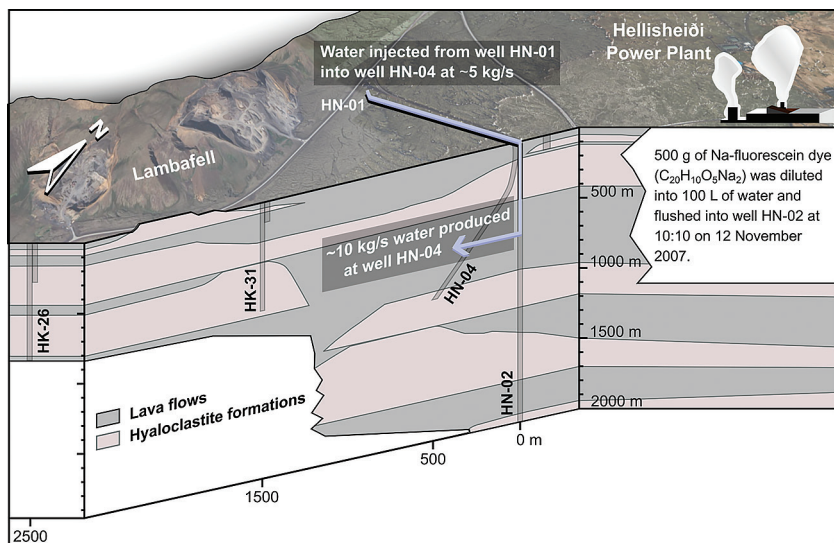


Figure 4.13 Geological cross section and wells at the CarbFix1 injection site at the time of Na-fluorescein slug test. Water was pumped from well HN-01 and injected into well HN-02 at 5 kg/s, and produced out of HN-4 at 10 kg/s. Note that at the time of the slug test, HN-32 monitoring well had not been drilled. Modified from Alfredsson *et al.* (2013).

A flow field was induced by the continuous injection of water into HN-02 at a rate of 5 kg/s, and continuous pumping of water out of well HN-04 at a rate of 10 kg/s. The operation of this “doublet” started 3 days prior to the tracer injection to develop a steady state flow field. A mass of 500 g Na-fluorescein dye (C₂₀H₁₀O₅Na₂), was diluted into 100 litres of water. This solution was flushed as

a slug into well HN-02, at 10:10 on 12th November 2007. The background level of this fluorescent dye was insignificant. The detection limit was about 10 ppt (Khalilabad, 2008; Smith and Pretorius, 2002).

Fluids were collected from the HN-4 monitoring well and analysed through early May 2008. Samples were also taken from wells HN-01 and HK-31 (Fig. 4.13). Well HN-01 supplied the water for the injection, and HK-31 was located 1.5 km downstream, to the south. No tracer was detected in these more distant monitoring wells. The measured Na-fluorescein concentrations in the HN-4 monitoring well are shown as square symbols in Figure 4.14.

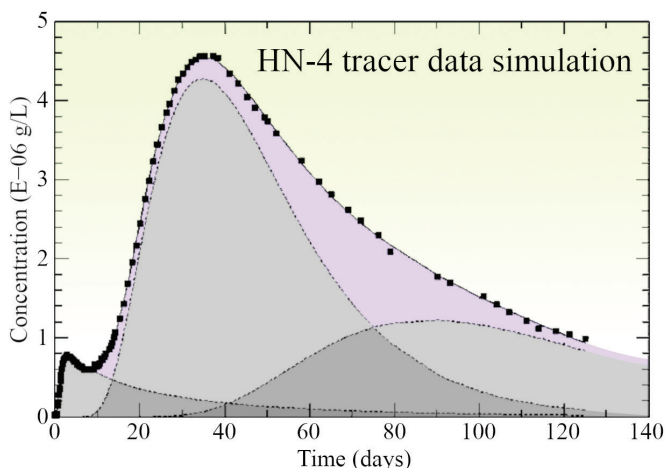


Figure 4.14 Observed and simulated Na-fluorescein recovery in well HN-04, assuming three distinct flow channels. The square symbols correspond to the measured tracer concentrations, the dashed curves to the simulated flow in three distinct flow channels, and the solid curve shows the overall simulated concentration of the tracer consisting of the sum of the three individual flow paths. Modified from Khalilabad (2008).

The observed Na-fluorescein concentration was interpreted assuming a set of one dimensional dispersion transport routes ignoring diffusion, adsorption and retardation (Axelsson *et al.*, 2005; Khalilabad, 2008; Khalilabad *et al.*, 2008). Three distinct flow paths were identified as indicated by the curves in Figure 4.14. The first flow path is located at 400 m depth in the monitoring well (with a 60 m distance between the wells), the second at 650 m depth (with a 150 m distance), and the third at 850 m depth (with a 360 m distance). The locations of these channels are based on stratigraphy (Alfredsson *et al.*, 2013), well logging and circulation losses during drilling of the wells (Helgadottir *et al.*, 2009). As the adopted solution is not unique, geological information and well logging data were considered to identify the aquifer depths. A total of 50 % of the injected tracer was recovered during the first 125 days of the tracer test.



The first peak in the tracer recovery data suggests the shallowest flow channel carries only 3.2 % of the water flow and may consist of a fracture between the wells at shallow depth. The second peak is likely caused by a much larger aquifer located at the depth of 650 m; this channel carries 34.5 % of the water flow. The shape of the last curve is characteristic of a homogeneous porous medium in the channel. This peak is likely caused by the presence of an aquifer located at ~850 m depth, transporting 12.3 % of the injected water. This aquifer responded to the tracer injection later because of its depth and greater distance between wells (Fig. 4.13). The rest of the injected water remained in the subsurface and likely transported deeper into the subsurface. The highest fluid velocity was measured in the shallowest aquifer, consistent with fracture flow. The velocity was slower in the middle aquifer; the deepest aquifer is predicted to have a greater velocity, but its contribution to the tracer recovery arrived later due to its longer flow path (Khalilabad, 2008; Khalilabad *et al.*, 2008). The shallowest aquifer has the smallest pore volume, as expected for a fracture. The middle aquifer represents a thicker layer with greater volume of pore space interpreted as a network of homogenous interconnected porosity. The deep aquifer has a large amount of pore space. Therefore, despite its depth, its contribution to the measured concentration was considerable (Fig. 4.14).

4.4.4 Pre-Injection Reactive Transport Modelling of the CarbFix1 Injection

Because of all the experimental work and field observations, it was possible to perform quantitative and detailed reactive transport modelling of the CarbFix1 injection in advance of performing the injection. Two and three dimensional field scale reservoir models of CO₂ mineral sequestration were developed (Aradottir *et al.*, 2012a). The principal hydrological properties were lateral and vertical intrinsic permeabilities of 300 and 1700 × 10⁻¹⁵ m², respectively, effective matrix porosities of 8.5 % and a natural regional groundwater flow velocity of 25 m/yr. Reactive chemistry was coupled to the calibrated hydrological model and predictive mass transport and reactive transport simulations carried out for 1) a 1,200 ton “pilot CO₂” injection, and 2) a scaled-up 400,000 ton CO₂ injection. These modelled “pilot injections” were considerably larger than the 230 tons of CO₂ injected later at the CarbFix1 site during January-August 2012 (Sigfusson *et al.*, 2015; Matter *et al.*, 2016).

In the simulation of the hypothetical 1,200 ton “pilot CO₂”, 3 kg/s of carbonated water saturated at 30 bar CO₂ pressure was assumed to be injected continuously into well HN-02 for 6 months (see Fig. 4.15). Simultaneously, the first monitoring well HN-04 was assumed to produce 1 kg/s of fluid continuously for the first 12 months of the pilot test, and an additional 1 kg/s production of fluid was assumed out of the new well HK-34 from months 6 to 18 (Aradottir *et al.*, 2012). The initial primary reservoir rock was assumed to consist of 43 vol. % plagioclase, 39 vol. % pyroxene, 13 vol. % olivine, and 5 vol. % basaltic glass, which is close to the mineral abundance in the rocks used in the experiments



of Gudbrandsson *et al.* (2011), shown in Figure 4.11. Figure 4.15 shows a cross-sectional view of the calculated dissolved inorganic carbon concentration (depicted as HCO_3^-) in the injected “plume” as predicted by three dimensional reactive transport simulations after 1, 5, and 10 years from the beginning of injection. The dissolved inorganic carbon concentration decreases after CO_2 injection is stopped due to dilution, diffusion, and chemical reactions. These processes result in the plume disappearing after 10 years. Carbonate mineral formation increases gradually, and all the 1,200 tons of the injected CO_2 were predicted to have been mineralised after ~10 years (Aradottir *et al.*, 2012a). The carbonate minerals formed are dominated by Fe-Mg carbonates close to the injection well, but calcite further downstream at lower $p\text{CO}_2$ pressure and higher pH (Fig. 4.16). Pure SiO_2 phases; amorphous, moganite and quartz were predicted to be enriched close to the injection well (Aradottir *et al.*, 2012a, 2015).

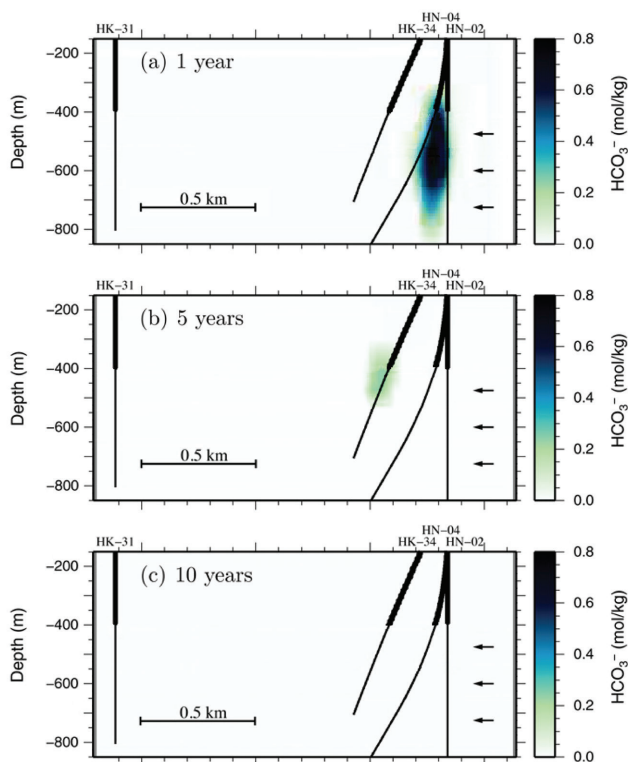


Figure 4.15

Cross-sectional view of modelled reservoir water-dissolved inorganic carbon concentration depicted as HCO_3^- concentration, in the 1,200 ton hypothetical “ CO_2 pilot” injection after (a) 1 year, (b) 5 years, and (c) 10 years, as predicted by three dimensional reactive transport simulations. Modified from Aradottir *et al.* (2012a).



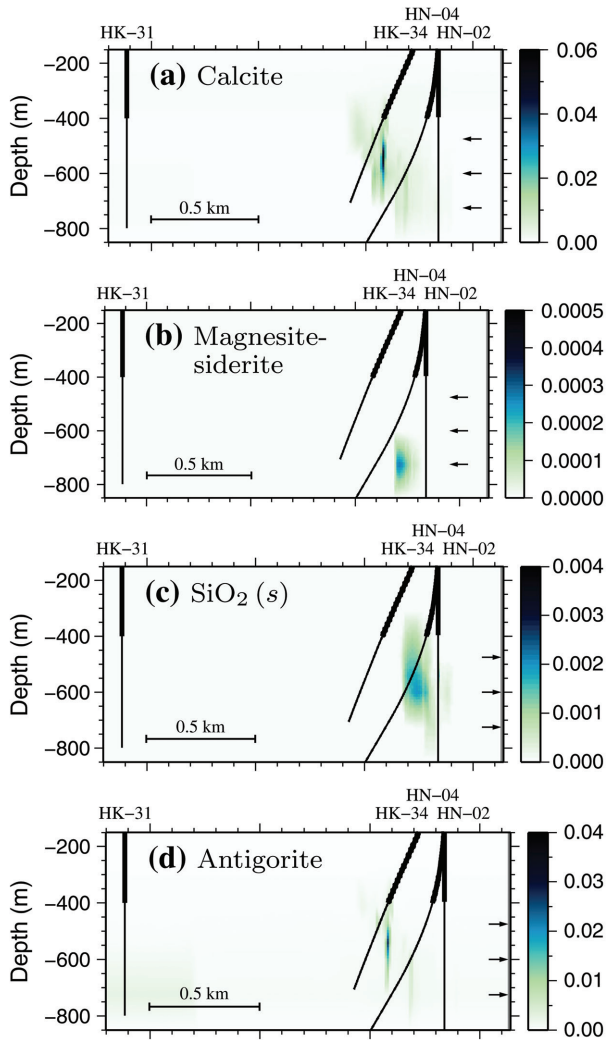


Figure 4.16

Cross-sectional reservoir view downstream from the injection well HN-02 (Fig. 4.13) of selected precipitated minerals (in vol. % of total mineral assemblage) 10 years after the 1,200 ton CO₂ was injected, as predicted by a three dimensional reactive transport simulation. The figure shows different minerals forming at different temperature/depth and pressure/depth conditions. Note the difference in vol. % scale in the diagrams. Modified from Aradottir *et al.* (2015).



The extensive field, experimental, and modelling effort all showed the likelihood that CO₂ injected into the CarbFix1 site would lead to the rapid storage of the injected water-dissolved gas within years. The only thing that remained was to test this directly in the field.

4.5 CarbFix1

All the laboratory experiments, field analogies, and geochemical modelling indicated that the injection of water-dissolved CO₂ into the subsurface basalts at Hellisheði would lead to the mineralisation of the injected gas over relatively short periods of time. What remained was to demonstrate that the subsurface mineralisation of basaltic rocks would actually work. This leads us to the CarbFix1 injections. The CarbFix research team quickly realised that buoyant supercritical CO₂ could not be injected into the young, fractured, and tectonically active rocks of the rift zone in Iceland. It would easily find its way back to the surface due to its low density compared to that of water. Therefore, we had to design an injection system where pressurised CO₂ gas was co-injected with meteoric water at depth within the reservoir well, sourced from the target formation.

4.5.1 The CarbFix1 Injection Well

The shallowest CarbFix1 subsurface basaltic aquifer is located at a depth of ~500 m depth in the HN-02 injection well. The water level in this well is at about 100 m depth. Consequently, the fluid pressure in the reservoir is about 40 bars at the depth of the shallowest target aquifer. The injectivity of the well that was used to inject water into a hydrostatically pressured reservoir was sufficiently high for the water to flow down-well by gravity alone. Our simple solution was to just release the CO₂ into the downflowing water through a sparger. The sparger was used to assure a continuous release of bubbles of less than 1 mm in diameter into water. We located the sparger at a depth of 350 m from the surface, such that the water pressure at this depth was roughly 25 bars. We injected the CO₂ into the well at a pressure of just above 25 bars. Note the CO₂ would not flow into the water if its pressure was less than that of the water at the depth of the sparger. The water to CO₂ ratio was chosen to be greater than the solubility of CO₂ at the depth of its release into the water. This assures the complete dissolution of the CO₂ before it arrives in the target subsurface aquifer. It turns out that 25 bars of pressure is close to an optimal pressure for water-dissolved CO₂ injection, based on the variation of CO₂ solubility as a function of pressure and the costs of CO₂ compression (Gislason *et al.*, 2018; Snaebjornsdottir *et al.*, 2020).

A schematic illustration of the CarbFix1 injection system is shown in Figure 4.17. The buoyancy of the CO₂ gas bubbles depends on the density difference between the water and the gas and the size of the bubble. The smaller the bubble, the less buoyancy. Furthermore, a critical water velocity is needed to overcome this buoyancy force. The bubbles dissolved during their descent



down the well from about 350 to 540 m depth within the polyethylene mixing pipe. This descent takes four and a half minutes on average (Sigfusson *et al.*, 2015). At the applied CO₂ pressure and at about 20 °C the *in situ* pH of the fully CO₂-charged water is 3.89 ± 0.1, due to the 0.82 mol/kg solubility of CO₂ at these conditions and the dissociation of the dissolved carbonic acid.

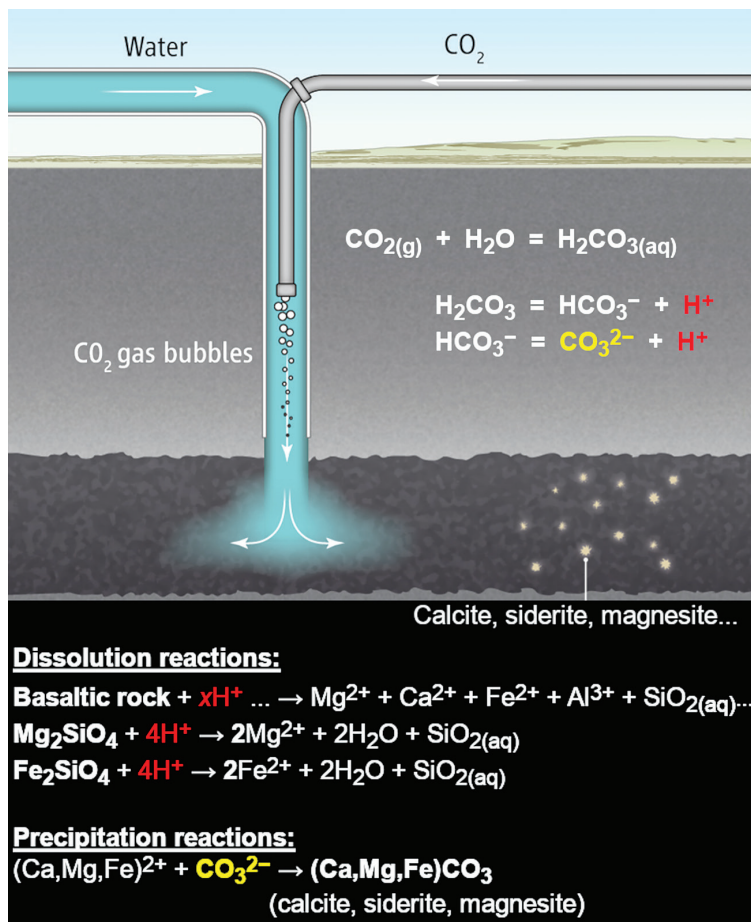


Figure 4.17

Carbon storage in basaltic rocks *via* the CarbFix1 method. The CO₂ is dissolved into water during its injection into porous basaltic rocks. No cap rock is required because the dissolved CO₂ is not buoyant once it is dissolved. Solubility trapping occurs immediately (Sigfusson *et al.*, 2015). The CO₂-charged water is denser than the formation water and has the tendency to sink. Over time the bulk of the carbon is trapped in minerals *via* the reactions shown in this figure. Modified from Gislason and Oelkers (2014).



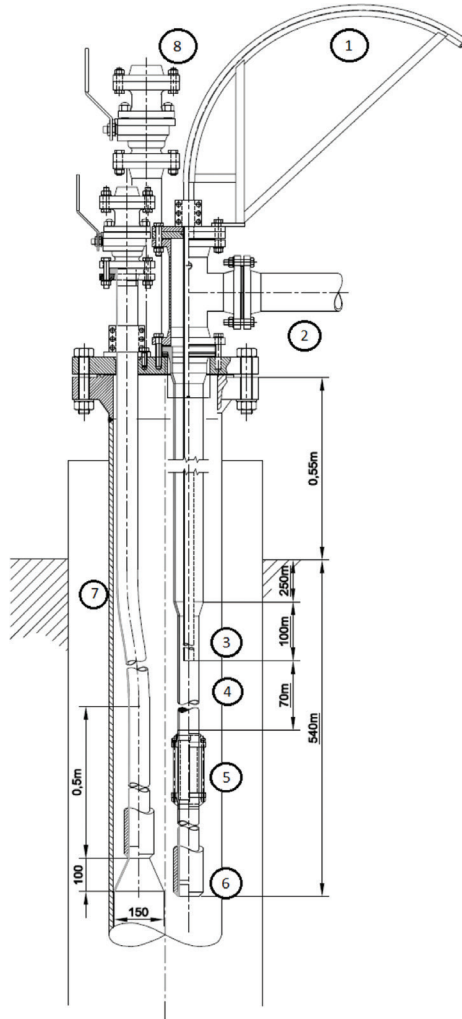


Figure 4.18

Design of the carbon dioxide injection system used during CarbFix1. The natural water level in the injection well HN-02 is about 100 m below the surface. (1) Polybutylene CO₂ injection pipe, (2) polyethylene water injection pipe, (3) stainless steel CO₂ sparger located at a depth of 330–360 m, (4) outer polyethylene mixing pipe extending to a depth of 540 m, (5) a Kenics, 1.5-KMS-6 static mixer located at 420 m, (6) fluid outlet at 540 m, (7) a polyethylene service pipe for downhole sampling and observations, spotted with holes for camera observations, (8) a service entry to well headspace. Modified from Sigfusson *et al.* (2015).



A detailed design of the injection equipment and a photo of the HN-02 injection wellhead are shown in Figures 4.18 and 4.19. The CO₂ and H₂O were injected *via* separate polybutylene and polyethylene pipes, respectively. The CO₂ is injected *via* the sparger into the downflowing H₂O. The sparger consisted of a 0.67 m long stainless steel pipe with the lowest 0.57 m containing 54 spirally aligned 1 mm holes, ensuring release of sufficiently small gas bubbles so that they were carried in the water stream to greater depths in the injection well. The mixture was carried from the sparger *via* a polyethylene mixing pipe that has a smaller diameter than the inlet polyethylene water pipe. Hence the water velocity increased as the CO₂ bubbles were released into the down going water stream. This water velocity acceleration helps to overcome the buoyancy force of the gas bubbles. The pipe extended down to 540 m where the CO₂-charged water was released to the bare subsurface rocks. A Kenics, 1.5-KMS-6 static mixer was located at a depth of 420 m to aid CO₂ dissolution.



Figure 4.19 The HN-02 injection wellhead with the attached polybutylene CO₂ gas pipe, polyethylene water pipe, sampling pipe for high pressure sampler and video camera, and opening into the headspace above the water level. The graduate students that monitored the well fluids before, during and after the injection are also shown from left to right; Sandra Snaebjornsdottir, Kiflom Mesfin, and Helgi Alfredsson.

The temporal variation of the CO₂ and H₂O injection rates during 2011 and 2012 is shown in Figure 4.20. Overall, 175 t of pure CO₂ were injected into the subsurface in dissolved form together with approximately 5,000 t of H₂O from 15 to 17 March 2011 and 10 January to 15 March 2012. Following the injection of

the pure CO₂ stream, a mixture of CO₂ and H₂S gas captured directly from the powerplant was injected into the system between June and August 2012. The typical fluid injection rate was 1800 g s⁻¹. To focus and to accelerate the subsurface flow of the gas-charged water into the monitoring wells, about 1 kg s⁻¹ of fluid was pumped out of well HN-04 and about 1 kg s⁻¹ from well HK-34 during and after the injection. Verification of the complete dissolution of CO₂ during its injection was done using a digital downhole camera and by high pressure well water bailer sampler (Alfredsson *et al.*, 2015; Sigfusson *et al.*, 2015). Digital images and videos were taken using a slimline water well inspection camera on 16 March 2011 at depths from 90 to 550 m. The camera and the high pressure bailer travelled within the service pipe (number 7 in Fig. 4.18), outside the polyethylene mixing pipe (number 4 in Fig. 4.18). No bubbles were observed by this camera at the 540 m depth of the subsurface feed zone (Sigfusson *et al.*, 2015). As shown in Figure 4.20, the measured *in situ* dissolved inorganic carbon concentration of the fluid sampled near the end of the polyethylene mixing pipe, using a high pressure bailer (Alfredsson *et al.*, 2015), was on average within 5 % of the 0.82 mol/kg. This is equal to the DIC concentration calculated based on the measured CO₂ and H₂O mass flow rates into the well and the measured fluid pH was 3.89 ± 0.1. This measurement thus confirms the complete dissolution of the CO₂ during its injection (Sigfusson *et al.*, 2015).

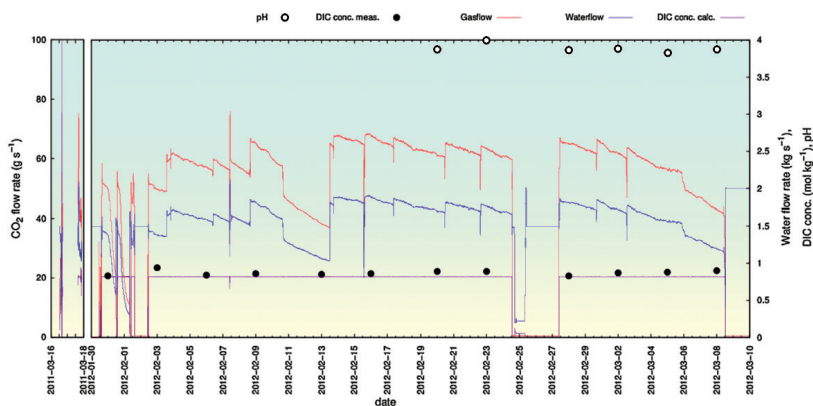


Figure 4.20 Temporal evolution of the fluid flow rates, fluid pH and dissolved organic carbon concentration in the CarbFix1 HN-02 injection well during 2011 and 2012. The CO₂ and H₂O injection rates are shown by the red and blue curves, respectively. Dissolved CO₂ concentrations (DIC) determined by mass balance are shown by the purple line, measured dissolved CO₂ concentrations are shown as black dots and measured *in situ* fluid pH values are shown as white circles. Gas and water pressures at the wellhead were between 20–25 bar and 0.5–1.5 bar, respectively, during injection. From Sigfusson *et al.* (2015) with permission from Elsevier.



4.5.2 The Chemistry of the Monitoring Well Fluids

Carbon dioxide-charged water is corrosive and dissolves both crystalline and glassy basalt as it penetrates the host rock (Oelkers *et al.*, 2008; Gislason *et al.*, 2010). Simplified reactions of this process for olivine and basalt dissolution are provided in Figure 4.17. Note that the reaction for basalt dissolution in this figure is not balanced. The dissolution of the host silicate rocks releases divalent metals, Ca, Mg, and Fe, together with other elements like Na, Si and Al, while H^+ is consumed, causing pH and dissolved carbonate (CO_3^{2-}) concentrations to increase. These changes provoke carbonate mineral precipitation at some distance from the injection well. The above series of processes is clearly evidenced by the compositions of the fluids collected from the HN-04 monitoring well. A schematic cross section showing the location of this HN-04 diverted monitoring well is provided in Figure 4.21.

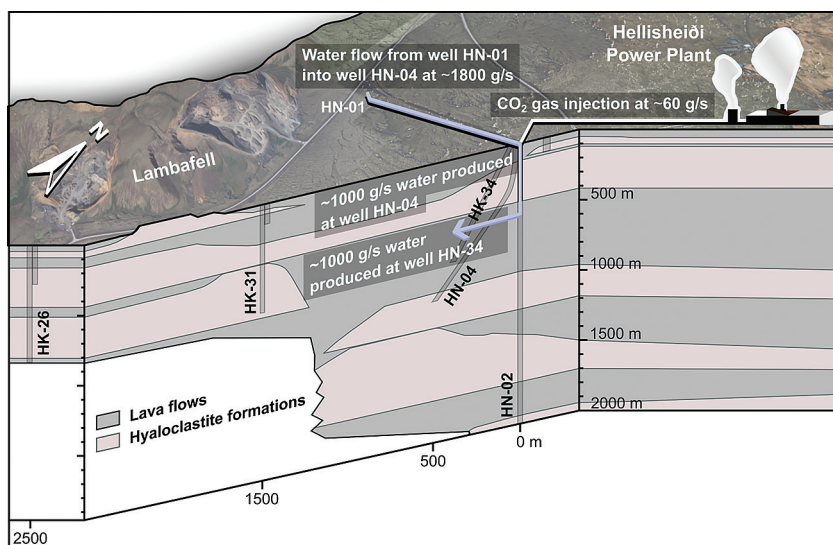


Figure 4.21 Geological cross-section of the CarbFix1 injection site, showing the location of the HN-01 water source well, the HN-02 injection well and HN-04, the first diverted monitoring well. The CO_2 and later a CO_2 - H_2S gas mixture fully dissolved in HN-01 water within the HN-02 injection well at the depth interval of 350–540 m. Fluid samples were collected from the source well HN-01, the injection well HN-02 and the closest monitoring well HN-04. Modified from Alfredsson *et al.* (2013).

We followed the progress of the subsurface reactions by the regular collection and analysis of fluid samples collected from the HN-04 monitoring well. The pH of these fluids first decreased from its original 9–10 value down to 6.5 and subsequently increased to its pre-injection values in 1–2 years as shown

in Figure 4.22. This pH behaviour stems from subsurface basalt-fluid reactions. The initial decrease in pH is indicative of the arrival of the carbonic acid acidified the water, as is confirmed by the measured dissolved inorganic carbon (DIC) concentrations that are also shown in Figure 4.22; a peak in DIC concentration coincides with the decrease in pH of the monitoring fluids. Over time the acidity was neutralised with a base, basaltic rock, the most massive “base” in the Earth’s crust. Near the injection well, the major basaltic minerals and glass were under-saturated in the pH 3.9 gas-charged injection fluid, resulting in porosity production. At some distance away from the injection well, this acid is neutralised and secondary minerals precipitate. The secondary minerals consume pore volume and might eventually clog up the flow paths. If CO₂ is continuously injected, however, the “CO₂ plume” and precipitated carbonate and other secondary minerals “travel” downstream by re-dissolution and precipitation as shown in Figures 4.15 and 4.16 (Aradottir *et al.*, 2012, 2015). As the CO₂ and secondary mineral plume moves from the injection well, the volume available for mineral precipitation increases, potentially further limiting the risk of flow path clogging.

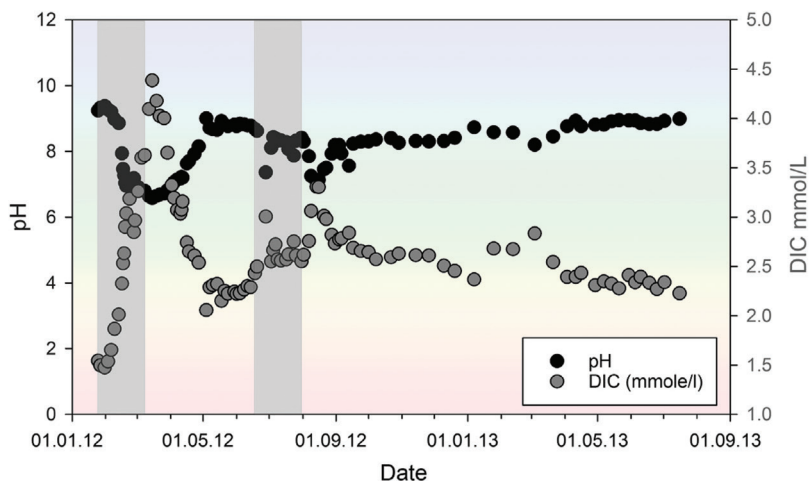


Figure 4.22 Measured values of the pH and dissolved inorganic carbon concentration (DIC) of the fluids collected from the HN-04 monitoring well before, during and after the CarbFix1 injections. The timings of both the pure CO₂ and the subsequent CO₂ + H₂S gas injections are indicated by grey bars. Modified from Snaebjornsdottir *et al.* (2017).

The concentrations of Ca, Mg, Fe and Si in the monitoring well fluids before, during and after the CarbFix1 injections are shown in Figure 4.23. The concentration of each of these elements rose rapidly as soon as the gas-charged water arrived, consistent with the dissolution of the subsurface basalt by the



injected acidic CO₂-charged waters. The Fe concentration was brought down to pre-injection values shortly after the injections, Ca about 500 days after the injection and Mg in less than 300 days after the injection.

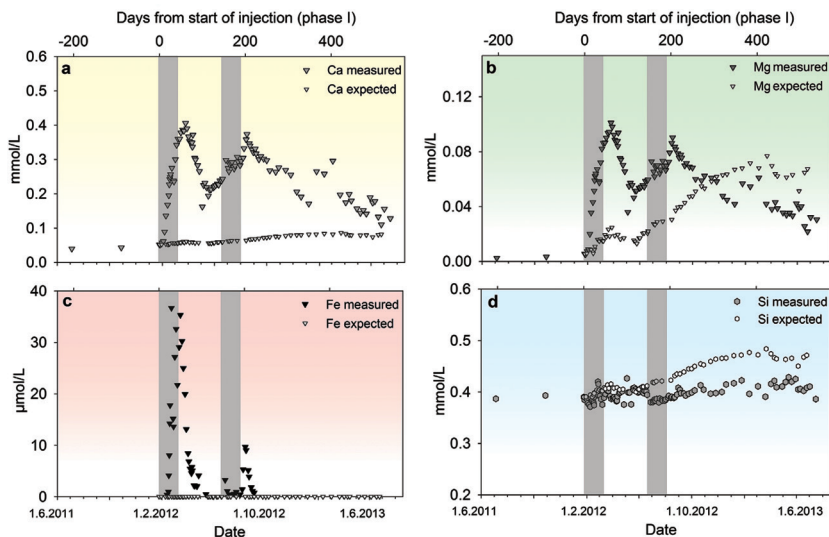


Figure 4.23

Comparison of calculated and measured Ca, Mg, Fe and Si concentrations in samples collected from the HN-04 monitoring well prior to, during and after the injection of CO₂ and CO₂/H₂S into the CarbFix1 subsurface storage site. The timing of both the pure CO₂ and the subsequent CO₂ + H₂S gas injections is indicated by grey bars. The “expected” concentrations were determined by assuming that the only subsurface process was the mechanical mixing of the injected gas-charged water and subsurface formation water. The “expected” concentrations were generated from mass balance constraints, taking into account the measured concentrations of conservative tracers. Modified from Snaebjornsdottir *et al.* (2017).

4.5.3 The Saturation State of the Monitoring Well Fluids

The measured dissolved element concentrations in the monitoring well fluids were used to calculate the saturation state of these fluids with respect to potentially precipitating secondary minerals. The results of some of these calculations are shown in Figure 4.24. As shown in this figure, the sampled monitoring well fluids were saturated with respect to siderite about four weeks after the injections began, then the fluids reached calcite saturation about three months after each injection. Several other carbonates were saturated or supersaturated at some stage during or after the injection, but magnesite never became saturated (Snaebjornsdottir *et al.*, 2017). Such results indicate the capacity of these fluids to fix CO₂ in



stable carbonate minerals in the subsurface. Pyrite was supersaturated prior to and during the mixed gas injection and in the following months, indicating the ability of this system to fix the injected H_2S by precipitating pyrite. The likelihood that these minerals being precipitated is indicated by the concentrations of Ca and Fe in the monitoring well fluids, as they decrease considerably after peaking upon the arrival of the initial DIC plume.

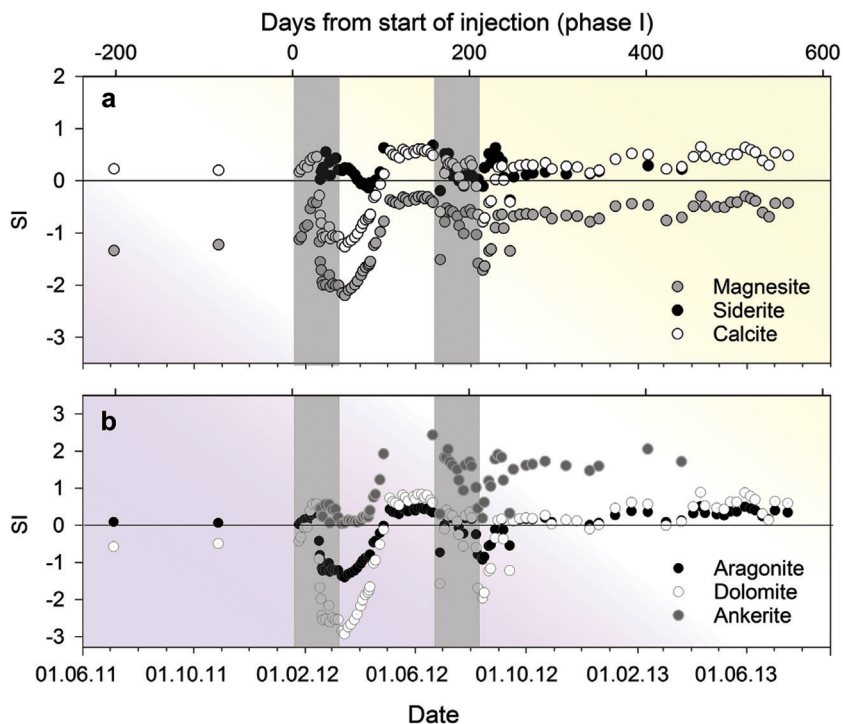


Figure 4.24 Saturation indices (SI) of HN-04 monitoring well water samples before, during, and after the injection of pure CO_2 and a CO_2 - H_2S gas mixture with respect to (a) magnesite, siderite and calcite, (b) dolomite, aragonite and ankerite. All saturation indices were calculated assuming the oxygen fugacity was controlled by equilibrium of the H_2S/SO_4^{2-} redox couple. The timing of both the pure CO_2 and the subsequent $CO_2 + H_2S$ gas injections is indicated by grey bars. Modified from Snaebjornsdottir *et al.* (2017).



4.5.4 Quantifying the Mass of CO₂ Fixed in Minerals

Critical to any carbon storage project is the quantification of the exact amount of carbon stored. This is a challenging task in the subsurface, which we overcame with the use of a suite of non-reactive tracers (Matter *et al.*, 2016; Snaebjornsdottir *et al.*, 2017, 2018). The approach itself is simple. The non-reactive tracers are injected into the subsurface in a constant proportion to the CO₂. Any changes in the tracer to DIC proportion of the monitoring well fluids indicated the fixation or liberation of CO₂ from the subsurface rocks. Two non-reactive tracers were used in CarbFix1, 1) volatile sulfur hexafluoride (SF₆) during the pure CO₂ injection, and 2) volatile trifluoromethyl sulfur pentafluoride (SF₅CF₃) during the CO₂-H₂S gas mixture injection. An additional reactive isotopic tracer, ¹⁴C was also co-injected with CO₂ during CarbFix1. Fluid samples for SF₆, SF₅CF₃, and ¹⁴C analyses were collected without degassing using a high pressure sampler from the injection well HN-02 (Alfredsson *et al.*, 2015) and with a submersible pump from the first monitoring well, HN-04. The temporal variation in the conservative tracer concentrations in the HN-04 monitoring well during and after the injections is shown in Figure 4.25. The arrival of the injectate from the pure CO₂ injection at the monitoring well HN-04 was confirmed by an increase in SF₆ concentrations. The arrival of this tracer coincided with a sharp decline in pH and increase in DIC. The SF₆ data suggest that the initial breakthrough peak in HN-04 occurred 56 days after injection. Subsequently, the SF₆ concentration slightly decreased before a further increase in concentration occurred, with peak concentration 406 days after initiation of the injection (Matter *et al.*, 2016). This double peak in the conservative tracer under forced flow is similar to the first Na-fluorescein tracer test, shown in Figure 4.14 (Khalilabad, 2008; Khalilabad *et al.*, 2008), suggesting that the subsurface contained a relatively homogenous porous media intersected by a low volume and fast flow path that channels about 3 % of the tracer flow between HN-02 and HN-04. The conservative SF₅CF₃ tracer co-injected with the CO₂-H₂S gas mixture injection behaves similarly (Fig. 4.25); its initial arrival peak was detected 58 days after initiation of the CO₂-H₂S injection.

We quantified the fate of the injected CO₂ using mass balance equations based on these tracer concentrations (Matter *et al.*, 2016). The DIC concentrations of the monitoring well fluids in the absence of any reaction could be calculated by simply multiplying the measured tracer concentration by the constant tracer to CO₂ injection ratio, after taking account of the background DIC concentration. The results of these calculations are compared to the measured DIC concentrations in Figure 4.26. The DIC and ¹⁴C concentrations expected in the absence of chemical reactions are far higher than those measured in monitoring well samples indicating a loss of DIC and ¹⁴C along the subsurface flow path from the injection to the monitoring well. The differences between calculated and measured DIC and ¹⁴C in Figure 4.26 indicate that >95 % of the injected CO₂ was mineralised through water-CO₂-basalt reactions between the HN-02 injection and the HN-04 monitoring wells within 2 years. All evidence points to this lost carbon precipitating as carbonate minerals.



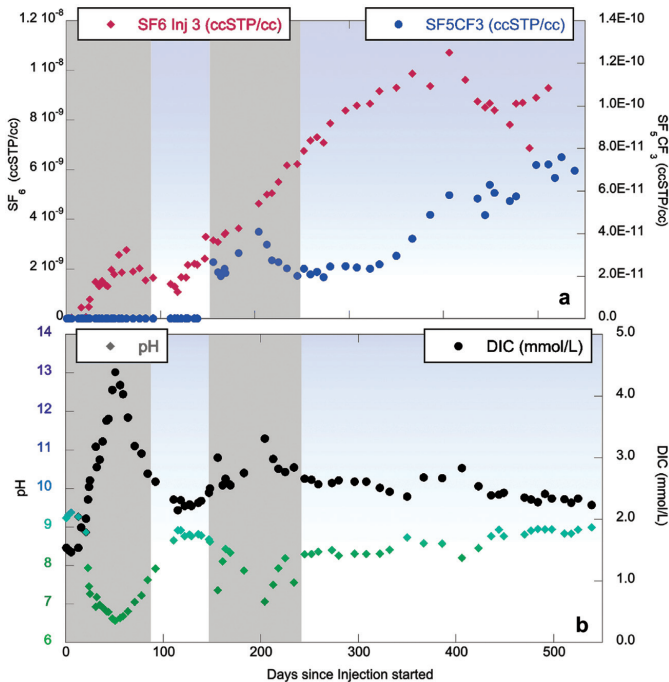


Figure 4.25 Temporal evolution of SF₆ and SF₅CF₃ tracer concentrations over time in monitoring well HN-04 during and after the CarbFix1 injections. Reproduced for comparison are the corresponding measured pH and DIC of these fluids. The shaded area indicates the timing of the pure CO₂ injection and CO₂-H₂S injections into the CarbFix1 site. Modified from Matter *et al.* (2016).

Corresponding mass balance calculations were made for the concentrations of Ca, Mg, Fe, and Si as shown in Figure 4.23. In each case the measured concentrations differ from the corresponding values calculated from measured non-reactive tracer concentrations on the assumption that there were no subsurface reactions. For the case of Si, the measured concentration is lower than the corresponding calculated values, consistent with the continuous dissolution of the host basalt coupled to the precipitation of Si as chalcedony; note that chalcedony readily precipitates at the low pH of the injected gas-charged fluids. The measured concentrations of Ca, Mg, and Fe are much higher than their calculated counterparts and then these values tend to converge with time. This behaviour is consistent with the initial release of these elements from the basalt and their subsequent precipitation in secondary carbonate and/or sulfide minerals as pH increases.



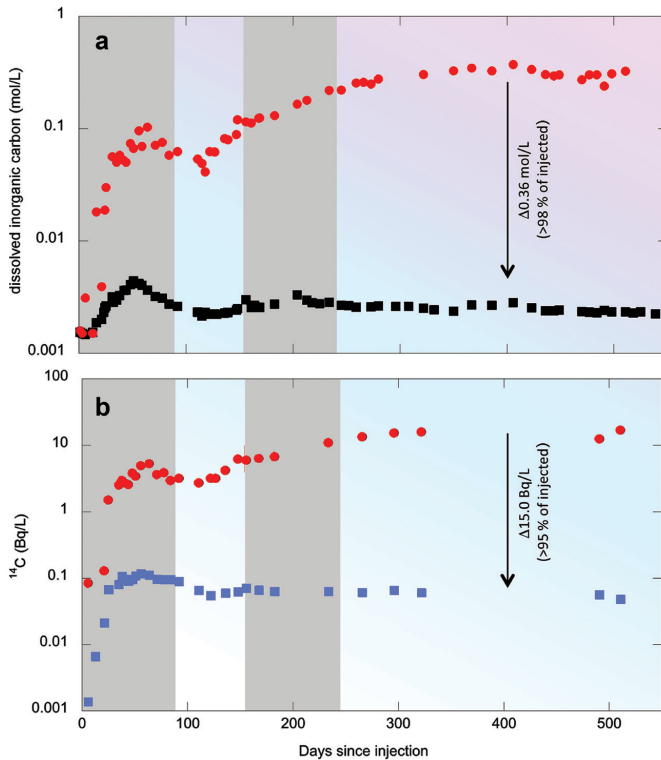


Figure 4.26

Comparison of calculated and measured DIC and ^{14}C concentrations in the HN-04 monitoring well fluids. The calculated values were generated assuming a non-reactive mechanical mixing of the HN-01 CO_2 -charged injection water and the formation water as measured in the monitoring well HN-04 before injection. **(a)** Time series of calculated (red solid circles) versus measured (black solid squares) DIC (mol/kg) in monitoring well HN-04. The difference between these points indicates the >98 % conversion of injected CO_2 to carbonate minerals. **(b)** Time series of calculated (red solid circles) versus measured (blue solid squares) $^{14}\text{C}_{\text{DIC}}$ (Bq/litre) in monitoring well HN-04. The difference between these points indicates that >95 % of the injected CO_2 was converted to carbonate minerals. The shaded area indicates the pure CO_2 injection and $\text{CO}_2\text{-H}_2\text{S}$ injection period. Modified from Matter *et al.* (2016).

The conclusion that the injected carbon dioxide was fixed as carbonate minerals was also confirmed by direct observation of precipitated minerals. After 550 days, the submersible pump used to sample the HN-04 monitoring well broke down after continuous pumping for more than 550 days. This resulted in a 3 month gap in the monitoring data. When brought up for inspection, the pump was clogged and coated with calcite containing the ^{14}C labelled carbon we injected.

The fast conversion rate of dissolved CO₂ to calcite minerals in the CarbFix1 storage reservoir is most likely due to a number of factors, including (1) the injection of water-dissolved CO₂ into the subsurface, (2) the relatively rapid dissolution rate of basalt, consuming H⁺ and releasing Ca, Mg, and Fe ions required for the CO₂ mineralisation, (3) the mixing of injected water with pH 9–10 formation waters, and (4) the dissolution of pre-existing secondary carbonates at the onset of the CO₂ injection. This latter factor may have contributed to the neutralisation of the injected CO₂-rich water *via* the reaction $\text{CaCO}_3 + \text{H}^+ = \text{Ca}^{2+} + \text{HCO}_3^-$. The dissolution of pre-existing calcite is supported by the ¹⁴C/¹²C ratio of the collected fluid samples, suggesting a 50 % dilution of the carbon in the fluid, most likely *via* calcite dissolution just after the gas-charged water arrived in the basaltic reservoir. Nevertheless, the mass balance calculations clearly demonstrate that these pre-existing carbonates re-precipitated during the mineralisation of the injected CO₂ (Matter *et al.*, 2016).

CarbFix1 generated a new, more rapid pathway to generating the secure storage of CO₂ through mineralisation in the subsurface, as summarised in Figure 4.27. The CO₂ is dissolved within minutes as it is co-injected with water into the subsurface. The CO₂ charged water accelerates the dissolution of the reactive rocks in the reservoir and the storage of CO₂ within carbonate minerals within several years. This is orders of magnitude more rapid than the conventional CCS approach of injecting a pure CO₂ phase into a non-reactive sedimentary basin.

4.5.5 Development of Novel Isotopic Tracers to Quantify the Fate of CO₂ Injected into the Subsurface

The improved understanding of the fractionation factors of stable metal isotopes provided us with the opportunity to use the isotopic compositions of the CarbFix1 rocks and fluids to further clarify the fate of CO₂ injected into the subsurface. Notably both Mg and Ca have a number of stable isotopes that fractionate distinctly in response to the precipitation of minerals. The measurement of the isotopic compositions of the sampled CarbFix1 monitoring well fluids before, during, and after the injection of CO₂, together with the measured isotopic compositions of the basalt in the CarbFix1 reservoir enabled us to both confirm the identity of the precipitated carbonate minerals and to develop an alternative method to determine the mass of CO₂ fixed as calcite in the subsurface.

Magnesium isotopes exhibit a distinct behaviour during the formation of secondary silicate minerals compared to secondary carbonate minerals. Mg-bearing clay minerals preferentially take up isotopically heavy Mg, whereas Mg-bearing carbonate minerals preferentially take up isotopically light Mg (*e.g.*, Pogge von Strandmann *et al.*, 2008; Mavromatis *et al.*, 2012, 2014; Teng, 2017). This difference makes Mg isotope compositions of coexisting fluids and rocks an effective tool for identifying the fate of Mg during water-rock interaction. Taking advantage of this behaviour, Oelkers *et al.* (2019) measured Mg isotopic



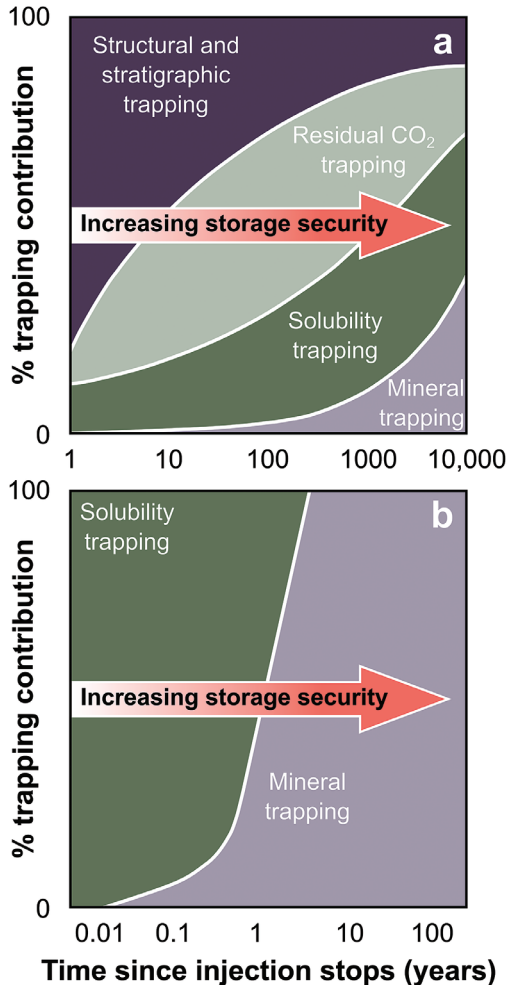


Figure 4.27

Schematic comparison of the processes of carbon storage in the subsurface by (a) conventional storage and (b) mineral storage via the CarbFix1 method. In CarbFix1 gaseous CO₂ is compressed to about 15–25 bar pressure and injected into down flowing water stream into porous reactive rocks. The gas bubbles dissolve in less than 5 minutes at about 25 °C (leading to rapid solubility trapping). No cap rock is required because the dissolved CO₂ is not buoyant and does not migrate back to the surface. This CO₂ charged water is corrosive with pH less than 4, leaches divalent cations from the rocks, eventually leading to supersaturation with respect to carbonates and sulfides at some distance from the injection well, resulting in mineral trapping of the water soluble gases within 2 years. In contrast, mineralisation of injected CO₂ by conventional carbon storage may take thousands of years if mineralisation occurs at all. Modified from Snaebjornsdottir *et al.* (2017).



compositions of the CarbFix1 monitoring well fluids over time. These results are shown in Figure 4.28. The measured fluid Mg compositions are isotopically lighter than the basalts present in the subsurface reservoir and continue to become increasingly lighter for at least two years after the gas-charged water injection was stopped. The results indicate the formation of isotopically heavy Mg clays rather than isotopically light Mg carbonates from the fluids. This conclusion is consistent with the observation that magnesite remains undersaturated during and after the CO₂ gas injections (see Fig. 4.24). Isotope mass balance calculations suggest that more than 70 % of the Mg liberated from the basalt by the injected gas-charged water was precipitated as Mg clays, with this percentage increasing with time after the injection. This interpretation is consistent with the continued precipitation of Mg clays over the whole of the study period.

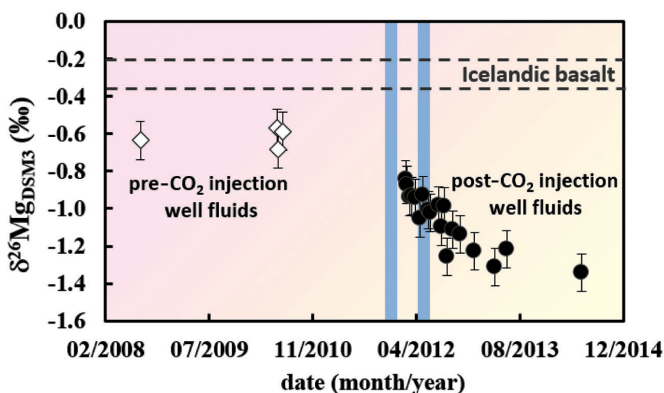


Figure 4.28

The temporal evolution of $\delta^{26}\text{Mg}$ of fluids collected from the CarbFix1 monitoring well. Open diamonds illustrate the compositions of monitoring well fluids prior to the injection, whereas the filled circles represent the compositions of monitoring well samples after the injection. The dashed horizontal lines show the compositions of the basalts at the CarbFix1 site, whereas the timing of the two CarbFix1 injections is indicated by the two blue bars. Modified from Oelkers *et al.* (2019).

In contrast to the behaviour of Mg, both silicate minerals, including zeolites and smectites, and carbonate minerals preferentially take up light Ca (Hindshaw *et al.*, 2013). Nevertheless, by assuming that calcite was the only Ca-bearing mineral precipitated in response to subsurface fluid-basalt interaction during and after the CarbFix1 injection, Pogge von Strandmann *et al.* (2019) quantified the amount of calcite precipitated, and therefore CO₂ stored by this process (Fig. 4.29). The assumption that calcite dominated Ca-bearing secondary minerals formed in the system is supported by the close correlation between the measured Ca isotope compositions and the saturation state of calcite in the sampled fluids.



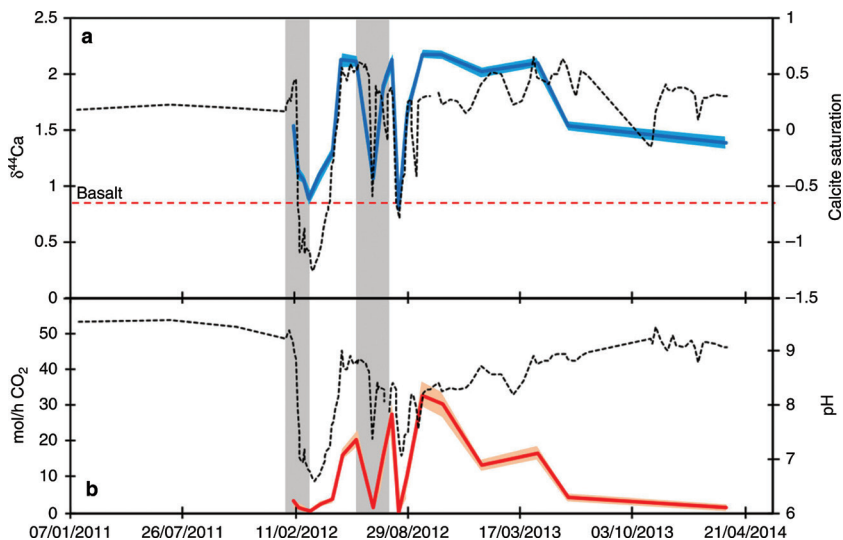


Figure 4.29

The temporal variation of calcite saturation state and Ca isotopic composition of HN-04 monitoring well fluids before, during and after CarbFix1 CO₂ injections. **(a)** Ca isotope ratios (blue line) and calcite saturation index (dotted black line). The blue shaded area represents the 2 σ analytical uncertainty of the isotope measurements. **(b)** The evolution of pH (dotted black line) and the calculated CO₂ precipitation rate based on Ca isotopes (red line). The red shaded area represents the 2 σ propagated uncertainty of the individual precipitation rates. The grey shaded areas represent the CO₂ injection periods. From Pogge von Strandmann *et al.* (2019).

The Ca isotope ratios of the CarbFix1 fluids rapidly increase with the pH and calcite saturation state, consistent with calcite precipitation. In total, this analysis of Ca isotope compositions suggests that 165 ± 8.3 tons of the injected CO₂ were precipitated into calcite, an overall carbon storage efficiency of 72 ± 5 % of the total 230 ton CO₂ injected. The non-reactive tracer approach illustrated in Figure 4.23 suggests that 95 to 98 % of the 230 ton injected CO₂ mineralised (Matter *et al.*, 2016). Both approaches concur that most of the injected CO₂ was efficiently fixed in carbonate minerals due to subsurface basalt-fluid interaction.

The results of these isotopic studies indicate that the precipitation of Ca carbonate dominated over those of Fe and Mg carbonates following the CarbFix1 injection. During continuous large scale CO₂ injections, however, a higher partial pressure of CO₂ might increase the role of Fe and Mg carbonate precipitation as suggested by modelling (Gysi and Stefansson, 2011; Snaebjornsdottir *et al.*, 2018), experiments (Clark *et al.*, 2019) and natural analogues (Rogers *et al.*, 2006). Such removal of CO₂ by the precipitation of Fe- and/or Mg-bearing carbonate

minerals could account for the lower carbonation estimate obtained from Ca isotope mass balance considerations, compared to the more direct measurement of dissolved inorganic carbonate measurements (e.g., Fig. 4.26).

4.5.6 Toxic and Trace Element Mobility in Response to the CarbFix1 Injections

A major concern we had during the CarbFix1 injection is that the dissolution of basalt, due to its interaction with the acidic, CO₂-charged injection water would increase the mobility of toxic and heavy metals. Basalts commonly contain significant amounts of toxic metals; numerous past studies have provided evidence for the trace element mobility during water-basalt interaction (e.g., Humphris and Thompson, 1978). There is evidence for the initial mobilisation of metals during the CarbFix1 injection. Just after the first arrival of the CO₂-charged water that passed through the fast flow path that transmitted about 3 % of the injected gas-charged waters towards the HN-04 monitoring well, the concentrations of Ba, Sr, Fe, Mn, Co, Ni and Zn rose sharply (Snaebjornsdottir, 2017). At the same time, however, the concentrations of Al, As, and V fell abruptly. Other trace and toxic metal concentrations were scattered in these fluids, probably because their concentrations were close to the analytical detection limit. The monitoring well fluid Pb and Cr concentrations were elevated just after the beginning of the second, H₂S-bearing injection (Snaebjornsdottir, 2017). All these elements can affect the quality of drinking water (although the water in the CarbFix1 reservoir is not intended for human consumption). The concentrations of none of these elements exceeded the health based values allowed for drinking water, as specified by the World Health Organization (WHO) (World Health Organization, 2017). The highest Fe concentrations, however, in some of the collected monitoring well fluids exceeded values proposed by the European Commission (European Commission, 2015) for the acceptability of drinking water.

The concentrations of all these metals decreased over time as the fluid pH increased. It seems likely that these metals were immobilised by their co-precipitation with carbonates, sulfides and/or other secondary minerals, similar to the processes in the natural analogues described in Section 4.4 (Flaathen *et al.*, 2009b; Olsson *et al.*, 2014a,b).

The role of fluid pH in immobilising toxic and heavy metals is also evident when comparing the measured fluid concentrations of the CarbFix1 monitoring well fluids with those of the reactive fluids collected in the high pressure laboratory column experiments of Galeczka *et al.* (2014) described in Section 4.4. The concentrations of Fe, Mn, Cr, Al, and As collected from the column experiments all exceeded the European and Icelandic standards for allowable concentrations in drinking and surface waters (Galeczka *et al.*, 2014; Umhverfisráðuneyti, 2001). Note, however, that the minimum pH of the CarbFix1 monitoring well fluids was 6.5 but the pH during the high pressure laboratory column experiments was 4.5. The higher pH of fluids in CarbFix1 favour the precipitation of a number of secondary phases that could scavenge trace and toxic elements.



4.5.7 The Co-Injection of CO₂ + H₂S and End of the CarbFix1 Injections

Once all of the purchased 175 tons of CO₂ were injected into the subsurface, efforts were made to inject a combination of CO₂ and H₂S captured directly from the Hellisheiði powerplant into the CarbFix1 site. This effort experienced some growing pains as the gas capture plant at Hellisheiði was still in development. The mass of gas available to inject was irregular and its flow often stopped for several days or up to a week. After a 48 day long injection period of which only 29 days were active, the CarbFix1 injection well became clogged. Only 73 tons of the gas mixture were injected, of which 58 tons were CO₂, 14 tons H₂S and 0.35 tons H₂. This clogging perplexed us, and we sought to understand and resolve the issue. A simple way to recover the injectivity of a well is to reverse the flow for a short time by airlifting, clearing out debris in the well. This process was unsuccessful in restoring the injectivity of the well. We thought that it was possible that the irregular composition of the fluids injected into the well, and in particular changes in the pH of this fluid, which increased from 3.9 to >9, while gas injection was stopped but while water injection continued, provoked the formation of well-clogging secondary minerals near the injection well. We thought of injecting some dilute acid to help dissolve these minerals.

This mystery was resolved eventually, however, by Benedicte Menez and her research group in Paris. This group collected water from both the CarbFix1 monitoring wells and injection wells before and after the clogging of the injection well (Trias *et al.*, 2017). They observed a bloom in lithoautotrophic iron oxidising bacteria. The bloom likely led to the blocking of fluid flow paths near the injection well. The cause of this bacterial bloom was likely the changing oxidation state of the injected fluids containing H₂S. At that time we were unaware that the petroleum industry commonly co-injects biocide to avoid such issues (*e.g.*, Youssef *et al.*, 2009). The demonstration of bioclogging at the CarbFix1 site motivated Daval *et al.* (2018) to argue that much of the carbon stored by CarbFix1 injections was due to the formation and growth of subsurface biota. Such speculative claims, however, are inconsistent with the carbon isotope compositions of the CarbFix1 monitoring well waters, which are, in contrast, consistent with the fixation of the injected CO₂ within carbonate minerals.

4.5.8 CarbFix1 Epilogue

The original CarbFix1 injection site remained unused for roughly 6 years, although through the efforts of Reykjavík Energy, the injectivity of the injection well has been recovered, and is again being used for subsurface carbon storage. Starting in September 2020, the Orca project, a combined effort of the Carbfix company and Climeworks, captures about 4,000 tons *per* year of pure CO₂ directly from the atmosphere. This CO₂ has been and is still being injected at the CarbFix1 site using the CarbFix1 approach, with an injection rate similar to that of the original CarbFix1 injection rates. To date, no detailed monitoring results are available for this more recent injection.



With CarbFix1 we demonstrated that more than 95 % of 233 tons of injected CO₂, labelled with ¹⁴C and co-injected with non-reactive tracers, were mineralised in less than two years (Sigfusson *et al.*, 2015; Matter *et al.*, 2016; Snaebjornsdottir *et al.*, 2017; Pogge von Strandmann *et al.*, 2019; Oelkers *et al.*, 2019). As part of the CarbFix1 project we trained 11 PhD students and several postdocs in the various aspects of the CarbFix method for subsurface carbon mineralisation. Many of these students and postdocs are now employed by the Carbfix company and at research institutes worldwide, promoting carbon capture and storage.

4.6 CarbFix2

The CarbFix2 project was designed to upscale the original CarbFix1 project into a functioning, cost effective ongoing industrial process. This goal required both several additional technological developments and the use of a larger subsurface system than used in the original CarbFix1 injection. One major technological advance by CarbFix2 was the development of a relatively low cost and effective scrubber to capture CO₂ from the emissions of the Hellisheiði power plant. A schematic illustration of this scrubber is shown in Figure 4.30. What makes this system so effective is its simplicity. Pure water, obtained from condensed powerplant steam, and the emission gas from the powerplant are pressurised to 6 bars. The water is released into the top of the scrubbing tower as a shower and descends to the bottom of the tower; the exhaust gas is released into the bottom of the scrubbing tower and ascends to the top of the tower. The average composition of the gas mixture as it enters the scrubber tower is 63 vol. % CO₂, 21 vol. % H₂S, 14 vol. % H₂, and 2 vol. % of other gases, predominantly N₂, Ar, and CH₄. The scrubbing tower is filled with plastic pellets to enhance the interaction between the water and the exhaust gas. By the time the water reaches the bottom of the tower it is close to saturated with respect to CO₂ and H₂S. Note that the H₂S present in the exhaust stream has a solubility and acidity similar to that of CO₂, so they tend to dissolve into water in similar proportions. The exhaust gas, depleted in one third of CO₂ and nearly all of H₂S, is released to the atmosphere at the top of the scrubbing tower. The gas-charged water is then further pressurised to 9 bars and transferred to the injection well at this pressure.

The injection and mineralisation of the larger mass of CO₂ and H₂S captured from the powerplant required a larger subsurface mineral storage site. The cross-section of the CarbFix2 system is shown in Figure 4.31. This system has several important differences from the original CarbFix1 injection site. First it is substantially deeper; the target aquifers are approximately ~ 2,000 m below the surface; second, it is considerably warmer, the rocks in the target subsurface reservoir have a temperature of 250–260 °C; and third, the rocks in the CarbFix2 target reservoir are substantially altered due to the higher temperature. The alteration of this deeper, hotter basalt results in a low primary permeability. The rocks, however, are fractured due to past and ongoing tectonic activity,



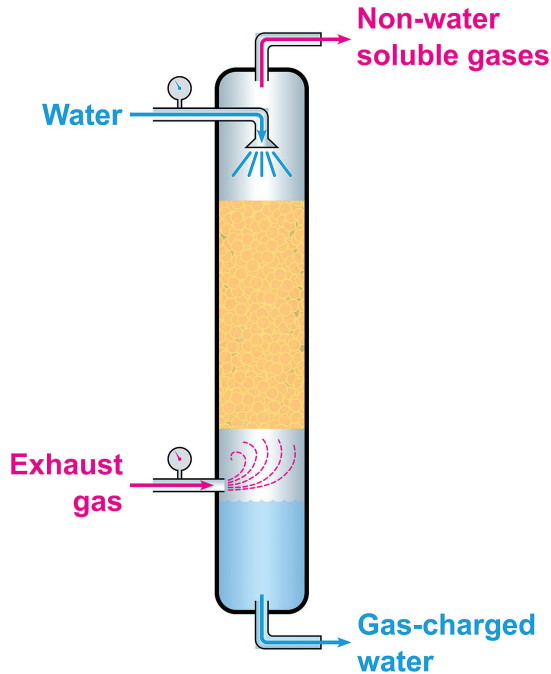


Figure 4.30 Schematic illustration of the scrubbing tower designed and in use at the Hellisheiði power plant to capture CO₂ and H₂S. The scrubbing tower is 12.5 m high, 1 m in diameter. The gas-water interaction volume in the scrubber is 4.7 m³. Nearly pure condensate water is injected into the top of the scrubber at 6 bars pressure and 20 °C. This water flows downwards as a shower and interacts with upflowing exhaust gas at this pressure while passing through a tortuous path around the plastic pellets within the scrubber. Remaining non-dissolved gases are vented at the top of the scrubbing unit and gas-charged water leaves the scrubbing tower from the bottom. From Gunnarsson *et al.* (2018) with permission from Elsevier.

providing efficient flow paths for gas-charged injection water. Both the injection and the monitoring/production wells are deviated to intersect vertical fault planes, providing high capacity flow paths as shown in Figure 4.32. The fluids in the monitoring wells are continuously produced and used in the production of electricity at the Hellisheiði power plant. The transmissivity of the injection wells can be as high as 150 kg/s.

The injection system consists of the HN-16 injection well and the HE-31, HE-48, and HE-44 monitoring wells. These three monitoring wells are located 984, 1356, and 1482 m from the injection well at the reservoir depth. The average

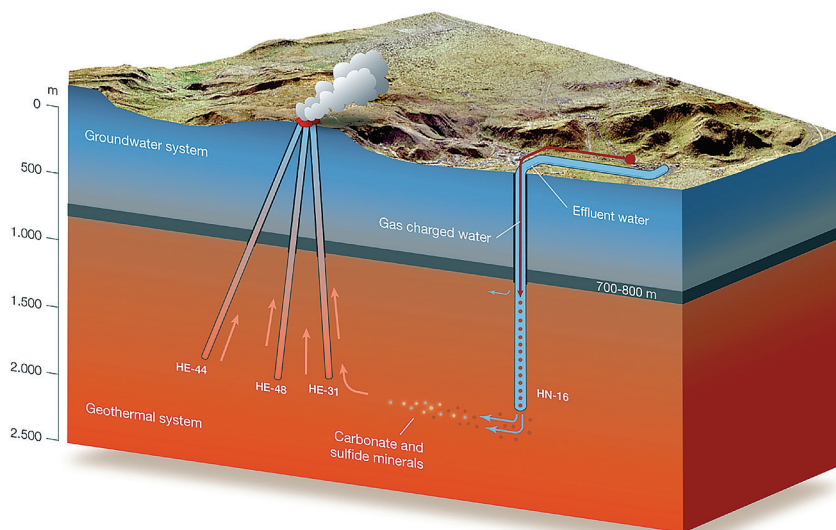


Figure 4.31 Schematic cross-section of the CarbFix2 injection site. The CO₂-H₂S gas mixture is captured in a pressurised water scrubber located next to the Hellisheiði power plant. The gas-charged water and effluent water are injected separately to a depth of 750 m into well HN-16, then allowed to mix until they enter the target aquifers at depths of 1900–2200 m. This combined fluid flows down a hydraulic pressure gradient to monitoring wells HE-31, HE-48, and HE-44 located 984, 1356, and 1482 m from the injection well at the reservoir depth. Water from the monitoring wells is constantly produced for energy generation. From Gunnarsson *et al.* (2018) with permission from Elsevier.

time for water to travel between these wells is 4, 6 and 9 months, respectively, based on inert tracer tests performed prior to the CarbFix2 project (Kristjansson *et al.*, 2016).

The injection commenced in June 2014 into well HN-16. For six months during 2015–2016 injection was also made into well HN-14 which released fluids into the same feed zone as well HN-16, for maintenance of the original injection well. Injection into well HN-16 was restarted after the maintenance was complete. In each case, the gas-charged water from the scrubbing tower was injected to a depth of 750 m, where it was released into a downflowing effluent water from the powerplant. This effluent water was the original geothermal fluid obtained from tens of production wells to generate heat and electricity at the powerplant. These fluids were co-injected with the condensed steam and gas that was separated from the geothermal fluids at various steps within the power plant. The addition of effluent water is not necessary, but this choice was made to streamline the powerplant operations. The mass of CO₂ and H₂S fixed in the subsurface was determined through the comparison of measured



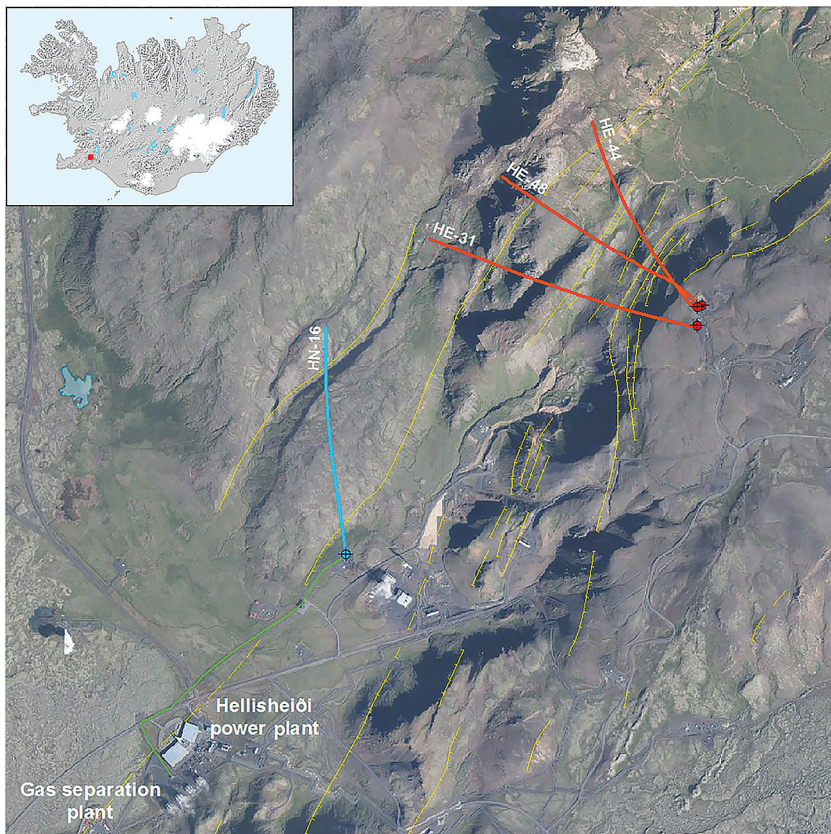


Figure 4.32 Overview of the CarbFix2 injection mineral storage site. The Hellisheiði power plant and the gas scrubbing tower are in the lower left of the figure. A 1.5 km long, gas-charged water pipe (shown in green) connects the gas scrubbing tower plant with the injection well. Injection was into well HN-16 (shown in blue). The three monitoring wells, HE-31, HE-48, and HE-44 (each shown in red) are located within 2 km down gradient from the injection well. Major faults and their relative movements are shown in yellow as well as the location of wells at the surface (blue and red dots). From Gunnarsson *et al.* (2018) with permission from Elsevier.

dissolved carbon and sulfur concentration in the monitoring well fluids, with corresponding values determined from mass balance calculations similar to those adopted in the original CarbFix1 project. For the purpose of the mass balance calculations, the inert tracer, 1-naftalensulfonic acid, was added to the injected gas-charged water at a constant proportion to the injected CO_2 and H_2S . The results of these mass balance calculations, shown in Figure 4.33, suggested

that during the first phase of the CarbFix2 injection, which lasted from June 2014 to July 2016, over 50 % of injected carbon and 76 % of sulfur mineralised within four to nine months. This time period is equal to the average time for the tracer to flow from the injection well to monitoring wells HE-31, HE-48, and HE-44 (Kristjansson *et al.*, 2016; Gunnarsson *et al.*, 2018). It was anticipated that further mineralisation of these gases continued as the injected water kept flowing in the subsurface system.

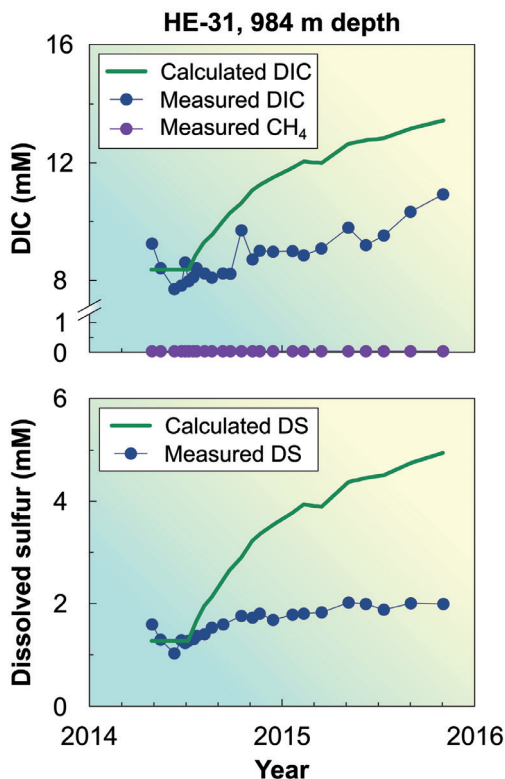


Figure 4.33

Comparison of the measured concentrations of total dissolved inorganic carbon (DIC) and total dissolved sulfur (DS) with those calculated from mass balance considerations in the HE-31 monitoring well located 984 m at depth from the HN-16 injection well. Measured concentrations are shown as blue symbols and the calculated values shown as green curves. The calculated values are based on assuming a non-reactive mechanical mixing of the injected gas-charged water with the subsurface formation fluids and taking account of the measured concentration of the 1-naftalensulfonic acid (1-ns) non-reactive tracer co-injected into the subsurface reservoir at a fixed proportion to the dissolved gases. The difference between the green curve and blue points correspond to the mass of injected gases fixed through mineralisation reactions. After Gunnarsson *et al.* (2018).



Owing to the success in mineralising injected CO₂ and H₂S over the first two years of operation, the injection rate of CO₂ and H₂S was doubled in July 2016. Dierdre Clark, one of our PhD students working with us on the CarbFix2 project, performed a detailed study of the fate of the injected gases before and after the doubling of the dissolved gas injection rate. Mass balance calculations indicated that the fraction of the injected gases fixed by mineral reactions increased four months after the doubling of the gas injection rate when over 60 % of injected carbon and over 85 % of injected sulfur mineralised within four to nine months between these wells (Clark *et al.*, 2020). This increase is attributed to the increased partial pressure of CO₂ and H₂S in the subsurface due to an increased injection rate.

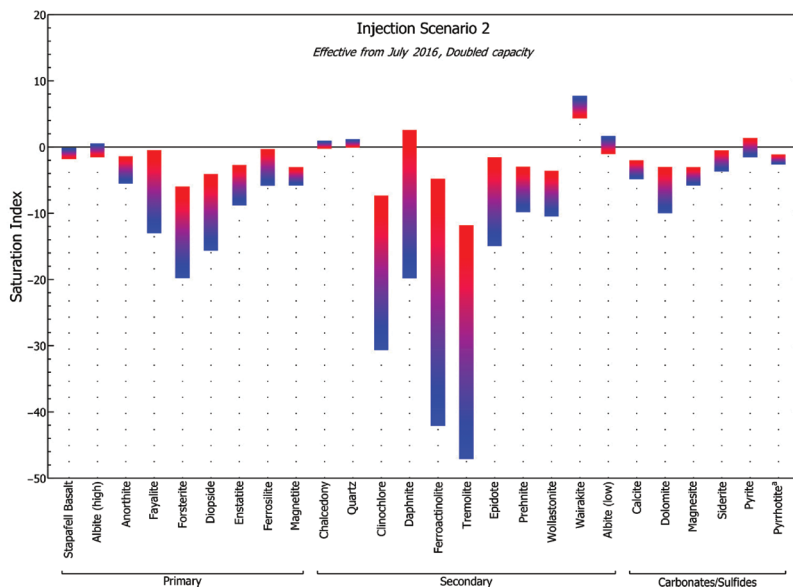


Figure 4.34

Calculated saturation indexes of primary and secondary minerals for the gas-charged fluid injected in CarbFix2, after the doubling of the injection rates in July 2016, as the fluid descended in the injection well and entered the target basaltic storage reservoir. Over this time the temperature of this water increased from 60 °C to 260 °C. The coolest temperature is represented by blue and the warmest by red. Note the starting effluent water temperature had a temperature of 80 °C. The saturation state of pyrrhotite does not increase continuously with temperature; its saturation index maximises at 150 °C. Modified from Clark *et al.* (2018).

To assess the potential for clogging the injection wells through mineral precipitation the saturation indexes of injected fluids with respect to a selection of possible minerals were calculated as shown in Figure 4.34. These calculations demonstrate that all primary minerals and glasses, and most alteration minerals,



are undersaturated in the injected gas-charged water/effluent water mixture as it leaves the injection well into the fracture-dominated basaltic aquifers (Clark *et al.*, 2018, 2020). The exceptions are chalcedony-quartz, low-albite, wairakite and pyrite. The permeability of the HN-16 injection well had increased steadily since June 2014, indicating that the dissolution of basalt near the injection well dominated over the precipitation of secondary minerals, a process that became important further away from the injection well, as observed in the monitoring wells. There calcite, dolomite, and sulfide minerals were all at saturation or supersaturated with respect to the gas-charged fluid. These minerals were saturated by the time the fluids arrived at the closest monitoring wells, as shown by the results of geochemical calculations as in Figure 4.35. Mass balance calculations indicated that sulfide precipitation was not limited by the availability of Fe or by the consumption of Fe by other secondary minerals. However, calcite precipitation was limited by the rate of Ca release from the reservoir rocks. Dolomite and hence aqueous Mg may have also played a role in the mineralisation of the injected carbon in this higher temperature system (Clark *et al.*, 2020).

The temperatures of the monitoring well fluids were 260 °C to 275 °C. This is near the upper temperature limit for carbon storage *via* the mineral carbonation of basalts using freshwater. As illustrated in Figure 4.36, higher temperatures will lead to the decomposition of carbonate and sulfide minerals. This is evident in natural systems as well. Wiese *et al.* (2008) quantified the amount and spatial distribution of CO₂ stored as calcite within the bedrock of three active geothermal systems in Iceland, before CO₂ injection, by measuring the concentration of carbon in drill-chips from these systems. The concentration ranged from 0 to 175 kg CO₂ per cubic metre of highly altered rock, mostly basalt, stored as calcite in these geothermal systems. The results for the Hellisheiði Geothermal system are summarised in Figure 4.37. Up to 100 kg of CO₂ was stored as calcite per cubic metre of basaltic rock at Hellisheiði prior to the CarbFix injections. Carbon storage is not seen, however, in places where the temperature of rocks exceeds ~280 °C, due to the decomposition of carbonate minerals. Similar results have been described by Franzson (1998) and Snaebjornsdottir *et al.* (2014). It should be noted, however, that geochemical modelling suggests the most efficient carbonation of injected CO₂ will occur at temperatures less than 200 °C, as at higher temperatures secondary silicate minerals become more efficient at consuming the divalent metal cations liberated by the dissolution of primary basaltic minerals (Marieni *et al.*, 2021; Galeczka *et al.*, 2022). When seawater rather than freshwater is used to dissolve the CO₂, this upper temperature limit is considerably lower due to precipitation of anhydrite at temperatures in excess of 150 °C, as will be discussed in the next section.



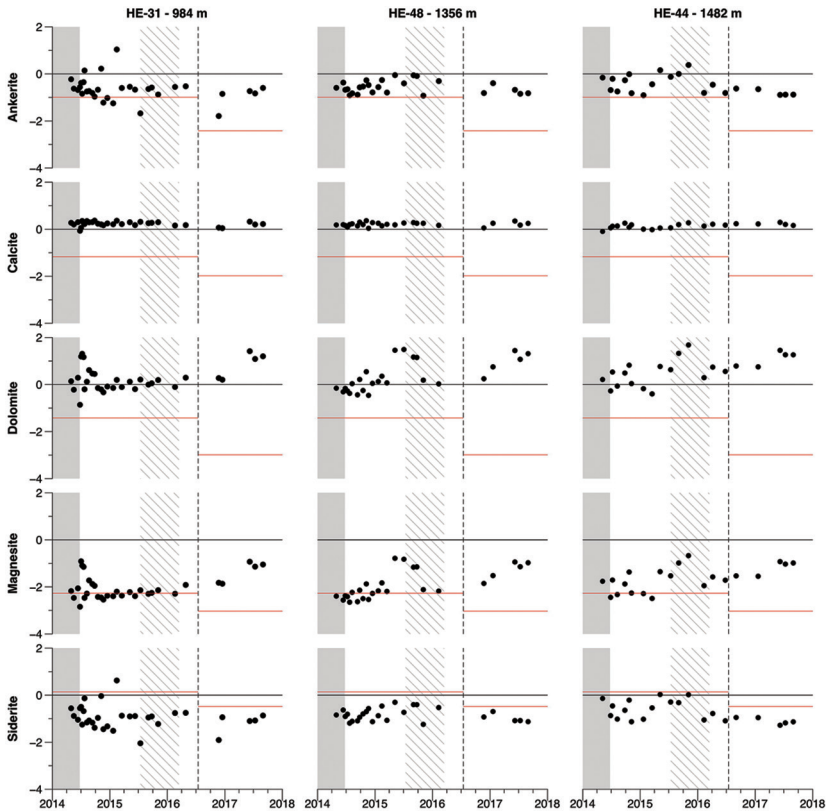


Figure 4.35

In situ saturation indices (SI) of the fluids, collected from the HE-31, HE-48, and HE-44 monitoring wells, with respect to carbonate minerals – ankerite, calcite, dolomite, magnesite, and siderite. The black symbols correspond to calculated fluid saturation indexes, the gray shaded area indicates times before the injection of gas-charged water into well HN-16, the diagonal lines denote times when well HN-14 was used for the injection of gas-charged waters, and the vertical dashed line signifies the time when the amount of CO₂ and H₂S injected into the subsurface was doubled. The SI of these minerals in the injected gas-charged waters, after mixing with geothermal effluent water and heating to 260 °C, but prior to their interaction with the rock, are depicted by the horizontal red lines. Modified from Clark *et al.* (2020).



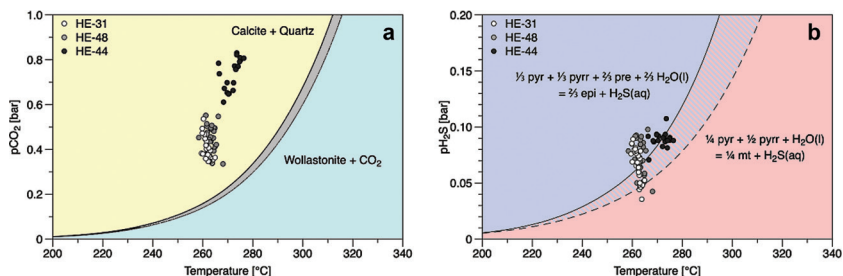


Figure 4.36

The *in situ* $p\text{CO}_2$ and $p\text{H}_2\text{S}$ of the fluids collected from the HE-31, HE-48, and HE-44 monitoring wells plotted against the calculated reservoir temperature. Curves represent the partial pressures of the indicated gases in equilibrium according to the reactions: (a) wollastonite and CO_2 formation from calcite and quartz at fixed total pressures from 1 to 300 bars based on Skippen (1977), (b) epidote (epi) and H_2S formation from pyrite (pyr), pyrrhotite (pyrr) and prehnite (pre), represented by the solid curve, and magnetite (mt) and H_2S formation from pyrite, pyrrhotite, and H_2O , represented by the dashed curve, based on data reported by Arnorsson *et al.* (2007) and Stefansson *et al.* (2011). Modified from Clark *et al.* (2018).

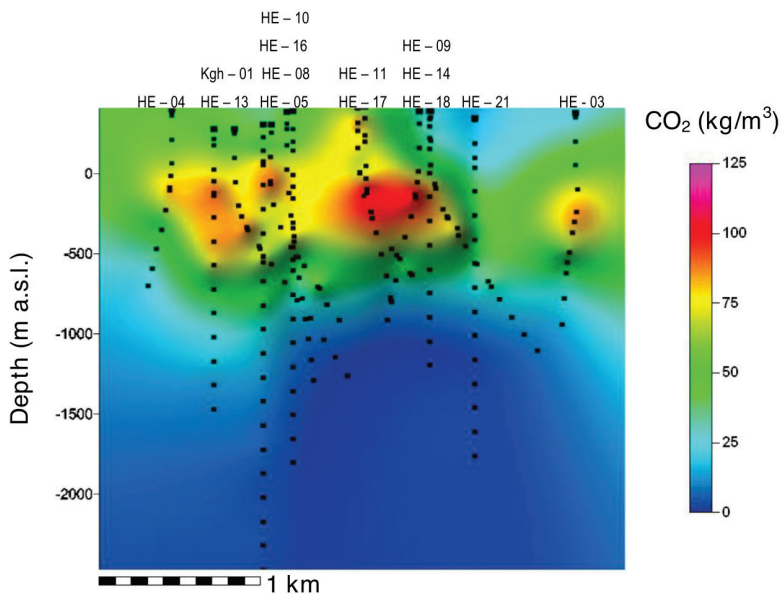


Figure 4.37

Cross-section extending from west to east (looking north) showing the distribution of the mass of CO_2 fixed in calcite within the Hellisheiði geothermal system by water-gas-rock interaction, before the CarbFix2 injection began in 2014. Mass of mineralised CO_2 is indicated by different colours, see the colour bar for scale. The width of this cross-section is approximately 4 km. From Wiesse *et al.* (2008) with permission from ISOR.



One concern when dissolving basaltic rocks with acidic CO₂- and H₂S-charged waters is the potential mobility of trace elements. Observations indicate, however, that although the trace elements Ba, Sr, Mn, As, Sb, and Mo, as well as the transition metal elements Ni, Cu, and Cr may have been transferred to the fluid phase by the dissolution of basalt, their concentrations were not enhanced in the monitoring well fluids during the CarbFix2 injections (Clark, 2019). Carbonates and sulfides likely incorporated these elements as they precipitated in the subsurface. Most notably, the concentrations of As in the monitoring well fluids have dropped substantially in response to the dissolved gas injection.

Since the beginning of the injection in 2014 until the time when this section was revised in September 2023, more than 95,000 tons of CO₂ have been injected into the subsurface at the CarbFix2 injection site. Some of the water injected into the reservoir has been recovered from the monitoring/production wells to generate heat and electricity at the powerplant, then reinjected into the HN-16 injection well. Through this process some fraction of the geothermal fluid used in the injection has been recirculated through the basaltic reservoir at least eight times, leaving thousands of tons of dissolved CO₂ and H₂S in the subsurface. The CarbFix2 injections are to be further upscaled in the future. Reykjavík Energy has now secured funds for capturing 95 % of the CO₂ emission and all the H₂S emissions from the power plant emitted after 2025. Although this is an impressive achievement, it is also a bit of a wakeup call. CarbFix was originally started in 2006, the complete capture and storage from the Hellisheiði powerplant will have taken 19 years to accomplish.

A key to the widespread acceptance of carbon capture and storage (CCS) is making it cost effective and ensuring public acceptance. Over the past two decades, CarbFix has done its best to address these issues. Cost estimates of CCS from concentrated point sources such as power plants or heavy industry, are difficult to estimate, but have been reported to range from US \$38 to US \$143/ton CO₂ (Global CCS Institute, 2011; Rubin *et al.*, 2015). Much of the cost involves CO₂ capture, which requires the separation of CO₂ from other gases in the gas stream. The more dilute the CO₂ is in the gas stream, the higher the cost. Far higher may be the cost to capture CO₂ directly from the atmosphere. Mazzotti *et al.* (2013) estimated that the direct capture of CO₂ from the atmosphere by the Climeworks approach may cost as much as US \$600/ton CO₂, as the CO₂ concentration is about 420 ppmv (0.042 %), or about 300 times more dilute than the CO₂ concentration in flue gas from a coal fired power plant (National Academies of Sciences, Engineering, and Medicine, 2019). Note, however, that cost estimates change regularly as technology advances, and accurate numbers are difficult to determine as many unsubstantiated claims exist in this industry. The total cost of capturing and storing a ton of the CO₂-H₂S gas mixture at Hellisheiði *via* CarbFix2 is US \$25 (Gunnarsson *et al.*, 2018). This cost is relatively low in part due to the relatively concentrated gas stream emitted from this powerplant, the low cost of electricity in Iceland, and the existence of substantial infrastructure at the Hellisheiði site. If a global average electricity price was used and the cost of wells needed to be drilled is included, this cost was estimated to increase to



\$48/ton of CO₂ captured, injected and mineralised (Gunnarsson *et al.*, 2018). The CarbFix method has not only been proven to be cost effective, but significantly, it results in carbon storage through the formation of stable carbonate minerals. The safest long term storage solution for carbon is to mineralise it – to turn it into stone. This leads to enhanced public acceptance and the potential for leakage is limited.

One of the keys to the success of CarbFix, and the reason it was allowed to continue over the years from 2011 to 2017 when the interest in CCS was at its lowest, is that it has proved to be financially advantageous to Reykjavík Energy. A law in Iceland was passed in 2010 requiring all industries to limit H₂S emissions to the atmosphere. The CarbFix approach equally captures and mineralises CO₂ and H₂S in the subsurface. The company has estimated that the financial savings from being able to use the CarbFix method to reduce H₂S emissions from the Hellisheiði power plant, compared to conventional industrial sulfur removal methods, was over 100 million EUR from June 2014 through March 2018 (U.S. Department of Energy, 2013; Morgunblaðið mbl.is., 2018; Sigfusson *et al.*, 2018). This cost savings has more than returned the investment made in designing, building, running and monitoring the CarbFix CO₂ capture and storage system at the Hellisheiði power plant.

4.7 Money Changes Everything

The original CarbFix legal document was signed among us two as members of the Scientific Steering Committee, Juerg Matter who stepped in for Wally Broecker from Columbia University and Einar Gunnlaugsson from Reykjavík Energy, at a very formal inauguration ceremony at the new Hellisheiði power plant on 29 September 2007. Present were the new CarbFix manager Holmfrídur Sigurdardóttir from Reykjavík Energy, Domenik Wolff-Boenish as University of Iceland's CarbFix project manager, the newly hired 7 PhD students and 2 MSc students (Fig. 4.38). The President of Iceland, Minister for the Environment, Rector of the University of Iceland, the Chairman of the board of Reykjavík Energy, the French and American ambassadors plus several other guests and the Icelandic press were there. This CarbFix document, slightly modified, was signed again over the period 23 April 2008 to 22 May 2008 by us, Juerg and Einar, the rector of the University of Iceland, the director of Reykjavík Energy, the Provost of Columbia University USA and the Déléguée Regionale of CNRS in Toulouse France. This document was to last for five years from the date signed, where it was stated that if CarbFix were to become viable business it would be co-owned among the four partners. From that time, we carried out most of the laboratory experiments, developed, tested, and eventually injected pure CO₂ and CO₂-H₂S gas mixture *via* the CarbFix1 method, where more than 95 % of the injected gases mineralised within two years. Over the next 11 years much of the funding to support the project was obtained by the academic partners in collaboration with Reykjavík Energy. Most papers reporting the technology were written by us and the PhD



students and published in the scientific literature, where the students were the first authors, as we have described in the previous sections.

At a January 2018 CarbFix2 partners' meeting in Zürich Switzerland we discussed the need for us to trademark the name CarbFix, as it was becoming very valuable. At the next CarbFix2 partners' meeting in September 2018 in Reykjavík Iceland, Edda Sif Aradóttir, a former CarbFix student and at this time acting as coordinator of the CarbFix2 EU-funded project, announced that Reykjavík Energy had trademarked the CarbFix name *on their own without the knowledge agreement of the other partners*. They had bought, on their own, the CarbFix logo rights from the artist and designer Marijo Murillo, the wife of Domenik Wolff-Boenish, the former University of Iceland CarbFix project manager. By this time, Domenik and Marijo had moved to Perth Australia. We were shocked, and Siggí commented that there had always in the past been complete trust between the CarbFix partners, and he was confident that this unilateral taking of CarbFix by Reykjavík would be rectified. Edda suggested that we instead should focus on submitting a CarbFix patent application and for all of us to continue to use the name and the logo - that from then on owned by Reykjavík Energy.

In December 2019 it was announced in the Icelandic media that Reykjavík Energy had established a subsidy with the name Carbfix⁴, fully owned by Reykjavík Energy, again without our prior knowledge. We had a very strange CarbFix2 partner meeting in Paris mid-January 2020, where we tried to determine our role. Did we even have permission from Carbfix (the company) to present or publish our research? We both were invited to remain as part of Carbfix as the company's unpaid scientific advisors. We felt insulted and refused. Subsequently, at Siggí's insistence, the University of Iceland started negotiations with Reykjavík Energy to try to resolve this issue. After substantial negotiation, the University of Iceland was allowed to *purchase* 10 % of the Carbfix company from Reykjavík Energy in 2022. Shortly after, as the Carbfix company grew, it required further funding. As the University was not legally allowed to invest further, Reykjavík Energy provided these funds and cut the University ownership to less than 0.1 percent without compensating the University. If Carbfix were to be sold at present, due to the current interest in carbon capture and storage it would likely be worth in excess of several millions of dollars.

There is no question to us at least that the taking of Carbfix, and all the jointly developed technology from the scientific partners by Reykjavík Energy was reprehensible. It is now clear to us that once money gets involved, public companies can be quick to change the rules to those which benefit the company at their convenience and without any advance notice.

4. Note again, in this text, the term *CarbFix* (upper case F) refers to the academic-industrial partnership from 2006 to 2020 led by us and others. The term *Carbfix* (lower case f) refers to the company created in 2020 without our prior knowledge or participation by Reykjavík Energy to exploit and profit from the results of the *Carbfix* consortium. The naming of the company 'Carbfix' gives the impression that the company generated the technology on their own from the beginning.



We have mixed feelings about Carbfix at this time. Although Reykjavík Energy had taken sole control of Carbfix and developed it into a multi-million dollar subsidiary, the Carbfix company has hired several of our former students and postdocs. Reykjavík Energy had provided us with field sites and the infrastructure to test our hypotheses in the subsurface; an opportunity few academics ever have. Through the Carbfix company our research has transformed into an internationally recognisable brand, and an important option to address a critical societal issue. Few in our community have had a chance in their careers to make such a large impact with their research, and for this we are grateful, for having the opportunity to make this impact with our students and postdocs. Nevertheless, this twist of events in the CarbFix story should serve as a warning to our fellow scientists. One needs to beware and wary of the actions of private sector partners. Once they sniff profit from one or more of your ideas, they have a large motivation to discard you once you develop the technology to the level that it is profitable.



Figure 4.38 The CarbFix members at the CarbFix signing ceremony 29th September 2007. Front row from left: Juerg Matter, management committee for Columbia University; Kristin Ingolfsdottir, Rector of the University of Iceland; Snorri Gudbrandsson, CarbFix student; Gudmundur Ingvarsson, CarbFix student; Gabrielle Stockmann, CarbFix student; Mahnaz R. Khalilabad, CarbFix student; Eric Oelkers, Scientific Steering Committee for CNRS; and Einar Gunnlaugsson, Scientific Steering Committee for Reykjavik Energy. Back row from left: Andri Stefansson, management committee for University of Iceland; Alexander Gysi, CarbFix student; Helgi Alfredsson, CarbFix student; Sigurdur Gislason, Chair of the Scientific Steering Committee for University of Iceland; and Domenik Wolff-Boenisch, CarbFix project manager for University of Iceland. The CarbFix students at this time who are not in the photo were Edda Aradottir, Therese Flaathen, and Elísabet Ragnheidardottir.



4.8 Water Demand and the Use of Seawater

A major challenge to carbon storage using the CarbFix method is its water demand. At least 25 tons of fresh water are required to capture and inject into the subsurface each ton of CO₂ at 25 bar CO₂ pressure at 25 °C. At this pressure and temperature, about 0.85 moles of CO₂ dissolve in each kg of pure water and 0.75 moles of CO₂ dissolve in each kg of seawater (Gislason *et al.*, 2010). At these conditions, the CO₂ mass percent is equal to or less than about 4 %. The solubility of CO₂ in water decreases with increasing temperature and water salinity but increases with increasing CO₂ pressure.

The water required to dissolve a ton of CO₂ in pure water and in seawater as a function of CO₂ pressure at 25 °C is shown in Figure 4.39 (Snaebjornsdottir *et al.*, 2020). Water demand decreases but the energy required for CO₂ and water compression increases with increasing CO₂ pressure. As freshwater may be scarce, it will be necessary to use seawater or other saline fluids for carbon storage *via* the CarbFix method in many parts of the world. Much of the ocean floor is made of basalts and numerous coastal regions, for example in Western India and Western Saudi Arabia, are made of basalts, providing opportunities for mineralising CO₂ *via* the CarbFix methods using seawater, onshore and/or offshore.

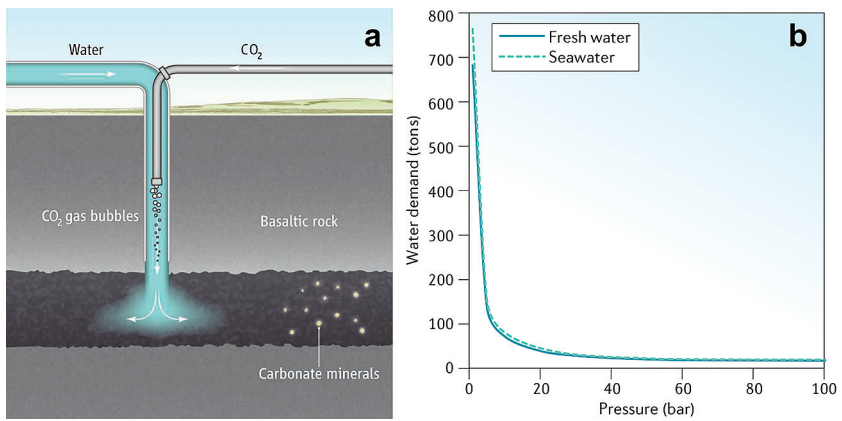


Figure 4.39 (a) CO₂ injection *via* the CarbFix1 method and, (b) the amount of freshwater and seawater needed at 25 °C to dissolve 1 t of CO₂ as a function of the CO₂ pressure. Values calculated using the real gas equation of state for solubility. Modified from Gislason and Oelkers (2014) and Snaebjornsdottir *et al.* (2020).

There is substantial evidence that the use of seawater for CO₂ dissolution and promotion of carbon mineralisation will be successful. Over millions of years, the interaction of submarine basalts with seawater in low temperature



ocean floor hydrothermal systems has led to the formation of calcite and aragonite (Coogan and Gillis, 2013; Voigt *et al.*, 2021). The presence of these minerals in marine basalts suggests substantial natural CO₂ fixation in the basaltic ocean crust. To assess the potential application of this natural process for carbon capture and storage, we measured the rate of mineralisation of CO₂ of Mid-Ocean Ridge Basalts (MORB) in CO₂-charged seawater in the laboratory at 130 °C (Voigt *et al.*, 2021). Experiments were performed at 130 °C, to obtain results within months, to keep the system sterile, and to keep the CO₂-charged seawater undersaturated with respect to anhydrite (CaSO₄). Note that the heating of pure seawater in an inert environment above 150 °C results in anhydrite precipitation and the consumption of Ca that otherwise could be used for CO₂ mineralisation by calcite or aragonite, the most common carbonates on the ocean floor and within the basaltic oceanic crust (*e.g.*, Coogan and Gillis, 2013). Some anhydrite may precipitate in the vicinity of injection wells at temperatures below 150 °C, due to the rapid release of Ca from the basaltic rocks. As a result, the potential formation of anhydrite limits the maximum temperature to about 130 °C, below which CO₂ can be efficiently mineralised using seawater.

Voigt *et al.* (2021) reported that calcite and aragonite were the first carbonate minerals to form in the experiments initiated with seawater charged with ~2.5 bar *p*CO₂, later possibly followed by siderite and ankerite. Magnesite, however, was the only carbonate mineral observed to form in experiments initiated with seawater charged with ~16 bar *p*CO₂. In total, approximately 20 % of the initial CO₂ in the reactors was mineralised within five months at 130 °C. This carbonation rate is similar to corresponding rates observed during the freshwater-basalt-CO₂ interaction experiments described in Section 4.4 and during the CarbFix field experiments at Hellisheiði, SW Iceland described in Sections 4.5 and 4.6. These laboratory experiments, therefore, suggest that CO₂-charged seawater injected into submarine basalts will lead to CO₂ mineralisation. Notably, at a *p*CO₂ of tens of bars, magnesite forms, limiting the formation of Mg-rich clays, which might otherwise compete for the Mg cations and pore space in the submarine basaltic crust. This suggests that the injection of CO₂-charged seawater into subsurface basalts can be an efficient and effective approach to the long term mineral storage of anthropogenic carbon (Voigt *et al.*, 2021).

Field experiments using seawater to capture the CO₂ *via* the CarbFix1 method (Fig. 4.39a) are now in preparation in a project called “CO₂-Seastone”, led by the “Carbfix” company and a Swiss based research Network called “DemoUpCARMA+Storage”. The CO₂-Seastone project will be the first full cycle of CO₂ capture, transportation, and subsurface mineralisation storage using seawater and the CarbFix1 method. In this project, CO₂ will be captured from a Swiss wastewater treatment plant, it will be compressed to liquid, transported over land to Rotterdam, and shipped to Reykjavík, Iceland, where it will be transported by truck to the storage site at Reykjanes peninsula, where seawater infiltrates the groundwater system. The injection will be onshore, using a seawater source well, injection well and monitoring wells at a location where



the water flows outward towards the ocean. Transport of CO₂ from Switzerland started during the summer of 2022, as well as drilling of the injection and monitoring wells (Carbfix, 2022).

4.9 Coupling Subsurface Mineralisation with Direct Air Capture (DAC)

A new partner was added to the EU funded CarbFix2 project in 2017, Climeworks Switzerland. Climeworks's role in the project was to start a small pilot experiment at the Hellisheiði injection site to capture CO₂ directly from the atmosphere every day of the year for about two years. The captured CO₂ would then be co-injected into the subsurface with water as part of the CarbFix2 project.

The Climeworks approach to DAC used alkaline functionalised amine adsorbents and a powerful fan to capture CO₂ directly from the atmosphere as shown in Figure 4.40. After the CO₂ was adsorbed from the atmosphere, the saturated amine surfaces were heated to about 100 °C to desorb the CO₂. The resulting gas was then compressed to more than 9 bars of pressure. The energy to drive the fan, to heat the adsorbent, and compress the CO₂ was provided by the Hellisheiði geothermal power plant. Finally, the pure compressed CO₂ was added to the downgoing CO₂-H₂S-charged water stream of the CarbFix2 injection well as described in Section 4.6.

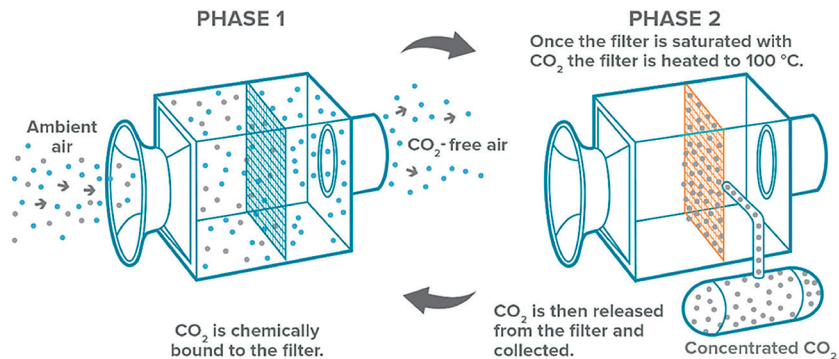


Figure 4.40 Schematic illustration of the Climeworks direct air capture process. From Gutknecht *et al.* (2018).

A Climeworks capture unit, with the capacity to capture 40–50 t CO₂/yr, was up and running in October 2017, ready for the harsh Icelandic winter (Fig. 4.41). This unit was kept running for about 2 years with surprisingly good performance. This led to the decision of Reykjavík Energy and Climeworks to upscale this direct air capture and storage (DACs) method to an industrial





Figure 4.41 The pilot Direct Air Capture (DAC) unit at Hellisheiði was launched in October 2017. This single unit had the capacity to capture 50 t CO₂ yr⁻¹.

phase. On September 8, 2021 Climeworks and two of Reykjavík Energy's new subsidiaries: the Carbfix company and On Power, inaugurated the largest direct air capture plant in the world at that time, aiming to capturing 4,000 t CO₂/yr and injecting this pure and compressed CO₂ at the original CarbFix1 injection site, *via* the CarbFix1 method described in Section 4.5.

On 28th of June 2022 Climeworks, the Carbfix company and On Power announced a tenfold increase to the current direct air CO₂ capture and storage capacity at the Hellisheiði site. This enlarged plant, named Mammoth, is expected to start operating within 18–24 months. The long term aim of these companies is to upscale these DAC's and Carbfix plants in Iceland and worldwide.

Direct air capture (DAC) of CO₂ from the atmosphere is independent of the CO₂ source; CO₂ released in New York can be captured few days later in Iceland. Hence, future direct air capture plants can be located where the best possible storage rocks and CO₂ emission-free energy sources are available. The main limitation of this approach at present is the cost. Direct air capture from the atmosphere, which contains 420 ppmv CO₂ is considerably more costly (600\$/t CO₂; Tollefson, 2018) than capturing CO₂ from concentrated point sources such as power plants and heavy industry (Global CCS Institute, 2011; Mazzotti *et al.*, 2013; Rubin *et al.*, 2015; Gunnarsson *et al.*, 2018; National Academies of Sciences, Engineering, and Medicine, 2019). It seems likely that this cost will need to be reduced substantially over the coming years for the wider acceptance and use of DAC.



4.10 Carbon Storage Alternatives

Although conventional and mineral storage has received large attention by the scientific community, several other CO₂ storage approaches have and are being considered. Among these are carbon storage in hydrates or clathrates, ocean storage of CO₂, forestation, and forest management.

4.10.1 Carbon Storage in Clathrates or Hydrates

At relatively low temperatures, CO₂ and H₂O form a phase that is referred to in the literature as a CO₂ hydrate. A gas hydrate is an ice-like substance formed when a low molecular weight gas combines with water into a clathrate structure. These hydrates trap CO₂ within a H₂O cage, which generally consists of 5.75 to 7.67 H₂O molecules for each CO₂ (Ferdows and Ota, 2006; see Fig. 4.42).

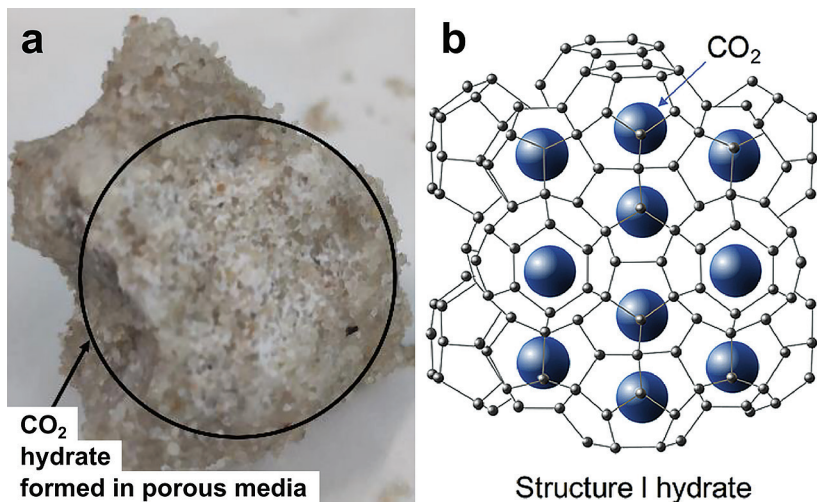


Figure 4.42 Left: Photo of a CO₂ hydrate formed in a porous medium. Right: representative structure of a CO₂ hydrate where a cage of H₂O molecules traps the CO₂ within its structure. Modified from Ansari *et al.* (2021) and Sa *et al.* (2017).

Insight into the potential for CO₂ hydrate storage can be gained from the phase diagram shown in Figure 4.43. The stability region for CO₂ hydrates is limited to a region along the pressures and temperatures of the pure CO₂ gas–pure CO₂ solid or CO₂ gas–pure CO₂ liquid phase boundaries. Most significantly, CO₂ hydrates are 1) stable at temperatures below 10 °C and CO₂ pressures of 10 to 40 bars, and 2) denser than water at these conditions (Sabil *et al.*, 2011).



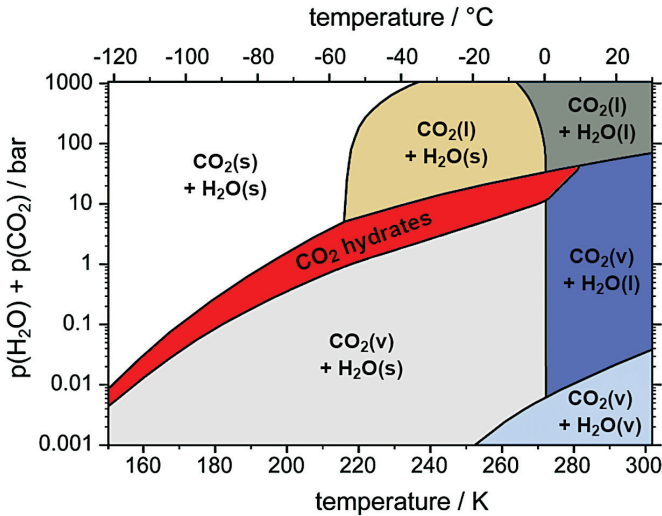


Figure 4.43 Phase diagram of the CO₂-H₂O system. The stability regions of ice, water, and water vapour are shown with white, dark blue and light blue backgrounds. The clear, tan and grey regions show the stability regions of CO₂ solid, liquid and gas, respectively. The red region shows the stability region of CO₂ hydrates. After Arzbacher *et al.* (2019).

Such temperature and pressure conditions can be found at relatively shallow depths in the oceans; CO₂ hydrates have been observed to form at depths of 500 to 900 m in CO₂-rich seawater (Sabil *et al.*, 2011). The stability and density of CO₂ hydrates have motivated some to propose the storage of CO₂ as hydrates on the shallow ocean floor or in seafloor sediments as illustrated in Figure 4.44 (Sabil *et al.*, 2011; Zheng *et al.*, 2020). If released at the appropriate depth, CO₂ would react with seawater to form CO₂ hydrates, which could accumulate on the ocean floor (Lee *et al.*, 2003; see Fig. 4.44a). Attention would have to be made to ensure that the depth of the ocean floor at the hydrate accumulation area should not exceed the stability region of the CO₂ hydrates. If deeper, the hydrates could decompose into buoyant liquid CO₂ and water, potentially releasing the CO₂ back to the atmosphere. The relatively limited stability region and rapid decomposition kinetics of CO₂ hydrates, however, makes such storage challenging to control (Brewer *et al.*, 1999). Alternatively, the injection of liquid CO₂ into the sediments located below the seafloor (Fig. 4.44b), where the seafloor is at depths where the pressure is in the CO₂ hydrate stability region has been considered as an option (Koide *et al.*, 1997; Qanbardi *et al.*, 2012; Teng and Zhang, 2018). As the injected liquid CO₂ rises to the sediment surface, the CO₂ pressure would decrease, leading to the formation of CO₂ hydrates. As CO₂ hydrates are solid and denser than water these hydrates could potentially serve as a trap for the liquid CO₂ below.



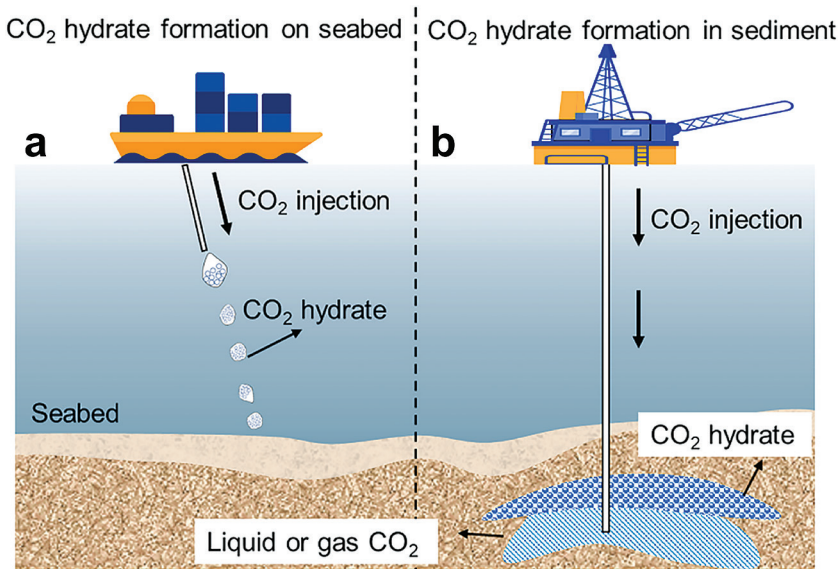


Figure 4.44 Schematic illustration of the potential strategies for CO₂ storage as hydrates in the oceans: **(a)** The release of CO₂ at appropriate depths could lead to the direct formation of CO₂ hydrates from the reaction of CO₂ with seawater. As the CO₂ hydrates are denser than water, they will sink and accumulate on the ocean floor. If the ocean floor at the target location is at depths within the CO₂ hydrate stability region, the hydrates could remain stable for substantial time. **(b)** The injection of liquid CO₂ into sediments below the stability field of CO₂ hydrates. As the liquid CO₂ rises towards the surface, it would enter the CO₂ hydrate stability region forming dense solid hydrates that could serve as a cap trapping the remaining liquid CO₂ below. From Wang *et al.* (2021a) with permission from John Wiley and Sons.

The storage of CO₂ within hydrates on or in the ocean floor would appear to be an attractive carbon storage alternative, as it would be a low cost solution, and seafloor at the appropriate depths is widely available. However, this option has not been embraced by the international community for several reasons. First, the environmental consequences of the vast formation of CO₂ hydrates on the ocean floors are poorly known and may be detrimental. Second, CO₂ hydrates may not be a stable storage solution. At the seawater-CO₂ hydrate interface CO₂ will dissolve into the aqueous phase where it would acidify ocean water and eventually find its way back to the atmosphere.

Alternatively, the formation of CO₂ hydrates has been explored as a potential carbon capture process (Duc *et al.*, 2007; Lee *et al.*, 2010; Babu *et al.*, 2013; Yang *et al.*, 2014). The basis for the separation or capture of the CO₂ is that at some temperatures, pressures and fluid compositions, the formed gas hydrate preferentially incorporates CO₂ compared to other gases (Kang and Lee,

2000; Linga *et al.*, 2007). Nguyen *et al.* (2022) concluded that CO₂ capture *via* hydrate formation has several advantages, including that 1) it is a water based process, (2) it has a high tolerance to the presence of impurities in the feed gas, and (3) it is energetically favourable compared to many alternatives.

4.10.2 Combining CO₂ Hydrate Storage with CH₄ Recovery

An interesting and potentially economically favourable option is to combine CO₂ storage with the production of methane (CH₄) by the exchange of these gases in subsurface hydrates (Jadhawar *et al.*, 2021; Wang *et al.*, 2021b; Liu *et al.*, 2022a). CH₄ hydrates are naturally occurring and, as is the case for CO₂ hydrates, are stable only over a range of low temperature, moderate pressure conditions. CH₄ hydrates are widespread in marine margin sediments and in permafrost regions. The potential mass of CH₄ hydrates worldwide is large (Collett *et al.*, 2014). Boswell and Collett (2011) estimated the global mass of CH₄ hydrates in surface and marine sediments to be 1,800 Gtons of carbon. This mass of carbon is equal to roughly 5 % of the carbon stored as dissolved CO₂ in the global oceans (37,100 Gtons of C). The global recoverable mass of CH₄ from hydrates has been estimated to be ~15 Gt C (Boswell and Collett, 2011). It has been proposed to inject CO₂ into natural CH₄ hydrate fields, where the injected gas would react with the natural hydrates, replacing the CH₄ with CO₂ in the hydrate structures (*e.g.*, Chong *et al.*, 2016). This process would liberate the CH₄ that could then be used as an energy source.

Although a potential energy source, CH₄ hydrate production has the potential to be a huge environmental challenge. CH₄ that escapes from sediments and soils and reaches the atmosphere could accelerate greatly global warming. Such a process has a strong positive feedback on climate (Ruppel and Kessler, 2017). Indeed, CH₄ concentrations in the atmosphere have increased by ~150 % since the pre-industrial age (Wuebbles and Hayhow, 2002), three times the percent change of atmospheric CO₂ over this time span. Methane is ~20 times more potent than CO₂ as a greenhouse gas. A leak of CH₄ from hydrates, therefore, either from inefficient efforts to harvest CH₄ from hydrates *via* CO₂ injection, or *via* natural warming can have a significant effect on global warming (Ruppel, 2011). CH₄, however, oxidises to CO₂ after about a decade in the atmosphere, such that the CO₂ released from CH₄ oxidation or from its burning for energy may play a larger role in global warming over the long term than CH₄ itself (Archer *et al.*, 2009).

4.10.3 Deep Ocean Storage of Liquid CO₂

The storage of CO₂ in the deep oceans was among the first CO₂ storage solutions considered by the scientific community (Marchetti, 1977). The key to this storage approach is that the density of liquid CO₂ increases with depth, so that at depths of 3,000–3,800 m it is denser than seawater (House *et al.*, 2006). If injected into the oceans below this depth, the denser liquid CO₂ would pool on the deep



ocean floor and become “trapped” by gravity in CO₂ lakes. The potential storage capacity of these deep ocean CO₂ lakes could be vast; Goldthorpe (2017) estimated that the CO₂ storage capacity of the Sunda trench alone is 19,000 gigatons of carbon. This option received serious consideration in the past due to its low cost and energy efficiency (Sheps *et al.*, 2009). The impact of such storage, however, would likely be detrimental to the deep subsurface marine biota. Numerous studies indicate that deep-living marine organisms are highly susceptible to the CO₂ and pH excursions that are likely to accompany deep sea CO₂ sequestration (Seibel and Walsh, 2001, 2003).

Deep sea liquid CO₂ storage is relatively short lived compared to some of the alternatives. Modelling studies indicate the CO₂ at the surface of deep sea CO₂ lakes would rapidly dissolve into the overlying seawater from the CO₂-lake surface, such that over several hundreds of years much of the CO₂ would be released from this lake (Adams and Caldera, 2008). This release would lead to both ocean acidification and the return of the injected CO₂ to the atmosphere. Model calculations reported by Adams and Caldera (2008) suggest that if anthropogenic carbon emissions were captured and stored in the deep oceans, after 2,000 years the atmosphere would have the same concentration as if no action was taken. Both deep ocean carbon storage or lack of action would lead to a decrease in ocean pH by 0.4 to 0.6 pH units. This decrease in pH has large detrimental impact on the marine biota (Fabry *et al.*, 2008; Hofmann *et al.*, 2010). Due to the limited storage duration and likely detrimental effects on the marine environment, the idea of storage of CO₂ in the deep ocean has largely been discarded by the scientific community over the past decade.

4.10.4 Carbon Storage through Forestry

The planting of trees and forest management is a popular possibility for carbon storage as it appears to be environmentally friendly and low cost (Bellassen and Luyssaert, 2014; Ni *et al.*, 2016). This approach builds upon the large current natural drawdown of CO₂ by forests. Forests are estimated to take up 2.4 Gton of carbon annually worldwide (Pan *et al.*, 2011; Zeng *et al.*, 2013); this is approximately 20 to 30 % of the total mass of anthropogenic CO₂ emissions. Much of this drawdown stems from growth in mature, unharvested, old growth forests. This carbon drawdown is somewhat enigmatic as mature forests might be expected to be carbon neutral as the rate of organic decay should roughly be equal to that of carbon capture by new growth. The current behaviour of mature forests as a carbon sink has been attributed to the increasing CO₂ concentration of the atmosphere; Luyssaert *et al.* (2008) argued that a higher atmospheric CO₂ content leads to accelerated tree growth.

There are two major challenges for optimising forests for large scale carbon storage. First, using forests for long term carbon storage competes with other land uses such as food production. Second, the net carbon uptake by forests decreases rapidly over time after they are planted. The decay of dead



forest organic material, including litter and dead wood from a newly planted forest is rapid. The global mean steady state turnover times of forest litter has been estimated to range from 1.4 to 3.4 years; the mean turnover time of partially-forested woodlands is estimated to be ~5 years, and turnover time for coarse woody detritus is estimated to be ~13 years (Matthews, 1997). It is of interest to note that plastics in the environment are far slower to degrade than natural organic material; the half-lives of plastics have been estimated to range from 58 years for plastic bottles to 1,200 years for plastic pipes (Chamas *et al.*, 2020). These contrasting half-lives would suggest that carbon storage within plastic waste is a longer term option than forestry. Nevertheless, the rapid decay rate of forest debris and dead wood suggests that the duration of carbon drawdown from a newly planted forest may only last for decades. Bernal *et al.* (2018) estimated that newly planted forest and woodlands have CO₂ removal rates ranging from 4.5 to 40.7 tons of CO₂ ha⁻¹ yr⁻¹ during their first 20 years of growth. This study also estimated that forests only have a positive net drawdown of CO₂ for the first 20 to 80 years after they are planted, depending on the type of forest and climatic conditions. Consequently, the efficient long term carbon removal by forests requires the removal and storage of wood and/or debris.

To address the challenge of wood and forest debris decay, forests can be harvested, made into products, or stored. Dry wood contains about 50 % carbon (Lamlom and Savidge, 2003). Domke *et al.* (2020) estimated that forests and harvested wood products take up the equivalent of more than 14 % of the annual CO₂ emissions in the United States, and this amount could be increased through improved forest management. Alternatively, dry wood could be stored in decommissioned coal mines or in facilities near the forests in the long term.

One of the more intriguing options for the storage of harvested wood and debris from forests is the creation and burial of biochar (Oni *et al.*, 2019). Biochar could be produced by the pyrolysis of forest products. Pyrolysis is a thermochemical technology for transforming biomass into biochar between 350 °C and 700 °C temperature in the absence of air (Varma *et al.*, 2018). The turnover rate of biochar depends strongly on the initial organic material, the method of pyrolysis, and the physical/chemical conditions into which they are buried. Nevertheless, the turnover rate of biochar buried into soils ranges from one hundred to one thousand years (Schmidt *et al.*, 2011; Yang *et al.*, 2015). The addition of biochar to soils also has the advantage of enhancing soil productivity (*e.g.*, Lehman *et al.*, 2011).

4.11 How Much Carbon Capture and Storage: Incentives and Costs?

During the final night of the Kyoto Protocol negotiations in Kyoto, Japan in December 1997, it was rumoured that Al Gore, then the Vice President of United States, said that the treaty would never get through the US Congress unless



the CO₂ emissions would be controlled by a CO₂ market rather than through direct taxation. A carbon market would allow carbon-emitting industries to buy the right to emit CO₂ from companies that capture and store CO₂ in a verified manner. The Kyoto Protocol entered into force in February 2005, committing countries to curb CO₂ emissions. It was ratified by 192 countries, but the Protocol was never ratified by the United States Congress.

The idea of a carbon trading market, however, motivated the creation of the European Emission Trading Scheme (ETS) in 2005. The ETS market is the largest multi-national, greenhouse gas emissions trading scheme in the world and covers almost half of the European Union's total CO₂ emissions (Wikipedia, 2022). Figure 4.45 shows the EU Carbon permit price from its beginning in 2005 until September 2023. During the first years there were large fluctuations in the EU Carbon permit price. From September 1, 2008, to August 1, 2018, the price was well below 20 €/tCO₂. This low price was a reflection of several factors, including an economic downturn in 2008, the outsourcing of CO₂ emissions



Figure 4.45 Time evolution of the market price of EU Carbon Permits, also referred to as Emission Trade Allowance (ETA) or Emission Trading Scheme (ETS), from its beginning to September 2023. Modified from Trading Economics (2023).

to non-European locations, overabundance of CO₂ permits, and a widespread disinformation campaign aimed at making the public sceptical about global warming (see Section 1.3). From November 2020, the price rose to the beginning of the war in Ukraine in February 2022. The estimated costs of carbon capture and storage *via* the geologic storage of CO₂ from concentrated point sources such as power plants or heavy industry are estimated to range from 38 to 143 US\$/tCO₂ (Global CCS Institute, 2011; Rubin *et al.*, 2015). Hence, there was little incentive for major emitters in Europe to develop CCS to curb their emissions during the



first 15 years of the ETS. Beginning in the year 2021, however, the emission prices rose above 40 US\$/tCO₂, driving a renewed interest in CCS. In September 2023, when this section was revised, the ETS carbon permit cost was 85 €/t CO₂. This cost is close that of CO₂ capture and storage from many of the concentrated point sources. The ETS market incentive is finally driving industry to take CCS seriously.

A similar carbon trading scheme has been initiated in China. The Chinese national carbon trading scheme started operating in 2021, and is now the largest in the world. The right to emit one ton of CO₂ was as high as €9/tCO₂ in China's national carbon market during 2022.

The only national financial incentive up to the end of 2022 to limit carbon emissions from concentrated sources in the United States is a tax credit up to US\$50/t CO₂ captured and stored in saline aquifers, and up to US\$35/t CO₂ for the use of CO₂ in enhanced oil recovery operations (Folger, 2018). It is, however, unclear, if enhanced oil operations actually lead to a net decrease in CO₂ emissions to the atmosphere (see Section 4.2).

In 2021, approximately 40 million tons of CO₂ were captured annually and stored in rocks *via* conventional CCS worldwide (see Section 1.2). The capture of this CO₂ is almost completely from concentrated point sources, which is less costly energetically and financially than capture directly from the atmosphere. At the same time anthropogenic CO₂ emissions are approximately 40 Gt CO₂/yr, such that only 0.1 % of emitted carbon was captured, stored in the subsurface, or used in 2021. Moreover, since roughly 90 % of the current geologic CCS projects are used for enhanced oil recovery (EOR), the percentage of “real CCS” goes down to 0.01 %. As discussed in Section 4.2, EOR is not a permanent CO₂ storage. Due to the slow growth in CCS, it is most likely that we will eventually be forced to capture huge amount of CO₂ directly from the atmosphere in the second half of this century to keep the average global temperature within 1.5 °C of its pre-industrial value.

The actual amount of carbon capture and storage, and direct air capture required to limit global warming to no more than 1.5 °C depends on both the future anthropogenic emissions to the atmosphere and the speed at which CCS is implemented. In October 2018, the Intergovernmental Panel on Climate Change published a report presenting four illustrative scenarios that could limit global temperatures to within 1.5 °C of its pre-industrial value (IPCC, 2018). Two of these scenarios are shown in Figure 4.46. Scenario P1 is the most optimistic, requiring the rapid decrease of CO₂ emissions to the atmosphere from fossil fuel burning, industry, and land use change. Scenario P4 is the most pessimistic, assuming a slow decrease in anthropogenic CO₂ emissions. The P1 scenario suggests that society becomes sustainable and efficiently phases out fossil fuel use over the next 40 years. Even agriculture, forestry, and other land use sectors (AFOLU) need to become carbon negative in the second half of this century. The P4 scenario assumes that anthropogenic CO₂ emissions will continue throughout



this century, and AFOLU will at best become carbon neutral. This latter scenario requires in excess of 20 Gton/yr CO₂ drawdown directly from the atmosphere over the second half of this century.

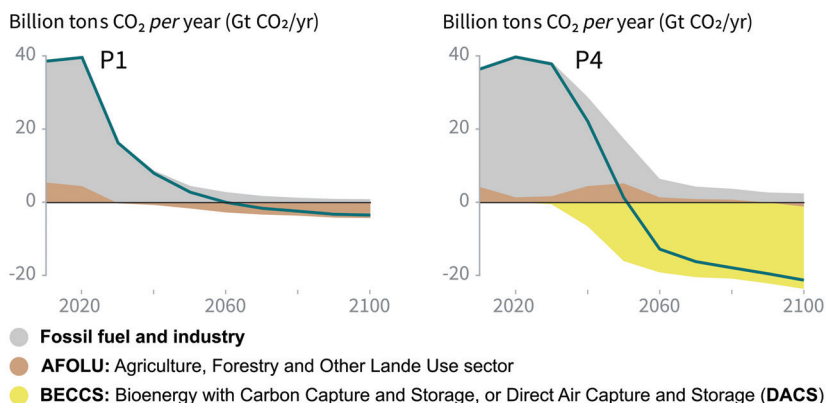


Figure 4.46 Illustration of two potential global carbon emission scenarios limiting global temperatures to within 1.5 °C of its pre-industrial value. On the left is an optimistic scenario where emissions from fossil fuel and industry are rapidly decreased through efficiency and sustainability. On the right is a pessimistic scenario where anthropogenic emissions decrease only slowly in the future. The grey shaded region corresponds to the annual mass of CO₂ emitted into the atmosphere from fossil fuel burning and industry; the brown shaded region shows the annual mass of CO₂ emissions to or removal from the atmosphere due to agriculture, forestry and land use changes; and the yellow shaded region shows the annual mass of CO₂ needed to be removed by direct air capture to limit global warming to no more than 1.5 °C. The green curve shows the net annual addition or removal of CO₂ to the atmosphere due to these efforts. Modified from IPCC Special Report (2018).

Several methods have been proposed for the direct carbon removal from the atmosphere. Some of these are summarised in Figure 4.47:

- 1) Afforestation and Reforestation to increase carbon storage in biomass and soil (see Section 4.10).
- 2) BioEnergy production combined with Carbon Capture and Storage (BECCS). This scheme consists of growing biomass to draw CO₂ out of the atmosphere and harvesting the biomass before it reaches steady state. This biomass can either be burned in a power plant for energy, or used to make liquid fuels for use in automobiles and/or airplanes. The emissions from these processes can be captured and stored in the subsurface.
- 3) Enhanced rock weathering (ERW) includes grinding reactive silicate rocks such as basalt to increase its specific surface area, and spreading the fine grained rock over agricultural fields or the ocean, where



water-rock interaction will raise the pH and alkalinity of the reacting fluid, resulting in binding the CO_2 as dissolved bicarbonate (HCO_3^-) in the water. To date, however, this process looks to be limited (see Section 4.3).

- 4) Finally, Direct Air Capture and Storage (DACs) as described in Section 4.9.

A detailed review of the costs and limitations of these technologies have been provided by Minx *et al.* (2018). The degree to which any of these approaches can be upscaled to address the global need for CCS is currently unclear, but it seems likely that each will be required at some scale (Fuss *et al.*, 2018). Upscaling and optimising these technologies are likely to be some of the great challenges of the scientific community over the coming decades.

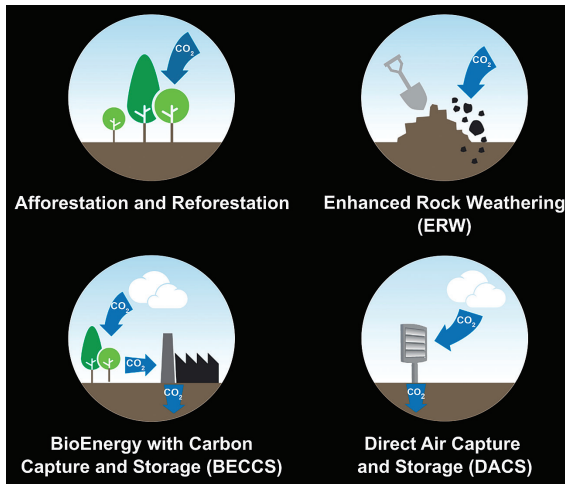


Figure 4.47 Some methods proposed for carbon removal from the atmosphere. Modified from Minx *et al.* (2017).



5. THE FUTURE

We wrote this *Geochemical Perspectives* in the fall of 2022. This was a curious time. During the summer of 2022 the world experienced some of the most unusual weather in years. Pakistan has experienced catastrophic floods. Much of Southern Europe experienced droughts more severe than seen in over a century. A heat-wave in the western United States during the fall of 2022 broke all-time temperature records in a number of cities. One might think such events would motivate the world to move yet faster on addressing the challenges of global warming by taking action to limit CO₂ emissions and accelerating efforts to develop technologies to attenuate the increasing CO₂ content of the atmosphere. On the contrary, many governments have decreased the cost of hydrocarbon fuels in response to the outcry of society. In France, the government lowered taxes on gasoline⁵; President Joe Biden of the United States called for a 3 month holiday on Federal gas taxes⁶. These actions highlight the conundrum faced by our governments in addressing the global warming challenge.

We all need energy. The availability of energy at an affordable price is the motor that makes society work. The culprit for global warming is not necessarily the petroleum industry, although they have attempted to discredit climate scientists in the past. The mandate of petroleum companies is to provide affordable energy while providing profit for their shareholders. This industry has provided energy for the world for decades, allowing us to heat our homes, ride in cars, buses, and airplanes, and help grow food to feed the world. When hydrocarbon-based energy becomes scarce and the prices go up, our society begins to break down through a weaker economy and social unrest becomes likely (Kilian, 2008; Thompson, 2012; Aminu *et al.*, 2018). The petroleum industry is certainly concerned about global warming and public perception, but they, like any other private company, need an incentive. The key to making the petroleum industry work towards low carbon-emitting solutions is public policy (Beck, 2020). If there is a financial incentive (or penalty) involved, this industry will find solutions to curb carbon emissions. Such potential financial actions that have or are being considered include a carbon tax, carbon trading or the creation of a carbon market as described in Section 4.11 (*e.g.*, Metcalf, 2020; Tsai, 2020).

For decades society has been paying for the production, refinement, and transport of hydrocarbon products, but has not paid for the disposal of its waste products, notably the disposal of CO₂. In many cases, the cost of disposing of waste products can exceed that of the product itself. Eric recently looked at his water bill and noted that the disposal of his wastewater costs more than the cost of the water being supplied to this home. But by paying this sum, however, we are helping to ensure the quality of our environment.

5. <https://www.france24.com/en/europe/20220312-france-to-offer-fuel-rebate-to-help-motorists>

6. <https://www.whitehouse.gov/briefing-room/statements-releases/2022/06/22/fact-sheet-president-biden-calls-for-a-three-month-federal-gas-tax-holiday/>



The question becomes who should pay for the disposal of CO₂. Over a decade ago, Eric had lunch with the head of research at a major petroleum company. When asked about the management of CO₂ emitted by the burning of petroleum, the response was something like; “We only sell the gasoline we do not burn it. The customer can just put it into his swimming pool”. This of course begs the question of who is responsible. Is it the producer, the consumer, or the government? The answer is that we all are and in the end the cost will be paid for either directly or indirectly by the consumer.

Once the cost to use hydrocarbon-based energies includes the capture and storage of its CO₂ waste products, the cost of this energy will increase. One benefit to this additional cost is that it will encourage the further development of renewable and potentially cleaner energy sources. Although it is currently being debated, the oil peak may occur over the next several years or decades as global resources dwindle (Sverdrup and Ragnarsdottir, 2014; Norouzi *et al.*, 2020). Other energy sources will be needed for our long term future.

Many petroleum companies have now promised to be net zero carbon emitters at some time in the future. The company BP, for example, has announced that they will strive to achieve “net zero carbon emissions from their operations by 2050 or sooner”⁷. Others making similar promises include Exxon-Mobile⁸, Chevron-Texaco⁹, and Total¹⁰. There are two things to keep in mind here. First, these promises are not to eliminate the carbon emissions from their products, but only from their operations. Second, these promises are for many years in the future, by the time much of the public may have long forgotten about them. It is therefore difficult to have much confidence in these promises of net zero emissions making a large difference to the overall carbon emissions to the atmosphere at the present time. Perhaps even more discouraging is that many of the major energy companies were using purchased carbon offsets from the voluntary carbon market to attain their limited net-zero goals. For example, Chevron relies almost totally on carbon offsets to attain net zero emission from their operations¹¹ - see section 5.1. Most of these offsets have been shown to provide little to no carbon drawdown¹².

7. <https://www.bp.com/en/global/corporate/news-and-insights/press-releases/bernard-looney-announces-new-ambition-for-bp.html>

8. https://corporate.exxonmobil.com/News/Newsroom/News-releases/2022/0118_ExxonMobil-announces-ambition-for-net-zero-greenhouse-gas-emissions-by-2050

9. <https://www.chevron.com/newsroom/2021/q4/chevron-sets-net-zero-aspiration-and-new-ghg-intensity-target>

10. <https://totalenergies.com/sites/g/files/nytnzq121/files/documents/2020-10/total-climate-report-2020.pdf>

11. <https://www.theguardian.com/environment/2023/may/24/chevron-carbon-offset-climate-crisis>

12. <https://www.zeit.de/wirtschaft/2023-01/co2-certificates-fraud-emissions-trading-climate-protection-english/komplettansicht>



5.1 Will Carbon Capture and Storage Ever Be Large Enough to Help Limit Global Warming?

The answer to this question is unclear at present. The Kyoto protocol was adopted in 1997. It is now 26 years later. Nevertheless, the annual mass of carbon captured and stored by all CCS operations including EOR amounts to less than 0.15 % of the annual global anthropogenic carbon emissions. The annual mass captured though all CCS operations has increased by a factor of less than 2 over the past decade. This rate increase will need to dramatically escalate for CCS to make a significant contribution to climate change before 2050.

History tells us that there are many potential factors that can slow or stop the further implementation of CCS. The combination of an economic crisis and a targeted misinformation campaign set back the development of new CCS facilities from 2011 to 2017. At present, one of the major risks looks to be dishonesty in the business world. Many of us might have wondered, why, if carbon offsets on the European Union Emissions Trading System (EU-ETS) cost roughly \$100 USD, is it possible to offset the CO₂ emitted on our plane flights for far less. The answer is that whereas the EU-ETS is government regulated, and covers emissions from major emitters, there are many companies offering carbon offsets on the largely unregulated voluntary carbon market. The voluntary carbon market allows companies developing CCS methods to create carbon credits in the amount of carbon they have captured and stored and sell these credits to carbon emitters. The cost of these largely unregulated carbon credits is substantially lower than those of the regulated EU-ETS and have been falling dramatically over the past year (Fig. 5.1). At the beginning of June 2022 one ton of carbon credit on the nature-based carbon credit market (NGEO) would have cost \$15 USD. By June of 2023 this price dropped to less than \$2 USD.

The reason for the dramatic drop in price is dishonestly. Many of us might think that most of the carbon offsets sold on the NGEO market originates from planting trees. But even easier than planting and growing trees is leasing forested land from governments and not cutting down the trees on the leased land. This is exactly what many companies marketing nature-based carbon credits have been doing. The carbon credits are based on comparing the percentage of trees removed from the leased land, located far from roads and population centres, with the percentage of trees removed from forested land located near roads and growing cities¹³. These carbon credits are then certified by a carbon credit company and sold on the open market. The largest of these carbon credit companies, is Verra, who certifies 75 % of the voluntary carbon credits on the market¹³. A number of academic studies have shown, however, that such projects offer little to no overall carbon reduction (West *et al.*, 2020, 2023). These conclusions have

13. <https://www.theguardian.com/environment/2023/jan/18/revealed-forest-carbon-offsets-biggest-provider-worthless-verra-aoe>





Figure 5.1 Market price for nature based general emission offsets (NGEOs). NGEOs are **carbon credits** generated by projects that reduce, remove, or prevent carbon emissions through nature-based solutions. Examples include forest conservation or restoration projects that sequester carbon in trees and soil, or agricultural practices that reduce emissions or enhance carbon storage. From Carbon Credits.com (<https://carboncredits.com/the-collapse-of-ngeo-carbon-prices-an-in-depth-analysis/>).

been made to the public through the popular press^{12,13}. Yet these projects were certified by Verra. The discrediting of the voluntary carbon market and companies certifying the offsets has led to a loss of confidence in many CCS companies. This makes it more difficult for them to raise the funds necessary to develop and market new and potentially more effective CCS technologies. Equally, many may not see the point in paying in excess of several hundred US dollars a ton for direct air capture technologies, when one can purchase NEGOS at a far lower price. It seems likely that clearly defined and honestly verified carbon removal, perhaps run by governments, will be required to assure a carbon market that will enable the growth of CCS to the scale need to attenuate future global warming.

5.2 Will Mineral Carbon Storage Move Forward?

There are abundant potential pathways to lowering future CO₂ concentrations in our atmosphere. Several of these were described briefly in the previous sections. Here we focus just on the possible role of carbon mineralisation processes to address this issue in the future.



5.2.1 *Ex situ* Mineralisation

There are numerous recently started private companies proposing to capture and store almost unbelievable quantities of CO₂ through some sort of *ex situ* mineral storage scheme (see Section 4.2). Such schemes include putting basalt particles into farmland (Beerling *et al.*, 2020), spreading crushed olivine-rich rock on beachfronts (Montserrat *et al.*, 2017), carbonating ultramafic mine wastes (Harrison *et al.*, 2013; Lechat *et al.*, 2016; Li *et al.*, 2018), and adding natural reactive minerals (Rigopoulos *et al.*, 2018) or some sort of activated mineral product to the oceans. Many of these companies promise gigaton-scale carbon removal starting in less than a decade¹⁴. According to Bill Gates, the Vesta company will use olivine dissolution to remove ‘a trillion tons of carbon dioxide from the atmosphere’¹⁵. This claim of course seems incredible as there are only 3.3 trillion tons of CO₂ in the atmosphere and this scale of carbon remove would likely provoke a new ice age. If one believes the websites, there is nothing at all to fear about global warming as the claims of these various startup companies would more than remove all annual anthropogenic CO₂ from the atmosphere. It is difficult to believe any of these large scale claims, recalling that the total weathering of the silicates on the global continents draws down roughly 0.5 Gt of CO₂ annually. It seems absurd that a single start-up company could “weather the planet” faster than all natural processes. And even if they were successful what other consequences would there be?

There is no doubt that some of these efforts will prove fruitful, though likely at a far smaller scale than some claim. Some will get wealthy as a result. It is unclear to us, however, that these efforts could be sufficiently upscaled to collectively draw down CO₂ from the atmosphere at the gigaton scale.

5.2.2 *In situ* Mineralisation

The success of the CarbFix1 and CarbFix2 projects has helped motivate further interest in the *in situ* mineralisation of CO₂ by its reactions with subsurface rocks. Hills *et al.* (2020) provided a list of the potential advantages of mineral storage in subsurface basaltic rocks. This list includes:

- the large size of the available reservoirs;
- the distribution of these reservoirs throughout the world;
- the long duration of the storage;
- the upscaling potential of the technology;

14. <https://smartstones.nl/enhanced-weathering-crushed-rocks-spread-on-farmland-can-capture-billions-of-tons-of-co2-year/>

15. <https://twitter.com/BillGates/status/1534572110470782976?lang=en>



They also list several potential disadvantages, including:

- the significant infrastructure required;
- the need to find sufficient porosity in the subsurface, and
- the current carbon credit status is not yet ensured.

In contrast to the large number of start-up companies promising to capture and store CO₂ at the surface of the Earth or in the oceans, there are relatively few companies focused on expanding efforts in subsurface storage of CO₂ through mineralisation. The relative lack of *in situ* mineralisation projects likely stems from 1) the costs of drilling injections and monitoring wells, 2) the poor characterisation of subsurface aquifers located in reactive rocks, 3) a continuing poor understanding of the process by decision makers, 4) a lack of laws and regulations for *in situ* mineralisation, and 5) difficulties of obtaining the right to inject CO₂ into the subsurface. Due to these challenges, it is probable that much of the near-term future of subsurface mineral storage of CO₂ will be led by petroleum companies and geothermal energy companies. These companies have the technology, the capital, and the experience in drilling and managing wells and obtaining permissions for the injection of water and brines in the subsurface. It seems likely that this technology might be first applied by geothermal energy companies as 1) geothermal energy wells are commonly located in reactive rocks such as basalts, 2) they often inject their wastewater into these rocks in part to help recharge the subsurface aquifer system (e.g., Khan, 2010), 3) they might be able to create additional revenue streams by creating carbon credits *via* subsurface storage, and 4) they can eliminate H₂S by its co-injection with CO₂ (see Sections 4.5 and 4.6). These efforts might be particularly favourable if geothermal energy companies teamed up together with companies that are experts in direct air capture of CO₂, as this combination would closely couple sources and sinks (e.g., Gutknecht *et al.*, 2018 and Section 4.9).

5.3 Future Carbfix Projects

We are happy to report, that despite elimination from the Carbfix company, this company is moving forward the technology that we developed on a number of fronts:

Carbon capture and storage at the Nesjavellir geothermal powerplant, Iceland: The geothermal power plant at Nesjavellir is a single-flash power plant and has been operating since 1990 with an installed capacity of 120 MW electricity and 300 MW thermal water (Gunnarsson *et al.*, 1992). The steam generated from the geothermal field is transported to the turbines for electricity generation and the separated hot water diverted into heat exchangers that heat cold groundwater for district heating and use in the city Reykjavík. The injection of water dissolved CO₂ and H₂S into the basalts adjacent to the Nesjavellir geothermal power plant is to begin during 2023 (Galeczka *et al.*, 2022). Plans call for the capture of a combined 1,000 tons of CO₂ and H₂S annually from the powerplant



by its dissolution in pure condensate water in accordance with the CarbFix2 approach and its co-injection into the subsurface together with waste geothermal brine (see Section 4.6). If successful, this approach will be upscaled to capture and store all the CO₂ and H₂S emitted from this power plant in future years.

The Silverstone Project: This project is a scale-up of the original CarbFix2 project at the Hellisheiði site described in Section 4.6, from about 1,200 tons to about 34,000 tons of CO₂ captured and stored annually. After this upscale, about 95 % of the CO₂ emission and all the H₂S emission will be captured from the Hellisheiði Power Plant. A new gas capture scrubber will be commissioned in 2025.

The Mammoth Direct Air Capture System: The Carbfix company has agreed with Climeworks company to install a new, larger direct air capture (DAC) facility close to the Hellisheiði power plant east of Reykjavík. This new DAC facility will capture 36,000 tons of CO₂ annually directly from the atmosphere for its injection close to the Mammoth plant *via* the CarbFix1 method, described in Section 4.5. This DAC facility is under construction and is due to be on line during 2024.

The CO₂-Seastone project: This project was designed to assess three major issues: 1) the ability to mineralise CO₂-charged seawater, 2) the legal and logistical issues associated with transporting substantial quantities of CO₂ across international borders, and 3) the cost and carbon footprint of the capture, transport, and storage. About 1,000 tons of liquid, pure CO₂ will be shipped over the course of a year or roughly about 100 tons *per* month. The source of the CO₂ is a water treatment plant located close to Basel, Switzerland. The captured pure CO₂ is first transported by truck and then train to Rotterdam, Holland. It is then shipped to Reykjavík, put on truck to the CO₂-Seastone injection site which is near Keflavík airport, SW Iceland. There it will be injected as gas along with seawater *via* the CarbFix1 method as described in Section 4.5. As of the writing of this section, the first containers have arrived in Iceland and cleared customs. Injection and monitoring wells are being drilled at the present with the aim to start the injection before the end of 2023. The results of this project will pave the way for the upscaling of this approach as part of the Coda terminal.

The Coda terminal: This is perhaps the most ambitious of the current Carbfix company projects. The project will consist of upgrading a harbour 25 km south of Reykjavík, and the drilling of a suite of source, injection and monitoring wells into the nearby subsurface basalts. The total investment cost of this facility is estimated to be 240 to 280 million Euros. Plans call for boats to ship CO₂ from Europe to be downloaded at the terminal and co-injected with seawater or freshwater into the subsurface for its mineral storage. Current estimates for the cost of storage range between 15–20 EUR *per* ton CO₂. The estimated maritime transport of CO₂ will cost between 20 and 45 EUR. This means that the total cost of transport and storage will be on the order of 35–65 EUR *per* ton of CO₂



stored¹⁶. The goal is to have one ship in operation by 2026 transporting 500 thousand tons of CO₂ per year, with an upgrade to 5 ships and up to 3 million tons of CO₂ transported and stored starting in the year in 2031.

5.4 Other Future Subsurface Mineral Storage Projects

5.4.1 Subsurface Basalt-Hosted Carbon Mineralisation in Other Parts of the World

The potential for CO₂ storage through its mineralisation in subsurface basalts are being considered in various locations throughout the world, including Saudi Arabia (Oelkers *et al.*, 2022), India (Jayaraman, 2007; Prasad *et al.*, 2009; Kumar *et al.*, 2019; Vishal *et al.*, 2021; Liu *et al.*, 2022b), Kenya (Okoko and Olaka, 2021), the Northwest coast of the United States (Goldberg *et al.*, 2018; Xiong *et al.*, 2018), the islands of Hawaii (DePaolo *et al.*, 2021), and beneath the seafloor (Goldberg *et al.*, 2009). The degree to which mineral carbon storage will be developed at these or other areas in the world is currently unclear, however, and it will depend greatly on public policy and perception.

5.4.2 Subsurface Mineralisation in Ultramafic Rocks

Another very favourable target for the subsurface mineralisation of injected CO₂ are ultramafic rocks. Such an approach is currently being championed by Peter Kelemen and co-workers (Kelemen *et al.*, 2011, 2020). Field evidence suggests that the carbonation of peridotite has substantially higher carbonation potential than that of basalts; in the ideal case the final reaction products of peridotite carbonation can be just magnesite plus quartz. This rock called listvenite can be observed in several natural systems (Beinlich *et al.*, 2012; Falk and Kelemen, 2015; Kelemen *et al.*, 2022). Numerous potential targets exist, notably in Oman, United Arab Emirates, New Caledonia, Papua New Guinea, and the US Pacific Northwest.

The injection of water dissolved CO₂ into subsurface ultramafic rocks for its subsurface storage has yet to be demonstrated in the field. The company 44.01¹⁷, however, is currently planning a pilot demonstration by the injection of air-captured CO₂ into ophiolites located in the United Arab Emirates.

16. <https://www.carbfix.com/codaterminal>

17. <https://4401.earth>



5.5 Future Research Directions

The scientific basis of subsurface mineralisation of water dissolved CO₂ has been well established in laboratory and modelling studies. Some details are still ripe for further laboratory and modelling studies, for example to address such issues as use of seawater rather than freshwater, improved methods for dissolving CO₂ in water, the evolution of permeability during CO₂ mineralisation at the core scale, and the effects of rock mineralogy and alteration state on mineral carbonation rates. The major challenges moving forward, however, must be addressed on the field scale, in small pilots and larger demonstration projects. Major issues that can only be assessed at the field level include the nature of subsurface permeability, the response of the field to the injection of water (*e.g.*, potential for induced seismicity), the rates of reactions in the subsurface, and the response of the subsurface to long term induced mineral reactions. Another issue is how can fracturing be induced to help create flow paths and mineral-fluid reactive surface area, facilitating mineral storage. Large scale demonstration and pilot projects, however, are very costly, require a large number of permissions, and expert engineering. This compels the creation of academic-industrial partnerships to join forces to move this field forward. The academic rewards of such partnerships are great. At present our community has only a limited understanding of the rates, extent, and consequences of subsurface geochemical processes. The running of such larger scale demonstration and pilot projects holds the promise to revolutionise our ability to quantify subsurface geochemical processes. In addition to moving subsurface carbon mineralisation forward, the projects could also lead to insights into the potential for mining through *in situ* leaching (*e.g.*, Akin *et al.*, 1996; Mudd, 2001), improved subsurface wastewater storage, and improved nuclear waste storage (*e.g.*, Tsang *et al.*, 2015).

Following a two day workshop presented on line to the Oil and Gas Climate Initiative (OGCI) during late 2020, we, along with Peter Kelemen, were asked to provide a list of some of the major remaining questions about the large scale implementation of subsurface mineral storage. We repeat some of our answers here to motivate our community towards moving the subject forward – see also Oelkers *et al.* (2023).

General Questions:

- What are the most significant technical gaps, if any, that must be addressed prior to wide scale deployment of subsurface carbon mineralisation?
- What financial models/incentives will make installation of subsurface mineral carbonation systems favourable?
- How do political issues and social acceptance affect adoption of mineral storage?



- What are the policy, regulatory and legal barriers to subsurface mineralisation?
- What are the geographical distributions and chemical compositions of rock formations that are legally accessible and located sufficiently close to large carbon sources? What is their storage capacity?

Demonstration and Pilot Project Questions:

- What demonstration size and duration of pilot projects are needed to measure success and what success metrics should be applied?
- How can the life cycle, net cost benefits and markets for subsurface mineral storage be defined?

Mineral/Fluid Chemistry and Interaction Questions:

- What minerals are reacting, at what rates, during carbonation of natural polyminerale rocks? How does this affect the multi-year time evolution of CO₂ uptake? For example, what is the role of glass in carbonation of young basalts? What is the role of rapidly reacting but volumetrically minor phases present in a given rock reservoir (*e.g.*, zeolite in altered basalt, brucite in altered peridotite)? What is the role of rock forming aluminosilicates (*e.g.*, epidote, prehnite, chlorite, albite, anorthite)? What is the role of abundant “ferromagnesian silicates” (*e.g.*, olivine, Ca-rich pyroxene, amphiboles)?
- What are the rates and proportions of Ca- and Mg-bearing mineral alteration products (*e.g.*, clays in basalt, serpentine in peridotite), that form in addition to carbonates during reaction with CO₂-rich aqueous fluids? How do these affect the rate and capacity of CO₂ storage *via* carbon mineralisation in different lithologies?
- What is the estimated storage capacity of different potential rock types, which are typically fractured crystalline units rather than sedimentary formations?
- What are the rates of carbonation reactions in different potential rock types, given limitations of multi-scale, fracture-controlled permeability and surface area?
- What are the limits and effects of different water compositions (*e.g.*, saline waters, seawater) on mineral carbonation efficiency?
- What are the optimal CO₂-water rock interaction durations in subsurface as a function of temperature, rock, and water composition?
- How long will the subsurface reactions continue? Will they slow down due to mineral precipitation and passivation of reactive surfaces? How does carbon mineralisation affect permeability?



- How efficiently are heavy metals that dissolve initially into the acid CO₂-charged water scavenged by the precipitation of secondary carbonates and silicates?
- Can the natural process of “reaction-driven cracking” be engineered? Instead, or in addition, will reservoir stimulation be required? How often?
- Given the potential for “solution trapping” to reduce or eliminate the need for an impermeable caprock above CO₂ storage reservoirs, are there advantages to inject into moderately tectonic-active areas where fracture permeability is readily available?

Engineering Issues:

- What are the best and most cost efficient ways to inject CO₂-charged water into the subsurface (well depth, favourable locations)?
- If stimulation is needed, what will be the advantages and disadvantages of re-opening fractures and generating new ones in fractured, crystalline rock reservoirs, compared to “fracking” in sedimentary oil and gas reservoirs?
- What biotic response might we see in the subsurface and how can we mitigate potential detrimental effects?
- What is the most efficient way of dissolving CO₂ and other soluble gases into water for promoting carbon mineralisation?
- How does one optimise CO₂ capture with water dissolution to limit costs?
- What is the long term durability of wells in response to injection of acidic CO₂-rich water?
- What are the industry-level costs for large scale deployment, including financing, payroll, drilling, well completion, well maintenance, and pressurisation of fluids and/or gases?

5.6 Over and Out

When one gets to the end of co-writing a long monograph such as this, one wonders if there is anything left to say. We have been fortunate to be able to do internationally recognised fundamental science, work with a large number of great colleagues and students, and provide a potential solution to a major societal issue.

Global warming is just one of the major challenges facing society today. Other major challenges include the need to provide secure access to resources and energy at an affordable price, and the safe and secure management of toxic



and radioactive waste products. We in the geochemical community hold a key position, and have the skillset to address these challenges. This is a great opportunity for our community. We may also have a moral obligation to address these issues as many of us are employed in public institutions and/or have unique abilities having been trained by top scientific experts. Our own experience tells us that working closely with private and public industrial companies on societal issues has led us to numerous scientific breakthroughs and opportunities that would not otherwise be possible. We encourage all to follow a similar path.



REFERENCES

- ADALSTEINSSON, H. (2000) Aurframburður á Eyjabökkum. OS-2000/071. Orkustofnun National Energy Authority, Reykjavik. (In Icelandic)
- ADAMS, E.E., CALDERA, K. (2008) Ocean Storage of CO₂. *Elements* 4, 319-324.
- ADLER, R.F., GU, G. WANG, J.J., HUFFMAN, G.J., CURTIS, S., BOLVIN, D. (2008) Relationships between global precipitation and surface temperature on interannual and longer timescales (1979-2006). *Journal of Geophysical Research* 113, D22104.
- AKIN, H., GOTZ, H., LOEWER, R., CATCHPOLE, G., BECKER, J. (1996) Mining uranium by the in-situ leach method. *ATW Int. Atomwirtschaft Atomtechnik*, 41, 94-97.
- ALFREDSSON, H.A., OELKERS, E.H, HARDARSSON, B.S, FRANZSON, H., GUNNLAUGSSON, E., GISLASON, S.R. (2013) The geology and water chemistry of the Hellisheiði, SW-Iceland carbon storage site. *International Journal of Greenhouse Gas Control* 12, 399-418.
- ALFREDSSON, H.A., MESFIN, K.H., WOLFF-BOENISCH, D. (2015) The syringe sampler: An inexpensive alternative borehole sampling technique for CO₂-rich fluids during mineral carbon storage. *Greenhouse Gases: Science and Technology* 6, 167-177.
- ALLEN, J.G., MACNAUGHTON, P., SATISH, U., VALLARIBO, J., SPENGLER, J.D. (2016) Associations of cognitive function scores with carbon dioxide, ventilation, and volatile organic compound exposures in office workers.: A controlled study of green and conventional office environments. *Environmental Health Perspectives* 124, 805-812.
- ALLEN, J.G., MACNAUGHTON, P., CEDENO-LAURENT, J.G., CAO, X., FLANIGAN, S., VALLARIBO, J., RUEDA, F., DONNELLY, MCLAY, D., SPENGLER, J.D. (2018) Airline pilot flight performance on 21 manoeuvres in a flight simulation under varying carbon dioxide concentrations. *Journal of Exposure Science and Environmental Epidemiology* 29, 457-468.
- AMINU, N., MEENAGH, D., MINFORD, P. (2018) The role of energy prices in the Great Recession – A two-sector model with unfiltered data. *Energy Economics* 71, 14-34.
- ANDREWS, M.G., TAYLOR, L.L. (2019) Combating climate change through enhanced weathering of agricultural soils. *Elements* 15, 253-258.



- ANSARI, A.A., RAVESH, R., PANIGRAHI, P.K., DAS, M.K. (2021) Influence of sand particle size on the kinetics of CO₂ hydrate formation in a pilot scale reactor. *Energy Proceedings* 20, 846.
- ARADÓTTIR, E.S.P., SONNENTHAL, E.L., BJÖRNSSON, G., JÓNSSON, H. (2012a) Multidimensional reactive transport modeling of CO₂ mineral sequestration in basalts at the Hellisheiði geothermal field, Iceland. *International Journal of Greenhouse Gas Control* 9, 24-40.
- ARADÓTTIR, E.S.P., SONNENTHAL, E.L., JÓNSSON, H. (2012b) Development and evaluation of a thermodynamic dataset for phases of interest in CO₂ sequestration in basaltic rocks. *Chemical Geology* 304-305, 26-38.
- ARADÓTTIR, E.S.P., SIGFÚSSON, B., SONNENTHAL, E.L., BJÖRNSSON, G., JÓNSSON, H. (2013) Dynamics of basaltic glass dissolution – Capturing microscopic effects in continuum scale models. *Geochimica et Cosmochimica Acta* 121, 311-327.
- ARADÓTTIR, E.S.P., GUNNARSSON, I., SIGFÚSSON, B., GUNNARSSON, G., JÚLÍUSSON, B.M., GUNNLAUGSSON, E., SIGURDARDÓTTIR, H., ARNARSON, M.TH, SONNENTHAL, E. (2015) Towards Cleaner Geothermal Energy Utilization: Capturing and Sequestering CO₂ and H₂S Emissions from Geothermal Power Plants. *Transport in Porous Media* 108, 61-84.
- ARCHER, D., BUFFETT, B., BROVKIN, V (2009) Ocean methane hydrates as a slow tipping point in the global carbon cycle. *Proceedings of the National Academy of Sciences* 106, 20956-20601.
- ARNALDS, O., OLAFSSON, H., DAGSSON-WALDHAUSEROVA, P. (2014) Quantification of iron-rich volcanogenic dust emissions and deposition over the ocean from Icelandic dust sources. *Biogeosciences* 11, 6623-6632.
- ARNDT, N.T., FONTBOTE, L., HEDENQUIST, J.W., KESLER, S.E., THOMPSON, J.F.H., WOOD, D.G. (2017) Future Global Mineral Resources. *Geochemical Perspectives* 6, 1-171.
- ARNÓRSSON, S., STEFÁNSSON, A., BJARNASON, J.O. (2007) Fluid-fluid interactions in geothermal systems. *Reviews in Mineralogy and Geochemistry* 65, 259-312.
- ARRHENIUS, S. (1896) On the Influence of Carbonic Acid in the Air Upon the Temperature of the Ground. *Philosophical Magazine* 41, 237-276.
- ARSOUZE, T., DUTAY, J.C., LACAN, F., JEANDEL, C. (2007) Modeling the neodymium isotopic composition with a global ocean circulation model. *Chemical Geology* 239, 165-177.
- ARZBACHER, S., RAHMATIAN, N., OSTERMANN, A., MASSANI, B., LOERTING, T., PETRASCH, J. (2019) Macroscopic defects upon decomposition of CO₂ clathrate hydrate crystals. *Physical Chemistry Chemical Physics* 21, 9694-9708.
- ASSIMA, G.P., LARACHI, F., MOLSON, J., VEAUDOIN, G., MOLSON, J. (2013) Accurate and direct quantification of native brucite in serpentine ores – New methodology and implications for CO₂ sequestration by mining residues. *Thermochemica Acta* 566, 281-291.
- AXELSSON, G., BJÖRNSSON, G., MONTALVO, F. (2005) Quantitative interpretation of tracer test data. In: Horne, R., Okandan, E. (Eds.) *Proceedings of the World Geothermal Congress 2005*, Antalya, Turkey.
- AYACHE, M, DUTAY, J.C, ARSOUZE, T., RÉVILLON, S., BEUVIER, J., JEANDEL, C. (2016) High-resolution neodymium characterization along the Mediterranean margins and modelling of Nd distribution in the Mediterranean basins. *Biogeosciences* 13, 5259-5276.
- AZUMA, K., KAGI, N., YANAGI, U., OSAWA, H. (2018) Effects of low-level inhalation exposure to carbon dioxide in indoor environments: a short review on human health and psychomotor performance. *Environment International* 121, 51-56.
- BABU, P., KUMAR, R., LINGA, P. (2013) Pre-combustion capture of carbon dioxide in a fixed bed reactor using the clathrate hydrate process. *Energy* 50, 364–373.
- BAILEY, B., TEMPLETON, A., STAUDIGEL, H., TEBO, B.M. (2009) Utilization of Substrate Components during Basaltic Glass Colonization by Pseudomonas and Shewanella Isolates. *Geomicrobiology Journal* 26, 648-656.
- BECK, L. (2020) Carbon capture and storage in the USA: the role of US innovation leadership in climate-technology commercialization. *Clean Energy* 4, 2-11.



- BEERLING, D.J., LEAKE, J.R., LONG, S.P., SCHOLES, J.D., TON, J., NELSON, P.N., BIRD, M., KANTZAS, E., TAYLOR, L.L., SARKAR, B., KELLAND, M., CELUCIA, E., KANTOLA, I., MULLER, C., RAU, G., HANSEN, J. (2018) Farming with crops and rocks to address global climate, food and soil security. *Nature Plants* 4, 138-147.
- BEERLING, D.J., KANTZAS, E.P., LOMAS, M.R., WADE, P., EUFRASIO, R.M., RENFORTH, P., SARKAR, B., ANDREWS, M.G., JAMES, R.H., PEARCE, C.R., MERCURE, J.F., POLLITT, H., HOLDEN, P.B., EDWARDS, N.R., KHANNA, M., KOH, L., QUEGAN S., PIDGEON N.F., JANSSENS, I.A., HANSEN, J., BANWART, S.A. (2020) Potential for large-scale CO₂ removal via enhanced rock weathering with croplands. *Nature* 583, 242-248.
- BEINLICH, A., PLÜMPER, O., HÖVELMANN, J., AUSTRHEIM, H., JAMTVEIT, B. (2012) Massive serpentinite carbonation at Linnajavri, N-Norway. *Terra Nova* 24, 446-455.
- BELLASSEN, V., LUYSSAERT, S. (2014) Carbon sequestration: Managing forests in uncertain times. *Nature* 506, 153-155.
- BENSON, S.M., COLE, D.R. (2008) CO₂ Sequestration in Deep Sedimentary Formations. *Elements* 4, 325-331.
- BENSON, S.M., HOVERSTEN, M., GASPERIKOVA, E., HAINES, M. (2005) Monitoring protocols and life-cycle costs for geologic storage of carbon dioxide. In: M. Wilson, E.S. Rubin, D.W. Keith, C.F. Gilboy, T. Morris, K., Thambimuthu, J. Gale (Eds.) *Proceedings of the 7th International Conference on Greenhouse Gas Control Technologies*. Elsevier, 1259-1265.
- BERNAL, B., MURRAY, L.T., PEARSON, T.R.H. (2018) Global carbon dioxide removal rates from forest landscape restoration activities. *Carbon Balance Manage* 13, 22.
- BERNER, R.A. (2004) *The Phanerozoic Carbon Cycle: CO₂ and O₂*. Oxford University Press, Oxford, UK, 158 pp.
- BERNER, R.A. (2012) Jacques-Joseph Ebelmen, the founder of Earth System Science. *Comptes Rendus Geoscience* 344, 544-548.
- BERNER, R.A., LASAGA, A.C., GARRELS, R.M. (1983) The carbonate-silicate geochemical cycle and its effect on atmospheric carbon dioxide and climate. *American Journal of Science* 283, 641-683.
- BLUM, J.D., GAZIS, C. A., JACOBSON, A.D., CHAMBERLAIN, C.P. (1998) Carbonate versus silicate weathering in the Raikhot watershed within the High Himalayan Crystalline Series. *Geology* 26, 411-414.
- BLUTH, G.J.S., KUMP, L.R. (1994) Lithologic and climatologic controls of river chemistry. *Geochimica et Cosmochimica Acta* 58, 2341-2359.
- BONNEVILLE, S., MORGAN, D.J., SCHMALENBERGER, A., BRAY, A., BROWN, A., BANWART, S.A., BENNING, L.G. (2011) Tree-mycorrhiza symbiosis accelerate mineral weathering: Evidences from nanometer-scale elemental fluxes at the hypha-mineral interface. *Geochimica et Cosmochimica Acta* 75, 6988-7005.
- BOSCHI, C., DINI, A., BANESCHI, I., BEDINI, F., PERCHIAZZI, N., CAVALLO, A. (2017) Brucite-driven CO₂ uptake in serpentinized dunites. (Ligurian Ophiolites, Montecastelli, Tuscany). *Lithos* 288-289, 264-281.
- BOSWELL, R., COLLETT, T.S. (2011) Current perspectives on gas hydrate resources. *Energy & Environmental Science* 4, 1206-1215.
- BRANTLEY, S.L. (2008) Kinetics of mineral dissolution. In: S.L. Brantley, J.D. Kubicki, A.F. White (Eds.) *Kinetics of Water Rock Interaction*. Springer, New York, 151-210.
- BREWER, P.G., FRIEDERICH, G., LETZTER, E.T., ORR, F.M. (1999) Direct experiments of the ocean disposal of fossil CO₂. *Science* 284, 943-945.
- BROECKER, W. (1975) Climatic change: Are we on the brink of a pronounced global warming? *Science* 189, 460-463.
- BROECKER, W.S. (2012) The Carbon Cycle and Climate Change: Memoirs of my 60 years in Science. *Geochemical Perspectives* 1, 221-340.
- BROECKER, W. (2018) CO₂: Earth's climate driver. *Geochemical Perspectives* 7, 117-196.
- BROECKER, W.S., KUNZIG, R. (2008) *Fixing climate: what past climate changes reveal about the current threat and how to counter it*. Hill and Wang, New York.



- BROHAN, P., KENNEDY, J.J., HARRIS, I., TETT, S.F., JONES, P.D. (2006) Uncertainty estimates in regional and global observed temperature changes: A new data set from 1850. *Journal of Geophysical Research* 111, D12106.
- BROWN, C.W., KEELING, C.D. (1965) The concentration of atmospheric carbon-dioxide in Antarctica. *Journal of Geophysical Research* 70, 6077-6085.
- BRUNAUER S., EMMET P.H., TELLER E. (1938) Adsorption of gases in multimolecular layers. *Journal of the American Chemical Society* 60, 309-319.
- BRULLE, R.J. (2019) Networks of opposition: A structural analysis of U.S climate change countermovement coalitions 1989-2015. *Social Inquiry* 91, 603-624.
- BUDYKO, M.I. (1969) The effect of solar radiation variations on the climate of the Earth. *Tellus* 21, 611-619.
- BUICK, R. (2008) When did oxygenic photosynthesis evolve? *Philosophical Transactions of the Royal Society B* 363, 2731-2743.
- BURKE, A., PRESENT, T.M. PARIS, G., RAE, E. C.M., SANDILANDS, B.H., GAILLARDET, J., PEUKER-EHRENBRINK, B., FISHER, W.W., MCCLELLAND, J.W., SPENCER, R.G.M., VOSS, B.M. ADKINS, J.F. (2018) Sulfur isotopes in rivers: Insights into global weathering budgets, pyrite oxidation, and the modern carbon cycle. *Earth and Planetary Science Letters* 496, 168-177.
- BURTON, M.R., SAWYER, G.M., GRANIERI, D. (2013) Deep carbon emissions from volcanoes. *Reviews in Mineralogy and Geochemistry* 75, 323-354.
- CAILLON, N., SVERERINGHAUS, J.P., JOZEL, J., BARNOLA, J.-M., KANG, J., LIPENKOV, V.Y. (2003) Timing of atmospheric CO₂ and Antarctic changes across Termination III. *Science* 299, 1728-1731.
- CALENDAR, G.S. (1938) The artificial production of carbon dioxide and its influence on temperature. *Quarterly Journal of the Royal Meteorological Society* 64, 223-237.
- CALENDAR, G.S. (1961) Temperature fluctuations and trends over the Earth. *Quarterly Journal of the Royal Meteorological Society* 87, 1-12.
- CALMELS, D., GALLI, A., HOVIUS, N., BICKLE, M., WEST, A.J., CHEN, M.-C., CHAPMAN, H. (2011) Contribution of deep groundwater to the weathering budget in a rapidly eroding mountain belt, Taiwan. *Earth and Planetary Science Letters* 202, 48-58.
- CAMPBELL, I.H., ALLEN, C.M. (2008) Formation of supercontinents linked to increases in atmospheric oxygen. *Nature Geoscience* 1, 554-558.
- CANADELL, J.G., MONTEIRO, P.M.S., COSTA, M.H., COTRIM DA CUNHA, L., COX, P.M., ELISEEV, A.V., HENSEN, S., ISHII, M., JACCARD, S., KOVEN, C., LOHILA, A., PATRA, P.K. AND PIAO, S., ROGELJ, J., SYAMPUNGANI, S., ZAEHLE, S., ZICKFELD, K. (2021) Global Carbon and other Biogeochemical Cycles and Feedbacks. In: Masson-Delmotte, V., Zhai, P., Pirani, A., Connors, S.L., Péan, C., Berger, S., Caud, N., Chen, Y., Goldfarb, L., Gomis, M.I., Huang, M., Leitzell, K., Lonnoy, E., Matthews, J.B.R., Maycock, T.K., Waterfield, T., Yelekçi, O., Yu, R., Zhou, B. (Eds.) *Climate Change 2021: The Physical Science Basis. Contribution of Working Group I to the Sixth Assessment Report of the Intergovernmental Panel on Climate Change*. Cambridge University Press, Cambridge, United Kingdom and New York, NY, USA, 673-816.
- CANFIELD, D.E. (2005) The early history of atmospheric oxygen: Homage to Robert M. Garrels. *Annual Review of Earth and Planetary Sciences* 33, 1-36.
- CARBFIX (2022) Project CO₂-SeaStone <https://www.carbfix.com/co2-seastone> accessed 27 June 2022.
- CATLING, D.C., CLAIRE, M.W. (2005) How Earth's atmosphere evolved to and oxic state: A status report. *Earth and Planetary Science Letters* 237, 1-20.
- CHAMAS, A., MOON, H., ZHENG, J., QIU, Y., TABASSUM, T., JANG, J.H., ABU-OMAR, M., SCOTT, S. L., SUH, S. (2020) Degradation rates of plastics in the Environment. *ACS Sustainable Chemistry and Engineering* 8, 3494-3511.
- CHONG, Z.R., YANG, S.H.B., BABU, P., LINGS, P., LI, X.-S. (2016) Review of natural gas hydrates as an energy resource: Prospects and challenges. *Applied Energy* 162, 1633-1652.
- CLARK, D.E. (2019) Mineral storage of carbon in basaltic rocks at elevated temperatures. A field and experimental study. Ph.D. dissertation, Faculty of Earth Sciences, University of Iceland, 183 pp.



- CLARK, D.E., GUNNARSSON, I., ARADÓTTIR, E.S., ARNARSON, M.P., THORGEIRSSON, TH. A., SIGURDARDÓTTIR, S.S., SIGFÚSSON, B., SNAEBJÖRNSDÓTTIR, S.O., OELKERS, E.H., GISLASON, S.R. (2018) The chemistry and potential reactivity of the CO₂-H₂S charged injected waters at the basaltic CarbFix2 site, Iceland. *Energy Procedia* 146, 121-128.
- CLARK, D.E., GALECZKA, I., DIDERIKSEN, K., VOIGT, M., WOLFF-BOENISCH, D., GISLASON, S.R. (2019) Experimental observations of CO₂- water-basaltic glass interaction in a large column reactor experiment at 50°C. *International Journal of Greenhouse Gas Control* 89, 9-19.
- CLARK, D.E., OELKERS, E.H., GUNNARSSON, I., SIGFUSSON, B., SNAEBJORNSDOTTIR, S.O., ARADÓTTIR E.S., GISLASON S.R. (2020) CarbFix2: CO₂ and H₂S mineralization during 3.5 years of continuous injection into basaltic rocks at more than 250° C. *Geochimica et Cosmochimica Acta* 279, 45-66.
- COLE, D.R., OELKERS, E.H. (2008) Carbon dioxide sequestration. *Elements* 4, 289-360.
- COLLETT, T., BAHK, J.-J., BAKER, R., BOSWELL, R., DIVINS, D., FRYE, M., GOLDBERG, D., HUSEBØ, J., KOH, C., MALONE, M., MORELL, M., MYERS, G., SHIPP, C., TORRES, M. (2014) Methane Hydrates in Nature – Current Knowledge and Challenges. *Journal of Chemical & Engineering Data* 60, 319-329.
- COOGAN, L.A., GILLIS, K.M. (2013) Evidence that low-temperature oceanic hydrothermal systems play an important role in the silicate-carbonate weathering cycle and long-term climate regulation. *Geochemistry, Geophysics and Geosystems* 14, 1771-1786.
- COONEY, G., LITTLEFIELD, J., MARRIOTT, J., SKONE, T.J. (2015) Evaluating the climate benefits of CO₂-enhanced oil recovery using life cycle analysis. *Environmental Science and Technology* 49, 7491-7500.
- CRUTZEN, P.J. (2002) Geology of mankind. *Nature* 415, 23-24.
- DASGUPTA, R., HIRSCHMANN, M.M. (2010) The deep carbon cycle and melting in Earth's interior. *Earth and Planetary Science Letters* 298, 1-13.
- DAVAL, D. (2018) Carbon dioxide sequestration through silicate degradation and carbon mineralization: Promises and uncertainties. *Materials Degradation* 2, 11.
- DEFOE, O.K., COMPTON, A.H. (1925) The density of rock salt and calcite. *Physical Review* 25, 618-620.
- DEPAOLO, D., THOMAS, D., CHRISTENSEN, J., ZHANG, S., ORR, F., MAHER, K., BENSON, S., LAUTZE, N., XUE, Z., MITO, S. (2021) Opportunities for large-scale CO₂ disposal in coastal marine volcanic basins based on the geology of northeast Hawaii. *International Journal of Greenhouse Gas Control* 110, 103396.
- DELERCE, S., HEŘMANSKÁ, M., BÉNÉZETH, P., SCHOTT, J., OELKERS, E.H. (2023a) The dissolution rates of naturally altered basalts at pH 3 and 120 °C: Implications for the in-situ mineralization of CO₂ injected into the subsurface. *Chemical Geology* 621, 121353.
- DELERCE, S., HEŘMANSKÁ, M., BÉNÉZETH, P., SCHOTT, J., OELKERS, E.H. (2023b) Experimental determination of the reactivity of basalts as a function of their degree of alteration. *Geochimica et Cosmochimica Acta*, doi: 10.1016/j.gca.2023.09.007.
- DOMKE, G.M., OSWALT, S.N., WALTERS, B.F., MORIN, R.S. (2020) Tree planting has the potential to increase carbon sequestration capacity of forests in the United States. *Proceedings of the National Academy of Sciences* 117, 24649-24651.
- DUAN, Z., MOLLER, N., WEARE, J.H. (1992) An equation of state for the CH₄-CO₂-H₂O system: I. Pure systems from 0 to 1000 °C and 0 to 8000 bar. *Geochimica Cosmochimica Acta* 56, 2605-2617.
- DUARTE, C.M., JAREMKO, L., JAREMKO, M. (2020) Hypothesis: Potentially systemic impacts of elevated CO₂ in the human proteome and health. *Frontiers in Public Health* 8, 543322.
- DUC, N.H., CHAUVY, F., HERRI, J.-M. (2007) CO₂ Capture by Hydrate Crystallization – A Potential Solution for Gas Emission of Steelmaking Industry. *Energy Conversion and Management* 48, 1313-1322.
- DUNCAN, M.S., DASGUPTA, R. (2017) Rise of Earth's atmospheric oxygen controlled by efficient subduction of organic carbon. *Nature Geoscience* 10, 387-392.
- EBELMEN, J.J. (1845) Sur les produits de la décomposition des espèces minérales de la famille des silicates. *Annales des Mines Series* 4, 7, 3-66. (In French)



- EDMOND, J.M., PALMER, M.R., MEASURES, C.I., GRANT, B., STALLARD, R.F. (1995) The fluvial geochemistry and denudation rates of the Guyana shield in Venezuela, Colombia and Brazil. *Geochimica et Cosmochimica Acta* 59, 3301-3325.
- ETHERIDGE, D.M., STEELE, L.P., LANGENFELDS, R.L., FRANCEY, R.J., BARNOLA, J.-M., MORGAN, V.I. (1996) Natural and anthropogenic changes in atmospheric CO₂ over the last 1000 years from air in Antarctic ice and firn. *Journal of Geophysical Research* 101, 4115-4128.
- EIRIKSDOTTIR, E.S., LOUVAT, P., GISLASON, S.R., ÓSKARSSON, N., HARDARDÓTTIR, J. (2008) Temporal variation of the chemical and mechanical weathering in NE-Iceland, evaluation of a steady state model of erosion. *Earth and Planetary Science Letters* 272, 78-88.
- EIRIKSDOTTIR, E.S., GISLASON, S.R., OELKERS, E.H. (2013) Does temperature or runoff control the feedback between chemical denudation and climate? Insights from NE Iceland. *Geochimica et Cosmochimica Acta* 107, 65-81.
- EIRIKSDOTTIR, E.S., GISLASON, S.R., OELKERS, E.H. (2015) Direct evidence of the feedback between climate and nutrient, major, and trace element transport to the oceans. *Geochimica et Cosmochimica Acta* 166, 249-266.
- EIRIKSDOTTIR, E.S., OELKERS, E.H., HARDARDÓTTIR, J., GISLASON, S.R. (2017) The impact of damming on riverine fluxes to the ocean: A case study from Eastern Iceland. *Water Research* 113, 124-138.
- EUROPEAN COMMISSION (2015) *Council Directive (EU) 2015/1787 amending Annexes II and III to Council Directive 98/83/EC on the quality of water intended for human consumption*, European Union.
- FABRY, V.J., SEIBEL, B.A., FEELY, R.A., ORR, J.C. (2008) Impacts of ocean acidification on marine fauna and ecosystem processes. *ICES Journal of Marine Science* 65, 414-432.
- FALK, E.S., KELEMEN, P.B. (2015) Geochemistry and petrology of listvenite in the Oman Ophiolite: Complete carbonation of peridotite during ophiolite emplacement. *Geochimica et Cosmochimica Acta* 160, 70-90.
- FALKOWSKI, P., SCHOLES, R. J., BOYLE, E., CANADELL, J., CANFIELD, D., ELSER, J., GRUBER, N., HIBBARD, K., HÖGBERG, P., LINDER, S., MACKENZIE, F. T., MOORE, B., PEDERSEN, T., ROSENTHAL, Y., SEITZINGER, S., SMETACEK, V., STEFFEN, W. (2000) The global carbon cycle: a test of our knowledge of Earth as a system. *Science* 290, 291-296.
- FASIHI, M., EFIMOVA, O., BREYER, C. (2019) Techno-economic assessment of CO₂ direct air capture plants. *Journal of Cleaner Production* 224, 957-980.
- FERDOWS, M., OTA, M. (2006) Density of CO₂ hydrate by Monte Carlo simulation. *Proceedings of the Institution of Mechanical Engineers, Part C: Journal of Mechanical Engineering Science* 220, 691-696.
- FLAATHEN, T.K., GISLASON S.R., OELKERS, E.H. SVEINBJÖRNSDÓTTIR, A.E. (2009a) Chemical evolution of the Mt. Hekla, Iceland, groundwaters: A natural analogue for CO₂ sequestration in basaltic rock. *Applied Geochemistry* 24, 463-474.
- FLAATHEN, T.K., GISLASON, S.R., OELKERS, E.H. (2009b) The effect of aqueous sulphate on basaltic glass dissolution rates. *Chemical Geology* 277, 345-354.
- FOLGER, P. (2018) Carbon capture and sequestration (CCS) in the United States. *Congressional Research Service*.
- FRANTA, B. (2021) Early oil industry disinformation of global warming. *Environmental Politics* 30, 663-668.
- FRANZSON, H. (1998) The Nesjavellir high-temperature field, SW-Iceland, reservoir geology. *Proceedings 19th Annual PNOG-EDC Geothermal Conference, Manila, Philippines*, 13-20.
- FRIEDLINGSTEIN, P., JONES, M.W., O'SULLIVAN, M., ANDREW, R.M., BAKKER, D.C.E., HAUCK, J., LE QUÉRE, C., PETERS, G.P., PETERS, W., PONGRATZ, J., SITCH, S., CANADELL, J.G., CIAIS, P., JACKSON, R.B., ALIN, S.R., ANTHONI, P., BATES, N.R., BECKER, M., BELLOUIN, N., BOPP, L., CHAU, T.T.T., CHEVALLIER, F., CHINI, L.P., CRONIN, M., CURRIE, K.I., DECHARME, B., DJEUTCHOUANG, L., DOU, X., EVANS, W., FEELY, R.A., FENG, L., GASSER, T., GILFILLAN, D., GKRIZALIS, T., GRASSI, G., GREGOR, L., GRUBER, N., GÜRSES, Ö., HARRIS, I., HOUGHTON, R.A., HURTT, G. C., IIDA, Y., ILYINA, T., LUIJKX, I.T., JAIN, A.K., JONES, S.D., KATO, E., KENNEDY, D., KLEIN GOLDEWIJK, K., KNAUER, J., KORSBAKKEN,



- J.I., KÖRTZINGER, A., LANDSCHÜTZER, P., LAUVSET, S.K., LEFÈVRE, N., LIENERT, S., LIU, J., MARLAND, G., MCGUIRE, P.C., MELTON, J.R., MUNRO, D. R., NABEL, J.E.M.S., NAKAOKA, S.-I., NIWA, Y., ONO, T., PIERRROT, D., POULTER, B., REHDER, G., RESPLANDY, L., ROBERTSON, E., RÖDENBECK, C., ROSAN, T.M., SCHWINGER, J., SCHWINGSACKL, C., SÉFÉRIAN, R., SUTTON, A.J., SWEENEY, C., TANHUA, T., TANS, P.P., TIAN, H., TILBROOK, B., TUBIELLO, F., VAN DER WERF, G., VUICHARD, N., WADA, C., WANNINKHOF, R., WATSON, A., WILLIS, D., WILTSHIRE, A.J., YUAN, W., YUE, C., YUE, X., ZAEHLE, S., ZENG, J. (2022) Global Carbon Budget 2021. *Earth System Science Data* 14, 1917-2005.
- FUSS, S., LAMB, W.F., CALLAGHAN, M. W., HILAIRE, J., CREUTZIG F., AMANN, T., BERINGER, T., DE OLIVEIRA GARCIA, D. HARTMANN, J., KHANNA, T., LENZI, D., LUDERER, G., NEMET, G.F., ROGELJ, J., SMITH, P., VICENTE VICENTE, J.L., WILCOX, J., DEL MAR ZAMORA DOMINGUEZ, M., MINX, J.C. (2018) Negative emissions – Part 2: Costs, potentials and side effects. *Environmental Research Letters* 13, 063002.
- GADIKOTA, G. (2021) Carbon mineralization pathways for capture, storage and utilization. *Communication Chemistry* 4, 23.
- GAILLARD, F., SCAILLET, B., ARNDT, N.T. (2011) Atmospheric oxygenation caused by a change in volcanic degassing pressure. *Nature* 478, 229-232.
- GAILLARDET, J., DUPRE, B., LOUVAT, P., ALLÈGRE, C.J. (1999a) Global silicate weathering and CO₂ consumption rates deduced from the chemistry of large rivers. *Chemical Geology* 159, 3-30.
- GAILLARDET, J., DUPRE, B., ALLÈGRE, C.J. (1999b) Geochemistry of large river suspended sediments: Silicate weathering of crustal recycling? *Geochimica et Cosmochimica Acta* 63, 4037-4051.
- GAILLARDET, J., VIERS, J. DUPRE, B. (2003) Trace Elements in river waters. In: Drever, J.I. (Ed) *Surface and groundwater weathering, Erosion and Soils. Treatise in Geochemistry, Volume 5*. Elsevier, Amsterdam, The Netherlands, 225-272.
- GALECZKA, I.M., WOLFF-BOENISCH, D., JONSSON, T.H., SIGFUSSON, B., STEFÁNSSON, A., GISLASON, S.R. (2013) A novel high pressure column flow reactor for experimental studies of CO₂ mineral storage. *Applied Geochemistry* 30, 91-104.
- GALECZKA, I.M., WOLFF-BOENISCH, D., OELKERS, E.H., GISLASON, S.R. (2014) An experimental study of basaltic glass-H₂O-CO₂ interaction at 22 and 50 °C: Implications for subsurface storage of CO₂. *Geochimica et Cosmochimica Acta* 126, 123-145.
- GALECZKA, I.M., STEFÁNSSON, A., KLEINE, B.L., GUNNARSSON-ROBIN, J., SNÆBJÖRNSDÓTTIR, S.Ó., SIGFÚSSON, B., GUNNARSÓTTIR, S.H., WEISENBERGER, T.B., OELKERS, E.H. (2022) A pre-injection assessment of CO₂ and H₂S mineralization reactions at the Nesjavellir (Iceland) geothermal storage site. *International Journal of Greenhouse Gas Control* 115, 103610.
- GALY, A., FRANCE-LANORD, C. (1999) Weathering process in the Ganges-Brahmaputra basin and the riverine alkalinity budget. *Chemical Geology* 159, 31-60.
- GILFILLAN, S., LOLLAR, B.S., HOLLAND, G., BLAGBURN, D., STEVENS, S., SCHOELL, M., CASSIDY, M., DING, Z., ZHOU, Z., LACRAMPE-COULOUME, G. AND BALLENTINE, C.J. (2009) Solubility trapping in formation water as dominant CO₂ sink in natural gas fields. *Nature* 458, 614-618.
- GISLASON, S.R. (2005) Chemical weathering, chemical denudation and the CO₂ budget for Iceland. In: Caseldine, C., Russell, A., Hardardóttir, J., Knudsen, O. (Eds.) *Iceland: Modern Processes, Past Environments*. Elsevier, Amsterdam, The Netherlands, 289-307.
- GISLASON, S.R. (2008) Weathering in Iceland. *Jökull* 58, 387-408.
- GISLASON, S.R., EUGSTER, H.P. (1987a) Meteoric water-basalt interactions: I. A laboratory study. *Geochimica et Cosmochimica Acta* 51, 2827-2840.
- GISLASON, S.R., EUGSTER, H.P. (1987b) Meteoric water-basalt interactions: II. A field study in NE Iceland. *Geochimica et Cosmochimica Acta* 51, 2841-2855.
- GISLASON, S.R., OELKERS, E.H. (2003) The mechanism, rates and consequences of basalt glass dissolution: II. An experimental study of the dissolution rates of basaltic glass as a function of pH and temperature. *Geochimica et Cosmochimica Acta* 65, 3817-3832.



- GISLASON, S.R., ARNORSSON, S., ARMANNSSON, H. (1996) Chemical weathering of basalt as deduced from the composition of precipitation, rivers, and rocks in SW Iceland. *American Journal of Science* 296, 837-907.
- GISLASON, S.R., HEANEY, P.J., OELKERS, E.H., SCHOTT, J. (1997) Kinetic and thermodynamic properties of moganite, a novel silica polymorph. *Geochimica et Cosmochimica Acta* 61, 1193-1204.
- GISLASON, S.R., OELKERS, E.H., SNORRASON A. (2006) Role of river suspended material in the global carbon cycle. *Geology* 34, 49-52.
- GISLASON S.R., OELKERS, E.H., EIRIKSDOTTIR, E.S., KARDJILOV, M.I., GISLADOTTIR, G., SIGFUSSON, B., SNORRASON, A., ELEFSEN, S.O., HARDARDOTTIR, J., TORSSANDER, P., OSKARSSON, N. (2009) Direct evidence of the feedback between climate and weathering. *Earth and Planetary Science Letters* 277, 213-222.
- GISLASON, S.R., WOLFF-BOENISCH, D., STEFÁNSSON, A., OELKERS, E.H., GUNNLAUGSSON, E., SIGURDARDÓTTIR, H., SIGFÚSSON, B., BROECKER, W.S., MATTER, J.M., STUTE, M. (2010) Mineral sequestration of carbon dioxide in basalt: A pre-injection overview of the CarbFix project. *International Journal of Greenhouse Gas Control* 4, 537-545.
- GISLASON, S.R., OELKERS, E.H. (2014) Carbon Storage in Basalt. *Science* 344, 373-374.
- GISLASON, S.R., SIGURDARDÓTTIR, H., ARADÓTTIR, E.S.P., OELKERS, E.H. (2018) A brief history of CarbFix: Challenges and victories of the project's pilot phase. *Energy Procedia* 146, 103-114.
- GLOBAL CCS INSTITUTE (2011) Economic Assessment of Carbon Capture and Storage Technologies: 2011 Update <https://www.globalccsinstitute.com/archive/hub/publications/12786/economic-assessment-carbon-capture-and-storage-technologies-2011-update.pdf> accessed 23 September 2023.
- GLOBAL CCS INSTITUTE (2020) Global status of CCS 2020 <https://www.globalccsinstitute.com/wp-content/uploads/2021/03/Global-Status-of-CCS-Report-English.pdf> accessed 23 September 2023.
- GLOBAL CCS INSTITUTE (2021) Global status of CCS 2021. CCS Accelerating to Net Zero https://www.globalccsinstitute.com/wp-content/uploads/2021/10/2021-Global-Status-of-CCS-Report_Global_CCS_Institute.pdf accessed 23 September 2023.
- GLOBAL ROUNDTABLE ON CLIMATE CHANGE (2006) https://en.wikipedia.org/wiki/Global_Roundtable_on_Climate_Change#:~:text=The%20Global%20Roundtable%20on%20%20Climate.issues%20associated%20with%20climate%20change accessed 23 September 2023.
- GOLDBERG, D.S., TAKAHASHI, T., SLAGLE, A.L. (2008) Carbon dioxide sequestration in deep-sea basalt. *Proceedings of the National Academy of Science* 105, 9920-9925.
- GOLDBERG, D., TAKAHASHI, T., SLAGEL, A.L. (2009) Carbon dioxide sequestration in deep-sea basalt. *Proceedings of the National Academy of Science* 105, 9920-9925.
- GOLDBERG, D., ASTON, L., BONNEVILLE, A., DEMIRKANLI, I., EVANS, C., FISHER, A., GARCIA, H., GERRARD, M., HEESEMANN, M., HNOTTAVANGE-TELLEN, K., HSU, E., MALINVERNO, C., MORAN, K., PARK, A.-H.A., SCHERWATH, M., SLAGLE, A., STUTE, M., WEATHERS, T., WEBB, R., WHITE, M., WHITE, S. (2018) Geological storage of CO₂ in sub-seafloor basalt: the CarbonSAFE pre-feasibility study offshore Washington State and British Columbia. *Energy Procedia* 146, 158-165.
- GOLDSCHMIDT, V.M. (1934) Drei Vorträge über Geochemie. *Geologiska Föreningen i Stockholm Förhandlingar* 56, 385-427. (In German)
- GOLDTHORPE, S. (2017) Potential for very deep ocean storage of CO₂ without ocean acidification. A discussion paper. *Energy Procedia*, 114, 5417-5429.
- GRIMM, C., MARTINEZ, R.E.M., POKROVSKY, O.S., BENNING, L.G., OELKERS, E.H. (2019) Enhancement of cyanobacteria growth by riverine particulate material. *Chemical Geology* 525, 143-167.
- GRIMM, C., FEURTET-MALZEL, A., POKROVSKY, O.S., OELKERS, E.H. (2023) Riverine particulate matter enhances the growth and viability of the marine diatom *Thalassiosira weissflogii*. *Minerals* 13, 183.



- GUDBRANDSSON, S., WOLFF-BOENISCH, D., GISLASON, S.R., OELKERS, E.H. (2011) An experimental study of crystalline basalt dissolution from $2 \leq \text{pH} \leq 11$ and temperatures from 5 to 75°C. *Geochimica et Cosmochimica Acta* 75, 5496-5509.
- GUDBRANDSSON, S., WOLFF-BOENISCH, D., GISLASON, S.R., OELKERS, E.H. (2014) Experimental determination of plagioclase dissolution rates as a function of its composition and pH at 22 °C. *Geochimica et Cosmochimica Acta* 139, 154-172.
- GUMSLEY, A.P., CHAMBERLAIN, K.R., BLEEKER, W., SODERLUND, U., DE KOCK, M.O., LARSSON, E.R., BEKKER, A. (2017) Timing and tempo of the Great Oxidation Event. *Proceedings of the National Academy of Science* 114, 1811-1816.
- GUNNARSSON, A., STEINGRIMSSON, B.S., GUNNLAUGSSON, E., MAGNUSSON, J., MAACK, R. (1992) Nesjavellir geothermal co-generation power plant. *Geothermics* 21, 559-583.
- GUNNARSSON, I., ARADOTTIR, E.S., OELKERS, E.H., CLARK, D.E., ARNARSON, M.P., SIGFUSSON, B., SNAEBJORNSDOTTIR, S.O., MATTER, J.M., STUTE, M., JÚLIÚSSON, B.M., GISLASON, S.R. (2018) The rapid and cost-effective capture and subsurface mineral storage of carbon and sulfur at the CarbFix2 site. *International Journal of Greenhouse Gas Control* 79, 117-126.
- GUNTER, W.D., WIWCHAR, B., PERKINS, E.H. (1997) Aquifer disposal of CO₂-rich greenhouse gases: Extension of the time scale of experiment for CO₂-sequestering reactions by geochemical modelling. *Mineralogy and Petrology* 59, 121-140.
- GUTKNECHT, V., SNAEBJORNSDOTTIR, S.O., SIGFUSSON, B., ARADOTTIR, E.S., CHARLES, L. (2018) Creating a carbon dioxide removal solution by combining rapid mineralization of CO₂ with direct air capture. *Energy Procedia* 146, 129-134.
- GYSI, A.P., STEFÁNSSON, A. (2011) CO₂-water-basalt interaction. Numerical simulation of low temperature CO₂ sequestration into basalts. *Geochimica et Cosmochimica Acta* 75, 4728-4751.
- GYSI, A.P., STEFÁNSSON, A. (2012a) CO₂-water-basalt interaction. Low temperature experiments and implications for CO₂ sequestration into basalts. *Geochimica et Cosmochimica Acta* 81, 129-152.
- GYSI, A.P., STEFÁNSSON, A. (2012b) Experiments and geochemical modelling of CO₂ sequestration during hydrothermal basalt alteration. *Chemical Geology* 306-307, 10-28.
- HANSEN, J., JOHNSON, D., LACIS, A., LEBEDEFF, S., LEE, P., RIND, D., RUSSELL, G. (1981) Climate impact of increasing carbon dioxide. *Science* 213, 957-966.
- HANSEN, J., LEBEDEFF, S. (1987) Global trends of measured surface air temperature. *Journal of Geophysical Research* 92, 13345-13372.
- HARRISON, A.L., POWER, I.M., DIPPLE, G.M. (2013) Accelerated carbonation of brucite in mine tailings for carbon sequestration. *Environmental Science & Technology* 47, 126-134.
- HARTMANN, J. (2009) Bicarbonate-fluxes and CO₂-consumption by chemical weathering on the Japanese Archipelago – application of a multi-lithological model framework. *Chemical Geology* 265, 237-271.
- HARTMANN, J., JANSEN, N., DÜRR, H.H., KEMPE, S., KÖHLER, P. (2009) Global CO₂-consumption by chemical weathering: What is the contribution of highly active weathering regions? *Global and Planetary Change* 69, 185-194.
- HELGADOTTIR, H.M., FRANZSON, H., SIGURDSSON, Ó., ÁSMUNDSSON, R.K., (2009) Helliheiði – Hola HN-2. 1st, 2nd and 3rd stage: Drilling for security casing down to 153 m, production casing down to 403 m and production part down to 2001 m depth. Iceland GeoSurvey, Reykjavík, report ÍSOR 2009/031. (In Icelandic)
- HENRICH, S.M., REEBURGH, W.S. (1987) Anaerobic mineralization of marine sediment organic matter: Rates and the role of anaerobic processes in the oceanic carbon economy. *Geomicrobiology Journal* 5, 191-237.
- HERMAN, M., VOIGT, M.J., MARIANI, C., DECLERCQ, J., OELKERS, E.H. (2022) A comprehensive and internally consistent mineral dissolution rate database: Part I: Primary silicate minerals and glasses. *Chemical Geology* 597, 120807.
- HERMAN, M., VOIGT, M.J., MARIANI, C., DECLERCQ, J., OELKERS, E.H. (2023) A comprehensive and internally consistent mineral dissolution rate database: Part II: Secondary silicate minerals. *Chemical Geology* 363, 121632.



- HILLS, C.D., TRIPATHI, N., CAREY, P.J. (2020) Mineralization technology for carbon capture, utilization and storage. *Frontiers in Energy Research* 8, 142.
- HINDSHAW, R.S., BOURDON, B., VON STRANDMANN, P.A.P., VIGIER, N., BURTON, K.W. (2013) The stable calcium isotopic composition of rivers draining basaltic catchments in Iceland. *Earth and Planetary Science Letters* 374, 173-184.
- HOFMANN, G.E., BARRY, J.P., EDMUNDS, P.J., GATES, R.D., HUTCHINS, D.A., KLINGER, T., SEWELL, M.A. (2010) The effect of ocean acidification on calcifying organisms in marine ecosystems: An organism-to-ecosystem perspective. *Annual Review of Ecology, Evolution, and Systematics* 41, 127-147.
- HOLLAND, H.D. (1962) Model for the evolution of the Earth's atmosphere. In: Angel, A.E.J., James, H.L., Leonard, B.F. (Eds.) *Petrologic Studies: A Volume in Honor of A.F. Buddington*. Geological Society of America, Boulder, Colorado, 447-477.
- HOLLAND, H.D. (2009) Why the atmosphere became oxygenated: A proposal. *Geochimica et Cosmochimica Acta* 73, 5241-5255.
- HOSTETLER, P.B., COLEMAN, R.G., MUMPTON, F.A., EVANS, B.W. (1966) Brucite in alpine serpentines. *American Mineralogist* 51, 75-98.
- HOUSE, K.Z., SCHRAG, D.P., HARVEY, C.F., LACKNER, K.S. (2006) Permanent carbon dioxide storage in deep-sea sediments. *Proceedings of the National Academy of Sciences* 103, 12291-12295.
- HUMPHRIS, S.E., THOMPSON, G. (1978) Trace element mobility during hydrothermal alteration of oceanic basalts. *Geochimica et Cosmochimica Acta* 42, 127-136.
- HUTCHEON, I., SHEVALIER, M., DUROCHER, K., BLOCH, J., JOHNSON, G., NIGHTINGALE, M., MAYER, B. (2016) Interactions of CO₂ with formation waters, oil and minerals and CO₂ storage at the Weyburn IEA EOR site, Saskatchewan, Canada. *International Journal of Greenhouse Gas Control* 53, 354-370.
- INGALL, E., VAN CAPPELLEN, P. (1990) Relation between sedimentation-rate and burial of organic phosphorus and organic-carbon in marine sediments. *Geochimica et Cosmochimica Acta* 54, 373-386.
- IPCC (2005a) IPCC Special Report on Carbon Dioxide Capture and Storage (2005) In: Metz, B., Davidson, O., de Coninck, H.C., Loos, M., Meyer, L.A. (Eds.) *Prepared by Working Group III of the Intergovernmental Panel on Climate Change*. Cambridge University Press, Cambridge, United Kingdom and New York, NY, USA, 442 pp.
- IPCC (2005b) Underground geological storage. In: Metz, B., Davidson, O., de Coninck, H.C., Loos, M., Meyer, L.A. (Eds.) *IPCC Special Report on Carbon Dioxide Capture and Storage, prepared by Working Group III of the Intergovernmental Panel on Climate Change*. Cambridge University Press, Cambridge, UK, and New York, USA, pp 195-276.
- IPCC (2014) Climate Change 2014: Synthesis Report. Contribution of Working Groups I, II and III to the Fifth Assessment Report of the Intergovernmental Panel on Climate Change. Core Writing Team, Pachauri, R.K., Meyer, L.A. (Eds.). Intergovernmental Panel on Climate Change, Geneva, Switzerland, 151 pp.
- IPCC (2018) Summary for Policymakers. In: Masson-Delmotte, V., Zhai, P., Pörtner, H.O., Roberts, D., Skea, J., Shukla, P.R., Pirani, A., Moufouma-Okia, W., Péan, C., Pidcock, R., Connors, S., Matthews, J.B.R., Chen, Y., Zhou, X., Gomis, M.I., Lonnoy, E., Maycock, T., Tignor, M., Waterfield, T. (Eds.) *Global warming of 1.5°C. An IPCC Special Report on the impacts of global warming of 1.5°C above pre-industrial levels and related global greenhouse gas emission pathways, in the context of strengthening the global response to the threat of climate change, sustainable development, and efforts to eradicate poverty*. World Meteorological Organization, Geneva, Switzerland, 32 pp.
- JACOBSON, A.D., ANDREWS, M.G., LEHN, G.O., HOLMDEN, C. (2015) Silicate versus carbonate weathering in Iceland: New insights from Ca isotopes. *Earth Planetary Science Letters* 416, 132-142.
- JACOBSON, T.A., KLER, J. S., HERNKE, M.T., BRAUN, R.K., MEYER, K.C., FUNK, W.E. (2019) Direct human health risks of increased atmospheric carbon dioxide. *Nature Sustainability* 2, 691-701.



- JADHAWAR, P., YANG, J., CHAPOY, A., TOHIDI, B. (2021) Subsurface carbon dioxide sequestration and storage in methane hydrate reservoirs combined with clean methane energy recovery. *Energy Fuels* 35, 1567-1579.
- JARAMILLO, P., GRIFFIN, W.M., MCCOY, S.T. (2009) Life cycle inventory of CO₂ enhanced oil recovery. *Environmental Science and Technology* 21, 8027-8032.
- JAYARAMAN, K.S. (2007) India's carbon dioxide trap. *Nature* 445, 350.
- JEANDEL, C. (2016) Overview of the mechanisms that could explain the 'Boundary Exchange' at the land-ocean contact. *Philosophical Transactions of the Royal Society A*, 374, 20150287.
- JEANDEL, C., OELKERS, E.H. (2015) The influence of terrigenous particulate material dissolution on ocean chemistry and global element cycles. *Chemical Geology* 395, 50-66.
- JICKELLS, T.D. AN, Z.S., ANDERSEN, K.K., BAKER, A.R., BERAGAMETTI, G., BROOKS, N., CAO, J.J., BOYD, P.W., DUCE, R.A., HUNTER, K.A., KAWAHATA, H., KUBILAY, N., LAROCHE, J., LISS, P.S., MAHOWAD, N., PROSPERO, J.M., RIDGWELL, A.J., TEGEN, I., TORRES, R. (2005) Global iron connections between desert dust, ocean biogeochemistry, and climate. *Science* 308, 67-71.
- JÓHANNESSON, H., SAEMUNDSSON, K. (1998) Geological Map of Iceland — Bedrock Geology. The Icelandic Institute of Natural History, Reykjavik, Iceland.
- JÓHANNESSON, T., AÐALGEIRSDÓTTIR, G., BJÖRNSSON, H., CROCHET, P., ELÍASSON, E.B., GUDMUNDSSON, S., JÓNSDÓTTIR, J.F., ÓLAFSSON, H., PÁLSSON, F., RÖGNVALDSSON, O., SIGURÐSSON, O., SNORRASON, A., SVEINSSON, O.G.B., THORSTEINSSON, T. (2007) Effect of climate change on hydrology and hydro-resources in Iceland. OS-2007-011. Orkustofnun National Energy Authority, Reykjavik, 91 pp. <https://orkustofnun.is/gogn/Skyrslur/OS-2007/OS-2007-011.pdf>
- JOHNSON, J.W., OELKERS, E.H., HELGESON, H.C. (1992) SUPCRT92 software package for calculating the standard molal thermodynamic properties of minerals, gases, aqueous species and reactions from 1 to 500 bars and 0 to 1000°C. *Computers & Geosciences* 18, 889-947.
- JONES, P.D., RAPER, S.C.B., WIGLEY, T.M.L. (1986a) Southern Hemisphere surface air temperature variations: 1851-1984. *Journal of Climate and Applied Meteorology* 25, 1213-1230.
- JONES, P.D., RAPER, S.C.B., BRADLEY, R.S., DIAZ, H.F., KELLY, P.M., WIGLEY, T. (1986b) Northern Hemisphere surface air temperature variations: 1851-1984. *Journal of Climate and Applied Meteorology* 25, 161-179.
- JONES, M.T., PEARCE, C.R., OELKERS, E.H. (2011) An experimental study of basaltic riverine particulate material and seawater. *Geochimica et Cosmochimica Acta* 77, 108-120.
- JONES, M.T., PEARCE, C.R., OELKERS, E.H. (2012a) An experimental study of the interaction of basaltic riverine particulate material and seawater. *Geochimica et Cosmochimica Acta* 77, 108-120.
- JONES, M.T., PEARCE, C.R., JEANDEL, C., GISLASON, S.R., EIRIKSDOTTIR, E., MAVROMATIS, V., OELKERS, E.H. (2012b) Riverine particulate material dissolution as a significant flux of strontium to the oceans. *Earth and Planetary Science Letters* 355, 51-59.
- JONES, M.T., GISLASON, S.R., BURTON, K.W., PEARCE, C.R., MAVROMATIS, V., POGGE VON STRANDMANN, P.A.E., OELKERS, E.H. (2014) Quantifying the impact of riverine particulate dissolution in seawater on ocean chemistry. *Earth and Planetary Science Letters* 395, 91-100.
- JONES, M.T., GISLASON, S.R., BURTON, K.W., PEARCE, C.R., MAVROMATIS, V., POGGE VON STRANDMANN, P.A.E., OELKERS, E.H. (2014) Quantifying the impact of riverine particulate dissolution in seawater on ocean chemistry. *Earth and Planetary Science Letters* 395, 91-100.
- KANG, S.-P., LEE, H. (2000) Recovery of CO₂ from Flue Gas Using Gas Hydrate: Thermodynamic Verification through Phase Equilibrium Measurements. *Environmental Science & Technology* 34, 4397-4400.
- KANTOLA, I.B., MASTERS, M.D., BEERLING, D.J., LONG, S.P., DELUCIA, E.H. (2017) Potential of global croplands and bioenergy crops for climate change mitigation through deployment for enhanced weathering. *Biology Letters* 13, 20160714.
- KARDJILOV, M.I. (2008) Riverine and terrestrial carbon fluxes in Iceland. Doctoral Thesis. University of Iceland, Reykjavik, Iceland, 83 pp.



- KARNAUSKAS, K., MILLER, S.L., SCHAPIRO, A.C. (2020) Fossil fuel combustion is driving indoor CO₂ levels harmful to human cognition. *GeoHealth* 4, e2019GH000237.
- KASTING, J.F. (2013) What caused the rise of atmospheric O₂? *Chemical Geology* 362, 13-23.
- KASTING, J.F. (2019) The Goldilocks Planet? How silicate weathering maintains Earth 'Just right'. *Elements* 15, 325-240.
- KEITH, D.W., HOLMES, G., ST. ANGELO, D., HEIDEL, K (2018) A process for capturing CO₂ from the atmosphere. *Joule* 2, 1573-1594.
- KELEMEN, P.B., MATTER, J.M. (2008) *In situ* carbonation of peridotite for CO₂ storage. *Proceedings of the National Academy of Science USA* 105, 17295-17300.
- KELEMEN, P.B., MATTER, J.M., STREIT, E.E., RUDGE, J.F., CURRY, W.B., BLUSZTAJN, J. (2011) Rates and mechanisms of mineral carbonation in peridotite: Natural processes and recipes for enhances, *in situ* CO₂ capture and storage. *Annual Review of Earth and Planetary Sciences* 39, 545-576.
- KELEMEN, P.B., MCQUEEN, N., WILCOX, J., RENFORTH, P., DIPPLE, G., VANKEUREN, A.P. (2020) Engineered carbon mineralization in ultramafic rocks for CO₂ removal from air: Review and new insights. *Chemical Geology* 550, 119628.
- KELEMEN, P.B., DE OBESO, J.C., LEONG, J.A., GODARD, M., OKAZAKI, K., KOTOWSKI, A.J., MANNING, C.E., ELLISON, E.T., MENZEL, M.D., URAI, J.L., HIRTH, G., RIOUX, M., STOCKLI, D.F., LAFAY, R., BEINLICH, A.M., COGGON, J.A., WARSI, N.H., MATTER, J.M., TEAGLE, D.A.H., HARRIS, M., MICHIBAYASHI, K., TAKAZAWA, E., AL SULAIMANI, Z., THE OMAN DRILLING PROJECT SCIENCE TEAM (2022) Listvenite formation during mass transfer into the leading edge of the mantle wedge: Initial results from Oman Drilling Project Hole BT1B. *Journal of Geophysical Research* 127, e2021JB022352.
- KHALILABAD, M.R. (2008) Characterization of the Hellisheiði – Threngslí CO₂ Sequestration Target aquifer by Tracer Testing. M.Sc. Thesis, Faculty of Earth Sciences, University of Iceland, 44 pp.
- KHALILABAD M.R., AXELSSON, G., GISLASON, S.R. (2008) Aquifer characterization with tracer test technique; permanent CO₂ sequestration into basalt, SW Iceland. *Mineralogical Magazine* 72, 121-125.
- KHAN, M.A. (2010) The geysers geothermal field. An injection success story. Proceedings World Geothermal Congress 2010 Bali, Indonesia, 25-29 April 2010. <https://www.geothermal-energy.org/pdf/IGAstandard/WGC/2010/0620.pdf>
- KILIAN, L. (2008) The Economic Effects of Energy Price Shocks. *Journal of Economic Literature* 46, 871-909.
- KIPP, M., KRISSENSAN-TOTTON, M., CATLING, D. (2021) High organic burial efficiency is required to explain mass balance in Earth's early carbon cycle. *Global Biogeochemical Cycles* 35, e2020GB006707, doi: 10.1029/2020GB006707.
- KIRSCHVINK, J.L., GAIDOS, E.J., BERTANI, L.E., BEUKES, N.J., GUTZMER, J., MAEPA, L.N., STEINBERGER, R.E. (2000) Paleoproterozoic snowball Earth: Extreme climatic and geochemical global change and its biological consequences. *Proceedings of the National Academy of Sciences* 97, 1400-1405.
- KOIDE, H., TAKAHASHI, M., SHINDO, Y., TAZAKI, Y., IIJIMA, M., ITO, K., KIMURA, N., OMATA, K. (1997) Hydrate formation in sediments in the sub-seabed disposal of CO₂. *Energy* 22, 279-283.
- KOLBERT, E. (2011) Enter the Anthropocene, age of man. *National Geographic* 219, 60-85.
- KÖPPEN, W. (1881) Über mehrjährige Perioden der Witterung – III. Mehrjährige Änderungen der Temperatur 1841 bis 1875 in den Tropen der nördlichen und südlichen gemässigten Zone, an den Jahresmitteln untersucht. *Zeitschrift der Österreichischen Gesellschaft für Meteorologie* Bd XVI, 141-150. (In German)
- KRISSENSAN-TOTTON, M., KIPP, M., CATLING, D. (2021) Carbon cycle inverse modelling suggests large changes in fractional organic burial are consistent with the carbon isotope record and may have contributed to the rise in oxygen. *Geobiology* 19, 342-363.



- KRISTJANSSON, B.R., AXELSSON, G., GUNNARSSON, G., GUNNARSSON, I., OSKARSSON, F. (2016) Comprehensive tracer testing in Hellsheiði Geothermal field in SW-Iceland. In Proceedings of the 41st Workshop on Geothermal Reservoir Engineering.
- KUMAR, A., SHRIVASTAVA, J.P. (2019) Thermodynamic modelling and experimental validation of CO₂ mineral sequestration in Mandla Basalt of the Eastern Deccan Volcanic Province. India. *Journal of the Geological Society of India* 93, 269-277.
- KUMP, L.R. (2008) The rise of atmospheric oxygen. *Nature* 451, 277-278.
- LABAT, D., GODDÉRIIS, Y., PROBST, J.L., GUYOT, J.L. (2004) Evidence for global runoff increase related to climate warming *Advances in Water Resources* 27, 631-642.
- LAMLON, S.H., SAVIDGE, R.A. (2003) A reassessment of carbon content in wood: variation within and between 41 North American species. *Biomass Bioenergy* 25, 381-388.
- LE TREUT, H., SOMERVILLE, R., CUBASCH, U., DING, Y., MAURITZEN, C., MOKSSIT, A., PETERSON, T., PRATHER, M. (2007) Historical Overview of Climate Change. In: Solomon, S., Qin, D., Manning, M., Chen, Z., Marquis, M., Averyt, K.B., Tignor, M., Miller, H.L. (Eds.) *Climate Change 2007: The Physical Science Basis. Contribution of Working Group I to the Fourth Assessment Report of the Intergovernmental Panel on Climate Change*. Cambridge University Press, Cambridge, United Kingdom and New York, NY, USA, 93-127.
- LEE, C.-T.A., JIANG, H., DASGUPTA, B., TORRES, M. (2019) A framework for understanding whole Earth carbon cycling. In: Orcutt, B., Daniel, I., Dasgupta, R. (Eds.) *Deep Carbon: Past to present*. Cambridge University Press, Cambridge, 313-357.
- LEE, S., LIANG, L., RIESTENBERG, D., WEST, O.R., TSOURIS C., ADAMS, E. (2003) CO₂ hydrate composite for ocean carbon sequestration. *Environmental Science and Technology* 37, 3701-3708.
- LEE, H.J., LEE, J.D., LINGA, P., ENGLEZOS, P., KIM, Y.S., LEE, M.S., KIM, Y.D. (2010) Gas hydrate formation process for pre-combustion capture of carbon dioxide. *Energy* 35, 2729-2733.
- LEE, H., MUIRHEAD, J.D., FISCHER, T.P., EBINGER, C.J., KATTENHORNM, S.A., SHARP, Z.D., KIANJI, G. (2016) Massive and prolonged deep carbon emissions associated with continental rifting. *Nature Geoscience* 9, 145-149.
- LEHAMMN, J., RILLIG, M., THIES, J., MASIELLO, C.A., HOCKADAY, W.C., CROELEY, D. (2011) Biochar effects on soil biota – A review. *Soil Biology and Biochemistry* 43, 1812-1836.
- LEISEROWITZ, A.A., MAIBACH, E.W., ROSER-RENOUF, C., SMITH, N., DAWSON, E. (2012) Climategate, public opinion, and the loss of trust. *American Behavioral Scientist* 57, 818-837.
- LEONG, J.A.M., ELY, T., SHOCK, E.L. (2021) Decreasing extents of Archean serpentinization contributed to the rise of an oxidized atmosphere. *Nature Communications* 12, 1-11.
- LI, G., HARTMANN, J., DERRY, L.A., WEST, A.J., YOU, C.-F., LONG, X., ZHAN, T., LI, L., LI, G., QIU, W., LI, T., LIU, L., CHEN, Y., Ji, J., ZHAO, L., CHEN, J. (2016) Temperature dependence of basalt weathering. *Earth and Planetary Science Letters* 443, 59-69.
- LI, S.-L., CALMALS, D., HAN, G., GAILLARDET, J., LIU, C.-Q. (2008) Sulfuric acid as an agent of carbonate weathering constrained by dC_{DIC}: Examples from Southwest China. *Earth and Planetary Science Letters* 270, 189-199.
- LI, J., HITCH, M., POWER, I.M., PAN, Y. (2018) Integrated mineral carbonation of ultramafic mine deposits—a review. *Minerals* 8, 147.
- LINGA, P., KUMAR, R., ENGLEZOS, P. (2007) The clathrate hydrate process for post and pre-combustion capture of carbon dioxide. *Journal of Hazardous Materials* 149, 625-629.
- LINKE, T., OELKERS, E.H., MÖCKEL, S., GISLASON, S.R. (2023) Direct evidence of CO₂ drawdown through enhanced weathering. Preprint (version v1) available at Research Square, doi: 10.21203/rs.3.rs-3439312/v1.
- LITTLE, S.H., VANCE, D., MCMANUS J., SEVERMANN, S. (2016) Key role of continental margin sediments in the oceanic mass balance of Zn and Zn isotopes. *Geology* 44, 207-210.
- LITTLE, S.H., ARCHER, C., MILNE, A., SCHLOSSER, C., ACHTERBERG, E.P., LOHAN, M.C., VANCE, D. (2018) Paired dissolved and particulate phase Cu isotope distributions in the South Atlantic. *Chemical Geology* 502, 29-43.



- LIU, T., WU, P., CHEN, Z., LI, Y. (2022a) Review on carbon dioxide replacement of natural gas hydrate: Research progress and perspectives. *Energy Fuels* 36, 7321-7336.
- LIU, D., AGARWAL, R., LIU, F., YANG, S., LI, Y. (2022b) Modeling and assessment of CO₂ geological storage in the Eastern Deccan Basalt of India. *Environmental Science and Pollution Research International* 29, 85465-85481.
- LOUVAT, P. (1997) Étude géochimique de l'érosion fluviale d'îles volcaniques à l'aide des bilans d'éléments majeurs et traces. Thesis, Institut de Physique du Globe de Paris, France, 223 pp. (In French)
- LOUVAT, P., GISLASON, S.R., ALLÈGRE, C.J. (2008) Chemical and mechanical erosion rates in Iceland as deduced from river dissolved and solid material. *American Journal of Science* 308, 679-726.
- LOWE, R.J., HUEBNER, G.M., ORESZCZYN, T. (2018) Possible future impacts of elevated levels of atmospheric CO₂ on human cognitive performance and on the design and operation of ventilation systems in buildings. *Building Services Engineering Research Technologies* 39, 698-711.
- LUO, G., ONO, S., BEUKES, N.J., WANG, D.T., XIE, S., SUMMONS, R.E. (2016) Rapid oxygenation of Earth's atmosphere 2.33 billion years ago. *Science Advances* 2, 1600134.
- LUYSSAERT, S., SCHULZE, E.D., BÖRNER, A., KNOHL, A., HESSENMOLLER, D., LAW, B.E., CIAIS, P., GRACE, J. (2008) Old-growth forests as global carbon sinks. *Nature* 455, 213-215.
- LYONS, T.W., REINHARD, C.T., PLANAVSKY, N.J. (2014) The rise of oxygen in Earth's early ocean and atmosphere. *Nature* 506, 307-315.
- MACFARLING MEURE, C., ETHERIDGE, D., TRUDINGER, C., STEELE, P., LANGENFELDS, R., VAN OMMEN, T., SMITH, A., ELKINS, J. (2006) Law Dome CO₂, CH₄ and N₂O ice core records extended to 2000 years BP. *Geophysical Research Letters*, 33.
- MACKENZIE, F.T., ANDERSSON, A.J. (2013) The marine carbon system and ocean acidification during Phanerozoic time. *Geochemical Perspectives* 2, 1-227.
- MANABE, S., STOUFFER R.J. (1980) Sensitivity of a Global Climate Model to an increase of CO₂ concentration in the atmosphere. *Journal of Geophysical Research* 85, 5529-5554.
- MARCHETTI, C. (1977) On geoengineering and the CO₂ problem. *Climatic Change* 1, 59-68.
- MARIENI, C., VOIGT, M., CLARK, D.E., GISLASON, S.R., OELKERS, E.H. (2021) Mineralization potential of water-dissolved CO₂ and H₂S injected into basalts as function of temperature: Freshwater versus Seawater. *International Journal of Greenhouse Gas Control* 109, 103357.
- MATTHEWS, E. (1997) Global litter production, pools, and turnover times: Estimates from measurement data and regression models. *Journal of Geophysical Research: Atmospheres* 102, 18771-18800.
- MATTER, J.M., STUTE, M., SNÆBJÖRNSDÓTTIR, S.Ó., OELKERS, E.H., GISLASON, S.R., ARADOTTIR, E.S., SIGFUSSON, B., GUNNARSSON, I., SIGURDARDOTTIR, H., GUNNLAUGSSON, E., AXELSSON, G., ALFREDSSON, H.A., WOLFF-BOENISCH, D., MESFIN, K., FERNANDEZ DE LA REGUERA TAYA, D., HALL, J., DIDERIKSEN, K., BROECKER, W.S. (2016) Rapid carbon mineralization for permanent and safe disposal of anthropogenic carbon dioxide emissions. *Science* 352, 1312-1314.
- MARTY, B., TOLSTIKHIN, I.N. (1998) CO₂ fluxes from mid-ocean ridges, arcs and plumes. *Chemical Geology* 145, 233-248.
- MAVROMATIS, V., PEARCE, C.R., SHIROKOVA, L.S., BUNDELEVA, I.A., POKROVSKY, O.S., BENEZETH, P., OELKERS, E.H. (2012) Magnesium isotope fractionation during hydrous magnesium carbonate precipitation with and without cyanobacteria. *Geochimica Cosmochimica Acta* 76, 161-174.
- MAVROMATIS, V., MEISTER, P., OELKERS, E.H. (2014) Using stable Mg isotopes to distinguish dolomite formation mechanisms: A case study from the Peru Margin. *Chemical Geology* 385, 84-91.
- MAZZOTTI, M., BACIOCCHI, R., DESMOND, M.J., SOCOLOW, R.H. (2013) Direct air capture of CO₂ with chemicals: Optimization of a two-loop hydroxide carbonate system using a countercurrent air-liquid contactor. *Climatic Change* 118, 119-135.



- MCGRAIL P.B., SCHAEF, H.T., HO, A.M., CHIEN, Y.J., DOOLEY, J.J., DAVIDSON, C.L. (2006) Potential for carbon dioxide sequestration in flood basalts. *Journal of Geophysical Research: Solid Earth* 111, B12.
- MCGRAIL, B.P., SPANE, F.A., AMONETTE, J.E., THOMPSON, C.R., BROWN, C.F. (2014) Injection and monitoring at the Wallula basalt pilot project. *Energy Procedia* 63, 2939-2948.
- MCGRAIL, B.P., SCHAEF, H.T., SPANE, F.A., CLIFF, J.B., QAFOKU, O., HORNER, J.A., THOMPSON, C.J., OWEN, A.T., SULLIVAN, C.E. (2017) Field validation of supercritical CO₂ reactivity with basalts. *Environmental Science & Technology Letters* 4, 6-10.
- MCQUEEN, N., KELEMAN, P.B., DIPPLE, G., RENFORTH, P., WILCOX, J. (2020) Ambient weathering of magnesium oxide for CO₂ removal from air. *Nature Communications* 11, 3299.
- METCALF, G.E. (2020) Designing a carbon tax to reduce US greenhouse gas emissions. *Review of Environmental Economics and Policy* 3, 1.
- MINX, J.C., WILLIAM F. LAMB, W.F., CALLAGHAN. M.W., BORNMANN, L., SABINE FUSS, S. (2017) Fast growing research on negative emissions. *Environmental Research Letters* 12, 035007.
- MINX, J.C., LAMB, W.F., CALLAGHAN, M. W., FUSS, S., HILAIRE, J., CREUTZIG F., AMANN, T., BERINGER, T., DE OLIVEIRA GARCIA, D. HARTMANN, J., KHANNA, T., LENZI, D., LUDERER, G., NEMET, G.F., ROGELJ, J., SMITH, P., VICENTE VICENTE, J. L., WILCOX J., DEL MAR ZAMORA DOMINGUEZ, M. (2018) Negative emissions – Part 1: Research landscape and synthesis. *Environmental Research Letters* 13, 063001.
- MILLS, B.J.W., LENTON, T., WATSON, A. (2014) Proterozoic oxygen rise linked to shifting balance between seafloor and terrestrial weathering. *Proceedings of the National Academy of Sciences* 111, 9073-9078.
- MITCHELL, J.M., JR. (1963) On the world-wide pattern of secular temperature change. In: *Changes of Climate. Proceedings of the Rome Symposium Organized by UNESCO and the World Meteorological Organization, 1961 (UNESCO Arid Zone Research Series, 20)*. UNESCO, Paris, 161-181.
- MITCHELL, J.M., JR. (1972) The natural breakdown of the present interglacial and its possible intervention by human activities. *Quaternary Research* 2, 436-445.
- MOLNAR, Z., PEKKER, P., DODONY, I., POSFAI, M. (2021) Clay minerals affect calcium (magnesium) carbonate precipitation and aging. *Earth and Planetary Science Letters* 567, 116971.
- MOLNAR, Z., DODONY, I., POSFAI, M. (2023) Transformation of amorphous calcium carbonate in the presence of magnesium, phosphate, and mineral surfaces. *Geochimica et Cosmochimica Acta* 345, 90-101.
- MONTERRAT, F., RENFORTH, P., HARTMANN, J., LEERMAKERS, M., KNOPS, P., MEYSMANN, F.J.R. (2017) Olivine dissolution in seawater: Implications for CO₂ sequestration through enhanced weathering in coastal environments. *Environmental Science & Technology* 51, 3960-3972.
- MOORBATH, S., SIGURDSSON, H., GOODWIN, R. (1968) K–Ar ages of the oldest exposed rocks in Iceland. *Earth and Planetary Science Letters* 4, 197-205.
- MOOSDORF, N., RENFORTH, P., HARTMANN, J. (2014) Carbon dioxide efficiency of terrestrial enhanced weathering. *Environmental Science and Technology* 48, 4809-4816.
- MORGUNBLAÐIÐ MBL.IS. (2018) Milljarða sparnaður vegna vísindastarfs (Saving billions of Icelandic kronas by scientific collaborations) https://www.mbl.is/frettir/innlent/2018/03/14/milljarða_sparnadur_vegna_visinda/ accessed 20 September 2023. (In Icelandic)
- MUDD, G.M. (2001) Critical review of acid in situ leach uranium mining: 1. USA and Australia. *Environmental Geology* 41, 390-403.
- MUNGAN, N. (1981) Carbon dioxide flooding – fundamentals. *Journal of Canadian Petroleum Technology* 20, 81-01-03.
- MUNGAN, N. (1992) Carbon dioxide flooding as an enhanced oil recovery process. *Journal of Canadian Petroleum Technology* 31, 92-09-01.
- MÜLLER, P.J., SUESS, E. (1979) Productivity, sedimentation rate, and sediment organic matter in the oceans. *Deep Sea Research Part A. Oceanographic Research Papers* 26, 1347-1362.



- NATIONAL ACADEMIES OF SCIENCES, ENGINEERING, AND MEDICINE (2019) Negative Emissions Technologies and Reliable Sequestration: A Research Agenda. Washington, DC, The National Academies Press.
- NOAA (2022) Global Monitoring Laboratory, Carbon Cycle Greenhouse Gases, Trends in Atmospheric Carbon Dioxide <https://gml.noaa.gov/ccg/trends/> accessed 20 January 2022.
- NOAA (2023) National Oceanic & Atmospheric Administration Global Monitoring laboratory. Daily and weekly average CO₂ at Mauna Loa <https://gml.noaa.gov/ccg/trends/weekly.html> accessed 19 September 2023.
- NEUHOFF, P.S., FRIDRIKSSON, T., ARNORSSON, S., BIRD, D.K. (1999) Porosity evolution and mineral paragenesis during low-grade metamorphism of basaltic lavas at Teigarhorn, eastern Iceland. *American Journal of Science* 299, 467-501.
- NI, Y., ESKELAND, G.S., GISKE, J., HANSEN, J.-P. (2016) The global potential for carbon capture and storage from forestry. *Carbon Balance Management* 11, 3.
- NICHOLS, C., WALLACE, M., BALASH, P.C. (2012) A note on sources of CO₂ supply for enhanced oil recovery <https://www.osti.gov/servlets/purl/1507996> accessed 2 September 2023.
- NGUYEN, N.N., LA, V.T., HUYNH, C.D., NGUYEN, A.V. (2022) Technical and economic perspectives of hydrate-based carbon dioxide capture. *Applied Energy* 307, 118237.
- NOROUZI, N., FANI, M., ZIARANI, Z.K. (2020) The fall of oil age: A scenario planning approach over the last peak oil of human history by 2040. *Journal of Petroleum Science and Engineering* 188, 106827.
- NUNEZ-LOPEZ, V., GIL-EGUI, R., HOSSEINI, S.A. (2019) Environmental and operational performance of CO₂-EOR as a CCUS technology: A Cranfield example with dynamic LCA considerations. *Energies* 12, 448.
- NUNEZ-LOPEZ, V., MOSKAL, E. (2019) Potential of CO₂-EOR for near-term decarbonization. *Frontiers in Climate* 10.3389.
- OELKERS, E.H., SCHOTT, J. (1998) Does organic acid adsorption affect alkali-feldspar dissolution rates? *Chemical Geology* 151, 235-245.
- OELKERS, E.H., GISLASON S.R. (2001) The mechanism, rates and consequences of basalt glass dissolution. I. An experimental study of the dissolution rates of basaltic glass as a function of aqueous Al, Si, and oxalic acid concentration at 25 C and pH = 3 and 11. *Geochimica et Cosmochimica Acta* 65, 3671-3681.
- OELKERS, E.H., SCHOTT, J. (2001) An experimental study of enstatite dissolution and the mechanism of pyroxene/pyroxenoid dissolution. *Geochimica et Cosmochimica Acta* 65, 1219-1231.
- OELKERS, E.H., COLE, D.R. (2008) Carbon dioxide sequestration: Solution to a global problem. *Elements* 4, 305-310.
- OELKERS, E.H., GISLASON, S.R., MATTER, J. (2008) Mineral Carbonation of CO₂. *Elements* 4, 333-337.
- OELKERS, E.H., GISLASON, S.R., EIRIKSDOTTIR, E.S., JONES, M., PEARCE, C. R., JEANDEL, C. (2011) The role of riverine particulate material of the global cycle of the elements. *Applied Geochemistry* 26, S65-S369.
- OELKERS, E.H., GISLASON, S.R., EIRIKSDOTTIR, E.S., JONES, M., PEARCE, C. R., JEANDEL, C. (2012) Riverine particulate material dissolution in seawater and its implications for the global cycles of the elements. *Comptes Rendus Geosciences* 344, 646-651.
- OELKERS, E.H., DECLERCQ, J., SALDI, G.D., GISLASON, S.R., SCHOTT, J. (2018) Olivine dissolution rates: A critical review. *Chemical Geology* 500, 1-19.
- OELKERS, E.H., BUTCHER, R., POGGE VON STRANDMANN, P.A.E., SCHUESSLER, J.A., BLANCKENBURG, F., SNÆBJÖRNSDÓTTIR, S.Ó., MESFIN K., ARADÓTTIR, E.S.P, GUNNARSSON, I., SIGFÚSSON, B., GUNNLAUGSSON, E., MATTER, J.M., STUTE, M., GISLASON, S.R. (2019) Using stable Mg isotope signatures to assess the fate of magnesium during the in-situ mineralisation of CO₂ and H₂S at the CarbFix site in SW-Iceland. *Geochimica et Cosmochimica Acta* 245, 542-555.



- OELKERS, E.H., ARKADAKSKIY, S., AFIFI, A.M., HOTEIT, H., RICHARDS, M., FEDORIK, J., DELAUNAY, A., TORRES, J.E., AHMED, Z.T., KUNNUMMAL, N., GISLASON, S.R. (2022) The subsurface carbonation potential of basaltic rocks from the Jizan region of Southwest Saudi Arabia. *International Journal of Greenhouse Gas Control* 120, 103772.
- OELKERS, E.H., GISLASON, S.R., KELEMAN, P.B. (2023) Moving subsurface carbon mineral storage forward. *Carbon Capture Science & Technology* 6, 100098.
- OIL-CLIMATE INDEX (2015) Carnegie Endowment for International Peace <http://oci.carnegieendowment.org/#total-emissions> accessed 24 September 2023.
- OKOKO, G.O., OLAKA, L.A. (2021) Can East African rift basalts sequester CO₂? Case study of the Kenya rift. *Scientific African* 13, e00924.
- OLAFSSON, J., OLAFSDOTTIR, S.R., BENOIT-CATTIN, A., DANIELSEN, M., ARNARSON, T.S., TAKAHASHI, T. (2009) Rate of Iceland Sea acidification from time series measurements. *Biogeosciences Discussions* 6, 5251-5270.
- OLSSON, J., STIPP, S.L.S., MAKOVICKY, E., GISLASON, S.R. (2014a) Metal scavenging by calcium carbonate at the Eyjafjallajökull volcano: A carbon capture and storage analogue. *Chemical Geology* 384, 135-148.
- OLSSON, J., STIPP, S.L.S., GISLASON, S.R. (2014b) Element scavenging by recently formed travertine deposits in the alkaline springs from the Oman Semail Ophiolite. *Mineralogical Magazine* 78, 1479-1490.
- ONI, B.A., OZIEGBE, O., OLAWOLE, O.O. (2019) Significance of biochar application to the environment and industry. *Annals of Agricultural Science* 64, 222-236.
- OSHA (1989) Carbon dioxide, Industrial exposure and control technologies for OSHA regulated hazardous substances, Volume I of II, Substance A-I. *Occupational Safety and Health Administration, US Department of Labor, US Government Printing Office, Washington DC.*
- OSKIERSKI, H.C., DLUGOGORSKI, B.Z., JACOBSEN, G. (2013) Sequestration of atmospheric CO₂ in chrysotile mine tailings Woodreef Asbestos Mine, Australia: quantitative mineralogy, isotopic fingerprinting and carbonation rates. *Chemical Geology* 358, 156-169.
- PAN, Y., BIRDSEY R.A., FANG, J., HOUGHTON, R., KAUPPI, P.E., KURZ, W.A., PHILLIPS, O.L., SHVIDENKO, A., LEWIS, S.L., CANDELL, J., G., CIAIS, P., JACKSON, R.B., PACALA, S.W., MCGUIRE, A.D., PIAO, S., RAUTIAINEN, A., SITCH, S., HAYES, D. (2011) A large and persistent carbon sink in the world's forests. *Science* 333, 988-993.
- PÁLSSON, S., VIGFÚSSON, G.H. (1996) Gagnasafn aurburðarmaelninga 1963-1995 (Results of suspended load and discharge measurements 1963-1995). OS-96032/VOD-05 B. Orkustofnun, National Energy Authority, Reykjavik. (In Icelandic)
- PALES, J.C., KEELING, C.D. (1965) The concentration of atmospheric carbon dioxide in Hawaii. *Journal of Geophysical Research* 70, 6053-6076.
- PEARCE, C.R., JONES, M.T., OELKERS, E.H. (2013) The effect of particulate dissolution on the neodymium (Nd) isotope and Rare Earth Element (REE) composition of seawater. *Earth and Planetary Science Letters* 369, 138-147.
- PENMAN, D.E., CAVES RUGENSTEIN, J.K., IBARRA, D.E. WINNICK, M.J. (2020) Silicate weathering as a feedback and forcing in Earth's climate and carbon cycle. *Earth-Science Reviews* 209, 103298.
- PETIT, J.R., JOUZEL, J., RAYNAUD, D., BARKOV, N.I., BARNOLA, J.-M., BASILE-DOELSCH, I., BENDER, M., CHAPPELLAZ, J., DAVIS, M., DELAYGUE, G., DELMOTTE, M.F., KOTLYAKOV, V.M., LEGRAND, M., LIPENKOV, V.Y., LORUS, C., PEPIN, L., RITZ, C., SALTZMAN, E., STEVENARD, M. (1999) Climate and atmospheric history of the past 420,000 years from the Vostok ice core, Antarctica. *Nature* 399, 429-436.
- PLANAVSKY, N.J., ASAEL, D., HOFMANN, A., REINHARD, C.T., LALONDE, S.V., KUNDSÉN, A., WANG, X., OSSA OSSA, F. PECOITS, E., SMITH, A.J.B., BEUKES, N.J., BEKKER, A., JOHNSON, T.M., KORNHAUSER, K.O., LYONS, T.W., ROUXEL, O.J. (2014) Evidence of oxygenic photosynthesis half a billion years before the Great Oxygenation Event. *Nature Geoscience* 7, 283-286.



- POGGE VON STRANDMANN, P.A.E., BURTON, K.W., JAMES, R.H., VAN CALSTEREN, P., GISLASON, S.R., SIGFUSSON, B. (2008) The influence of weathering processes on riverine magnesium isotopes in a basaltic terrain. *Earth Planetary Science Letters* 276, 187-197.
- POGGE VON STRANDMANN, P.A.E., JENKYN, H., WOODFINE, R. (2013) Lithium isotope evidence for enhanced weathering during Oceanic Anoxic Event 2. *Nature Geoscience* 6, 668-672.
- POGGE VON STRANDMANN, P.A.E., BURTON, K.W., SNÆBJÖRNSDÓTTIR, S.O., SIGFÚSSON, B., ARADÓTTIR, E.S., GUNNARSSON, I., ALFREDSSON, H.A., MESFIN, K.G., OELKERS, E.H., GISLASON, S.R. (2019) Rapid CO₂ mineralisation into calcite at the CarbFix storage site quantified using calcium isotopes. *Nature Communications* 10, 1983.
- POKROVSKY, O.S., SCHOTT J. (2000) Kinetics and mechanism of forsterite dissolution at 25°C and pH from 1 to 12. *Geochimica et Cosmochimica Acta* 64, 3313-3325.
- POKROVSKY, O.S., SCHOTT, J. (2004) Experimental study of brucite dissolution and precipitation in aqueous solutions: surface speciation and chemical affinity control. *Geochimica et Cosmochimica Acta* 68, 31-45.
- POWER, I.M., HARRISON, A.L., DIPPLE, G.M., WILSON, S.A., BARKER, S.L.L., FALLON, S.J. (2019) Magnesite formation in playa environments near Atlin, British Columbia, Canada. *Geochimica et Cosmochimica Acta* 255, 10-24.
- POWER, I.M., WILSON, S.A., THOM, J.M., DIPPLE, G.M., SOUTHAM, G. (2007) Biologically induced mineralization of dyspingite by cyanobacteria from an alkaline wetland near Atlin, British Columbia, Canada. *Geochimica et Cosmochimica Acta* 71, 16.
- PRASAD, P.S.R., SARMA, D.S., SUDHAKAR, L., BASAVARAJU, U., SINGH, R. S., BEGUM, Z., ARCHANA, K.B., CHAVAN, C.D., CHARAN, S.N. (2009) Geologic sequestration of carbon dioxide in Deccan basalts: Preliminary laboratory study. *Current Science* 96, 288-291.
- QANBARI, F., POOLADI-DARVISH, M., TABATABAIE, S.H., GERAMI, S. (2012) CO₂ disposal as hydrate in ocean sediments. *Journal of Natural Gas Science and Engineering* 8, 139-149.
- QUADE, J., ENGLISH, N., DECELLES, P.G. (2003) Silicate versus carbonate weathering in the Himalaya: A comparison of the Arun and Seti River watersheds. *Chemical Geology* 202, 275-296.
- RAISTRICK, M., MAYER, B., SHEVALIER, M., PEREZ, R.J., HUTCHEON, I., PERKINS, E., GUNTER, B. (2006) Using chemical and isotopic data to quantify ionic trapping of injected carbon dioxide in oil field brines. *Environmental Science and Technology* 40, 6744-6749.
- RENFORTH, P., WASHBOURNE, C.-L., TAYLOR, J., MANNING, D.A.C. (2011) Silicate production and availability of mineral carbonation. *Environmental Science and Technology* 45, 2035-2041.
- RIGOPOULOS, I., HARRISON, A.L., DELIMITIS, A., IOANNOU, I., EFSTATHIOU, A.M., KYRATSI, T., OELKERS, E.H. (2018) Carbon sequestration via enhanced weathering of peridotites and basalts in seawater. *Applied Geochemistry* 91, 197-207.
- RIST, S. (1956) Íslenzk Vötn. Icelandic Fresh Waters. National Energy Authority Report, The State Electricity Authority Hydrological Survey, Reykjavík, 127 pp. (In Icelandic)
- ROBERTSON, D.S. (2001) The rise in the atmospheric concentration of carbon-dioxide and the effects on human health. *Medical Hypotheses* 56, 513-518.
- ROBERTSON, D.S. (2006) Health effects of increase in concentration of carbon dioxide in the atmosphere. *Current Science* 12, 1607-1609.
- ROGERS, J.R., BENNETT, P.C. (2004) Mineral stimulation of subsurface microorganisms: Release of limiting nutrients from silicates. *Chemical Geology* 203, 91-108.
- ROGERS, K.L., NEUHOFF, P.S., PEDERSEN, A.K., BIRD, D.K. (2006) CO₂ metasomatism in a basalt-hosted petroleum reservoir, Nuussuaq, West Greenland. *Lithos* 92, 55-82.
- ROSS, H. (2006) More knobs to control global environment. *Reasons to Believe*. <https://reasons.org/explore/publications/articles/more-knobs-to-control-global-environment>
- ROUSI, E., KORNHUBER, K., BEOBIDE-ARSUAGA, G., LUO, F., COUMOU, D. (2022) Accelerated western European heatwave trends linked to more-persistent double jets over Eurasia. *Nature Communications* 13, 3851.
- RUBIN, E.S., DAVIDSON, J.E., HERZOG, H.J. (2015) The cost of CO₂ capture and storage. *International Journal of Greenhouse Gas Control* 40, 378-400.



- RUDDIMAN, W.F. (2003) The anthropogenic greenhouse area began thousands of years ago. *Climate Change* 61, 261-293.
- RUPPEL, C.D. (2011) Methane Hydrates and Contemporary Climate Change. *Nature Education Knowledge* 3, 29.
- RUPPEL, C.D., KESSLER, J.D. (2017) The interaction of climate change and methane hydrates. *Reviews of Geophysics* 55, 126-168.
- SA, J.-H., KWAK, G.-H., LEE, B.R., HAN, K., CHO, S.-J., LEE, J.D., LEE, K.-H. (2017) Phase equilibria and characterization of CO₂ and SF₆ binary hydrates for CO₂ sequestration. *Energy* 126, 306-311.
- SABIL, K.M., AZMI, N., MUKHTAR, H. (2011) A review on carbon dioxide hydrate potential in Technological Applications. *Journal of Applied Sciences* 11, 3534-3540.
- SALDI, G., KOHLER, S.J., MARTY, N., OELKERS, E.H. (2007) Dissolution rates of talc as a function of solution composition, pH and temperature *Geochimica et Cosmochimica Acta* 71, 3446-3457.
- SALDI, G.D., JORDAN, G., SCHOTT, J., OELKERS, E.H. (2009) Magnesite growth rates as a function of temperature and saturation state. *Geochimica Cosmochimica Acta* 73, 5646-5657.
- SALDI, G.D., SCHOTT, J., POKROVSKY, O.S., GAUTIER, Q., OELKERS, E.H. (2012) An experimental study of magnesite precipitation rates at neutral to alkaline conditions and 100-200 °C as a function of pH, aqueous solution composition and chemical affinity. *Geochimica Cosmochimica Acta* 83, 93-109.
- SATISH, U., MENDELL, M.J., SHEKHAR, K., HOTCHI, T., SULLIVAN, D., STREUFERT, S., FISK, W.J. (2012) Is CO₂ an indoor pollutant? Direct effects of low-to-moderate CO₂ concentrations on human decision-making performance. *Environmental Health Perspectives* 124, 805-812.
- SCHAEF, H.T., MCGRAIL, B.P., OWEN, A.T. (2010) Carbonate mineralisation of volcanic province basalts. *International Journal of Greenhouse Gas Control* 4, 249-261.
- SCHMIDT, M., TORN, M., ABIVEN, S., DITTMAR, T., GUGGENBERGER, G., JANSSENS, I.A., KLEBER, M., KOGEL-KNABNER, I., LEHMANN, J., MANNING, D.A.C., NANNIPIRI, P., RASSE, D.P., WEINER, S., TRUMBORE, S.E. (2011) Persistence of soil organic matter as an ecosystem property. *Nature* 478, 49-56.
- SCHOTT, J., POKROVSKY, O.S., OELKERS, E.H. (2009) The Link Between Mineral Dissolution/Precipitation Kinetics and Solution Chemistry. *Reviews in Mineralogy And Geochemistry* 70, 207-258.
- SEIBEL, B.A., WALSH, P.J. (2001) Potential impacts of CO₂ injection on deep-sea biota. *Science* 294, 319-320.
- SEIBEL, B.A., WALSH, P.J. (2003) Biological impacts of deep-sea carbon dioxide injection inferred from indices of physiological performance. *Journal of Experimental Biology* 206, 641-650.
- SHEPS, K.M., MAX, M.D., OSEGOVIC, J.P., TATRO, S.R., BRAZEL, L.A. (2009) A case for deep-ocean CO₂ sequestration. *Energy Procedia* 1, 4961-4968.
- SHEVALIER, M., NIGHTINGALE, M., MAYER, B., HUTCHEON, I., DUROCHER, K., PERKINS, E.H. (2013) Brine geochemistry changes induced by CO₂ injection observed over a 10 year period in the Weyburn oil field. *International Journal of Greenhouse Gas Control* 16, S160-S176.
- SHIROKOVA, L.S., MAVROMATIS, V., BUNDELEVA, I.A., POKROVSKY, O.S., BENEZETH, P., GERARD, E., PEARCE, C.R., OELKERS, E.H. (2013) Using Mg isotopes to trace cyanobacterially mediated magnesium carbonate precipitation in alkaline lakes. *Aquatic Geochemistry* 19, 1-24.
- SIGFUSSON, B., GISLASON, S.R., MATTER, J.M., STUTE, M., GUNNLAUGSSON, E., GUNNARSSON, I., ARADOTTIR, E.S., SIGURDARDOTTIR, H., MESPIN, K., ALFREDSSON, H.A., WOLFF-BOENISCH, D., ARNARSSON, M.T., OELKERS, E.H. (2015) Solving the carbon-dioxide buoyancy challenge: The design and field testing of a dissolved CO₂ injection system. *International Journal of Greenhouse Gas Control* 37, 213-219.
- SIGFUSSON, B., ARNARSON, M.P., SNÆBJÖRNSDÓTTIR, S.Ó., KARLSDÓTTIR, M.R., ARADÓTTIR, E.S.P., GUNNARSSON, I. (2018) Reducing emissions of carbon dioxide and hydrogen sulphide at Hellisheiði power plant in 2014-2017 and the role of CarbFix in achieving the 2040 Iceland climate goals. *Energy Procedia* 146, 135-145.



- SIGURDSSON, F., ÍNGIMARSSON, J. (1990) Lekt íslenskra jarðefna. In: Sigbjarnarson, G. (Ed.) *Vatnid og landid Vatnafröediradstefna*. Orkustofnun, Reykjavik, 121-128. (In Icelandic)
- SKIPPEN, G.B. (1977) Dehydration and decarbonation equilibria. In: Greenwood, H.J. (Ed) *Application of Thermodynamics to Petrology and Ore Deposits Short Course*, 2 Mineralogical Association of Canada. Evergreen Press Limited, Vancouver.
- SMIT, M.A., MEZGER, K. (2017) Earth's early O₂ cycle suppressed by primitive continents. *Nature Geoscience* 10, 788-792.
- SMITH, M.R., MYERS, S.S. (2020) Impact of anthropogenic CO₂ emission on global human nutrition. *Nature Climate Change* 8, 834-839.
- SMITH, S.A., PRETORIUS, W.A. (2002) The conservative behaviour of Fluorescein. *Water SA* 28, 403-406.
- SMITS, M.M., BONNEVILLE, S., BENNING, L.G., BANWART, S.A., LEAKE, J.R. (2012) Plant-driven weathering of apatite – the role of an ectomycorrhizal fungus. *Geobiology* 10, 445-456.
- SNÆBJÖRNSDÓTTIR, S.O., WEISE, F., FRÍDKSSON, T., ÁRMANSSON, H., EINARSSON, G. M., GISLASON, S.R. (2014) CO₂ storage potential of basaltic rocks in Iceland and the oceanic ridges. *Energy Procedia* 63, 4584-4600.
- SNÆBJÖRNSDÓTTIR, S.O. (2017) *Mineral storage of carbon in basaltic rocks*. PhD dissertation, Faculty of Earth Sciences, University of Iceland, 156 pp.
- SNÆBJÖRNSDÓTTIR, S.O., OELKERS, E.H., MESFIN, K., ARADÓTTIR, E.S., DIDERIKSEN, K., GUNNARSSON, I., GUNNLAUGSSON, E., MATTER, J.M., STUTE, M., GISLASON, S.R. (2017) The chemistry and saturation states of subsurface fluids during the in-situ mineralisation of CO₂ and H₂S at the CarbFix site in SW-Iceland. *International Journal of Greenhouse Gas Control* 58, 87-102.
- SNÆBJÖRNSDÓTTIR, S.O., GISLASON, S.R., GALECZKA, I.M., OELKERS, E.H. (2018) Reaction path modelling of in-situ mineralisation of CO₂ at the CarbFix site at Hellisheiði, SW-Iceland. *Geochimica et Cosmochimica Acta* 220, 348-366.
- SNÆBJÖRNSDÓTTIR, S.O., SIGFÚSSON, B., MARIENI, C., GOLDBERG, D., GISLASON, S.R., OELKERS, E.H. (2020) Carbon dioxide storage through mineral carbonation. *Nature Reviews Earth & Environment* 1, 90-102.
- SPENCER, R.J., CHOU, I.-M. (Eds.) (1990) Fluid-Mineral Interactions: A Tribute to H.P. Eugster. The Geochemical Society Special Publication 2. The Geochemical Society, St. Louis. <https://www.geochemsoc.org/publications/sps/v2fluidmineralinteractions>
- STEFÁNSSON, A., ARNÓRSSON, S., GUNNARSSON, I., KAASALAINEN, H., GUNNLAUGSSON, E. (2011) The geochemistry and sequestration of H₂S into the geothermal system at Hellisheiði, Iceland. *Journal of Volcanology and Geothermal Research* 202, 179-188.
- STEFÁNSSON, A., GISLASON, S.R. (2001) Chemical weathering of basalts, SW Iceland: effect of rock crystallinity and secondary minerals on chemical fluxes to the oceans. *American Journal of Science* 301, 513-556.
- STEWART, R.J., HASZELDINE, R.S. (2014) Carbon Accounting for Carbon Dioxide Enhanced Oil Recovery. Scottish Carbon Capture and Storage <https://era.ed.ac.uk/bitstream/handle/1842/15717/SCCS-CO2-EOR-JIP-WP2-Carbon-Balance.pdf?sequence=1&isAllowed=y> accessed 24 September 2023.
- STEWART, R.J., HASZELDINE, R.S. (2015) Can producing oil store carbon? Greenhouse gas footprint of CO₂EOR, offshore North Sea. *Environmental Science & Technology* 49, 5788-5795.
- STEWART, R.J., JOHNSON, G., HEINEMANN, N., WILKINSON, M., HASZELDINE, R.S. (2018) Low carbon oil production: Enhanced oil recovery with CO₂ from North Sea residual oil zones. *International Journal of Greenhouse Gas Control* 75, 235-242.
- STOCKMANN, G.J., WOLFF-BOENISCH, D., GISLASON, S.R., OELKERS, E.H. (2011) Do carbonate precipitated affect dissolution kinetics? 1: Basaltic glass. *Chemical Geology* 284, 306-316.
- STOCKMANN, G.J., SHIROKOVA, L.S., POKROVSKY, O.S., BENEZETH, P., BOVET, N., GISLASON, S.R., OELKERS, E.H. (2012) Does the presence of heterotrophic bacterium *Pseudomonas* reactants affect basaltic glass dissolution rates? *Chemical Geology* 296-297, 1-18.



- STOCKMANN, G.J., WOLFF-BOENISCH, D., GISLASON, S.R., OELKERS, E.H. (2013) Do carbonate precipitated affect dissolution kinetics? 2. Diopside. *Chemical Geology* 337, 56-66.
- STOCKMANN, G.J., WOLFF-BOENISCH, D., BOVET, N., GISLASON, S.R., OELKERS, E.H. (2014) The role of silicate surfaces on calcite precipitation kinetics. *Geochimica et Cosmochimica Acta* 135, 231-250.
- SUAREZ C.A., EDMONDS M., JONES A.P. (2019) Catastrophic Perturbations to Earth's Deep Carbon Cycle. *Elements* 15, 301-306.
- SUDEK, L.A., WANGER, G., TEMPLETON, A.S., STAUDIGEL, H., TEBO, B.M. (2017) Submarine Basaltic Glass Colonization by the Heterotrophic Fe(II)-Oxidizing and Siderophore-Producing Deep-Sea Bacterium *Pseudomonas stutzeri* VS-10: The Potential Role of Basalt in Enhancing Growth. *Frontiers in Microbiology* 8, doi: 10.3389/fmicb.2017.00363.
- SUN, H., XIAO, Y., ZHANG, G., CASEY, J.F., SHEN, Y. (2018) Rapid enhancement of chemical weathering recorded by extremely light seawater lithium isotopes at the Permian-Triassic boundary. *Proceedings of the National Academy of Sciences* 115, 3782-3787.
- SVERDRUP, H., RAGNARSÓTTIR, K.V. (2014) Natural resources in a planetary perspective. *Geochemical Perspectives* 3, 129-341.
- SYVITSKI, J.P.M., VOROSMARTY, C.J., KETTNER, A.J., GREEN, P. (2005) Impact of humans on the flux of terrestrial sediment to the global coastal oceans. *Science* 308, 376-380.
- TAKAHASHI, T., SUTHERLAND, S.C., WANNINKHOF, R., SWEENEY, C., FEELY, R.A., CHIPMAN, D.W., HALES, B., FRIEDERICH, G., CHAVEZ, F., SABINE, C., WATSON, A., BAKKER, D.C.E., SCHUSTER, U., METZL, N., YOSHIKAWA-INOUE, H., ISHII, M., MIDORIKAWA, T., NOJIRI Y., KÖRTZINGER, A., STEINHOFFM, T., HOPPEMAN, M., OLAFSSON, J., ARNARSON, TH.S., TLBROOK, B., JOHANNESSEN, T., OLSEN, A., BELLERBY, R., WONG, C.S., DELILLE, B., BATES, N.R., DE BAAR, H.J.W. (2009) Climatological mean and decadal change in surface ocean pCO₂ and net sea-air CO₂ flux over the global oceans. *Deep-Sea Research, Part II-Topical Studies in Oceanography* 56, 554-577.
- TANZER, S.E., RAMIREZ, A. (2019) When are negative emissions negative emissions? *Energy and Environmental Science* 12, 1210-1288.
- TENG, F.-Z. (2017) Magnesium Isotope Geochemistry. *Reviews in Mineralogy and Geochemistry* 82, 219-287.
- TENG, Y., ZHANG, D. (2018) Long-term viability of carbon sequestration in deep-sea sediments. *Science Advances* 4, eaao6588.
- THAMATRAKOLN, K., HILDEBRAND, M. (2008) Silicon uptake in diatoms revisited. A model for saturable and nonsaturatable uptake kinetics and the role of silicon transporters. *Plant Physiology* 146, 1397-1407.
- THOMPSON, D. (2012) Rick Santorum is right: Gas prices caused the great recession. *The Atlantic*. <https://www.theatlantic.com/business/archive/2012/02/rick-santorum-is-right-gas-prices-caused-the-great-recession/252790/>
- THOMPSON, V., KENNEDY-ASSER, A.T., VOSPER, E., LO, Y. T. E., HUNTINGFORD, C., ANDREWS, O., COLLINS, M., HEGERL, G.C., MITCHELL, D. (2022) The 2021 western North America heat wave among the most extreme events ever recorded globally. *Science Advances* 8, eabm6860.
- TIPPER, E.T., BICKLE, M.J., GALY, A., WEST, A.J., POMIE, S., CHAPAMAN, H.J. (2006) The short-term climatic sensitivity of carbonate and silicate weathering fluxes: insight from seasonal variations in river chemistry. *Geochimica et Cosmochimica Acta* 70, 2737-2754.
- TOLLEFSON, J. (2018) Price of sucking CO₂ from air plunges. *Nature* 558, 173.
- TORP, T.A., GALE, J. (2003) Demonstrating storage of CO₂ in geological reservoirs: the Sleipner and SACS projects. In: Gale, J., Kaya, Y. (Eds.) *Proceedings of the 6th International Conference on Greenhouse Gas Control Technologies*, 311-316, Pergamon.
- TÓMASSON, H. (1990) Suspended material in Icelandic rivers. In: Guttormur, S. (Ed.) *Vatnid og Landid*. Orkustofnun, Reykjavik, 169-174.



- TÓMASSON, H., PÁLSSON, S., VIGFÚSSON, G.H., HAFSTAD, T. (1996) Framburður Þjórsár við Þjórsárver. Botnskið og svifaur. OS-96010/VOD-03 B. Orkustofnun, Reykjavík. 29 pp. (In Icelandic)
- TRADING ECONOMICS (2022) Markets <https://tradingeconomics.com/commodity/carbon> accessed 24 September 2023.
- TRIAS, R., MÉNEZ, B., CAMPION, P., ZIVANOVIC, Y., LECOURT, L., LECOEVRE, A., SCHMITT-KOPPLIN, P., UHL, J., GISLASON, S.R., ALFREDSSON, H.A., MESFIN, K.G., SNÆBJÖRNSDÓTTIR, S.Ó., ARADÓTTIR, E.S.P., GUNNARSSON, I., MATTER, J.M., STUTE, M., OELKERS, E.H., GÉRARD, E. (2017) High reactivity of deep biota under anthropogenic CO₂ injection into basalt. *Nature Communications* 8, 1063.
- TSAI, W.-H. (2020) Carbon Emission Reduction – Carbon Tax, Carbon Trading, and Carbon Offset. *Energies* 13, 6128.
- TSANG, C.-F. NERETNIEKS, I., TSANG, Y. (2015) Hydrologic issues associated with nuclear waste depositories. *Water Resources Research* 51, 6923-6972.
- TUCKER, J.M., MUKHOPADHYAY, S., GONNERMANN, H.M. (2018) Reconstructing mantle carbon and noble gas contents from degassed mid-ocean ridge basalts. *Earth and Planetary Science Letters* 496, 108-119.
- UMHVERFISRÁÐUNEYTI (2001) *Reglugerð 536/2001 um neysluvatn*. (Regulations in drinking ewater) Stjórnarráð Íslands. (In Icelandic)
- UREY, H.C. (1952) *The planets, their origin and development*. Yale University Press, New Haven, CT, USA, 245 pp.
- U.S. DEPARTMENT OF ENERGY (2013) More Economical Sulfur Removal for Fuel Processing Plants. Energy Efficiency & Renewable Energy http://www1.eere.energy.gov/office_eere/pdfs/tda_sbir_case_study_2010.pdf accessed 22 September 2023.
- VAN'T VELD, K., MASON, C.F., LEACH, A. (2013) The economics of CO₂ sequestration through enhanced oil recovery. *Energy Procedia* 37, 6909-6919.
- VARMA, A.K., SHANKAR, R., MONDAL, P. (2018) A Review on Pyrolysis of Biomass and the Impacts of Operating Conditions on Product Yield, Quality, and Upgradation In: Sarangi, P.K., Sonil, N. Pravakar, M. (Eds.) *Recent Advancements in Biofuels and Bioenergy Utilization*. Springer, 227-259.
- VIERS, J., DUPRE, B., GAILLARDET, J. (2009) Chemical composition of suspended sediments in world rivers. *Science of the Total Environment* 407, 835-868.
- VIERS, J., OLIVA, P., DANDURAND, J.-L., DUPRÉ, B., GAILLARDET, J. (2014) 7.6 - Chemical Weathering Rates, CO₂ Consumption, and Control Parameters Deduced from the Chemical Composition of Rivers. In: Holland, H.D., Turekian, K.K. (Eds.) *Treatise on Geochemistry*. Second Edition, Elsevier, Amsterdam, 175-194.
- VIGIER, N., BURTON, K.W., GISLASON, S.R., ROGERS, N.W., DUCHENE, S., THOMAS, L., HODGE, E., SCHAEFER, B. (2006) The relationship between riverine U-series disequilibria and erosion rates in a basaltic terrain. *Earth and Planetary Science Letters* 249, 258-273.
- VISHAL, V., VERMA, Y., CHANDRA, D., ASHOK, D. (2021) A systematic assessment and classification of geologic CO₂ storage systems in India. *International Journal of Greenhouse Gas Control* 111, 103458.
- VOIGT, M., MARIENI, C., BALDERMANN, A., GALECZKA, I.M., WOLFF-BOENISCH, D., OELKERS, E.H., GISLASON, S.R. (2021) An experimental study of basalt-seawater-CO₂ interaction at 130 °C. *Geochimica et Cosmochimica Acta* 308, 21-41.
- WATERS, C.N., TURNER, S.D. (2022) Defining the onset of the Anthropocene. *Science* 378, 706-708.
- WALKER, J.C.G., HAYS, P.B., KASTING, J.F. (1981) A negative feedback mechanism for the long-term stabilization of Earth's surface temperature *Journal of Geophysical Research* 86, 9776-9782.
- WALLING, D.E. (2006) Human Impact on land-sediment transfer by the world's rivers. *Geomorphology* 79, 192-216.
- WALLING, D.E., WEBB, B.W. (1986) Solutes in river systems. In: Trudgill, S.T. (Ed.) *Solute Processes*. Wiley, Chichester, 251-327.



- WANG, P., TENG, Y., ZHAO, Y., ZHU, J. (2021a) Experimental studies on gas hydrate-based CO₂ storage: State-of-the-art and future research directions. *Energy Technology* 9, 2100004.
- WANG, Y., LANG, X., FAN, S., WANG, S., YU, C., LI, G. (2021b) Review on enhanced technology of natural gas hydrate recovery by carbon dioxide replacement. *Energy Fuels* 35, 3659-3674.
- WEST, T.A.P., BORNER, J., SILLS, E.O., KONTOLEON (2020) Overstated carbon emission reduction from voluntary REDD+ projects in the Brazilian Amazon. *Proceedings of the National Academy of Science* 117, 241188-24194.
- WEST, T.A.P., WUNDER, S., SILLS, E.O., BORNER, J., KONTOLEON (2023) Action needed to make carbon offsets from forest conservation work for climate change. *Science* 381, 873-877.
- WIESE, F., FRIDRIKSSON, TH., ÁRMANNSSON, H. (2008) CO₂ Fixation by Calcite in High-temperature Geothermal Systems in Iceland. Tech. Rep. ISOR-2008/003, Iceland Geosurvey <https://gogn.orkustofnun.is/Skyrslur/ISOR-2008/ISOR-2008-003.pdf> accessed 24 September 2023.
- WIKIPEDIA (2022) https://en.wikipedia.org/wiki/Carbon_emission_trading#Market_trend accessed 30 June 2022.
- WILLETT, H.C. (1950) Temperature trends of the past century. In: *Centenary Proceedings of the Royal Meteorological Society*. Royal Meteorological Society, London, pp 195-206.
- WILSON, W., MONEA, M. (2004) *IEA GHG Weyburn CO₂ monitoring & storage project: Summary Report 2000-2004*. Petroleum Technology Research Center, Vancouver, 2004.
- WILSON, S.A., HARRISON, A.L., DIPPLE, G.M., POWER, I.M., BARKER, S.L.L., MAYER, K.U., FALLON, S.J., RAUDSEPP, M., SOUTHAM, G. (2014) Offsetting CO₂ emissions by air capture in mine tailings at the Mount Keith Nickel Mine, Western Australia: Rates controls and prospects for carbon neutral mining. *International Journal of Greenhouse Gas Control* 25, 121-140.
- WOLFF-BOENISCH, D., GISLASON, S.R., OELKERS, E.H. (2004a) The effect of fluoride on the dissolution rates of natural glasses at pH 4 and 25 °C. *Geochimica et Cosmochimica Acta* 68, 4571-4582.
- WOLFF-BOENISCH, D., GISLASON, S.R., OELKERS, E.H. (2004b) The effect of fluoride on the dissolution rates of natural glasses at pH 4 and 25°C. *Geochimica et Cosmochimica Acta* 68, 4571-4582.
- WOLFF-BOENISCH, D., GISLASON, S.R., OELKERS, E.H. (2006) The effect of crystallinity on dissolution rates and CO₂ consumption capacity of silicates. *Geochimica et Cosmochimica Acta* 70, 858-870.
- WOLFF-BOENISCH, D., WENAU, S., GISLASON, S.R., OELKERS, E.H. (2011) Dissolution of basalts and peridotite in seawater, in the presence of ligands, and CO₂: Implications for mineral sequestration of carbon dioxide. *Geochimica et Cosmochimica Acta* 75, 5510-5525.
- WORLD HEALTH ORGANIZATION (2017) *Guidelines for drinking-water quality: fourth edition incorporating the first addendum*. World Health Organization.
- WORLD METEOROLOGICAL ORGANIZATION (2022) 2021 one of the seven warmest years on record, WMO consolidated data shows. <https://public.wmo.int/en/media/press-release/2021-one-of-seven-warmest-years-record-wmo-consolidated-data-shows>
- WUEBBLES, D., HAYHOW, K. (2002) Atmospheric Methane and Global Change. *Earth Science Reviews* 57, 177-210.
- XIONG, W., WELLS, R.K., HORNER, J.A., SCHASF, H. T., SKEMER, P.A., GIAMMAR, D.E. (2018) CO₂ mineral sequestration in naturally porous basalt. *Environmental Science & Technology Letters* 5, 142-147.
- YANG, M., SONG, Y., JIANG, L., ZHAO, Y., RUAN, X., ZHANG, Y., WANG, S. (2014) Hydrate-Based Technology for CO₂ Capture from Fossil Fuel Power Plants. *Applied Energy* 116, 26-40.
- YANG, J., XIONG, Z., KUZYAKOV, Y. (2015) Biochar stability in soil: Meta-analysis of decomposition and priming effects. *GBD Bioenergy* 8, 512-523.
- YOUSSEF, N., ELSHAHED, M.S., MCINERNEY, M.J. (2009) Microbial processes in oil fields: Culprits, problems, and opportunities. *Advances in Applied Microbiology* 66, 141-251.



- ZENG, N., KING, A.W., ZAITCHIK, B., WULLSCHEGGER, S.D., GREGG, J., WANG, S., KIRK-DAVIDOFF, D. (2013) Carbon sequestration via wood harvest and storage: an assessment of its harvest potential. *Climatic Change* 118, 245-257.
- ZHENG, J., CHONG, Z.R., QURESHI, M.F., LINGA, O. (2020) Carbon dioxide sequestration via gas hydrates: A potential toward decarbonization. *Energy Fuels* 34, 10529-10547.
- ZARANDI, A.E., LARCHI, F., BEAUDOIN, G., PLANTE, B., SCIORTINO, M. (2017) Ambient mineral carbonation of different lithologies of mafic to ultramafic mining waste/tailings – A comparative study. *International Journal of Greenhouse Gas Control* 63, 392-400.



INDEX

A

agricultural soils 248
Agriculture, Forestry and Other Land Use (AFOLU) 308
alkalinity 205, 207, 213, 215, 248, 310
anhydrite 206, 290, 298
anthropocene 233
atmospheric CO₂ content 187, 189, 194-198, 207, 237, 238, 305

B

bedload 223-227, 230, 231
bioclogging 283
Bioenergy Carbon Capture and Storage (BECCS) 309
bioenergy production 309
Borgarfjörður Estuary 226, 227
Broecker, Wally 183, 186, 187, 189, 250, 251, 254, 294
brucite 246, 247, 320

C

¹⁴C 275, 277, 284
Ca flux 202, 204, 205

calcium isotopes 281
carbonate weathering 197
carbon credits 313, 314, 316
carbon reservoirs 192, 235, 236
chemical denudation rate 216-218, 221
clathrates 301
climategate 190
climeworks 283, 293, 299, 300, 317
CO₂-H₂S gas mixture 253, 271, 274, 275, 286, 293, 294
CO₂ solubility 266
coda terminal 317
cognitive and neurological effects 239
cumulative anthropogenic CO₂ 236

D

deep ocean storage 304
density 231, 234, 266, 302, 304
Direct Air Capture and Storage (DACs) 299, 310
Direct Air Capture (DAC) 253, 299, 300, 317
dissolution rates 183, 246-248, 257, 258
dissolved flux 205, 223
divine intervention 215



E

Eiríksdóttir, Eydis 198, 199, 201-204, 207, 210, 212, 213, 218, 219, 221, 224
Emission Trading Scheme (ETS) 307
enhanced oil recovery 241-244, 308
Enhanced Rock Weathering (ERW) 309
estuarine material 225
Eugster, Hans 181, 182, 218
European Emission Trading Scheme (ETS) 307
ex situ mineralisation 245, 315

F

Fellsá river 221
forestry 305, 306, 308, 309
fossil CO₂ emissions 235
fracturing 319

G

Gates, Bill 315
global CO₂ emission 187, 233, 234
global temperature 179, 187-190, 194-198, 207, 215, 237, 308
Gore, Al 189, 306
Great Oxygenation Event (GOE) 228
greenhouse effect 195, 207, 215
Grimsson, Olafur Ragnar 189, 250, 254
Gunnlaugsson, Einar 183, 250, 251, 294, 296

H

Hekla volcano 181, 216, 256
Helgeson, Harold 184, 185
human health 179, 238, 239
Hvítá river 225
hydrates 301-304

I

induced seismicity 319
injection system 266, 268, 285
IPCC report 191, 240

J

Jökulsá á Brú 199
Jökulsá á Dal 198-200, 202-205, 210, 218-220
Jökulsá í Fljótsdal 198, 200, 201, 207, 208, 212-214, 221

K

Kyoto agreement 188

L

laboratory experiments 230, 257, 266, 294, 298
Lagarfljót river 219, 220
limiting nutrients 209, 228-230

M

magmatic gases 216
magnesium isotopes 278
Mammoth Direct Air Capture System 317
mass balance 224, 226, 270, 273, 275, 276, 278, 280, 282, 287-290
methane 194, 304
mineral carbonation 180, 240, 245, 246, 259, 290, 319, 320
mineral cycling 249, 250
mineral saturation state 255, 273, 280, 281, 289
mineral trapping 241-243
mine waste 246, 247
Mississippi river bedload 230, 231
monitoring well 261-263, 271-278, 280-283, 287-290, 293

N

Na-fluorescein 261, 262, 275
natural analogues 281, 282
Nature-Based Global Emissions Offset (NGEO) 313
negative feedback 179, 215
Neoproterozoic Oxygenation Event (NOE) 228
Nesjavellir geothermal powerplant 316
net zero carbon emissions 312

O

ocean acidification 179, 192, 237, 240, 305
olivine 218, 246-248, 258, 259, 263, 271, 315, 320
organic carbon burial 229, 231

P

Particulate Organic Carbon (POC) 209, 210
particulate-seawater interaction 228



$p\text{CO}_2$ 259, 260, 264, 292, 298
photosynthesis 193, 194, 220, 229, 246,
248
physical trapping 242
plastics 306
porosity 242, 256, 263, 272, 316
power laws 201
primary productivity 209, 224, 228, 231
public acceptance 293, 294

R

residence time 189, 193, 194, 220, 235, 260
residual trapping 241
Reykjavík Energy 183, 250, 251, 255, 260,
283, 293-296, 299, 300
river discharge 199, 201, 204, 218
rock age 200, 213, 216-218, 222

S

scrubber 284, 285, 286, 317
Seastone (CO_2 -Seastone) 298, 317
seawater 189, 224-228, 235, 248, 297, 298,
302-305, 317, 319, 320
 SF_5CF_3 275, 276
 SF_6 275, 276
Silverstone Project 317
snowball Earth 228-231
solubility trapping 241, 267
stratigraphic trapping 241, 243
strontium isotopes 224
subsurface flow paths 261
suspended material 183, 201, 202, 205,
207, 215, 219, 220, 222, 223
Synechococcus sp 230

T

total chemical denudation rate 216, 217,
218, 221
toxic metals 257, 282
trace elements 205, 221, 293
tracers 273, 275, 278, 284
trademark 295

U

ultramafic rocks 180, 229, 248, 253, 257,
318
Utsira formation 240, 241

V

Verra 313
voluntary carbon market 312-314
Vostok ice core 190

W

Wallula project 253
water demand 297
weathering feedback 209, 215
weathering rates 179, 195, 198, 200, 205,
207, 209, 211, 213, 215, 216, 218, 220,
222
Weyburn oil fields 242





ERIC H. OELKERS is an international leader in carbon capture and storage technology. Eric was a co-founder and co-director of CarbFix from 2006 to 2020. Eric received his undergraduate degrees in Chemistry and in Earth and Planetary Sciences from the Massachusetts Institute of Technology, and his doctorate from the University of California. He has been employed as Professor at the University College London, UK, as Research Director at the CNRS GET Laboratory in Toulouse, France, and as Adjunct Professor at the University of Iceland. He has previously served as president of the European Association of Geochemistry, director of the Geochemical Society, founding co-editor of *Geochemical Perspectives* and *Geochemical Perspective Letters*, co-editor of *Chemical Geology*, associate editor of *Geochimica et Cosmochimica Acta*, and guest editor of 6 thematic journal issues.



SIGURDUR R. GISLASON received his PhD in geochemistry from Johns Hopkins University and is a research professor at University of Iceland. He has focused on field and laboratory experiments related to mineral storage of CO₂ in basaltic rocks, chemical and physical erosion rates of basaltic terrains and their role in the global carbon cycle, and the environmental impact of volcanic eruptions. He was co-founder and co-director of the CarbFix project from 2006 to 2020, and served as president of the European Association of Geochemistry in 2019-2020. He is a Geochemistry Fellow of the European Association of Geochemistry and Geochemical Society, Fellow of the International Association of Geochemistry, recipient of the Geochemical Society Patterson Award, and a Falling Walls 2021 Winner in Physical Sciences. The President of Iceland invested him with the Order of The Falcon in 2020.